

**Clinical application
of genomics- and
phosphoproteomics-based selection
of targeted therapy in patients
with advanced solid tumors**

Hanneke van der Wijngaart

**Clinical application
of genomics- and
phosphoproteomics-based selection
of targeted therapy in patients
with advanced solid tumors**

Hanneke van der Wijngaart

The author gratefully acknowledges the Barcode for Life foundation (BFL), the Center for Personalized Cancer Treatment (CPCT), the Dutch Cancer Society (KWF) and the Dutch Research Council (NWO) for financially supporting the research in this thesis. Amgen, AstraZeneca, Bayer, Boehringer Ingelheim, Bristol-Myers Squibb, Clovis Oncology, Eisai, Eli Lilly, Ipsen, Janssen, Merck Sharp & Dohme, Novartis, Pfizer and Roche generously provided drugs and financial support for the DRUP trial.

ISBN: 978-94-6483-538-0

doi:10.5463/thesis.350

Provided by thesis specialist Ridderprint, ridderprint.nl

Printing: Ridderprint

Layout and cover design: Timo Wolf Kamp, persoonlijkproefschrift.nl

Copyright © 2023, Hanneke van der Wijngaart

All rights reserved. No part of this book may be reproduced, stored in a retrieval system, or transmitted, in any form or by any means, electronic, photocopying, or otherwise, without the permission of the author, or, when appropriate, of the publishers of the publications.

VRIJE UNIVERSITEIT

**CLINICAL APPLICATION OF GENOMICS- AND PHOSPHOPROTEOMICS-BASED
SELECTION OF TARGETED THERAPY IN PATIENTS WITH ADVANCED SOLID
TUMORS**

ACADEMISCH PROEFSCHRIFT

ter verkrijging van de graad Doctor aan
de Vrije Universiteit Amsterdam,
op gezag van de rector magnificus
prof.dr. J.J.G. Geurts,
in het openbaar te verdedigen
ten overstaan van de promotiecommissie
van de Faculteit der Geneeskunde
op vrijdag 15 december 2023 om 9.45 uur
in een bijeenkomst van de universiteit,
De Boelelaan 1105

door

Hanneke van der Wijngaart

geboren te Ridderkerk

promotoren: prof.dr. H.M.W. Verheul
prof.dr. E.E. Voest

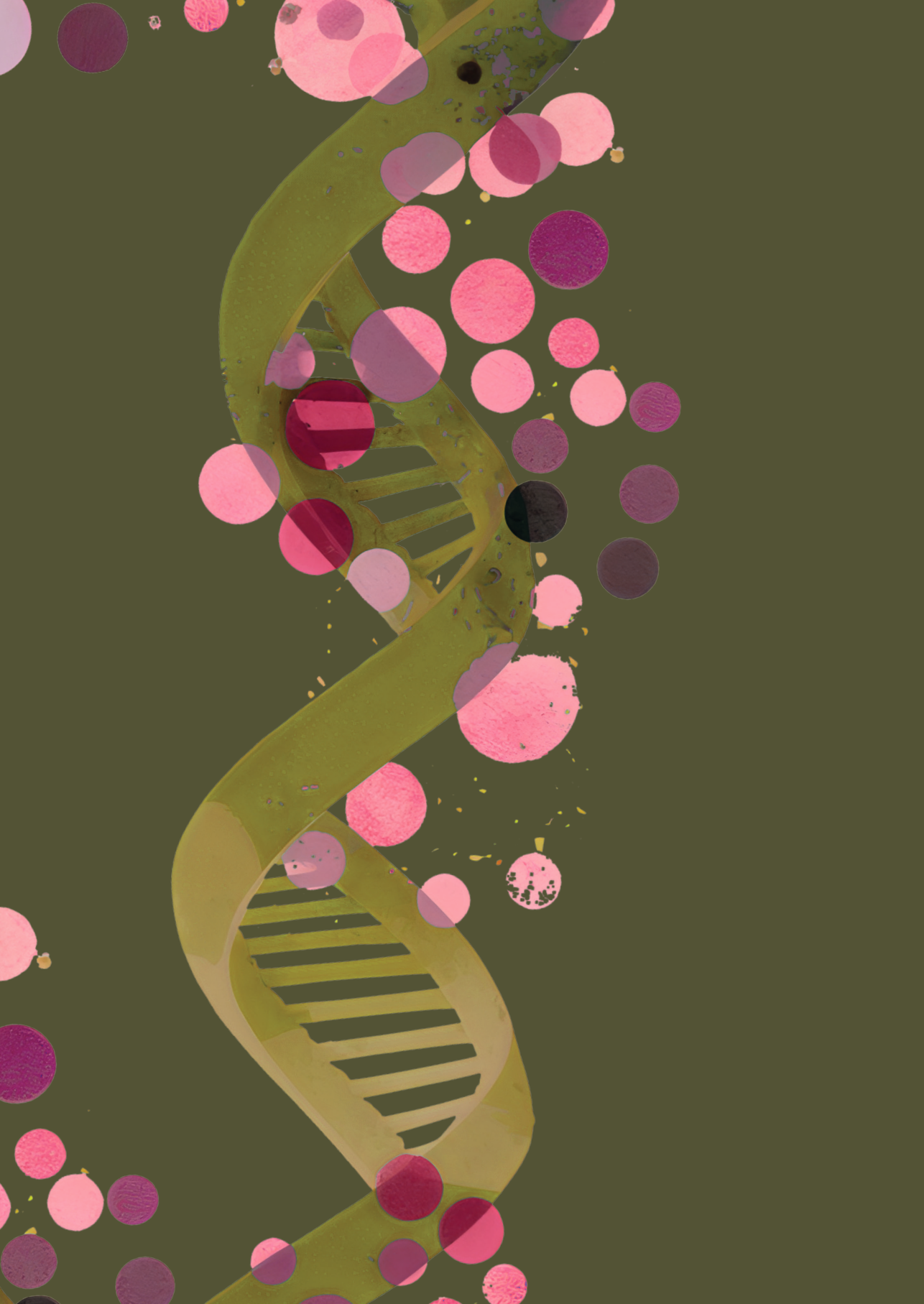
copromotor: dr. M. Labots

promotiecommissie: prof.dr. J. Berkhof
prof.dr. M.J.L. Ligtenberg
prof.dr. K. Taskén
prof.dr. C.M.L. van Herpen
dr. M.A.J. van Limbeek
dr. M. van Dongen
dr. M. van Linde

Voor mijn moeder

TABLE OF CONTENTS

Chapter 1	General introduction	9
Chapter 2	The Drug Rediscovery protocol facilitates the expanded use of existing anticancer drugs	23
Chapter 3	Patients with Biallelic BRCA1/2 Inactivation Respond to Olaparib Treatment Across Histologic Tumor Types	55
Chapter 4	Candidate biomarkers for treatment benefit from sunitinib in patients with advanced renal cell carcinoma using mass spectrometry-based (phospho)proteomics	87
Chapter 5	Advancing wide implementation of precision oncology: A liquid nitrogen-free snap freezer preserves molecular profiles of biological samples	129
Chapter 6	Summarizing discussion and future perspectives	157
Chapter 7	Nederlandse samenvatting	177
Chapter 8	Appendices	187
	Dankwoord	188
	Curriculum vitae	195
	List of publications	196





CHAPTER 1

| General Introduction

GENERAL INTRODUCTION

Accounting for almost one in six deaths, cancer is the second leading cause of death worldwide¹. In 2020, an estimated 19.3 million new cancer cases occurred, and nearly 10 million people have died from the disease². The global cancer burden continues to increase and a 47% rise in incidence is expected between 2020 and 2040 to an incidence of 28.4 million cases².

A GENETIC DISEASE

Cancer is a generic term for a large group of diseases characterized by the uncontrolled growth and spread of abnormal cells that can result in death if not treated¹. It is a genetic disease with nine essential characteristics (Hallmarks): self-sufficiency in growth signals, evasion of growth suppressors, resistance to cell death, replicative immortality, induction of angiogenesis, activation of invasion and metastasis, reprogramming of energy metabolism, evading immune destruction and the creation of a “tumor microenvironment”. Underlying these Hallmarks are two enabling capabilities: genome instability and mutation and tumor-promoting inflammation^{3,4}. Using these Hallmarks to describe the pathophysiology of cancer provides a better understanding of the drivers and enablers of the disease, and, equally important, may contribute to the development of new effective systemic anti-cancer treatments.

SYSTEMIC ANTI-CANCER TREATMENT: CHEMOTHERAPY

The first written prescriptions of remedies for the treatment of cancer date back to 2000 BC, usually in the form of ointments, medicated herbal solutions and powders⁵. Luckily, we have come a long way since then, and the systemic anti-cancer therapies have become more and more effective. Between 1948 and 1956, folic acid antagonists, vinca alkaloids and methotrexate were introduced as effective chemotherapies for the treatment of different types of cancer⁵. These agents were among the first modern chemotherapeutic drugs and are still in use today. Since the late 1950's, systemic anti-cancer therapies have continued to improve in terms of efficacy and survival due to the discovery of new chemotherapeutic agents, new combinations of drugs, new dosing regimens and the use of chemotherapy (neo)adjuvant to surgery and radiotherapy⁶. Conventional chemotherapy interferes with the DNA, hindering cell division and thereby stopping tumor growth but also damaging healthy tissues. Not all tumors respond (equally) to treatment with chemotherapy while most patients experience (serious) toxic side effects. It has proven to be difficult to upfront predict which patients will benefit from the treatment. Part of the solution to the problem of treatment selection for individual patients may lie in the fact that cancer is a genetic disease, which is characterized by dysregulation of growth signaling cascades and the escape from suppressive signaling and the immune response.

NEW CLASSES OF ANTI-CANCER DRUGS

In the past 30 years, global overall cancer survival and five-year relative survival has improved significantly⁷. Many factors have contributed to this worldwide decrease in mortality⁷. Development of, and access to, new types of anti-cancer drugs has played a major role in multiple tumor types. Especially drugs that interfere with aberrantly activated signaling cascades (i.e.

protein kinase inhibitors (PKI's)) or the immune system (i.e. immune checkpoint inhibitors (ICI)), or that target specific weaknesses in cancer cells caused by genetic aberrations (e.g. PARP inhibitors), have proven to be effective. For patients with metastatic melanoma or renal cell carcinoma for example, these new treatment options have dramatically improved the overall survival and quality of life.

Historically, patients with advanced melanoma, an aggressive and chemotherapy-resistant form of cancer, had a median overall survival of around 8 months and a 5-year survival of 10%. With the introduction of immune checkpoint inhibitors ipilimumab (monoclonal antibody (mAb) directed against CTLA4), nivolumab and pembrolizumab (mAb directed against PD-1) and combinations of these drugs, the overall survival has improved to several years, with a 5-year survival of 52%⁸. Approximately 50% of patients with advanced melanoma has a pathogenic mutation in the V-Raf Murine SarcomaViral Oncogene Homolog B (*BRAF*) gene in their tumor DNA. Treatment of these patients with an inhibitor of *BRAF* combined with an inhibitor of mitogen-activated protein kinase 1 (*MEK1* or *MAP2K1*) resulted in a median progression free survival of 9.9 months, with an objective response rate of 68%⁹. Treatment strategies combining these *BRAF*/*MEK* inhibitors with ICI are currently under investigation¹⁰.

For patients with metastatic clear cell renal cell carcinoma, the introduction of anti-angiogenic tyrosine kinase inhibitors (TKI's), such as sunitinib, sorafenib, axitinib, pazopanib and cabozantinib, has also dramatically improved survival. Since their introduction, the median overall survival (OS) has improved from 15-17 months before 2004¹¹⁻¹⁴ to 23-29 months with TKI monotherapy¹⁵⁻¹⁷. Combining TKI's with ICI has further improved the 12-month overall survival rate from 72%¹⁸ to 90%^{19,20}.

MOLECULAR PROFILING TO ASSESS TUMOR BIOLOGY

A corner stone for successful targeted treatment of patients with cancer is the presence of a biomarker that is associated with sensitivity for a certain targeted agent. Targets for treatment can be identified in multiple layers of cancer cell biology, but the challenge remains where to look for the most reliable biomarkers that best predict the treatment outcome to a targeted therapy.

DNA holds a permanent copy of the genetic information. The genes in DNA encode proteins, the driving force of cellular function, including intracellular signaling and immune response. All genetic information together is called the *genome*. The conversion of the genetic information stored in DNA to a functional product, such as a protein, is a complicated process that has two major steps. First, during transcription, the information in the double-stranded DNA is transferred to a messenger RNA (mRNA) molecule, which is a single-stranded temporary copy of the gene²⁶. The sum of all the mRNA molecules expressed from the genes is called the *transcriptome*. During the process of translation, the second major step, the transcribed code on the mRNA molecules is used to assemble a chain of specifically sequenced amino acids

that form a protein²⁶. All proteins in an organism together are called the *proteome*. Through regulation of gene expression, cellular functions can be controlled.

Another way that the function and activity of proteins are regulated is through reversible chemical changes to the protein after translation, known as posttranslational modifications (PTM). Phosphorylation is one of the most common PTM. During phosphorylation, a phosphate group is added to one of the amino acids tyrosine, serine or threonine by a kinase, thereby regulating the protein function. Especially tyrosine phosphorylation (pTyr) plays an important role in the regulation of signaling cascades in cancer. All phosphorylated proteins together are called the *phosphoproteome*.

GENOMICS-BASED PRECISION ONCOLOGY

The development of a large number of targeted- and immunotherapies, targeting specific molecular alterations and aberrant pathways in tumor cells, has dramatically changed the treatment paradigm in oncology. Coming from a histology-centered one-size-fits-all approach, the major focus has now shifted to precision oncology, a patient-centered biomarker-driven personalized approach to systemic treatment of patients with cancer²¹. Precision oncology is also known in literature as “personalized oncology”, “personalized cancer medicine” or “precision cancer medicine”. Many targeted- and immunotherapies have already received FDA/EMA approval and are available for patients with certain tumor types, harboring a specific molecular feature that predicts sensitivity for these drugs^{9,22-24}.

Though this is an important step towards precision oncology, the maximum potential of this approach is currently not used. A pan-cancer whole-genome analysis of metastatic solid tumors showed that in 31% of patients, across tumor types, an “actionable” genomic event was identified that predicted sensitivity to a drug. In 18% this was a biomarker for which on-label medication was available, and 13% of patients had a genomic target for which drugs were available, but not for the tumor type²⁵. Due to the histology-specific registrations of these drugs, a significant number of patients with other tumor types harboring the qualifying genomic aberration does not have access to these potentially active treatment options. Clinical evidence for efficacy of these drugs in other tumor types is often not available, and large trials with conventional design are usually not feasible due to the small and diverse subgroups of patients.

PROTEOME- AND MULTI-OMICS-BASED PRECISION ONCOLOGY

For the identification of tissue-based biomarkers, research often focused on abnormal protein expression, as found by immunohistochemistry, or genomic aberrations, such as activating mutations or amplifications of oncogenes or deletions of tumor suppressor genes, as found by targeted or broad panel sequencing. With recent advancements in sequencing- and bioinformatics techniques, also more complex genomic features such as gene fusions, microsatellite instability (MSI) and homologous repair deficiency (HRD) signatures can be computed and may serve as genomic biomarkers for treatment response to targeted agents.

For single oncogene-driven tumors, such as malignant melanoma with a BRAF V600E mutation, genomics-based treatment is a valuable approach⁹. Unfortunately, not all tumors harbor a clear genomic driver mutation. Some may be driven by a multitude of aberrantly activated kinase signaling pathways, such as renal cell carcinoma²⁷. In these tumor types, a functional pathway analysis may be a more promising approach^{28,29}. (Phospho)proteomics based on liquid chromatography coupled to tandem mass spectrometry (LC-MS/MS) may offer insight in aberrantly activated kinase signaling pathways and potential drug targets through the global analysis of phosphorylated proteins. In particular, phosphotyrosine-(pTyr)-phosphoproteomics provides an opportunity for the identification of patient subgroups likely to benefit from tyrosine kinase inhibitors (TKI's)^{30,31}.

In the past decade, advances in technology have enabled us to generate large-scale molecular data, allowing characterization of complex biological systems in great detail. For quite some time, research efforts have focused on unidimensional approaches to discovery of clinically useful biomarkers, i.e. genomics, transcriptomics or proteomics analysis³². The new fields of research created by these efforts are often referred to as “omics”, a field of study that focusses on large-scale data/information to understand biology³³. The application of these omics techniques have enabled major improvements in the understanding of cancer biology, the identification of biomarkers and the personalized treatment of patients with cancer. The *integrated* use of multiple omics may hold an opportunity for further improvement of our knowledge of biological processes. This multi-omics approach is suggested by numerous recent reviews to greatly benefit the field of precision oncology³⁴⁻³⁶. To date, only limited examples of truly multi-omics studies are available³². Most so-called multi-omics analyses only describe one omics approach, complemented with a limited amount of data from additional techniques, often obtained through targeted analyses³². Given the fact that different omics datasets do not overlap extensively and the correlation between data sets is extremely limited, it is likely that different omics approaches assess disparate pieces of the puzzle of the complex pathophysiology of cancer development and progression. True multi-omics analysis of tissues obtained from patients with cancer is still in its infancy. Nevertheless, recent advances in each of the omics techniques bring the clinical application of multi-omics in the standard care for patients with cancer closer by the day.

PRE-ANALYTICAL REQUIREMENTS TO ENABLE MULTI-OMICS ANALYSIS

Development and wider implementation of multi-omics in clinical studies faces many challenges³².

One of the most critical hurdles is tissue availability. A true multi-omics analysis requires multiple techniques to be performed on a tissue of interest. To allow for optimal correlation between these types of omics, they are ideally performed on the same piece of tissue to minimize the effect of intra- and inter-patient heterogeneity. Each of the omics techniques has its own minimally required quantity, often expressed as, for example, minimal tumor cell percentage, nanograms of DNA or RNA, or milligrams of protein. Clinical tissue samples, however,

are often core needle biopsies, with a maximum tissue yield of only 3.5 – 7 mg when using a 16-gauge core needle³⁷. In recent years, the omics techniques have improved tremendously, resulting in a general lowering of minimally required quantity of tissue. Whole genome- and whole transcriptome sequencing can already be performed on a single cell³⁸⁻⁴⁰. In the field of phosphoproteomics, important steps have been made to optimize the techniques, to facilitate analysis of small clinical samples⁴¹. Single-cell mass spectrometry-based phosphoproteomics is considered a promising opportunity for improving our understanding of individual tumor biology and facilitating phosphoproteomics-based therapy selection for individual patients in the future^{42,43}.

Furthermore, a standardized suitable method of processing and handling the acquired tissue specimen is fundamentally important to allow for a comprehensive multi-layer analysis of cancer tissue. In the past, biopsy samples were often collected in buffers that stabilized DNA and RNA, but essentially rendering the tissue useless for proteomics analysis³². Instead, high-quality fresh frozen tumor samples are required⁴⁴. Standardized operating procedures for handling and preservation of the tissue are indispensable, since differences in pre-analytical handling can generate conflicting research results due to heterogeneity in the quality of samples and associated data^{45,46}. Moreover, posttranslational modifications may be affected by certain handling and storage conditions, such as cold ischemia time⁴⁷⁻⁵⁰ and possibly freezing rate⁵¹⁻⁵³. Standardized high-quality preservation of biospecimens, in order to harness the most accurate genomic, transcriptomic and protein expression properties of the tissue, is a basic requirement for the generation of these complex multi-omics data⁴⁶.

An even bigger challenge may be the urgent need for the development of an integrated bioinformatics pipeline for a comprehensive analysis of these high-throughput molecular assays^{32,54}. Such an integrated approach may further increase our understanding of cancer biology and support biomarker discovery and drug repurposing^{55,56}, both essential for the practice and advancement of precision oncology.

TREATMENT SELECTION TRIALS

Working towards a histology-agnostic biomarker-centric approach, many precision oncology clinical trials now focus on the use of registered or experimental (combinations of) targeted agents solely based on the presence of a validated biomarker, while evaluating the effect in the context of histology. New trial designs have been developed to investigate even modest signs of clinical activity of these targeted agents in small subgroups of patients with cancer. Many of these basket-, umbrella and *N*-of-1-trials have been conducted in the past ten years⁵⁷, some living up to the promise of precision medicine, and others reporting disappointing results⁵⁸⁻⁷⁰. Tsimberidou et al have reviewed and summarized all these completed and ongoing trials and their distinctive features and outcomes²¹. A fundamental question in precision oncology remains *how to select the right treatment for the right patient at the right time*. An important factor contributing to the success of a precision oncology approach may be the actual process of treatment selection and the arguments for prioritizing one treatment over another.

THESIS OUTLINE AND SCOPE

Clinical implementation of precision oncology for patients with advanced solid tumors continues to be challenging. This thesis focused on optimizing the approach to targeted treatment selection (patient-based approach) and on identification of predictive tissue-based biomarkers for treatment benefit (drug-based approach), while contributing to an optimized infrastructure as a basic requirement for multi-omics analysis.

Chapters 2 and 3 focus on the Drug Rediscovery Protocol (DRUP), an ongoing prospective, multicenter, non-randomized basket trial, in which patients with advanced solid tumors are being treated based on their tumor genomic profile, with targeted- or immunotherapy outside their registered indications.

Chapter 2 describes the design and feasibility of the DRUP trial, including treatment outcomes of the first 215 patients treated in the trial. The clinical benefit rate in the first completed cohort “*Nivolumab for MSI tumors*” is highlighted, as well as the value of WGS in identifying targeted treatment options for patients with advanced cancer.

In **chapter 3** we present the results of the DRUP cohort “*Olaparib for tumors with a BRCA1/2 mutation*”, in which 24 patients with treatment refractory cancer with BRCA1/2 loss of function mutations were treated with the PARP inhibitor olaparib. Clinical outcome of these patients is interpreted in the context of their tumor genomic characteristics, attempting to identify potential indicators of (lack of) treatment benefit to olaparib, with special emphasis on patients with non-BRCA-associated tumor types.

Chapter 4 focuses on the use of mass spectrometry-based phosphoproteomics for the identification of predictive biomarkers for response and resistance to the tyrosine kinase inhibitor sunitinib in patients with renal cell carcinoma. Using this functional read-out, we aimed to describe differences in biology between sensitive and primary resistant patients and to define a phosphosite signature for prediction of treatment outcome.

In **chapter 5** we describe a new liquid nitrogen-free snap freezer for snap freezing biospecimens, which was developed to conserve molecular profiles under standardized and optimized pre-analytical conditions. We compare the performance of the new snap freezer to the current golden standard for snap freezing (quenching in liquid nitrogen) in terms of conservation of phosphoproteomics- and transcriptomics profiles of samples, hypothesizing that a liquid nitrogen-free snap freezing method may advance implementation of precision oncology.

The main findings of this thesis are summarized and discussed in **chapter 6**. With special emphasis on the approaches we used for improving patient selection and prediction of treatment outcome, we place our findings in the broader context of multi-omics for improving effective and personalized care for patients with cancer, and give recommendations for future research.

REFERENCES

1. American Cancer Society. Cancer Facts & Figures 2022.

2. Sung H, Ferlay J, Siegel RL, et al. Global cancer statistics 2020: GLOBOCAN estimates of incidence and mortality worldwide for 36 cancers in 185 countries. *Ca-Cancer J Clin* 2021;71(3):209-249. (In English). DOI: 10.3322/caac.21660.

3. Hanahan D, Weinberg RA. Hallmarks of Cancer: The Next Generation. *Cell* 2011;144(5):646-674. (In English). DOI: 10.1016/j.cell.2011.02.013.

4. Hanahan D. Hallmarks of Cancer: New Dimensions. *Cancer Discov* 2022;12(1):31-46. (In English). DOI: 10.1158/2159-8290.Cd-21-1059.

5. Hajdu SI. 2000 years of chemotherapy of tumors. *Cancer-Am Cancer Soc* 2005;103(6):1097-1102. (In English). DOI: 10.1002/cncr.20908.

6. DeVita VT, Chu E. A History of Cancer Chemotherapy. *Cancer Research* 2008;68(21):8643-8653. (In English). DOI: 10.1158/0008-5472.Can-07-6611.

7. Santucci C, Carioli G, Bertuccio P, et al. Progress in cancer mortality, incidence, and survival: a global overview. *Eur J Cancer Prev* 2020;29(5):367-381. (In English). DOI: 10.1097/Cej.0000000000000594.

8. Larkin J, Chiarion-Sileni V, Gonzalez R, et al. Five-Year Survival with Combined Nivolumab and Ipilimumab in Advanced Melanoma. *New Engl J Med* 2019;381(16):1535-1546. (In English). DOI: 10.1056/NEJMoa1910836.

9. Larkin J, Ascierto PA, Dreno B, et al. Combined Vemurafenib and Cobimetinib in BRAF-Mutated Melanoma. *New Engl J Med* 2014;371(20):1867-1876. (In English). DOI: 10.1056/NEJMoa1408868.

10. Ziogas DC, Konstantinou F, Bouros S, Theochari M, Gogas H. Combining BRAF/MEK Inhibitors with Immunotherapy in the Treatment of Metastatic Melanoma. *Am J Clin Dermatol* 2021;22(3):301-314. (In English). DOI: 10.1007/s40257-021-00593-9.

11. Fisher RI, Rosenberg SA, Fyfe G. Long-term survival update for high-dose recombinant interleukin-2 in patients with renal cell carcinoma. *Cancer J Sci Am* 2000;6:S55-S57. (In English) (<Go to ISI>://WOS:000085283900012).

12. McDermott DF, Regan MM, Clark JI, et al. Randomized phase III trial of high-dose interleukin-2 versus subcutaneous interleukin-2 and interferon in patients with metastatic renal cell carcinoma. *Journal of Clinical Oncology* 2005;23(1):133-141. (In English). DOI: 10.1200/Jco.2005.03.206.

13. Motzer RJ, Murphy BA, Bacik J, et al. Phase III trial of interferon alfa-2a with or without 13-cis-retinoic acid for patients with advanced renal cell carcinoma. *Journal of Clinical Oncology* 2000;18(16):2972-2980. (In English). DOI: Doi 10.1200/Jco.2000.18.16.2972.

14. Negrier S, Escudier B, Lasset C, et al. Recombinant human interleukin-2, recombinant human interferon alfa-2a, or both in metastatic renal-cell carcinoma. *New Engl J Med* 1998;338(18):1272-1278. (In English). DOI: Doi 10.1056/Nejm199804303381805.

15. Hutson TE, Al-Shukri S, Stus VP, et al. Axitinib Versus Sorafenib in First-Line Metastatic Renal Cell Carcinoma: Overall Survival From a Randomized Phase III Trial. *Clin Genitourin Canc* 2017;15(1):72-76. (In English). DOI: 10.1016/j.clgc.2016.05.008.

16. Konishi S, Hatakeyama S, Tanaka T, et al. Comparison of axitinib and sunitinib as first-line therapies for metastatic renal cell carcinoma: a real-world multicenter analysis. *Med Oncol* 2019;36(1) (In English). DOI: ARTN 6 10.1007/s12032-018-1231-3.

17. Motzer RJ, Hutson TE, Cella D, et al. Pazopanib versus Sunitinib in Metastatic Renal-Cell Carcinoma. *New Engl J Med* 2013;369(8):722-731. (In English). DOI: 10.1056/NEJMoa1303989.

18. Schmidinger M, Bamias A, Procopio G, et al. Prospective Observational Study of Pazopanib in Patients with Advanced Renal Cell Carcinoma (PRINCIPAL Study). *Oncologist* 2019;24(4):491-497. DOI: 10.1634/theoncologist.2018-0787.

19. Rini BI, Plimack ER, Stus V, et al. Pembrolizumab plus Axitinib versus Sunitinib for Advanced Renal-Cell Carcinoma. *New Engl J Med* 2019;380(12):1116-1127. (In English). DOI: 10.1056/NEJMoa1816714.

20. Motzer RJ, Penkov K, Haanen J, et al. Avelumab plus Axitinib versus Sunitinib for Advanced Renal-Cell Carcinoma. *New Engl J Med* 2019;380(12):1103-1115. (In English). DOI: 10.1056/NEJMoa1816047.

21. Tsimberidou AM, Fountzilas E, Nikanjam M, Kurzrock R. Review of precision cancer medicine: Evolution of the treatment paradigm. *Cancer Treat Rev* 2020;86 (In English). DOI: ARTN 102019 10.1016/j.ctrv.2020.102019.

22. de Bono J, Mateo J, Fizazi K, et al. Olaparib for Metastatic Castration-Resistant Prostate Cancer. *N Engl J Med* 2020. DOI: 10.1056/NEJMoa1911440.

23. Marcus L, Lemery SJ, Keegan P, Pazdur R. FDA Approval Summary: Pembrolizumab for the Treatment of Microsatellite Instability-High Solid Tumors. *Clinical Cancer Research* 2019;25(13):3753-3758. (In English). DOI: 10.1158/1078-0432.Ccr-18-4070.

24. Scott LJ. Larotrectinib: First Global Approval. *Drugs* 2019;79(2):201-206. (In English). DOI: 10.1007/s40265-018-1044-x.

25. Priestley P, Baber J, Lolkema MP, et al. Pan-cancer whole-genome analyses of metastatic solid tumours. *Nature* 2019;575(7781):210-+. (In English). DOI: 10.1038/s41586-019-1689-y.

26. Clancy SB, W. . Translation: DNA to mRNA to Protein. *Nature Education* 2008;1(01):101.

27. Stommel JM, Kimmelman AC, Ying H, et al. Coactivation of receptor tyrosine kinases affects the response of tumor cells to targeted therapies. *Science* 2007;318(5848):287-90. DOI: 10.1126/science.1142946.

28. Clark DJ, Dhanasekaran SM, Petralia F, et al. Integrated Proteogenomic Characterization of Clear Cell Renal Cell Carcinoma. *Cell* 2019;179(4):964-983 e31. DOI: 10.1016/j.cell.2019.10.007.

29. Cutillas PR. Role of phosphoproteomics in the development of personalized cancer therapies. *Proteom Clin Appl* 2015;9(3-4):383-395. (In English). DOI: 10.1002/prca.201400104.

30. Jimenez CR, Verheul HM. Mass spectrometry-based proteomics: from cancer biology to protein biomarkers, drug targets, and clinical applications. *Am Soc Clin Oncol Educ Book* 2014:e504-10. DOI: 10.14694/EdBook_AM.2014.34.e504.

31. Klaeger S, Heinzlmeier S, Wilhelm M, et al. The target landscape of clinical kinase drugs. *Science* 2017;358(6367) (In English). DOI: ARTN eaan4368 10.1126/science.aan4368.

32. Olivier M, Asmis R, Hawkins GA, Howard TD, Cox LA. The Need for Multi-Omics Biomarker Signatures in Precision Medicine. *Int J Mol Sci* 2019;20(19) (In English). DOI: ARTN 4781 10.3390/ijms20194781.

33. Yadav SP. The wholeness in suffix -omics, -omes, and the word om. *J Biomol Tech* 2007;18(5):277. (<https://www.ncbi.nlm.nih.gov/pubmed/18166670>).

34. Gallo Cantafio ME, Grillone K, Caracciolo D, et al. From Single Level Analysis to Multi-Omics Integrative Approaches: A Powerful Strategy towards the Precision Oncology. *High Throughput* 2018;7(4). DOI: 10.3390/ht7040033.

35. Hasin Y, Seldin M, Lusis A. Multi-omics approaches to disease. *Genome Biol* 2017;18(1):83. DOI: 10.1186/s13059-017-1215-1.

36. Turanli B, Karagoz K, Gulfidan G, Sinha R, Mardinoglu A, Arga KY. A Network-Based Cancer Drug Discovery: From Integrated Multi-Omics Approaches to Precision Medicine. *Curr Pharm Des* 2018;24(32):3778-3790. DOI: 10.2174/1381612824666181106095959.

37. Lai HW, Wu HK, Kuo SJ, et al. Differences in accuracy and underestimation rates for 14- versus 16-gauge core needle biopsies in ultrasound-detectable breast lesions. *Asian J Surg* 2013;36(2):83-88. (In English). DOI: 10.1016/j.asjsur.2012.09.003.

38. Han YY, Wang D, Peng LS, et al. Single-cell sequencing: a promising approach for uncovering the mechanisms of tumor metastasis. *J Hematol Oncol* 2022;15(1) (In English). DOI: ARTN 59 10.1186/s13045-022-01280-w.

39. Tang XM, Huang YM, Lei JL, Luo H, Zhu X. The single-cell sequencing: new developments and medical applications. *Cell Biosci* 2019;9 (In English). DOI: ARTN 53 10.1186/s13578-019-0314-y.

40. Zhang YJ, Wang D, Peng M, et al. Single-cell RNA sequencing in cancer research. *J Exp Clin Canc Res* 2021;40(1) (In English). DOI: ARTN 81 10.1186/s13046-021-01874-1.

41. Labots M, van der Mijn JC, Beekhof R, et al. Phosphotyrosine-based-phosphoproteomics scaled-down to biopsy level for analysis of individual tumor biology and treatment selection. *J Proteomics* 2017;162:99-107. DOI: 10.1016/j.jprot.2017.04.014.

42. Polat AN, Ozlu N. Towards single-cell LC-MS phosphoproteomics. *Analyst* 2014;139(19):4733-4749. (In English). DOI: 10.1039/c4an00463a.

43. Lun XK, Bodenmiller B. Profiling Cell Signaling Networks at Single-cell Resolution. *Mol Cell Proteomics* 2020;19(5):744-756. (In English). DOI: 10.1074/mcp.R119.001790.

44. Mazur P. Stopping biological time. The freezing of living cells. *Ann N Y Acad Sci* 1988;541:514-31. DOI: 10.1111/j.1749-6632.1988.tb22288.x.

45. Mager SR, Oomen MH, Morente MM, et al. Standard operating procedure for the collection of fresh frozen tissue samples. *Eur J Cancer* 2007;43(5):828-34. DOI: 10.1016/j.ejca.2007.01.002.

46. Barnes RO, Parisien M, Murphy LC, Watson PH. Influence of evolution in tumor biobanking on the interpretation of translational research. *Cancer Epidemiol Biomarkers Prev* 2008;17(12):3344-50. DOI: 10.1158/1055-9965.EPI-08-0622.

47. Bray SE, Paulin FE, Fong SC, et al. Gene expression in colorectal neoplasia: modifications induced by tissue ischaemic time and tissue handling protocol. *Histopathology* 2010;56(2):240-50. DOI: 10.1111/j.1365-2559.2009.03470.x.

48. Buffart TE, van den Oord RAHM, van den Berg A, et al. Time dependent effect of cold ischemia on the phosphoproteome and protein kinase activity in fresh-frozen colorectal cancer tissue obtained from patients. *Clin Proteom* 2021;18(1) (In English). DOI: ARTN 8 10.1186/s12014-020-09306-6.

49. Freidin MB, Bhudia N, Lim E, Nicholson AG, Cookson WO, Moffatt MF. Impact of collection and storage of lung tumor tissue on whole genome expression profiling. *J Mol Diagn* 2012;14(2):140-8. DOI: 10.1016/j.jmoldx.2011.11.002.

50. Mertins P, Yang F, Liu T, et al. Ischemia in Tumors Induces Early and Sustained Phosphorylation Changes in Stress Kinase Pathways but Does Not Affect Global Protein Levels. *Mol Cell Proteomics* 2014;13(7):1690-1704. (In English). DOI: 10.1074/mcp.M113.036392.

51. Desrosiers P, Legare C, Leclerc P, Sullivan R. Membranous and structural damage that occur during cryopreservation of human sperm may be time-related events. *Fertil Steril* 2006;85(6):1744-52. DOI: 10.1016/j.fertnstert.2005.11.046.

52. Fabbri R, Porcu E, Marsella T, Rocchetta G, Venturoli S, Flamigni C. Human oocyte cryopreservation: new perspectives regarding oocyte survival. *Hum Reprod* 2001;16(3):411-6. DOI: 10.1093/humrep/16.3.411.

53. Hunt CJ. Cryopreservation: Vitrification and Controlled Rate Cooling. *Methods Mol Biol* 2017;1590:41-77. DOI: 10.1007/978-1-4939-6921-0_5.

54. Nicora G, Vitali F, Dagliati A, Geifman N, Bellazzi R. Integrated Multi-Omics Analyses in Oncology: A Review of Machine Learning Methods and Tools. *Front Oncol* 2020;10:1030. DOI: 10.3389/fonc.2020.01030.

55. Gottlieb A, Stein GY, Ruppin E, Sharan R. PREDICT: a method for inferring novel drug indications with application to personalized medicine. *Mol Syst Biol* 2011;7:496. DOI: 10.1038/msb.2011.26.

56. Napolitano F, Zhao Y, Moreira VM, et al. Drug repositioning: a machine-learning approach through data integration. *J Cheminformatics* 2013;5 (In English). DOI: ArtN 30 10.1186/1758-2946-5-30.

57. Park JJH, Hsu G, Siden EG, Thorlund K, Mills EJ. An overview of precision oncology basket and umbrella trials for clinicians. *Ca-Cancer J Clin* 2020;70(2):125-137. (In English). DOI: 10.3322/caac.21600.

58. Hainsworth JD, Meric-Bernstam F, Swanton C, et al. Targeted Therapy for Advanced Solid Tumors on the Basis of Molecular Profiles: Results From MyPathway, an Open-Label, Phase IIa Multiple Basket Study. *Journal of Clinical Oncology* 2018;36(6):536-+. (In English). DOI: 10.1200/Jco.2017.75.3780.

59. Le Tourneau C, Delord JP, Goncalves A, et al. Molecularly targeted therapy based on tumour molecular profiling versus conventional therapy for advanced cancer (SHIVA): a multicentre, open-label, proof-of-concept, randomised, controlled phase 2 trial. *Lancet Oncol* 2015;16(13):1324-1334. (In English). DOI: 10.1016/S1470-2045(15)00188-6.

60. Massard C, Michiels S, Ferte C, et al. High-Throughput Genomics and Clinical Outcome in Hard-to-Treat Advanced Cancers: Results of the MOSCATO 01 Trial. *Cancer Discov* 2017;7(6):586-595. (In English). DOI: 10.1158/2159-8290.Cd-16-1396.

61. Rodon J, Soria JC, Berger R, et al. Genomic and transcriptomic profiling expands precision cancer medicine: the WINTHER trial. *Nature Medicine* 2019;25(5):751-+. (In English). DOI: 10.1038/s41591-019-0424-4.

62. Rothwell DG, Ayub M, Cook N, et al. Utility of ctDNA to support patient selection for early phase clinical trials: the TARGET study. *Nature Medicine* 2019;25(5):738-+. (In English). DOI: 10.1038/s41591-019-0380-z.

63. Schwaederle M, Parker BA, Schwab RB, et al. Precision Oncology: The UC San Diego Moores Cancer Center PREDICT Experience. *Mol Cancer Ther* 2016;15(4):743-752. (In English). DOI: 10.1158/1535-7163.Mct-15-0795.

64. Sicklick JK, Kato S, Okamura R, et al. Molecular profiling of cancer patients enables personalized combination therapy: the I-PREDICT study. *Nature Medicine* 2019;25(5):744-+. (In English). DOI: 10.1038/s41591-019-0407-5.

65. Stockley TL, Oza AM, Berman HK, et al. Molecular profiling of advanced solid tumors and patient outcomes with genotype-matched clinical trials: the Princess Margaret IMPACT/COMPACT trial. *Genome Med* 2016;8 (In English). DOI: ARTN 109 10.1186/s13073-016-0364-2.

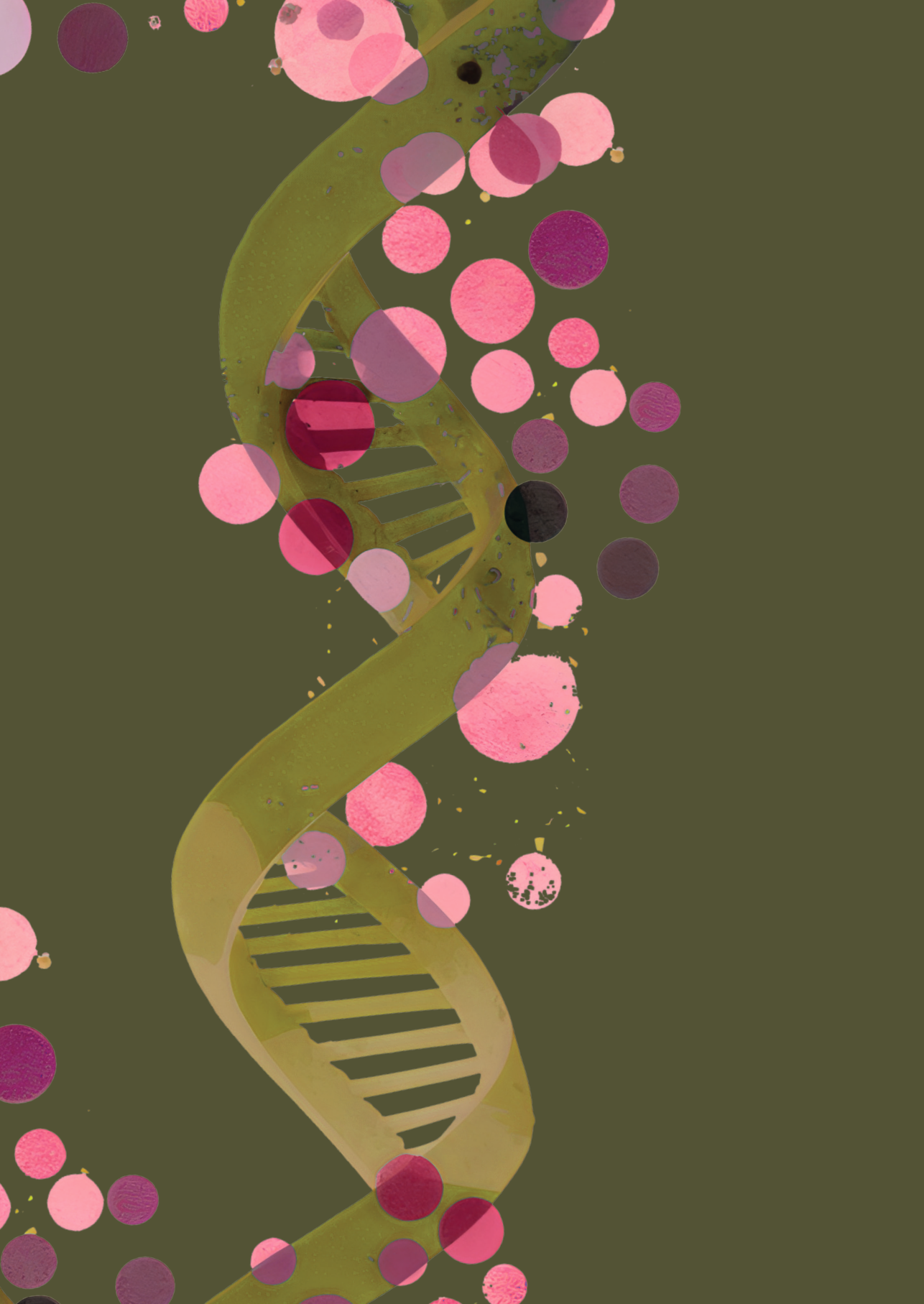
66. Tredan O, Wang Q, Pissaloux D, et al. Molecular screening program to select molecular-based recommended therapies for metastatic cancer patients: analysis from the ProfilER trial. *Ann Oncol* 2019;30(5):757-765. (In English). DOI: 10.1093/annonc/mdz080.

67. Tsimberidou AM, Hong DS, Ye Y, et al. Initiative for Molecular Profiling and Advanced Cancer Therapy (IMPACT): An MD Anderson Precision Medicine Study. *Jco Precis Oncol* 2017;1 (In English). DOI: Doi 10.1200/Po.17.00002.

68. Tsimberidou AM, Iskander NG, Hong DS, et al. Personalized Medicine in a Phase I Clinical Trials Program: The MD Anderson Cancer Center Initiative. *Clinical Cancer Research* 2012;18(22):6373-6383. (In English). DOI: 10.1158/1078-0432.Ccr-12-1627.

69. Von Hoff DD, Stephenson JJ, Rosen P, et al. Pilot Study Using Molecular Profiling of Patients' Tumors to Find Potential Targets and Select Treatments for Their Refractory Cancers. *Journal of Clinical Oncology* 2010;28(33):4877-4882. (In English). DOI: 10.1200/Jco.2009.26.5983.

70. Wheler JJ, Janku F, Naing A, et al. Cancer Therapy Directed by Comprehensive Genomic Profiling: A Single Center Study. *Cancer Research* 2016;76(13):3690-3701. (In English). DOI: 10.1158/0008-5472.Can-15-3043.





CHAPTER 2

The Drug Rediscovery protocol facilitates the expanded use of existing anticancer drugs

H. van der Wijngaart, D. L. van der Velden*, L. R. Hoes*, J. M. van Berge Henegouwen*, E. van Werkhoven, P. Roepman, R. L. Schilsky, W. W. J. de Leng, A. D. R. Huitema, B. Nuijen, P. M. Nederlof, C. M. L. van Herpen, D. J. A. de Groot, L. A. Devriese, A. Hoeben, M. J. A. de Jonge, M. Chalabi, E. F. Smit, A. J. de Langen, N. Mehra, M. Labots, E. Kapiteijn, S. Sleijfer, E. Cuppen, H. M. W. Verheul, H. Gelderblom, E. E. Voest*

** These authors contributed equally to this work*

Nature 2019 Oct;574(7776):127-131. ■

ABSTRACT

The large-scale genetic profiling of tumours can identify potentially actionable molecular variants for which approved anticancer drugs are available¹⁻³. However, when patients with such variants are treated with drugs outside of their approved label, successes and failures of targeted therapy are not systematically collected or shared. We therefore initiated the Drug Rediscovery protocol, an adaptive, precision-oncology trial that aims to identify signals of activity in cohorts of patients, with defined tumour types and molecular variants, who are being treated with anticancer drugs outside of their approved label. To be eligible for the trial, patients have to have exhausted or declined standard therapies, and have malignancies with potentially actionable variants for which no approved anticancer drugs are available. Here we show an overall rate of clinical benefit—defined as complete or partial response, or as stable disease beyond 16 weeks—of 34% in 215 treated patients, comprising 136 patients who received targeted therapies and 79 patients who received immunotherapy. The overall median duration of clinical benefit was 9 months (95% confidence interval of 8–11 months), including 26 patients who were experiencing ongoing clinical benefit at data cut-off. The potential of the Drug Rediscovery protocol is illustrated by the identification of a successful cohort of patients with microsatellite instable tumours who received nivolumab (clinical benefit rate of 63%), and a cohort of patients with colorectal cancer with relatively low mutational load who experienced only limited clinical benefit from immunotherapy. The Drug Rediscovery protocol facilitates the defined use of approved drugs beyond their labels in rare subgroups of cancer, identifies early signals of activity in these subgroups, accelerates the clinical translation of new insights into the use of anticancer drugs outside of their approved label, and creates a publicly available repository of knowledge for future decision-making.

MAIN

The precision treatment of cancer holds great promise for patients in terms of life extension and quality of life^{1,2,4-7}. However, early studies and experiences with genetically and molecularly informed decisions regarding treatment have also identified considerable hurdles, which may jeopardize the way in which we capitalize on precision medicine⁸⁻¹¹. First, populations of patients who are eligible for specific treatments or trials become smaller and trials accrue slower, owing to pre-selection by targeted sequencing of candidate variants and to slow implementation of pre-selection tests. Second, these candidate variants can, in general, be appreciated only when their tissue context is taken into consideration. However, with regards to drug sensitivity, the importance of a given genetic or molecular variant is usually tested in the subtype of cancer that most frequently contains this variant. The importance of the same variant in other cancers often remains unknown. Third, as drug development is challenging for rare subtypes of cancer, this can create inequality in care¹². Finally, with growing pressure from society to increase the success rate of drug-development trials¹³, there is hesitation amongst payers to reimburse large-scale sequencing efforts before they have proof that these efforts will make healthcare more sustainable. As a result, we are not using the full potential of rapidly expanding technological advances, knowledge of biomarkers and the spectrum of approved anticancer drugs for our patients.

The Center for Personalized Cancer Treatment was founded in 2010¹⁴ to address these issues. In this network (which now connects 45 hospitals in the Netherlands), patients with all types of metastatic cancer are offered the opportunity to undergo a fresh tumour biopsy for whole-genome sequencing (WGS) before starting systemic anticancer treatment. The WGS results are combined with treatment outcomes in a national, centralized database for research purposes, and returned to the physician who is treating the patient for future planning of treatment. This initiative has contributed to the identification of potentially actionable variants in cancers that are not routinely tested for these variants. To provide treatment opportunities for patients in whom such variants were identified (while simultaneously collecting clinical outcomes), we began the Drug Rediscovery protocol (DRUP), in which we seek to expand the use of targeted therapies that have been approved by the European Medicines Agency (EMA) and/or US Food and Drug Administration (FDA) beyond the approved indications of these therapies.

The DRUP is an ongoing, prospective multi-drug and pan-cancer trial. Patients who are eligible are those who have progression of an advanced or metastatic solid tumour, multiple myeloma or B-cell non-Hodgkin lymphoma, and no suitable standard-treatment options. A potentially actionable genetic or molecular variant, which can be matched to one of the drugs available in the study (Extended Data Table 1), must have been identified via regular diagnostics or by the Center for Personalized Cancer Treatment.

In recognition of the importance of tissue context, the trial design allows for an unlimited number of parallel cohorts (each defined by tumour type, molecular variant and study treatment) (Fig. 1). For selected variant categories (such as mutational load, microsatellite instabil-

ity and DNA-repair deficiency), the protocol allows for cohorts in which tumour types are combined. A Simon-like two-stage design is used per cohort^{15,16}, in which 8 patients are enrolled in stage I and up to 24 patients are enrolled in stage II—provided that clinical benefit (which we define as complete or partial response, or stable disease beyond 16 weeks, measured 2-or-more times, ≥ 28 days apart) is observed at least once in stage I. A drug warrants further investigation in a particular cohort if ≥ 5 out of 24 patients experience a clinical benefit. If fewer responses are observed, the cohort is closed; results will be made public whether or not the cohort is successful. This design has 85% power to reject a rate of clinical benefit of 10%, if the true percentage is 30% (α error rate of 7.8%). The analysis of closed cohorts with some activity allows for the opening of new cohorts with refined criteria for inclusion.

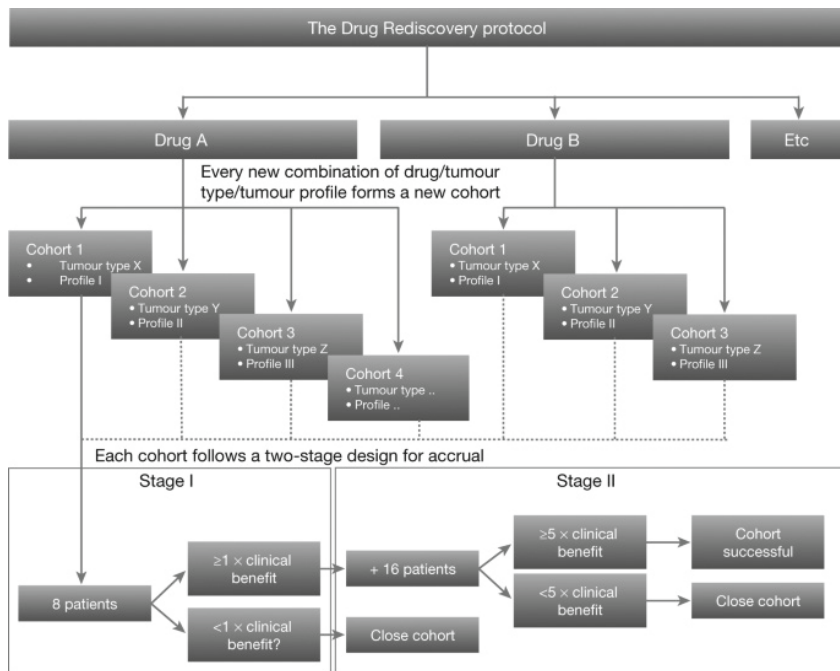


Figure 1. Study design. Schematic overview of the study and cohort design. For each study drug, a theoretically unlimited number of cohorts can be opened in parallel, depending on the tumour types and tumour profiles of submitted patients and the amount of the drug being studied that is available. A new cohort is opened for each combination of tumour type, tumour profile and study treatment. In each cohort, patients are enrolled in a two-stage design. Clinical benefit is defined as either complete or partial response, or absence of disease progression for ≥ 16 weeks, and must be measured 2 or more times and ≥ 28 days apart.

Between September 2016 and September 2018, over 600 cases were submitted for central review and 294 patients started study treatment. Extended Data Figure 1 provides details of the review process, and Extended Data Figure 2 provides an overview of case submissions. To allow for sufficient follow-up (≥ 5 months for patients on study treatment), here we pres-

ent the results of the first 215 patients who started study treatment. The enrolment of these 215 patients resulted in the initiation of 76 cohorts (Extended Data Table 2); the baseline characteristics of these patients are provided in Table 1.

■ **Table 1.** Baseline characteristics of the first 215 patients who started study treatment

WHO, World Health Organization. *All patients were required to have exhausted standard therapies, but some patients refused standard chemotherapy owing to fear of toxicity. In addition, on occasion the treating physician had well-argued reasons to refrain from a given standard therapy (such as the low response rate to standard therapies in specific subgroups of patients).

<i>n</i> = 215		
Age (approximately at consent)		
Median (range)	62	(23 – 87)
Gender		
Male	114	53%
Female	101	47%
WHO Performance Status		
WHO 0	60	28%
WHO 1	116	54%
WHO 2	14	7%
Not available	25	12%
Primary tumor types		
Colorectal cancer	49	23%
Non-small cell lung cancer	37	17%
Prostate cancer	19	9%
Breast cancer	16	7%
Gastro-intestinal stroma cell tumor	9	4%
Cervical cancer	8	4%
Salivary gland carcinoma	8	4%
Urothelial cell carcinoma	8	4%
Sarcoma	7	3%
Ovarian cancer	7	3%
Other	47	22%
Number of prior systemic therapies		
Median (range)	3	(0 – 12)*

Overall, clinical benefit was observed in 74 patients (34%) (Extended Data Table 3) with a median duration of 9 months (95% confidence interval, 8–11 months). Clinical benefit was observed across all types of treatment, comprising immunotherapy (*n* = 79 patients, clinical benefit rate of 38%), treatment with small-molecule inhibitors (including PARP inhibitors) (*n* = 81 patients, clinical benefit rate of 36%) and with monoclonal antibodies (*n* = 55 patients,

clinical benefit rate of 27%). The median progression-free survival and overall survival were 3 months (95% confidence interval 2–4 months) and 10 months (95% confidence interval 7–13 months), respectively (Figure. 2). To put this in perspective, a large database of 854 patients who were participating in phase I studies and were treated with molecularly targeted agents indicated a median progression-free survival and overall survival of 2 and 8 months, respectively¹⁷.

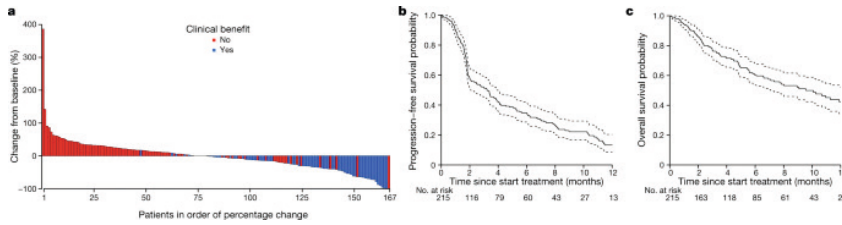


Figure 2. Response and survival plots.

- Waterfall plot of the best percentage change in the sum of target lesions compared to baseline tumour measurements according to ‘Response Evaluation Criteria in Solid Tumours’ (RECIST) 1.1, for all patients with ≥ 1 response evaluation and with a known change in the sum of target lesions ($n = 166$ patients). Patients with unequivocal disease progression at the first evaluation (on the basis of non-target lesions or non-RECIST measurements only) and patients who went off-study before their response could be evaluated are not included in this graph ($n = 49$ patients).
- Kaplan–Meier curve for estimated progression-free survival.
- Kaplan–Meier curve for estimated overall survival, with 95% confidence interval (dashed lines).

One hundred and forty-one patients (66%) did not experience a clinical benefit, either because of progressive disease ($n = 117$ patients) or because they went off-study before they could be classified as having experienced a clinical benefit or not ($n = 24$ patients). Reasons for early withdrawal from the study without obtaining radiologic or clinical diagnosis of progressive disease included death ($n = 9$ patients), adverse events ($n = 5$ patients), patient preference ($n = 3$ patients) or were unknown ($n = 7$ patients). Adverse events were consistent with those observed in standard of care (Extended Data Table 4). Overall, ten patients discontinued treatment owing to toxicity. Two suspected unexpected severe adverse reactions were reported: bacterial peritonitis in a patient with ovarian carcinoma and sinus thrombosis in a patient with breast cancer.

To date, two cohorts have completed accrual: the first is a tumour-type-agnostic cohort of patients with microsatellite-unstable (MSI) tumours treated with nivolumab. In total, 30 patients with 8 types of tumour were enrolled in this cohort. As of 3 May 2019, one patient (3%) had a complete response. Eleven patients (37%) had a partial response, and seven patients (23%) had stable disease at ≥ 16 weeks. Four patients (13%) had progressive disease as a best overall response, and seven patients (23%) went off study before evaluability was reached (that is, after fewer than two cycles of nivolumab treatment and/or with insufficient response evalu-

ations to determine clinical benefit). In this cohort, the rate of clinical benefit was 63%. The median progression-free survival was not reached after a median follow-up of 16.5 months. A summary of the clinical benefits to individual patients is presented in Figure 3. The results are consistent with previous reports for immunotherapy in MSI tumours^{18,19}. Overall, nivolumab was tolerated well, and adverse events were largely consistent with those that have previously been reported^{18,19} (Extended Data Table 5). One patient developed a grade-5 abdominal infection upon intestinal perforation, owing to shrinkage of a peritoneal tumour deposit. One patient experienced grade-5 dyspnoea, possibly attributable to disease progression. Baseline WGS for this cohort was successfully performed in 20 patients (67%) (Table 2). Assessment of MSI on the basis of WGS was highly representative for MSI identification on the basis of immunohistochemistry and PCR. On average, MSI tumours had 866 mutations (range of 614–1,111 mutations) in the genome.

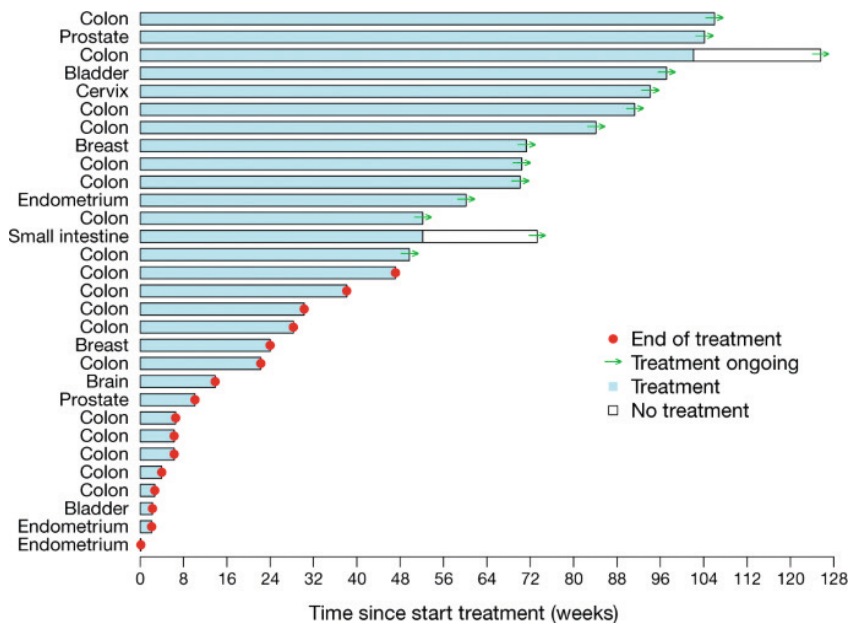


Figure 3. Treatment efficacy of nivolumab in completed MSI cohort.

Swimmer plot of the time on treatment (in weeks) for each patient ($n = 30$ patients). Patients marked with an arrow were still on treatment at the point of data cut-off (3 May 2019). The white bars represent the time period for which nivolumab treatment was interrupted (which was optional per protocol after 12 months of treatment) for patients, who still experienced clinical benefit.

■ **Table 2.** Tumour and biomarker details per patient of the MSI cohort

Histologic tumour type, biomarker characteristics and classification of clinical benefit per patient in the MSI cohort. CB, clinical benefit; PFS, progression-free survival (given in weeks, at data cut-off; > denotes benefit ongoing at cut-off); CRC, colorectal cancer; GBM, glioblastoma multiforme; Lynch, Lynch syndrome; ML, mutational load; MSIseq, microsatellite instability score; MSS, microsatellite stable; mut, mutation; NA, not applicable; NE, not evaluable; no., case number; PD, progressive disease; PR, partial response; SD, stable disease; somatic, different from germline DNA; UCC, urothelial cell carcinoma. ^aThe use of – denotes that no baseline WGS data are available. ^bCopy number gain of *CD274*. ^cUse of + denotes >20% prevalence of ‘Catalogue of Somatic Mutations in Cancer’ (COSMIC) mutational signature. Signatures are only mentioned in case of >10% prevalence (<https://cancer.sanger.ac.uk/cosmic/signatures>).

No.	Tumour type	Pre-enrolment Somatic or Lynch	MSI profile	Baseline WGS			CD274 ^b	COSMIC signature ^c	CB	PFS
				MSI seq ^a	ML	<i>JAK1</i> and/ or <i>JAK2</i> mutations				
1	CRC	Somatic	MLH1/PMS2 loss	–	–	–	–	–	NE	NA
2	CRC	Somatic	MLH1/PMS2 loss, <i>MLH1</i> methylation	76.9	1,589	3x	6+, 9, 15, 12, 17	PR	>105	
3	UCC	Lynch	<i>MSH2</i> mut, <i>MSH2</i> loss, MSI	35.2	973	3x	1+, 6+	PR	>92	
4	CRC	Somatic	MLH1/PMS2 loss	–	–	–	–	PD	8	
5	Cervix	Lynch	<i>MSH2</i> mut, <i>MSH2/MSH6</i> loss	23.1	776	2x	6+, 1+, 14, 12	PR	>88	
6	CRC	Somatic	MLH1/PMS2 loss, <i>MLH1</i> methylation	66.7	1,301	2x	12+, 6+, 9, 20	PR	>83	
7	CRC	Somatic	MLH1/PMS2 loss, <i>MLH1</i> methylation	17.1	638	2x	–	PR	>90	
8	CRC	Somatic	MLH1/PMS2 loss	–	–	–	–	NE	NA	
9	CRC	Somatic	MLH1/PMS2 loss, MSI, <i>MLH1</i> methylation	–	–	–	–	SD	23	
10	Breast	Somatic	MLH1/PMS2 loss, <i>MLH1</i> not methylated	20.9	287	<i>JAK2</i> p.Tyr20Asn	8x	6+, 12, 9, 1	PR	23
11	CRC	Somatic	MLH1/PMS2 loss, <i>MLH1</i> methylation	65.9	1,036	<i>JAK1</i> p.Ala639Val	2x	12+, 6+, 9	SD	24
12	CRC	Somatic	MLH1/PMS2 loss	10.6	346	–	2x	6+, 12	SD	>68
13	CRC	Somatic	MLH1/PMS2 loss, <i>MLH1</i> methylation	58.6	912	<i>JAK1</i> p.Lys860fs	2x	6+, 12, 21, 9	PR	>69
14	Breast	Somatic	MLH1/PMS2 loss, <i>MLH1</i> not methylated	–	–	–	–	PR	>72	
15	CRC	Somatic	MLH1/PMS2 loss, MSI, <i>BRAF</i> ^{KG0E} , <i>MLH1</i> methylation	0.5	73	2x	1+, 8, 17, 18, 11	NE	NA	

Table 2. Tumour and biomarker details per patient of the MSI cohort (continued)

No.	Tumour type	Pre-enrolment		Baseline WGS			CD274 ^b	COSMIC signature ^c	CB	PFS
		Somatic or Lynch	MSI profile	MSI seq ^a	ML	JAK1 and/or JAK2 mutations				
16	CRC	Lynch	MSH2 mut	-	-	-	-	-	SD	36
17	EC	Somatic	MLH1/PMS2 loss, MLH1 methylation	37.7	798	JAK2 p.Lys1055Glu, JAK2 c.3291 + 8delT	4x	12+, 26+, 6	NE	NA
18	EC	Somatic	MLH1/PMS2 loss, MLH1 methylation	-	-	-	-	-	SD	>58
19	CRC	Somatic	MSI, MLH1 not methylated	-	-	-	-	-	PR	>49
20	CRC	Lynch	PMS2 mut, MLH1/PMS2 loss, MLH1 not methylated	57.7	1,048	-	2x	6+, 15, 1, 9	SD	48
21	CRC	Somatic	MLH1/PMS2 loss, MLH1 methylation	85.8	1,558	JAK1 p.Lys860fs	2x	6+, 12+, 15, 9	SD	39
22	GBM	Lynch	PMS2 mut, PMS2 loss, MSS	42.4	6,137	JAK1 p.Gln437His, JAK2 p.Ala586Thr	2x	14+, 1+, 15	PD	13
23	Duodenum	Somatic	MSH6 loss, MSI	35.6	1,425	JAK2 p.Arg158Gln	2x	6+, 1, 12, 9	PR	>63
24	CRC	Somatic	MLH1/PMS2 loss, BRAF ^{V600E}	46.0	1,048	JAK2 c.3291 + 8delT	2x	6, 14, 12	PR	>120
25	UCC	Lynch	MSH6 mut, MSH6 loss	7.2	637	-	2x	1+, 6+	PD	5
26	Prostate	Lynch	MSH6 mut	-	-	-	-	-	SD	>98
27	Prostate	Somatic	MSI	12.0	543	-	3x	1+, 6+, 12	PD	15
28	CRC	Somatic	MLH1/PMS2 loss	60.4	820	-	2x	-	PD	6
29	CRC	Somatic	MSH2/MSH6 loss	-	-	-	-	-	SD	>51
30	EC	Somatic	MLH1/PMS2 loss	39.3	387	JAK1 p.Pro430fs, JAK1 c.2115 + 1G>A	2x	6+, 12+	NE	NA

The EMA has not yet approved checkpoint inhibitors for the MSI indication. However, on the basis of these DRUP data, the Dutch Health Care Institute and insurance agencies have now embraced a pay-for-performance model for this and future successful cohorts from the DRUP. This not only creates access to these drugs for patients with rare tumour profiles, but also allows further confirmation of clinical benefit in a larger cohort of patients²⁰.

Another immunotherapy cohort—pembrolizumab treatment for patients with microsatellite-stable colorectal cancer, with a tumour mutational load of between 140 and 290 (which corresponds to 11–22 mutations per megabase)—showed limited clinical benefit in stage I, and was therefore closed (Extended Data Table 6). Together, these two cohorts illustrate the potential for the DRUP to identify subgroups of patients who may benefit from a broader use of approved drugs, and to prevent unnecessary treatment in other subgroups.

Upon enrolment, the DRUP mandated a fresh baseline tumour biopsy for WGS. Baseline WGS results were used for the confirmation of previously identified variants, and for exploratory biomarker analyses. In the first 215 patients, baseline WGS was successfully performed in 131 patients (61%); the main reason for failure was insufficient tumour cells in the baseline biopsy (Extended Data Figure 3). The variant on the basis of which patients were included was confirmed in 121 patients (92%) with successful baseline WGS. Notably, in 112 patients (85%) with baseline WGS, potentially relevant additional information was revealed (Supplementary Table 1). This information included high mutational load, variants associated with therapy response or resistance, and variants that were potentially actionable with experimental or off-label agents (other than the current treatment that the patient was receiving in the DRUP). The latter may lead to re-enrolment upon failure of the first treatment administered to the patient in the DRUP.

Some limitations of the DRUP should be taken into account. One important caveat is the absence of comparator groups, owing to the non-randomized trial design. With the increasing availability of large, clinically and molecularly annotated databases, this may be addressed by methodologies such as trials within cohorts. Another concern is that, in a heterogeneous study population such as that of the DRUP, the correct interpretation of molecular aberrations is challenging. Fortunately, we were able to draw upon previous experiences with a much larger cohort²¹: we combined three large repositories of knowledge—‘Clinical Interpretation of Variants in Cancer’ (CIViC)²², ‘Precision Oncology Knowledge Base’ (OncoKB)²³ and ‘Cancer Genome Interpreter’ (CGI)²⁴. We also followed the ‘European Society for Medical Oncology (ESMO) Scale for Clinical Actionability of molecular Targets’ (ESCAT)²⁵ wherever possible.

The efficacy endpoints bear additional, inherent limitations²⁶: the objective response rate can detect tumour growth (or reductions in size) but cannot detect reductions in the rate of growth. By contrast, survival statistics cannot differentiate between a true effect of the treatment and a naturally slow growth rate. The progression-free-survival ratio (in which each patient

serves as their own control) might be able to overcome some of these challenges, but has its own limitations (as pre-study progression-free-survival data are collected retrospectively).

Taken together, the DRUP shows the feasibility of performing precision medicine in multiple, parallel cohorts driven by tumour type and tumour profile. It provides a framework through which patients with all types of tumours are able to acquire access to existing targeted therapies and immunotherapies, and in which treatment outcomes are monitored and publicly reported. This improves on current practice, in which individual physicians obtain anticancer drugs ‘off label’ for their patients without subsequent public reporting of clinical outcomes. The public availability of these data is especially relevant given recent concerns that the increasingly widespread use of genetic profiling could escalate the demand for off-label treatment²⁷. Furthermore, the importance of publicly reporting negative results cannot be underestimated, as it prevents patient exposure to ineffective agents with all their accompanying toxicities and financial costs. Another important advantage of the DRUP is that it enables the rapid incorporation of new drugs and scientific insights into clinical practice: matching rules can be adapted quickly, and cohorts based on new biomarkers may be opened almost instantaneously. In addition, our use of WGS identified many potentially actionable variants that were not identified by smaller gene panels, immunohistochemistry and/or in-situ hybridization. Eventually, WGS may thus identify more, or more-appropriate, treatment options for each patient. An integral part of our approach is a tiered review process that includes reviews of the literature and by multidisciplinary boards of experts, before patients are enrolled. This prevents the prescription of anticancer drugs when negative clinical data are available, or when the actionability of the variant is unknown or unlikely. Finally, our study design and informed consent both enable the sharing of data internationally. By combining cohorts from similar international studies, we will improve our knowledge of rare subsets of cancer, and the outcomes of their treatment. Most importantly, our approach shows that existing anticancer drugs may have value beyond their approved indications, which potentially expands the range of patients who may benefit from their use.

METHODS

The DRUP is a national, prospective, non-randomized multi-drug and multi-tumour study, designed and conducted on behalf of the Center for Personalized Cancer Treatment (CPCT) (clinicaltrials.gov: NCT02925234). The trial was approved by the Medical Ethical Committee of the Netherlands Cancer Institute in Amsterdam, and was conducted in accordance with good clinical practice guidelines and the Declaration of Helsinki’s ethical principles for medical research. Written informed consent was obtained from all study subjects. Patients were accrued at multiple hospitals throughout the Netherlands, and followed for 30 days after end of study treatment, or death, respectively, for toxicity and survival analyses. Figure 1 provides a schematic overview of the study design.

PATIENT POPULATION

Patients who were eligible for the study had an advanced or metastatic solid tumour, multiple myeloma or B cell non-Hodgkin lymphoma, and had exhausted standard-treatment options. A tumour genetic or protein-expression test (CPCT or regular diagnostics) had to have revealed a potentially actionable variant, for which FDA- and/or EMA-approved targeted therapy was available—but not for the tumour type in question. In addition, patients were required to be ≥ 18 years of age, with acceptable organ function and performance status (Eastern Cooperative Oncology Group (ECOG) score ≤ 2), and to have objectively evaluable disease of which a fresh baseline tumour biopsy could safely be obtained. For every study drug, further drug-specific selection criteria applied.

MATCHING RULES

Upon case submission, the study team attempted to match each patient to the appropriate study treatment (Extended Data Figure 1), according to pre-defined matching rules (Extended Data Table 1). For matching purposes, a potentially actionable molecular variant was defined following a previous publication²⁸, as either one of the following options: (1) the variant is the target of an approved drug for any cancer indication, or is known to predict sensitivity to an approved drug for any cancer indication; (2) the variant is in the same molecular pathway, but located upstream of the target of an approved drug for any cancer indication, and has been reported as an oncogenic or pathogenic mutation; (3) mutations that result in unique susceptibility to a specific molecular intervention (such as *BRCA1* and *BRCA2* mutations and PARP inhibitors, or MSI and PD-1 inhibitors); and (4) other variants that have appropriate justification for selection on the basis of published scientific evidence regarding their susceptibility to specific targeted therapies.

If multiple variant–drug matches could be made for one patient, the drug with the highest level of evidence was selected unless there was a rationale (such as drug intolerance) that justified selecting an agent with a lower level of evidence. Levels of evidence were adapted from a previous publication²⁸ and were defined as: the drug met a clinical endpoint (objective response, PFS or overall survival) in a prospective trial, in patients with the same variant and tumour type, and has not yet received regulatory approval for use in the tumour type of the patient (level 1); clinical studies have demonstrated an association between presence of the variant and drug activity against the tumour type of the patient (level 2); the drug is commercially available in the US and/or European Union (EU) for use in another tumour type that contains the same variant (level 3); and preclinical evidence of anti-tumour activity and target inhibition in model systems of the tumour type of the patient (level 4).

STUDY TREATMENT AND ASSESSMENTS

If a slot for a matching study treatment was available (to which the patient consented) the patient could be enrolled, if all drug-specific selection criteria were met. Once a fresh baseline tumour biopsy for biomarker analyses was obtained, the study treatment could be initiated. Treatment and follow-up were conducted according to the approved indication. All treat-

ment-related adverse events (following the Common Terminology Criteria for Adverse Events (CTCAE) version 4.03) of grade 3 or higher were documented. The response to the treatment was evaluated every 2 months (up to every 3 months for patients who remained in the study for ≥ 6 months), and classified by local investigators according to internationally accepted criteria for each tumour type²⁹⁻³³. The study treatment could continue until progressive disease (patients who were receiving immune-system-stimulating agents were permitted to continue treatment in case of pseudo-progression), unacceptable treatment-related toxicity, death, pregnancy, consent withdrawal or withdrawal from the study at the discretion of the investigator.

BASELINE TUMOUR BIOPSIES

A fresh, frozen tumour biopsy specimen was mandatory before treatment initiation (baseline biopsy had to be obtained ≤ 2 months before enrolment, and without any anticancer therapy within those ≤ 2 months), and was optional during and after study treatment. All biopsies were sent to the central sequencing institute of the CPCT (Hartwig Medical Foundation (HMF), Amsterdam, The Netherlands), together with a 10-ml blood sample to determine the background variation of the germline DNA of the patient. If the tumour-cell percentage was $\geq 30\%$ and the DNA yield was ≥ 300 ng, WGS and biomarker analyses were performed.

The WGS data and treatment details were stored in a national centralized database (at the HMF). In addition, a sequencing report was returned to the local principal investigator and could be used to re-assess eligibility if a patient progressed on initial study treatment. As the baseline biopsy was obtained after enrolment, the baseline WGS results did not affect the initiation of the study treatment. For each patient, a unique patient identification number was generated by the electronic case-report file system. This number was used by the study team and external researchers for data and sample collection and analysis, and could be tracked back to the individual patient only by the local sub-investigator.

In addition to a summary of somatic variants across cancer-related genes, the sequencing report contained information regarding complex molecular features of the tumour, including the mutational load and microsatellite instability. The tumour mutational load represents the total number of somatic missense variants across the protein-coding region of the tumour genome. The microsatellite (in)stability score represents the number of somatic insertions and deletions in short repeat sections across the tumour genome per megabase. This metric can be considered as a good marker for instability in microsatellite repeat regions³⁴, and has extensively been validated against the standard MSI-PCR assay used in routine practice (data not shown).

COHORT DESIGN

The study comprised multiple parallel cohorts, each defined by one histologic tumour type, one molecular tumour variant and one study treatment. For the purposes of cohort definition, the variant category was defined at the level of the gene or receptor that contains the

mutation, translocation, amplification, overexpression or homozygous deletion; for example, the *EGFR* mutant that was defined as the variant for purposes of cohort definition included all detected *EGFR* mutations.

The rate of clinical benefit for each treatment was analysed per cohort. Clinical benefit was defined as objective response, or absence of disease progression for ≥ 16 weeks (counted from treatment initiation until end of treatment or measurement of progressive disease, whichever came first), measured 2 or more times and ≥ 28 days apart (defined as a confirmed response). Per cohort, a rate of clinical benefit of $< 10\%$ was considered to be of no clinical interest. A rate of clinical benefit of $\geq 30\%$ was considered relevant and of sufficient interest to warrant further investigation. A Simon-like two-stage ‘admissible’ design¹⁵ was used for each cohort: in stage I, eight patients were enrolled. If no clinical benefit was observed in these first eight patients, the cohort was closed. Otherwise, 16 additional patients were enrolled. Cohorts with clinical benefit in ≤ 4 out of 24 patients were considered ineffective, whereas cohorts with clinical benefit in ≥ 5 patients were considered effective. This monitoring rule has 85% power and an α error rate of 7.8%. These operating characteristics were selected to represent a reasonable compromise between high power, low false-positive rates and a desire for small sample sizes, especially in stage I.

STUDY ENDPOINTS

The main study endpoints included (i) the percentage of submitted patients that started study treatment, and the main reasons for non-enrolment; (ii) the efficacy, including best overall response, response duration and rate of clinical benefit; and (iii) toxicity, including all treatment-related adverse events of grade 3 or higher. The sequencing-success rate of pre-treatment biopsies, and comparison of ‘historic’ and baseline tumour profiles formed an exploratory endpoint (endpoint iv). All endpoints were prospectively decided. For endpoint (i), all cases that were submitted for review were considered evaluable, and the reasons for non-enrolment were classified by two reviewers independently. For endpoint (ii), the best overall response was considered evaluable in patients who received at least one cycle of oral study medication or two cycles of intravenous study medication, and for whom response was radiologically or clinically evaluable (at the discretion of the treating physician). Clinical-benefit calculations included all enrolled patients, regardless of evaluability of the best overall response. All patients without clinical benefit had been followed for at least 16 weeks at the time of the analysis, so no censoring was necessary. All patients who received study treatment were considered evaluable for endpoint (iii), and all patients who were formally enrolled were considered evaluable for endpoint (iv).

STATISTICS

All statistical analyses were performed using R version 3.5.0 (<http://www.R-project.org/>). This trial was not randomized and investigators were not blinded to treatment allocation or outcome assessments. Patient characteristics, adverse events and tumour responses were summarized using descriptive statistics. In addition, a waterfall plot was used to illustrate

maximum tumour shrinkage compared to baseline sizes. Percentages were calculated with 95% confidence intervals using the Clopper–Pearson method. Kaplan–Meier methods were used to estimate overall survival (calculated from the first day of treatment administration to the date of death from any cause, censoring patients who were alive at the final follow-up), PFS (from the start of treatment to progression or death from any cause, whichever came first, and censoring patients who were alive without progression at final follow-up and time on treatment (censoring patients who had not finished treatment at the time of analysis).

ACKNOWLEDGEMENTS

We thank the Barcode for Life Foundation and the Dutch Cancer Society for their financial support; Amgen, Astra Zeneca, Bayer, Boehringer Ingelheim, Bristol-Myers Squibb, Eisai, Merck Sharp and Dohme, Novartis, Pfizer and Roche for their in-kind and financial support; the HMF for their in-kind support by performing sequencing and biomarker analyses on baseline biopsies; the Center for Personalized Cancer Treatment Multidisciplinary Expert Board for supporting the central case-review process; the Independent Data Monitoring Committee for their advice on cohort decisions and the monitoring of preliminary safety data; the Netherlands Cancer Institute's Biobank Facility, Scientific Department and Pharmacy for their facilitating services; A. P. Hamberg, L. V. Beerepoot and J. M. Meerum-Terwogt for their contributions to trial recruitment; and all participating hospitals for supporting and facilitating the conduct of the DRUP trial.

REFERENCES

1. Hainsworth, J.D., *et al.* Targeted Therapy for Advanced Solid Tumors on the Basis of Molecular Profiles: Results From MyPathway, an Open-Label, Phase IIa Multiple Basket Study. *Journal of Clinical Oncology* **36**, 536-+ (2018).

2. Hyman, D.M., *et al.* HER kinase inhibition in patients with HER2-and HER3-mutant cancers. *Nature* **554**, 189-194 (2018).

3. Hyman, D.M., *et al.* Vemurafenib in Multiple Nonmelanoma Cancers with BRAF V600 Mutations. *New Engl J Med* **373**, 726-736 (2015).

4. Colwell, J. NCI-MATCH Trial Draws Strong Interest. *Cancer Discov* **6**, 334-334 (2016).

5. Massard, C., *et al.* High-Throughput Genomics and Clinical Outcome in Hard-to-Treat Advanced Cancers: Results of the MOSCATO 01 Trial. *Cancer Discov* **7**, 586-595 (2017).

6. Meric-Bernstam, F., *et al.* Feasibility of Large-Scale Genomic Testing to Facilitate Enrollment Onto Genomically Matched Clinical Trials. *Journal of Clinical Oncology* **33**, 2753-U2761 (2015).

7. Stockley, T.L., *et al.* Molecular profiling of advanced solid tumors and patient outcomes with genotype-matched clinical trials: the Princess Margaret IMPACT/COMPACT trial. *Genome Med* **8**(2016).

8. Hyman, D.M., Taylor, B.S. & Baselga, J. Implementing Genome-Driven Oncology. *Cell* **168**, 584-599 (2017).

9. Le Tourneau, C., *et al.* Molecularly targeted therapy based on tumour molecular profiling versus conventional therapy for advanced cancer (SHIVA): a multicentre, open-label, proof-of-concept, randomised, controlled phase 2 trial. *Lancet Oncol* **16**, 1324-1334 (2015).

10. Prasad, V. The precision-oncology illusion. *Nature* **537**, S63-S63 (2016).

11. Tannock, I.F. & Hickman, J.A. Limits to Personalized Cancer Medicine. *New Engl J Med* **375**, 1289-1294 (2016).

12. Sleijfer, S., Bogaerts, J. & Siu, L.L. Designing Transformative Clinical Trials in the Cancer Genome Era. *Journal of Clinical Oncology* **31**, 1834-+ (2013).

13. Ellis, L.M., *et al.* American Society of Clinical Oncology Perspective: Raising the Bar for Clinical Trials by Defining Clinically Meaningful Outcomes. *Journal of Clinical Oncology* **32**, 1277-+ (2014).

14. Bins, S., *et al.* Implementation of a Multicenter Biobanking Collaboration for Next-Generation Sequencing-Based Biomarker Discovery Based on Fresh Frozen Pretreatment Tumor Tissue Biopsies. *Oncologist* **22**, 33-40 (2017).

15. Simon, R. Optimal 2-Stage Designs for Phase-Ii Clinical-Trials. *Control Clin Trials* **10**, 1-10 (1989).

16. Jung, S.H., Lee, T., Kim, K. & George, S.L. Admissible two-stage designs for phase II cancer clinical trials. *Stat Med* **23**, 561-569 (2004).

17. Garcia, V.M., *et al.* Dose-Response Relationship in Phase I Clinical Trials: A European Drug Development Network (EDDN) Collaboration Study. *Clinical Cancer Research* **20**, 5663-5671 (2014).

18. Le, D.T., *et al.* PD-1 Blockade in Tumors with Mismatch-Repair Deficiency. *New Engl J Med* **372**, 2509-2520 (2015).

19. Overman, M.J., *et al.* Nivolumab in patients with metastatic DNA mismatch repair-deficient or microsatellite instability-high colorectal cancer (CheckMate 142): an open-label, multicentre, phase 2 study. *Lancet Oncol* **18**, 1182-1191 (2017).

20. van Waalwijk van Doorn-Khosrovani, S.B., *et al.* Personalised reimbursement: a risk-sharing model for biomarker-driven treatment of rare subgroups of cancer patients. *Ann Oncol* (2019).

21. Priestley P, B.J., Lolkema M, *et al.* Pan-cancer whole genome analyses of metastatic solid tumors. *bioRxiv* (2018).

22. Griffith, M., *et al.* CIViC is a community knowledgebase for expert crowdsourcing the clinical interpretation of variants in cancer. *Nat Genet* **49**, 170-174 (2017).

23. Chakravarty, D., *et al.* OncoKB: A Precision Oncology Knowledge Base. *Jco Precis Oncol* **1**(2017).

24. Tamborero, D., *et al.* Cancer Genome Interpreter annotates the biological and clinical relevance of tumor alterations. *Genome Med* **10**(2018).

25. Mateo, J., *et al.* A framework to rank genomic alterations as targets for cancer precision medicine: the ESMO Scale for Clinical Actionability of molecular Targets (ESCAT). *Ann Oncol* **29**, 1895-1902 (2018).

26. Sleijfer, S. & Wagner, A.J. The Challenge of Choosing Appropriate End Points in Single-Arm Phase II Studies of Rare Diseases. *Journal of Clinical Oncology* **30**, 896-898 (2012).

27. T, R. CMS-Proposed Coverage of NGS Cancer Tests Could Lead to Off-Label Scripts, Oncologists Worry, 360Dx. (NEW YORK, GenomeWeb, 2018).

28. Meric-Bernstam, F., *et al.* A Decision Support Framework for Genomically Informed Investigational Cancer Therapy. *Jnci-J Natl Cancer I* **107**(2015).

29. Cheson, B.D., *et al.* Recommendations for Initial Evaluation, Staging, and Response Assessment of Hodgkin and Non-Hodgkin Lymphoma: The Lugano Classification. *Journal of Clinical Oncology* **32**, 3059-+ (2014).

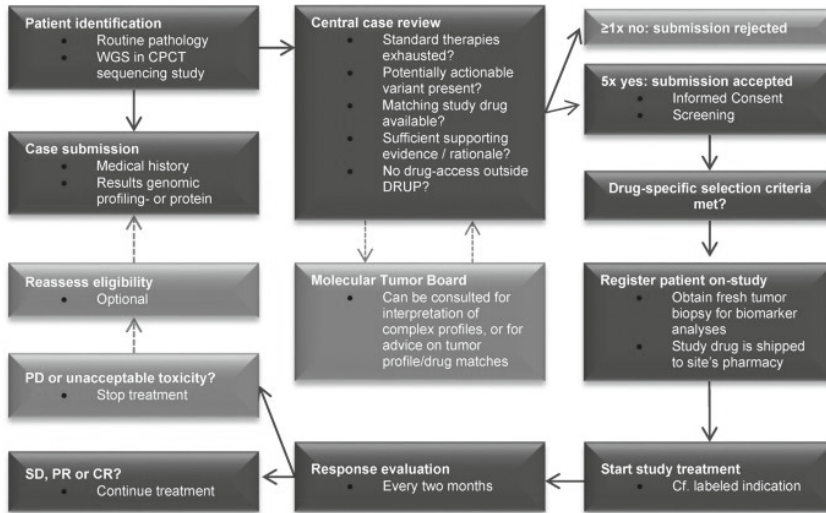
30. Rajkumar, S.V., *et al.* International Myeloma Working Group updated criteria for the diagnosis of multiple myeloma. *Lancet Oncol* **15**, E538-E548 (2014).

31. Rustin, G.J.S., *et al.* Definitions for Response and Progression in Ovarian Cancer Clinical Trials Incorporating RECIST 1.1 and CA 125 Agreed by the Gynecological Cancer Intergroup (GCIG). *Int J Gynecol Cancer* **21**, 419-423 (2011).

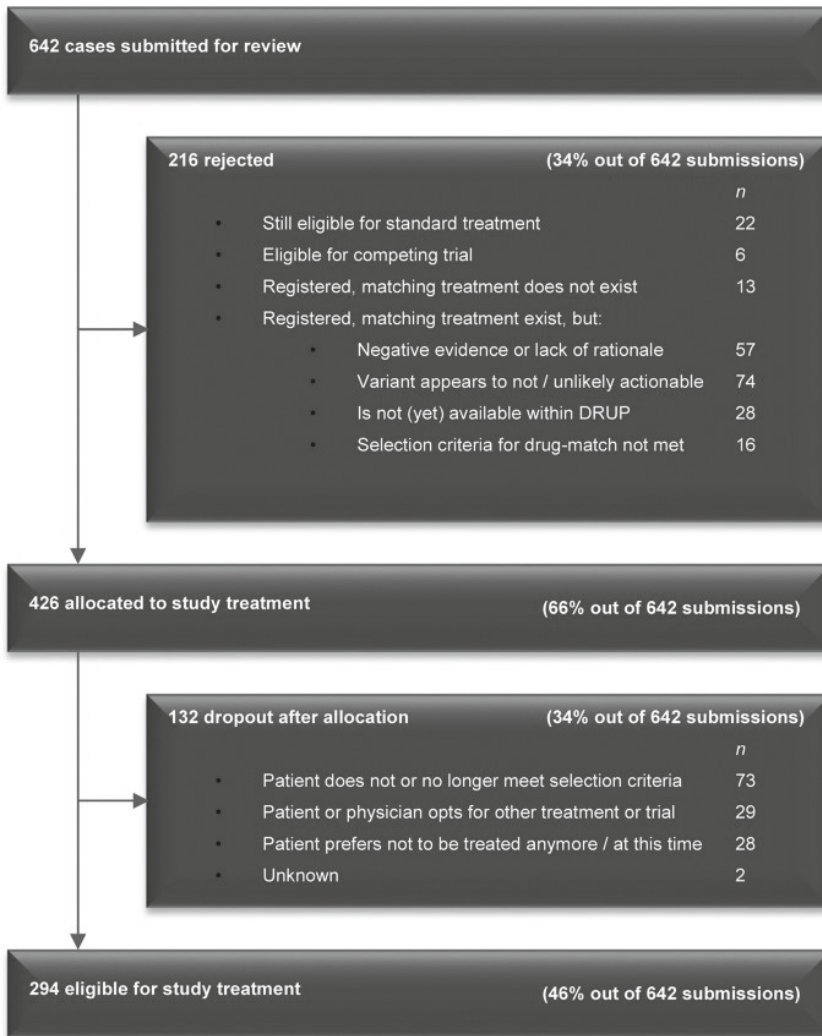
32. Therasse, P., *et al.* New guidelines to evaluate the response to treatment in solid Tumors. *J Natl Cancer I* **92**, 205-216 (2000).

33. Wen, P.Y., *et al.* Updated Response Assessment Criteria for High-Grade Gliomas: Response Assessment in Neuro-Oncology Working Group. *Journal of Clinical Oncology* **28**, 1963-1972 (2010).
 34. Huang, M.N., McPherson, J.R., Cutcutache, I., Teh, B.T., Tan, P. & Rozen, S.G. MSIseq: Software for Assessing Microsatellite Instability from Catalogs of Somatic Mutations. *Sci Rep-Uk* **5**(2015).
-

EXTENDED DATA FIGURES AND TABLES

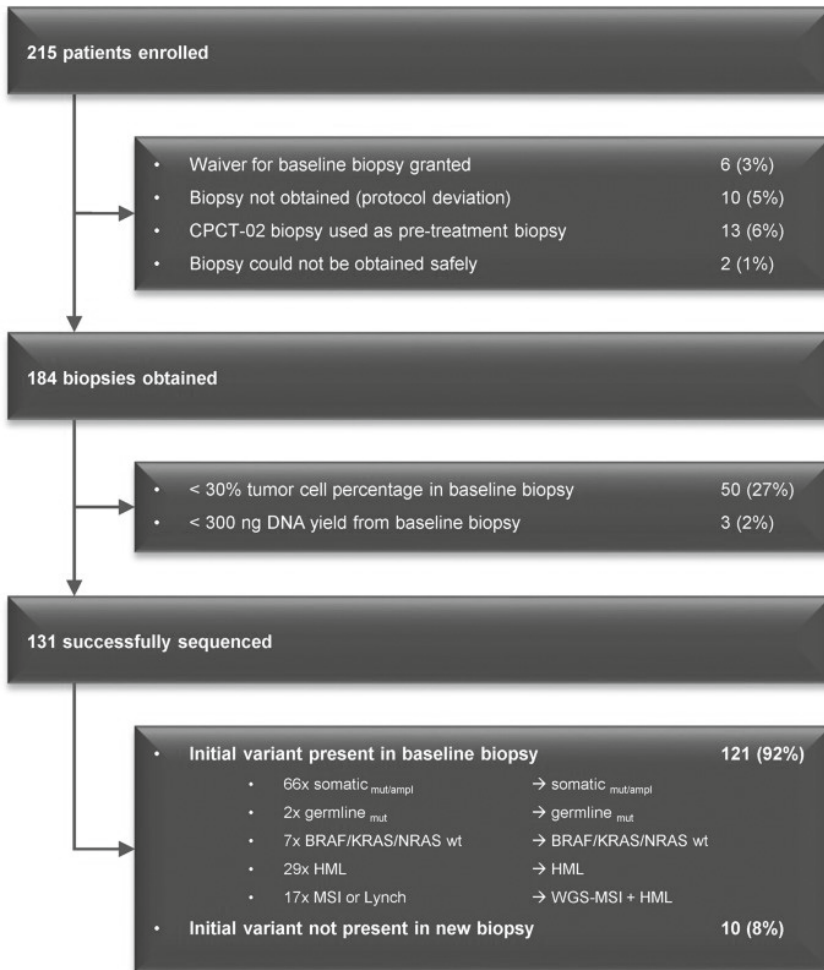
**Extended Data Figure 1.** Study flowchart

Patients may be identified via regular diagnostics or by WGS performed within the context of a CPCT sequencing study. Adult patients with advanced cancers and without standard-treatment options (but with a known potentially actionable variant in their molecular tumour profile) can be submitted for review. The central review is done by two or more reviewers independently, supported by the CPCT Molecular Tumour Board, and includes review of (i) the medical history of the patient, (ii) tumour-profiling test results, (iii) available literature and (iv) potential drug-access alternatives. Patients who are eligible for standard treatments are referred back to their treating physician. Genomic variants of unknown significance (VUS) that are not likely to be actionable are not considered acceptable drug targets. Negative trials are not repeated, nor are positive or ongoing phase II or III trials, unless drug access is not (or is not yet) facilitated. Drug access via other trials or access programmes is preferred, if available. Input for stages (iii) and (iv) of the review is derived from PubMed (<https://www.ncbi.nlm.nih.gov/pubmed/>), ClinicalTrials.gov and weekly automatic updates on publications that mention any drug in the study in their titles and/or abstracts. If the general selection criteria are met and the appropriate study treatment is available, the patient can be informed, screened and enrolled (if all drug-specific selection criteria are also met). Once a fresh baseline tumour biopsy is obtained, study treatment can be initiated. Patients are treated and followed according to the labelled indication for each drug. Response is evaluated once every two months. Patients can continue study treatment as long as clinical benefit is observed. Patients who discontinue study treatment can be resubmitted if their molecular tumour profile (as revealed by the baseline biopsy) contains additional actionable variants. CR, complete response, PR, partial response.



Extended Data Figure 2. Case submissions and reasons for non-accrual.

Overview of the first 642 case submissions (submitted between 1 September 2016 and 1 September 2018), as well as the reasons for not being enrolled in the study. Values are displayed as a percentage relative to these 642 case submissions, and as an absolute number per category. Cases that were erroneously submitted (owing to incomplete understanding of the study protocol and/or retraction of the submission by the treating physician) are not included in this overview ($n = 58$ cases).



2

Extended Data Figure 3. Baseline biopsies for biomarker analyses.

Overview and success rate of WGS on pre-treatment tumour biopsies. The bottom panel displays the number of patients for whom WGS succeeded, and indicates whether the initial variant (on the basis of which the patient started the study treatment) was also present in the fresh baseline biopsy. Values are displayed as absolute numbers and percentages, relative to the 131 successfully sequenced biopsies. CPCT-02, the national WGS programme of the CPCT; HML, high mutational load (defined as ≥ 140 somatic missense variants across the tumour genome overall); WGS-MSI, microsatellite instability suspected on the basis of WGS results; ampl, amplification; mut, mutation; wt, wild type.

■ **Extended Data Table 1.** Available drugs and matching rules

A list of the participating pharmaceutical companies, and the drugs that were available for this study. To be eligible for a given treatment, a patient needed to meet the description for the treatment that is marked with a + in this table (exclusion criteria are marked with -).

Supplier	Drug	Indications	Available
Amgen	Panitumumab	+ BRAF-KRAS-NRAS wild type tumors	September 2016
		- Patients eligible for on-label panitumumab and BRAF-KRAS-NRAS mutated tumors	
AstraZeneca	Olaparib	+ ATM, BARD1, BRCA1/2, BRIP1, CDK12, CHEK1/2, FANCL, PALB2, PP2R2A, RAD51B/C/D, RAD54L inactivating mutations	September 2016
		- Patients eligible for on-label olaparib or for the MEDIOLA, POLO, PROFOUND, REVIVAL or SUBITO trial.	
Bayer	Regorafenib	+ BRAF, CSF1(R), FLT1/4, KDR, KIT, PDGFRβ, RAF1, RET activating mutations, amplifications, fusion or overexpression	September 2016
Boehringer Ingelheim	Afatinib	- Patients eligible for on-label regorafenib	
		+ ERBB4 activating mutations or NRG1 activating mutations or fusions in non-small cell lung cancer	September 2017
Bristol-Myers Squibb	Nivolumab	- All tumor types and profiles not fulfilling the subscription above	
		+ High mutational load or micro-satellite instable tumors, with MLH1, MSH2/6 or PMS2 mutations or non-expression	September 2016
Eisai	Lenvatinib	- Patients eligible for on-label nivolumab	
		+ FGFR1/2/3/4 activating mutations, amplifications or fusions	October 2017
Merck Sharp & Dohme	Pembrolizumab	- Patients eligible for on-label lenvatinib	
		+ High mutational load tumors	September 2017
		- Patients eligible for on-label pembrolizumab and multiple myeloma	
Novartis	Dabrafenib	+ BRAF V600D/E/K/R activating mutations	September 2016
		- Patients eligible for on-label dabrafenib or for the ROAR trial, and tumors with MAP2K1/2 or NRAS mutations	
	Nilotinib	+ ABL1, KIT, PDGFRα, PDGFRβ activating mutations	September 2016

■ **Extended Data Table 1.** Available drugs and matching rules (continued)

Supplier	Drug	Indications	Available
Pfizer	Trametinib	- Patients eligible for on-label nilotinib, or for the SUSTRENUM or NAUT trial + MAP2K1/2/4, MAP3K1 or NRAS activating mutations	November 2016
	Axitinib	- Patients eligible for on-label trametinib or for the KRAS trial + FLT1/4 or KDR activating mutations, amplifications or overexpression	October 2017
	Crizotinib	- Patients eligible for on-label axitinib + ALK, MET, MST1R, ROS1 activating mutations, amplifications, fusions or overexpression	October 2017
	Sunitinib	- Patients eligible for on-label crizotinib, and tumors with known ALK-resistance mutations + CSF1R, FGFR1/2/3, FLT1/3/4, KDR, KIT, PDGFR α / β , RET, activating mutations, amplifications, fusions or overexpression	October 2017
	Palbociclib	- Patients eligible for on-label sunitinib, and tumors with KIT D842V mutations + CCND1, CDK4(R24)/6, FLT3, PIK3R4, GSK3b activating mutations, amplifications or overexpression. CDKN2A inactivating mutations.	August 2018
	Erlotinib	- Patients eligible for on-label palbociclib. + EGFR activating mutations or exon 19 deletions in the region E746_E759	September 2016
	Trastuzumab and pertuzumab	- Patients eligible for on-label erlotinib, and tumors with known EGFR-resistance mutations + ERBB2 activating mutations, amplifications exon 20 insertions or overexpression	September 2016
	Vemurafenib and cobimetinib	Patients eligible for on-label trastuzumab + pertuzumab or for the KAMELEON trial - BRAF V600D/E/K/R activating mutations Patients eligible for on-label vemurafenib + cobimetinib, and tumors with MAP2K1/2 or NRAS mutations	September 2016
	Vismodegib	+ PTCH1 activating mutations	September 2016
		- Patients eligible for on-label vismodegib, and tumors with known SMO-resistance mutations or with GLI2 amplification	

■ **Extended Data Table 2.** Opened cohorts

Overview of cohorts that have been opened for the first 215 patients who started study treatment. For each cohort cell in the table, the tumour type is indicated in top line, the tumour profile is indicated in the middle line and the number of evaluable or enrolled patients is indicated in bottom line. All patients were required to be refractory or intolerant to standard therapies. ACUP, adenocarcinoma of unknown primary; amp, amplification; cholangio, cholangiocarcinoma; esoph, oesophageal cancer; esthesioneurobl, esthesioneuroblastoma; fus, fusion; GIST, gastrointestinal stromal tumour; HML, high mutational load (defined here as the sum of all somatic missense variants across the protein-coding region of the tumour genome); HNSCC, head and neck squamous cell carcinoma; HRR, homologous recombination repair; hydradeno., hidradenocarcinoma; IMT, inflammatory myofibroblastic tumour; NEC, neuro-endocrine carcinoma; NSCLC, non-small-cell lung cancer; pre-specified indicates breast, gastric, ovarian, pancreatic, prostate and small-cell lung cancer pre-specified for olaparib.

*Three cohorts have been closed for enrolment. The dabrafenib + trametinib cohort for NSCLC with BRAF mutation has been closed because this treatment is now registered and reimbursed for this indication. The nivolumab–MSI cohort has completed stage I as well as stage II and is thus closed for further inclusion: the overall clinical benefit rate was 67%. The pembrolizumab cohort of patients with colorectal cancer with a high mutational load (140 to 290) has completed stage I. As no patient experienced clinical benefit, the cohort has been closed and will not be graduated to stage II. All other cohorts with >8 evaluable patients have been graduated to stage II, as clinical benefit was observed once or more in stage I.

Treatment	Cohorts (incl. tumor type, tumor profile, and number of evaluable/enrolled patients)			
Axitinib	CRC			
	FLT1 _{amp}			1/1
Crizotinib	Cholangio	CRC	IMT	
	ALK _{mut}	MET _{amp}	ALK _{fus}	1/1
Dabrafenib Trametinib	NSCLC*			
	BRAF _{mut}			0/1
Dabra-fenib	GBM	UCC		
	BRAF _{mut}	BRAF _{mut}		1/1
Lenvatinib	Anal	Breast	CRC	Sarcoma
	FGFR3 _{mut}	FGFR2	FGFR2 _{amp}	FGFR1 _{amp}
	0/1	2/3	1/1	1/1
				0/1

Extended Data Table 2. Opened cohorts (continued)

Treatment	Cohorts (incl. tumor type, tumor profile, and number of evaluable/enrolled patients)	
Nilotinib	GIST	Mesothelioma
	KIT _{mut} 7/8	PDGFRα _{mut} 1/1
Nivolumab	All	All*
	HML _{>450} 15/16	MSI 29/30
	All	All
Olaparib	ATM _{mut} 7/8	HRR _{def} 2/2
	BRCA1/2 _{mut} 11/12	HRR _{def} 3/3
Panitumumab	Carcinosarcoma	Pre-specified
	RAF/RAS _{wt} 1/1	HNSCC RAF/RAS _{wt} 1/1
	Cervical RAF/RAS _{wt} 1/1	Melanoma RAF/RAS _{wt} 1/1
		Meningeoma RAF/RAS _{wt} 1/1
		NSCLC EGFR _{mut} RAF/RAS _{wt} 1/1
	Salivary RAF/RAS _{wt} 1/1	Thyroid RAF/RAS _{wt} 1/1
	Sarcoma RAF/RAS _{wt} 3/3	CRC* HML ₁₄₀₋₂₉₀ 8/10
Pembrolizumab	All	HNSCC
	HML _{>290} 4/7	HML ₁₄₀₋₂₉₀ 2/3
Regorafenib	Esthesioneurobl.	Melanoma
	RET _{fus} 1/1	KIT _{mut} 1/1
Sunitinib	Thymus	Prostate
	KIT _{mut} 1/1	PDGFRα _{mut} 1/1
		Stomach/esoph. HML ₁₄₀₋₂₉₀ 3/4
		Other HML ₁₄₀₋₂₉₀ 3/4

Extended Data Table 2. Opened cohorts (continued)

Treatment	Cohorts (incl. tumor type, tumor profile, and number of evaluable/enrolled patients)						
Trametinib	ACUP	Cervical	CRC	NEC	NSCLC	NSCLC	
	MAP3K1 _{mut} 1/1	MAP3K1 _{mut} 1/1	MAP2K4 _{mut} 1/1	MAP3K1 _{mut} 1/1	MEK1 _{mut} 3/3	NRAS _{mut} 2/2	
	Ovarian						
	NRAS _{mut} 1/1						
Trastuzumab	Bladder	Cervical	Cholangio	CRC	CRC	Hydradeno.	
	ERBB2 _{amp} 2/2	ERBB2 _{amp} 2/2	ERBB2 _{amp} 1/1	ERBB2 _{amp} 7/7	ERBB2 _{mut} 0/1	ERBB2 _{amp} 1/1	
Pertuzumab	NSCLC	NSCLC	Ovarian	Salivary	Vulva		
	ERBB2 _{amp} 5/6	ERBB2 _{mut} 13/15	ERBB2 _{mut} 1/1	ERBB2 _{amp} 3/4	ERBB2 _{amp} 1/1		
Vemurafenib	ACUP	Ovarian	Thyroid				
	BRAF _{mut} 1/1	BRAF _{mut} 2/2	BRAF _{mut} 2/2				
Cobimetinib							
Vismodegib	Sarcoma						
	PTCH1 _{mut} 1/1						

■ **Extended Data Table 3.** Rates of response and clinical benefit

Rates of clinical benefit and response in the first 215 patients who started study treatment. Clinical benefit is defined as a complete or partial response or absence of disease progression at ≥ 16 weeks; it must be measured 2 or more times ≥ 28 days apart (defined as a confirmed response). Given that 29 patients had ongoing clinical benefit at the time of analyses, the actual mean duration is expected to exceed the current mean duration. The reasons for early withdrawal from study (other than progressive disease) included death (n = 9 patients), adverse events (n = 5 patients), patient preference (n = 3 patients) or were unknown (n = 7 patients).

		<i>n</i>	In total, over 215 patients	Median duration in months (95% CI)
Clinical benefit	Complete response (confirmed)	1		
	Partial response (confirmed)	32	34%	9 (8 – 11)
	Stable disease ≥ 16 weeks (confirmed)	41		
No clinical benefit	Stable disease <16 weeks / non-confirmed stable disease only	117	66%	
	Early study withdrawal, for other reasons than progressive disease	24		

■ **Extended Data Table 4.** Adverse events in the first 215 patients

Rates of clinical benefit and response in the first 215 patients who started study treatment. Clinical benefit is defined as a complete or partial response or absence of disease progression at ≥ 16 weeks; it must be measured 2 or more times ≥ 28 days apart (defined as a confirmed response). Given that 29 patients had ongoing clinical benefit at the time of analyses, the actual mean duration is expected to exceed the current mean duration. The reasons for early withdrawal from study (other than progressive disease) included death (n = 9 patients), adverse events (n = 5 patients), patient preference (n = 3 patients) or were unknown (n = 7 patients).

Adverse event	Grade 3	Grade 4	Grade 5
Abdominal infection			1
Abscess	2		
Adrenal insufficiency	1		
AF \uparrow	5		
ALT \uparrow	3		
AST \uparrow	6		
Amylase \uparrow	1		
Anal fistula or ulcer	2		
Anemia	8		
Arteritis	1		
Atrioventricular block	1		

■ **Extended Data Table 4.** Adverse events in the first 215 patients (continued)

Adverse event	Grade 3	Grade 4	Grade 5
Bacterial peritonitis		1	
Baseline biopsy-related bleeding	1		
Bile duct stenosis	2		
Bilirubin ↑	4		
Bleeding	3		
Blindness		1	
Cauda equina syndrome	1		
Cholangitis	1		
Cholecystolithiasis	1	1	
Delirium	1		
Diarrhea	3		
Duodenal Perforation			1
Dyspnea	8		2
Encephalopathy	1	1	
Ejection fraction ↓	1		
Fatigue	4		
Fever	2		
Flu like symptoms	2		
GGT ↑	16	1	
Gastro-enteritis	2		
General malaise	1		
Hepatic impairment	2		
Hip Fracture	1		
Hydronephrosis	2		
Hypercalcemia	1	1	
Hypertension	8		
Hypoalbuminemia	1		
Hyponatremia	3		
Hypophosphatemia	1		
Hypotension	1		
Hypoxia	1		
Infusion related reaction	1		
LDH ↑	1		
Lymphocyte count ↓	2		
Muscle weakness	1		
Nausea	4		

■ **Extended Data Table 4.** Adverse events in the first 215 patients (continued)

Adverse event	Grade 3	Grade 4	Grade 5
Pain	15		
Partial paralysis	1		
Peripheral sensory neuropathy	1		
Pleural effusion	2		
Pneumonia	3		
Pneumonitis		1	
Rectal perforation			1
Seizure	1		
Skin rash or infection	5		
Somnolence	1		
Syncope	1		
Tachycardia	1		
Thromboembolic event	3		
Urea ↑	1		
Vomiting	1		

■ **Extended Data Table 5.** Adverse events in the MSI cohort

All reported adverse events of grade 3 or higher that were (or could possibly be) attributed to treatment with nivolumab. Grades are given according to CTCAE version 4.03. a, For each adverse event, the number of patients is displayed in whom it was reported at grade 3, 4 or 5 as the highest grade. Upward-pointing arrows indicate an increase. b, The number of patients who had any grade 3 or higher, grade 4 or higher, or grade 5 or higher adverse event as their highest-grade adverse event is displayed. The denominator of the percentages is the total number of patients who started study treatment (n = 30 patients). Given that every patient could be counted only once per column in b, the numbers in b are not a summation of the numbers in a.

A. Adverse event	Grade 3	Grade 4	Grade 5
Abdominal infection			1
Abscess	1		
Adrenal insufficiency	1		
Alkaline phosphatase ↑	1		
Anal fistula	1		
Anemia	1		
Aspartate aminotransferase ↑	1		
Atrioventricular block	1		
Dyspnea			1
Fatigue	2		
Fever	1		

■ **Extended Data Table 5.** Adverse events in the MSI cohort (continued)

A. Adverse event	Grade 3	Grade 4	Grade 5
Gastric hemorrhage	1		
GGT ↑	2	1	
Hypertension	3		
Hypoalbuminemia	1		
Hypotension	1		
Nausea	3		
Serum amylase ↑	1		
Urinary tract obstruction	1		
Vomiting	1		

B. Any adverse event	Grade ≥3	Grade ≥4	Grade ≥5
<i>n</i>	14	2	2
% (95% CI)	46.7% (28.3 – 65.7%)	6.7% (0.8 – 22.1%)	6.7% (0.8 – 22.1%)

■ **Extended Data Table 6.** Treatment with pembrolizumab in the cohort of patients with MSS colorectal cancer with a high mutational load (between 140 and 290)

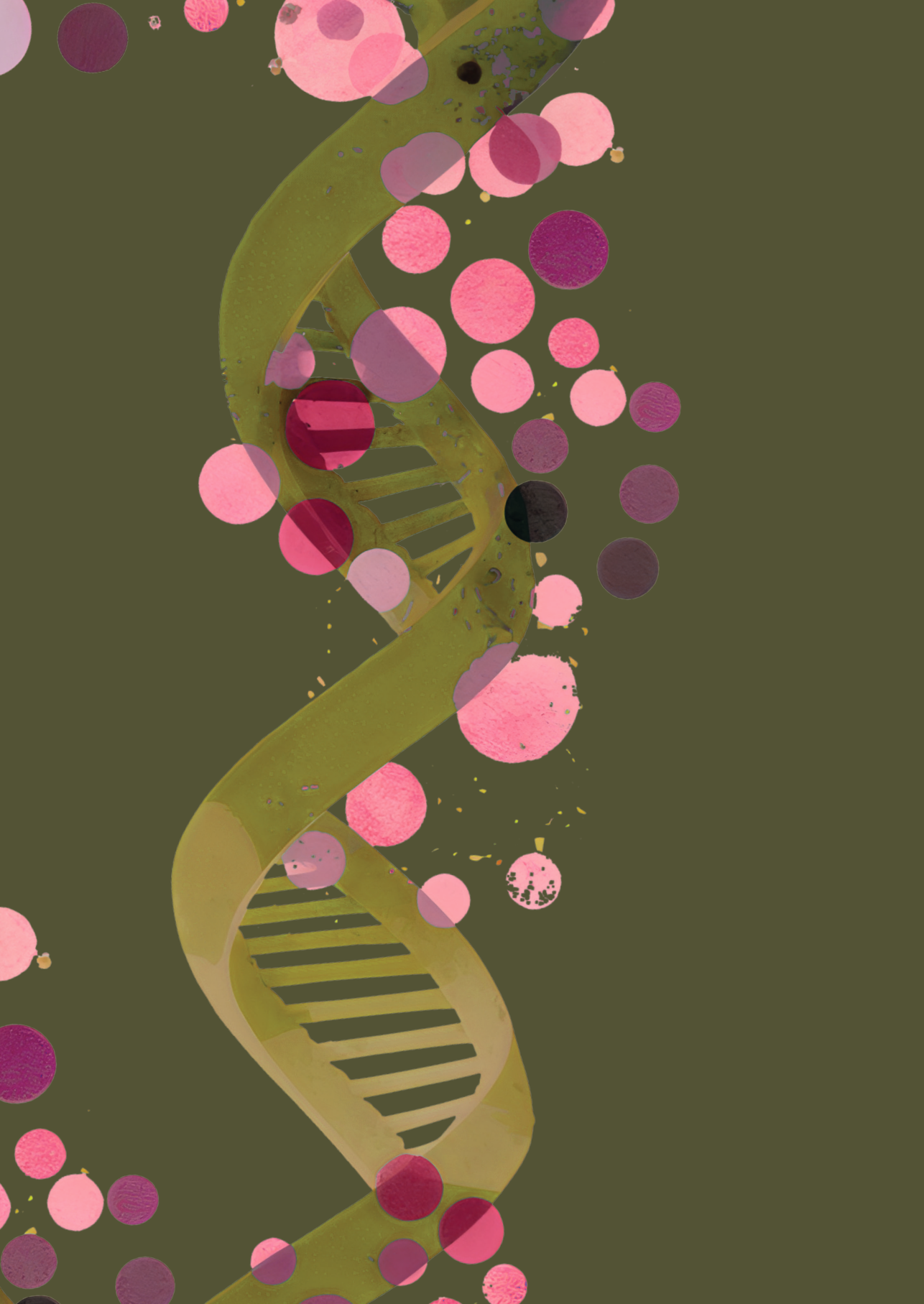
Overview of baseline characteristics and clinical benefit in ten patients who were treated within the cohort ‘pembrolizumab for patients with colorectal cancer with a high mutational load (between 140 and 290)’. Clinical benefit is defined as complete or partial response or absence of disease progression at ≥16 weeks. The reasons for early withdrawal from the study (other than progressive disease) included death ($n = 1$ patient) or adverse event ($n = 1$ patient), and were classified as having no clinical benefit.

<i>n = 10</i>		
Gender		
Male	9	90%
Female	1	10%
Age (approximately at consent)		
Median (range)	65	(59 – 71)
WHO Performance Status		
WHO 0	4	40%
WHO 1	6	60%
Number of prior systemic therapies		
Median (range)	4	(2 – 10)
Mutational load		
Median (range)	189	(149 – 215)
Clinical Benefit		
Yes	0	0%
No	10	100%

SUPPLEMENTARY INFORMATION

Supplementary Table 1 is available at Nature <https://www.nature.com/articles/s41586-019-1600-x#Sec13>

This table summarizes the molecular tumour profile of all enrolled patients for whom WGS data were available and the potentially relevant additional WGS findings per patient.





CHAPTER 3

Patients with Biallelic BRCA1/2 Inactivation Respond to Olaparib Treatment Across Histologic Tumor Types

*Hanneke van der Wijngaart, Louisa R Hoes, J Maxime van Berge Henegouwen,
Daphne L van der Velden, Laurien J Zeverijn, Paul Roepman, Erik van Werkhoven, Wendy W J de Leng,
Anne M L Jansen, Niven Mehra, Debbie G J Robbrecht, Mariette Labots, Derk Jan A de Groot,
Ann Hoeben, Paul Hamberg, Hans Gelderblom, Emile E Voest, Henk M W Verheul*

ABSTRACT

Purpose: To assess the efficacy of olaparib, a PARP inhibitor (PARPi) in patients with tumors with *BRCA1/2* mutations, regardless of histological tumor type.

Patients and methods: Patients with treatment-refractory *BRCA1/2* mutated cancer were included for treatment with off-label olaparib 300 mg twice daily until disease progression or unacceptable toxicity. In DRUP, patients with treatment-refractory solid malignancies receive off-label drugs based on tumor molecular profiles while whole genome sequencing (WGS) is performed on baseline tumor biopsies. The primary endpoint was clinical benefit (CB, defined as objective response or stable disease \geq 16 weeks according to RECIST 1.1). Per protocol patients were enrolled using a Simon-like two-stage model.

Results: Twenty-four evaluable patients with nine different tumor types harboring *BRCA1/2* mutations were included, 58% had CB from treatment with olaparib. CB was observed in patients with complete loss of function (LoF) of *BRCA1/2*, while 73% of patients with bi-allelic BRCA LoF had CB. In 17 patients with – and seven without current labeled indication, 10 and four patients had CB respectively. Treatment resistance in four patients with bi-allelic loss might be explained by an additional oncogenic driver which was discovered by WGS, including Wnt pathway activation, *FGFR* amplification and *CDKN2A* loss, in three tumor types.

Conclusion: These data indicate that PARPi is a promising treatment strategy for patients with non-BRCA associated histologies harboring bi-allelic *BRCA* LoF. WGS allows to accurately detect complete LoF of *BRCA* and HRD signature as well as oncogenic drivers that may contribute to resistance, using a single assay.

INTRODUCTION

Homologous recombination repair (HRR) is a crucial DNA repair pathway, essential for the repair of DNA double strand breaks (DSB)¹ that the genome is continuously subjected to². It allows for error-free restoration of DNA integrity and sequence, even when the genomic damage is extensive. The breast cancer susceptibility genes *BRCA1* and *BRCA2* are two of the most extensively studied tumor suppressor genes and are key players in the HR pathway³. Deleterious alterations in *BRCA1* or *BRCA2*, both germline⁴⁻⁶ and somatic^{7,8}, result in deficient homologous recombination repair (dHRR)^{9,10} and a high risk of developing cancer. dHRR due to bi-allelic loss of function (LoF) mutations in *BRCA1* or *BRCA2* is seen in 4.9% of patients with cancer across tumor types¹¹⁻¹³.

Tumor cells with dHRR can be specifically targeted by drugs inducing multiple DNA strand breaks. Inhibitors of poly(ADP-ribose) polymerase (PARP) specifically target the weakness of dHRR tumor cells¹⁴⁻¹⁶ by synthetic lethality^{17,18} leading to selective cytotoxicity and apoptosis.

Olaparib, an oral inhibitor of *PARP1*, is approved by the Food and Drug Administration (FDA) and European Medicines Agency (EMA) for several indications, among which the maintenance treatment of ovarian, fallopian tube and primary peritoneal cancer with germline or somatic *BRCA* mutations after response to first line platinum-based chemotherapy and, irrespective of *BRCA*-status, for recurrent ovarian, fallopian tube and primary peritoneal cancer after response to platinum-based chemotherapy. Olaparib was most recently approved as monotherapy for patients with metastatic castration-resistant prostate cancer with germline or somatic *BRCA* mutations (EMA) and mutations in other homologous repair deficiency (HRD) genes (FDA)¹⁹⁻²¹. Several other PARP inhibitors have been registered for the treatment of epithelial ovarian, fallopian tube and primary peritoneal cancer (rucaparib²², niraparib²³) and gBRCAm breast cancer (talazoparib)²⁴.

The majority of the phase II-III clinical trials performed focused on efficacy of PARPi monotherapy in *BRCA*-associated cancer types, often only based on the presence of a germline *BRCA* mutation, and lacking detailed biomarker information such as confirmation of bi-allelic *BRCA* LoF in tumor tissue. Data on the effectivity of PARPi in patients with somatic *BRCA* mutations are scarce.

In the Drug Rediscovery Protocol (DRUP, NCT02925234)²⁵ patients are being treated based on their tumor molecular profile with registered targeted treatments outside their labeled indications, systematically recording efficacy and safety data. Moreover, the DRUP creates opportunities for extensive biomarker analysis by performing whole genome sequencing (WGS) on baseline tumor biopsies. Within DRUP, we initiated a cohort in which patients were treated with olaparib based on a germline or somatic *BRCA1* or *BRCA2* loss of function (LoF) genomic event. Patients with a malignancy for which olaparib was not available as standard treatment were considered for this cohort. We hypothesized that a PARPi may be an effective

treatment option for patients with malignant tumors harboring *BRCA12* LoF mutations, both germline and somatic, independent of histology.

Here, we show that PARPi is a potentially effective treatment strategy for patients with complete LoF of *BRCA1/2* in the DRUP cohort of 24 patients “*Olaparib for tumors with a BRCA1/2 mutation*”. The importance of WGS, performed on baseline biopsies, is demonstrated by the correlation between complete LoF of *BRCA1/2* and clinical benefit from olaparib. WGS provides information on both germline and somatic mutations, and genomic mutational signatures, allowing for optimal patient selection using a single assay.

PATIENTS AND METHODS

STUDY DESIGN

The Drug Rediscovery Protocol (DRUP) is an ongoing prospective, multicenter, non-randomized basket trial in which patients with advanced solid malignancies are being treated based on their tumor molecular profile, with targeted- or immunotherapy outside their registered indications²⁵. The basket trial design allows for an unlimited number of parallel cohorts consisting of patients with the same histological tumor type, molecular target (defined at gene level) and study drug. Patients enrolled in the histology-agnostic cohort “*Olaparib for tumors with a BRCA1 or BRCA2 mutation*” received olaparib tablets 300 mg twice daily²⁶ in 28-day cycles until occurrence of disease progression or intolerable side effects. Dose reductions were allowed up to a minimum dose of 200 mg twice daily. Patients were enrolled in nine out of the 32 DRUP-participating hospitals in the Netherlands, between September 2016 and October 2019. To date, accrual in other cohorts of the DRUP is still ongoing.

This study is registered with ClinicalTrials.gov, number NCT02925234.

PATIENTS

Adult patients with advanced solid malignancies, for which standard treatment options were exhausted, and with no option for on-label or phase III study treatment with PARPi, were enrolled. Expansion of the reimbursed indications of olaparib during the course of the trial resulted in exclusion of patients with the new “on-label” histologies from that moment on. Patients with those histologies who were already enrolled in DRUP were not excluded, but continued treatment within the trial and were included in the efficacy analysis. Pre-enrollment, patients needed to have a pathogenic, inactivating *BRCA1* or *BRCA2* mutation or deletion confirmed in their tumor tissue, identified using any validated genetic test within the context of routine diagnostics or using WGS in the context of the Dutch CPCT-02 study²⁷. At the start of the trial, confirmation of bi-allelic LoF of *BRCA* was not a requirement for eligibility yet. During the course of the trial, literature emerged reporting on the importance of complete LoF for response to PARP inhibitors. Therefore, we added *bi-allelic* LoF of *BRCA* as a second requirement for eligibility in this cohort. In all submitted cases, the variant was reviewed

by two independent clinical molecular biologists, assessing the actionability of the variant. Actionable variants were homozygous deletions and inactivating bi-allelic somatic mutations or inactivating germline mutations with LOH. They advised the study team on the driver likelihood, after which the decision to include the patient was made by the study team.

For this cohort in DRUP, the general DRUP in- and exclusion criteria applied²⁵. Additionally, patients were not eligible if they had previously been treated with a PARP inhibitor, if they were immunocompromised or if they had features suggestive of myelodysplastic syndrome (MDS) or acute myeloid leukemia (AML). Patients were considered evaluable for the primary endpoint if at least one cycle of olaparib was completed. Non-evaluable patients were excluded for the efficacy analysis, but included in the safety analysis.

The study is conducted in accordance with the International Conference of Harmonization of Good Clinical Practice and the Declaration of Helsinki, and was approved by the independent ethics committee and by the institutional review boards in every participating hospital. Patients provided written informed consent upon enrollment.

STUDY ENDPOINTS

The primary end point of this study is the clinical benefit rate (CBR), defined as confirmed complete or partial response or stable disease for 16 weeks or more, according to RECIST 1.1 and measured at least twice, at least 28 days apart in a particular cohort. Tumor response was reported by the local investigator in the electronic case record form (eCRF).

Tumor assessments were done at baseline and after every second treatment cycle. If patients were on treatment ≥ 6 months, tumor assessments were performed after every three cycles. Secondary endpoints include: objective response rate (ORR, defined as partial or complete response), duration of response, progression free survival (PFS), overall survival (OS) and treatment related CTCAE grade ≥ 3 adverse events. Exploratory endpoints include biomarker analysis on fresh frozen tumor biopsies.

Safety is assessed by documentation of serious and study treatment-related grade ≥ 3 adverse events according to CTCAE v.4.03, and followed up until one month after the last dose of study drug. Safety within the trial is monitored by an Independent Data Monitoring Committee (IDMC) who is blinded for response rates per cohort during accrual.

STATISTICAL ANALYSIS

Cohorts are monitored using a Simon-like two-stage “admissible” monitoring plan^{28,29} to identify cohorts with evidence of activity. Clinical benefit (CB) of $\geq 30\%$ is considered of sufficient clinical interest to warrant further study in a confirmatory expansion cohort (stage III within the DRUP³⁰). The cohorts are evaluated in a two-stage design, if there would be 0 patients with CB in the first 8 participants in the cohort, the cohort would be closed. Otherwise, an additional 16 patients would be included in the cohort. Four or fewer patients with CB out of

24 would suggest a lack of (clinically meaningful) activity, while five or more patients with CB would suggest that further investigation of the drug in the tumor/variant cohort is warranted. The null hypothesis and alternative hypothesis to be tested are defined as CBR of 10% versus $\geq 30\%$. This monitoring rule has 85% power to reject the null hypothesis of a CBR of 10% when the true CBR is 30%, with a one-sided alpha error rate of 7.8%. Exact 95% confidence intervals (CI) were calculated using the Clopper-Pearson method.

BASELINE TUMOR BIOPSIES AND BIOMARKER ANALYSIS

At baseline, a new fresh frozen tumor biopsy was obtained from each patient. Biopsies were harvested and collected by the participating hospitals and sent to the Hartwig Medical Foundation (HMF), Amsterdam, The Netherlands), together with a 10-ml blood sample to determine the background variation of the germline DNA of the patient. For WGS, a minimum tumor cell percentage of 30% is required. A 6- μm section was collected for haematoxylin and eosin (H&E) staining and estimation of tumor cellularity by an experienced pathologist. If the sample tumor cellularity was $\geq 30\%$ and the DNA yield was ≥ 300 ng, WGS was performed.

WGS data were analyzed using an optimized, high-quality bioinformatic pipeline³¹, and per patient a summarizing report of all relevant findings was created, including information on tumor purity, ploidy, somatic variants, copy number variations, mutational load, and more complex genomic features such as gene fusions, COSMIC mutational signatures³² and microsatellite (in) stability. A Classifier of HOMologous Recombination Deficiency (CHORD) for pan-cancer HRD detection, as recently developed by HMF, was computed for each sample, hereafter referred to as “HRD-score”³³. Bi-allelic status of point mutations and the driver likelihood were assessed as described in previously published work³¹. All code and scripts used for analysis of the WGS data are available at GitHub (<https://github.com/hartwigmedical/>).

Before biomarker analysis was performed, all WGS samples (baseline study samples and pre-enrollment WGS samples) were re-analyzed using the most recent HMF bioinformatics pipeline, including computation of the HRD-score for each sample. The investigators and an independent clinical molecular biologist reviewed the baseline biopsy WGS results and confirmed presence of the qualifying BRCA mutation, assessed bi-allelic status of BRCA LoF and explored other identified oncogenic driver alterations. In cases where no baseline WGS data were available (i.e. failed sequencing due to low tumor cellularity), the call for bi-allelic or mono-allelic BRCA LoF was made based on the pre-enrollment molecular data. If pre-enrollment WGS data was available, a HRD-score was computed from that sample. Recent reports show a high spatiotemporal preservation of genomic driver alterations³⁶ which justifies this approach.

ROLE OF FUNDING SOURCE

This Investigator Initiated study receives funding from the Dutch Cancer Society (KWF), Barcode for Life and receives equal funding from a number of pharmaceutical companies, among which AstraZeneca. WGS was performed free of charge at HMF. Study medication was made available free of charge by the manufacturer.

AstraZeneca had no role in the design or execution of the study and no influence on the study report.

RESULTS

ACCRUAL IN THE COHORT “OLAPARIB FOR TUMORS WITH A BRCA1 OR BRCA2 MUTATION”

Between September 2016 and November 2019, 68 patients with advanced cancer harboring a *BRCA1* or *BRCA2* alteration, who had exhausted standard treatment options, were submitted to the study team for evaluation for potential study participation in the cohort “Olaparib for tumors with a *BRCA1* or *BRCA2* mutation”. Forty-five patients were approved by the study team to be screened for treatment with olaparib, 18 patients were ineligible for study participation (Supplementary Figure 1). Twenty-seven patients with nine tumor types were found eligible and started study treatment, of which the majority (41%, $N=11$) had prostate cancer. Nineteen patients were included despite their current labeled indication (prostate ($N=11$), breast ($N=3$), ovarian ($N=3$) and pancreatic cancer ($N=2$)), since at the time of enrollment PARPi treatment was still off-label and not reimbursed for their tumor type. Patients had a median number of four prior lines of systemic treatment (Table 1, Supplementary Table 1). The regimens varied greatly due to the different tumor types enrolled. Fifteen of 27 patients were treated with a platinum-containing regimen (carboplatin ($N=11$), oxaliplatin ($N=3$) and cisplatin ($N=1$)). Seven patients who were previously platinum resistant had clinical benefit of olaparib treatment. Three patients were not evaluable for the primary endpoint according to our protocol definition of evaluability and were excluded in the efficacy analysis (two had clinical progression and rapid deterioration (within 4 weeks) before finishing the first complete cycle, one patient suffered from intolerable side effects and stopped study treatment after six days). All 27 patients who received at least 1 dose of study medication were included in the safety analysis. Baseline characteristics are presented in Table 1. Twenty-four patients were evaluated in the efficacy analysis. From here on, only the results and characteristics of these 24 patients are described.

Table 1. Baseline characteristics of the 27 patients enrolled in the cohort “Olaparib for tumors with a BRCA1 or BRCA2 mutation”.

*All patients were required to have exhausted standard therapies, but six patients refused standard chemotherapy due to fear of toxicity. In addition, occasionally the treating physician had well-argued reasons to refrain from certain standard therapies (i.e. low response rate to standard therapies in specific patient subgroups). Abbreviations: WHO = World Health Organization.

	<i>n</i> = 27	
Gender		
Male	17	63%
Female	10	37%
Age (approximately at consent)		
Median (range)	57	(37 – 79)

Table 1. Baseline characteristics of the 27 patients enrolled in the cohort “Olaparib for tumors with a BRCA1 or BRCA2 mutation” (continued)

<i>n</i> = 27		
WHO Performance Status		
WHO 0	7	26%
WHO 1	18	67%
Not available	2	7%
Primary tumor types		
Prostate cancer	11	41%
Breast cancer	4	15%
Pancreatic cancer	3	11%
Ovarian cancer	2	7%
Colorectal cancer	2	7%
Cholangiocarcinoma	2	7%
Renal cell carcinoma	1	4%
Adrenal gland carcinoma	1	4%
Endometrial cancer	1	4%
Number of prior systemic therapy lines		
Median (range)	4	(1 – 6)*

PRE-ENROLLMENT MOLECULAR CHARACTERISTICS

Seventeen patients were included based on a *BRCA2* mutation, and seven patients had a *BRCA1* mutation. In 14 of 24 patients, the *BRCA* alteration was discovered by WGS, performed as part of the Dutch CPCT-02 study²⁷. In five patients, the target was found using an NGS panel (smMIP and/or MLPA). Four patients were included based on a germline test only, and in one patient, a germline test combined with two functional HRD tests was performed. This patient with breast cancer had a germline mono-allelic *BRCA2* c.9104A>C mutation that was classified as a variant of uncertain significance. Functional characterization of this variant using embryonic stem cell complementation showed 50% reduction in HR functionality³⁷. Additionally, a Recombination Capacity (RECAP) test³⁸ showed negative RAD51 staining after ex vivo irradiation of the tumor tissue, which is highly suggestive of HRD. Based on these results, the study team granted a waiver to include the patient. Twelve patients had a germline *BRCA* mutation. Six of them also had a somatic event in *BRCA*, or LOH in tumor tissue, resulting in complete *BRCA* LoF. Twelve patients were included based only on somatic *BRCA* alterations. In six of them, complete LoF of *BRCA* was confirmed pre-enrollment or based on the baseline WGS data (Supplementary Table 1).

BASELINE BIOPSIES AND WGS RESULTS

Baseline study biopsies were performed in 22 out of 24 patients. For two patients, a biopsy was not possible for medical reasons. Thirteen (59%) biopsies were successfully sequenced.

Eight biopsies could not be sequenced due to a low tumor cellularity (< 30%) and one was sequenced despite a tumor cellularity below the threshold, confirming the qualifying *BRCA* mutation, but HRD-score and bi-allelic call could not be extracted (Supplementary Table 1).

From seven of 13 patients with successful baseline biopsy WGS, pre-enrollment WGS data were also available. Additionally, from eight patients with failed baseline study WGS, pre-enrollment WGS data were available, and from three patients no WGS data were available and information on bi-allelic status and HRD-score from these patients could not be retrieved. Based on a consensus of findings from the pre-enrollment and the baseline study biopsies, 15 out of 24 patients had confirmed bi-allelic *BRCA* LoF and a high HRD-score (Supplementary Table 1). In two patients with prostate cancer the call for bi-allelic loss could not be made due to low tumor purity, but in one of them, the high HRD-score suggests complete LoF of *BRCA2*. In six other patients, baseline WGS showed a low HRD-score and only mono-allelic loss ($N=4$) or no *BRCA* variant at all ($N=2$, 9%) (Supplementary Table 1).

CLINICAL BENEFIT

Fourteen of 24 patients (58%, 95% CI 37% - 78%) had CB upon treatment with olaparib. The objective response rate was 29% (7/24 patients), median time on treatment was 5.8 months (95% CI 1.8 - 9.2 months). At data cut-off (5 November 2020), one patient was still on treatment. The median PFS in this cohort was 7 months (95% CI 2-8 months) and the median OS was 13 months (95% CI 7 - NA months) (Figure 1). CB was observed across tumor types, including non-*BRCA* histologies such as cholangiocarcinoma, and in patients with both germline and somatic *BRCA* alterations (Figure 2, Supplementary Table 1). In the group of patients with CB, the median treatment duration was 9.1 months (95% CI 8.4 - NA months). The difference in outcome between bi-allelic LoF of *BRCA1* and *BRCA2* was not statistically significant (Fishers' exact value 0.2445).

CB was predominantly observed in patients with tumors harboring a bi-allelic LoF alteration of *BRCA1* or *BRCA2*, and with an HRD genomic signature, with few exceptions: one patient with prostate cancer had prolonged stable disease, while having no signs of genomic bi-allelic *BRCA* loss. The pre-enrollment molecular data showed a somatic *BRCA2* mutation with 24% variant allele frequency (VAF), while in the baseline study biopsy WGS data, no evidence of a *BRCA* alteration or HRD was found. As indicated before, the most likely cause of this discordance is tumor heterogeneity. It is known that patients with *BRCA*-associated tumor types can benefit from PARPi even if the tumor has only mono-allelic *BRCA* LoF¹³. Another possible explanation for the clinical benefit in this patient may be that the dominant tumor clone indeed had a *BRCA2* alteration, in combination with a post-translational silencing of *BRCA2*, resulting in functional HRD. CB was also observed in two patients whose details regarding bi-allelic LoF and HRD-score were unknown. Both patients had *BRCA* associated tumor types and were included based on a germline test only, with no WGS results available to confirm the target. None of the four patients with confirmed mono-allelic loss had CB. Of the fifteen patients with confirmed bi-allelic *BRCA1/2* LoF, eleven had CB (73%).

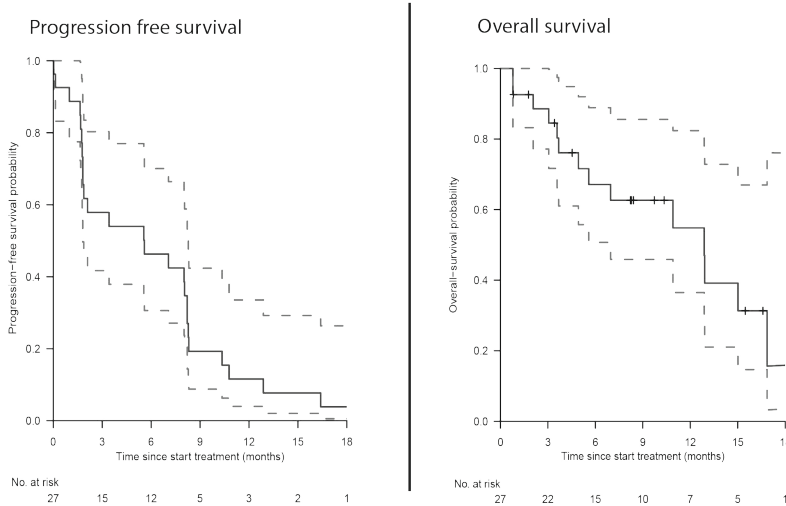


Figure 1. PFS and OS in the cohort “Olaparib for tumors with BRCA1/2 mutations”. Kaplan–Meier curves for estimated PFS (left) and OS (right), with 95% CI (dashed lines).

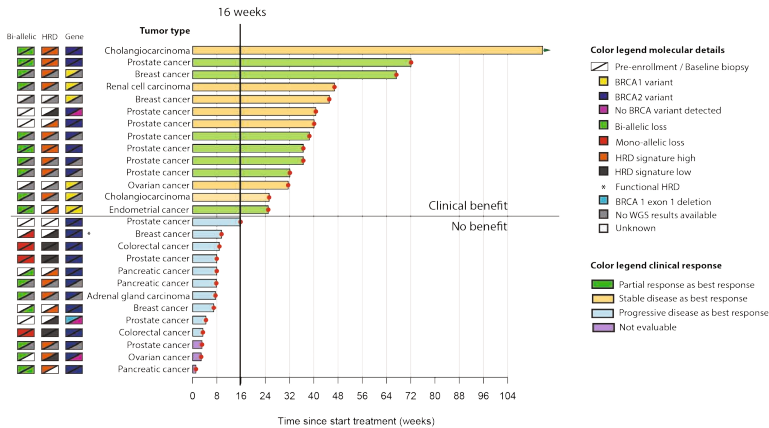


Figure 2. Treatment efficacy of olaparib in patients with tumors harboring BRCA1/2 alterations. Swimmer plot of the time on treatment (in weeks) for each patient (n = 27). Patients marked with an arrow were still on treatment (as per November 5th, 2020). On the left side of the figure, the molecular tumor profiles of preenrollment biopsies and DRUP baseline-study biopsies and the histologic tumor types are annotated.

NON-BRCA ASSOCIATED HISTOLOGIES

Seven patients in this cohort had non-*BRCA* associated tumor types. Of these, four (57%) had clinical benefit: two patients with cholangiocarcinoma, one with renal cell carcinoma and one with endometrial cancer. WGS data showed bi-allelic LoF of *BRCA* (Supplementary Table 1). Three patients with non-*BRCA* associated histologies had no benefit from olaparib. The WGS data from the two patients with colorectal cancer clearly showed no bi-allelic LoF of *BRCA* and

no evidence of HRD. This suggests that the *BRCA* mutations found in these patients are likely neutral passenger mutations and a consequence rather than a cause of tumorigenesis, in line with previous reports¹³. Both patients had *TP53*, *APC* and *KRAS* mutations and one also had a *SMAD4* mutation. One patient with adrenal gland carcinoma had bi-allelic *BRCA* LoF and HRD, however, a *CTNNB1* (β -catenin) p.Ser45Pro mutation was found, suggestive for WNT pathway activation, which is a known mechanism of PARPi resistance via N⁶-methyladenosine modification of *FZD10* mRNA, correlating with increased homologous recombination activity and reduced PARPi sensitivity³⁹. Additionally, this patient had a *TP53* mutation and *RB1* deletion (Supplementary Table 1).

LACK OF BENEFIT DUE TO OTHER DOMINANT NON-HRD MUTATIONAL PROCESSES

Apart from the patient with adrenal gland carcinoma described above, three other patients had no CB, despite having *BRCA*-associated tumor types, confirmed bi-allelic *BRCA* LoF and a high HRD-score. We analyzed WGS data to search for indicators of primary resistance to PARPi. In each patient, WGS analysis showed the presence of another (strong) oncogenic driver mutation that was not previously implied as possible PARPi resistance mechanism. One patient had breast cancer with an amplification (18 copies) of Fibroblast Growth Factor Receptor 1 (*FGFR1*), which is found in 6.9 - 19.7% of patients with metastatic breast cancer^{31,40} and has been reported as a possible driver alteration and potential therapeutic target in breast cancer⁴¹⁻⁴³. Another patient with pancreatic cancer had a homozygous loss of *CDKN2A* and a duplication of exon 3-6 of *TGFBR2*, likely leading to inactivation. *CDKN2A* (p16) is deleted or inactivated in 67% of patients with metastatic pancreatic cancer³¹. If expressed, it compromises efficient *BRCA1* dependent DNA repair⁴⁴ and it is associated with better radiosensitivity in vitro⁴⁵, while we hypothesize that the opposite may result in lower sensitivity to PARPi. Inactivation of *TGFRB2* may also contribute to decreased sensitivity to PARPi because active TGF β signaling in tumors enhances sensitivity to PARPi in vitro⁴⁶. In the third patient, also with pancreatic cancer, a *KEAP* p.Cys434* inactivating mutation, which is associated with drug resistance by regulation of expression of plasma membrane efflux pumps and detoxifying enzymes⁴⁷, and a *KRAS* p.Gly12Arg activating hotspot mutation were detected. In-vitro cell line data have indicated a role of *KRAS* mutation for PARPi resistance⁴⁸, but the clinical relevance remains uncertain. In all these patients, it is likely that the tumors were not dependent on *BRCA*, but rather on another dominant non-HRD mutational process.

SAFETY

Serious adverse events (SAE's) occurred in 37% of the enrolled patients (Table 2). No unexpected toxicity or CTCAE Grade ≥ 4 events were reported. Review of SAE's by the IDMC raised no safety concerns.

Table 2. Serious Adverse Events (SAEs): 16 SAE's occurred in 10 out of 27 patients. No grade ≥ 4 SAEs were reported. Grading according to Common Terminology Criteria for Adverse Events (CTCAE) 5.0.

Abbreviations: GGT = gamma glutamyltransferase.

SAE	Grade ≥ 3	
	No	%
Dehydration	1	3.7
Fatigue	2	7.4
Enterocolitis	1	3.7
Hydronephrosis	1	3.7
GGT increased	2	7.4
Spinal cord compression	1	3.7
Pain	2	7.4
Pneumonitis	1	3.7
Tachycardia	1	3.7
Anemia	1	3.7
Dyspnea	2	7.4
Pulmonary embolism	1	3.7

DISCUSSION

Precision medicine holds great promise for the future of patients with (advanced) cancer, but is hampered by many challenges, including target identification, prioritization and funding/reimbursement of biomarker identification and treatment, due to extremely low numbers of patients with similar molecular profiles. This makes established methods of randomized trials to generate solid evidence for determination of treatment benefit difficult. To circumvent this challenge, the innovative design of the DRUP allows evaluation of small groups of patients with rare cancer subtypes to determine the potential benefit of a targeted agent in a group of patients with a specific tumor molecular profile.

In patients with cancer harboring deleterious *BRCA1/2* mutations, regardless of histological tumor type, we here report that olaparib monotherapy is an effective and tolerable treatment option, for both germline and somatic alterations. The majority of patients (58%) derived CB from olaparib treatment. CB was almost exclusively observed in patients who had bi-allelic *BRCA* LoF and a high HRD-score, confirming the absence of a functional homologous repair system. Post hoc selection of only those patients with confirmed bi-allelic loss of *BRCA1/2* ($N=15$) revealed a CBR of 73% ($N=11$).

A considerable proportion of patients in this cohort had *BRCA*-associated tumor types (i.e. prostate, ovarian, breast and pancreatic cancer), of which we now know that olaparib is an effective treatment option⁴⁹⁻⁵³. Ten out of 15 evaluable patients with *BRCA*-associated histolo-

gies had CB, which may in part contribute to the success of the cohort. Seven of 24 patients had non-*BRCA* associated tumor types, of whom four (57%) had clinical benefit (Supplementary Table 1). These results indicate that patients with tumor types other than the known *BRCA* associated histologies can benefit from treatment with PARPi, provided that they have bi-allelic LoF of *BRCA*, resulting in HRD. It also emphasizes the importance of extensive molecular tumor profiling by means of WGS or large panel sequencing for all patients. Small tumor-specific sequencing panels would, in all seven patients in this cohort, not have identified the *BRCA* mutations, as *BRCA* diagnostics is not part of the regular reimbursed care for these tumor types.

An important limitation of this study is the small sample size of 24 patients. Nine different tumor types were enrolled in this histology-agnostic cohort, resulting in a heterogeneous population with large variations in biological tumor features and previous treatments. The number of patients per tumor type is low, there is a relative underrepresentation of patients with non-*BRCA* associated tumor types and since some important tumor types (i.e. non-Small Cell Lung Cancer) are not represented in our cohort, the results cannot simply be extrapolated to all patients with cancer. Though we find a clinically relevant signal of activity here, confirmation of our findings in a larger cohort is essential, with special emphasis on patients with non-*BRCA* tumor types.

Six patients ultimately did not have bi-allelic *BRCA* loss (mono-allelic loss: $N=4$; no *BRCA* variant: $N=2$). In two patients with prostate cancer, the qualifying *BRCA* variant could not be re-identified in the baseline biopsy WGS data, the exact reason for this discordance is unclear. No evidence for reversion of HRD (for example due to platinum-based chemotherapy) was found in the WGS data. A possible explanation in both cases could be inter- or intra-tumor heterogeneity. Alternatively, in the first patient the low VAF of 24% may suggest that *BRCA2* LoF was not the major driver of tumorigenesis and that the variant was lost in clonal evolution. However, the short time between pre-enrollment biopsy and baseline study biopsy did not support this. In the other patient with a *BRCA1* exon 1 deletion, an alternative explanation could be that the deletion of exon 1, which is located outside the open reading frame and contains the *BRCA1* promoter, could not be picked up by the bioinformatics pipeline. However, the low HRD-score suggests that there was no functional HRD, which points towards the more likely hypothesis of tumor heterogeneity. In three other patients, the information regarding bi-allelic status of *BRCA* could not be retrieved. In the early days of the trial, confirmation of complete LoF of *BRCA1* or *BRCA2* in this cohort may be considered a weakness but we regard it as an unintentional strength, as it underlines the importance of a sharply defined biomarker. Our data illustrate the contrast between the groups with and without complete LoF, in terms of CB to PARPi treatment (73% versus 17%). Clearly, this study is not powered to demonstrate a significant difference between these subgroups within the cohort due to the small number of patients. However, we noted this as an interesting signal that warrants confirmation in a larger independent cohort. Currently, pathologists and molecular biologists struggle to reliably call loss-of-heterogeneity and bi-allelic *BRCA* LoF using the available standard large

NGS panels. Experts are able to circumvent some of the struggles by adding a custom design of polymorphous single nucleotide polymorphisms (SNP's) around the *BRCA1/2* genes, but this requires experience and expertise that is not widely available yet, and an uncertainty margin remains when NGS panels are used, especially for samples with lower tumor percentages. Due to the reliable detection of tumor purities, WGS facilitates the diagnostic process by accurately informing physicians on tumor specific bi-allelic loss of function of *BRCA1/2* and HRD, as well as on the presence of additional mutations potentially causing resistance to PARPi, using a single assay. Prompt availability of this information allows for better patient selection for treatment with PARPi, preventing overtreatment of patients who will likely not benefit.

The availability of WGS data also allowed to explore possible reasons for unexplained lack of clinical benefit upon PARPi treatment in patients with HRD and bi-allelic *BRCA* LoF. As described, in the four patients who had no CB despite having a favorable HRD molecular profile, another dominant non-HRD mutational process was identified as possible explanation for the lack of benefit. Pan-cancer, it is known that tumors have a mean number of 5.7 candidate genomic driver events per patient³¹, likely occurring at different stages of tumor evolution. Some tumors may have multiple drivers occurring as early events in tumor development. In tumors with HRD, not responding to PARPi, one could also hypothesize that bi-allelic *BRCA* LoF and HRD may simply manifest as a consequence of genomic instability rather than being an early driving genomic event, especially in late stage cancers such as in our cohort. Although we did find potential underlying tumor biology contributing to resistance in these patients, it is still hypothetical and needs further investigation.

Although an association between clinical benefit from olaparib and platinum sensitivity has been described^{54,55}, we here found that platinum refractory tumors can still respond to PARPi treatment. Seven out of 12 patients previously treated with platinum-containing chemotherapy had CB upon olaparib treatment, one of them was primary resistant to carboplatin, which indicates that platinum-sensitivity alone may not be a good predictive biomarker for olaparib treatment outcome.

Baseline WGS was successfully performed on all biopsies that had sufficient tumor cellularity ($N=15$ (60%)). This is consistent with the overall WGS success rate within DRUP²⁵ and within the Dutch CPCT-02 study³¹. Currently, the minimum required tumor cellularity for clinical-grade WGS analysis has been further downscaled from 30% to 20% due to ongoing technical improvements and optimized data analysis (bioinformatics)⁵⁶, resulting in a current successful analysis of 71%⁵⁷.

The CBR observed in this cohort needs confirmation in a larger independent cohort. Currently, we are preparing an expansion cohort within DRUP. After the first example of a 3rd stage cohort “nivolumab for MSI tumors”, which is the first pilot of the new Dutch personalized reimbursement model that has been previously described³⁰, negotiations with the manufacturer, payers and health authorities are currently ongoing to work towards a second expansion cohort in

DRUP to study olaparib in *BRCA1/2*-mutated tumors. Based on our current findings and previous reports¹³, we have refined the qualifying biomarker to bi-allelic (somatic or germline) loss of function of *BRCA1* or *BRCA2*, and only off-label tumor types (non-*BRCA* histologies) will be eligible. In this expansion cohort, the financial risk will be shared between the manufacturer of olaparib and the insurance companies. For the first 16 weeks of treatment, the study drug is provided by the manufacturer. Upon confirmation of clinical benefit at 16 weeks, the subsequent treatment will be reimbursed by the health care insurance on an individual basis while efficacy and safety data collection continues to ultimately support expansion of the existing labeled indications of the drug.

CONCLUSION

Olaparib is an effective treatment option for patients with cancer harboring somatic and germline deleterious *BRCA1/2* alterations regardless of tumor type, who exhausted other treatment options. The CBR in this cohort was 58%, and CB was predominantly observed in patients harboring tumors with bi-allelic LoF of *BRCA* and HRD. In patients with non-*BRCA* associated tumor types, 57% had clinical benefit, suggesting PARPi as a promising treatment strategy and justifying a broad molecular diagnostic approach in all patients. In patients in this cohort who had complete LoF of *BRCA* and HRD in tumor tissue, but without clinical benefit of olaparib, another potential oncogenic driver was discovered by WGS. Further investigation and confirmation of this CBR in patients with non-*BRCA* histologies in an independent expansion cohort is warranted, and is currently in preparation within DRUP for patients with bi-allelic *BRCA* LoF.

ACKNOWLEDGMENTS

This Investigator Initiated study receives funding from the Dutch Cancer Society (KWF, grant number 10014/2016-1), Barcode for Life and receives equal funding from a number of pharmaceutical companies, among which AstraZeneca. Whole genome sequencing was performed free of charge at the Hartwig Medical Foundation. Study medication was made available free of charge by the manufacturer.

REFERENCES

1. Liang F, Han M, Romanienko PJ, Jasin M. Homology-directed repair is a major double-strand break repair pathway in mammalian cells. *Proc Natl Acad Sci U S A* 1998;95:5172-7.

2. Hoeijmakers JH. DNA damage, aging, and cancer. *N Engl J Med* 2009;361:1475-85.

3. Gudmundsdottir K, Ashworth A. The roles of BRCA1 and BRCA2 and associated proteins in the maintenance of genomic stability. *Oncogene* 2006;25:5864-74.

4. Foulkes WD, Knoppers BM, Turnbull C. Population genetic testing for cancer susceptibility: founder mutations to genomes. *Nat Rev Clin Oncol* 2016;13:41-54.

5. King MC, Marks JH, Mandell JB, New York Breast Cancer Study G. Breast and ovarian cancer risks due to inherited mutations in BRCA1 and BRCA2. *Science* 2003;302:643-6.

6. Nielsen FC, van Overeem Hansen T, Sorensen CS. Hereditary breast and ovarian cancer: new genes in confined pathways. *Nat Rev Cancer* 2016;16:599-612.

7. Cancer Genome Atlas Research N. Integrated genomic analyses of ovarian carcinoma. *Nature* 2011;474:609-15.

8. Robinson D, Van Allen EM, Wu YM, et al. Integrative clinical genomics of advanced prostate cancer. *Cell* 2015;161:1215-28.

9. Moynahan ME, Chiu JW, Koller BH, Jasin M. Brca1 controls homology-directed DNA repair. *Mol Cell* 1999;4:511-8.

10. Moynahan ME, Pierce AJ, Jasin M. BRCA2 is required for homology-directed repair of chromosomal breaks. *Mol Cell* 2001;7:263-72.

11. Riaz N, Bleuca P, Lim RS, et al. Pan-cancer analysis of bi-allelic alterations in homologous recombination DNA repair genes. *Nature Communications* 2017;8.

12. Levy-Lahad E, Friedman E. Cancer risks among BRCA1 and BRCA2 mutation carriers. *Br J Cancer* 2007;96:11-5.

13. Jonsson P, Bandlamudi C, Cheng ML, et al. Tumour lineage shapes BRCA-mediated phenotypes. *Nature* 2019;571:576-9.

14. Farmer H, McCabe N, Lord CJ, et al. Targeting the DNA repair defect in BRCA mutant cells as a therapeutic strategy. *Nature* 2005;434:917-21.

15. Gallmeier E, Kern SE. Absence of specific cell killing of the BRCA2-deficient human cancer cell line CAPAN1 by poly(ADP-ribose) polymerase inhibition. *Cancer Biol Ther* 2005;4:703-6.

16. Bryant HE, Schultz N, Thomas HD, et al. Specific killing of BRCA2-deficient tumours with inhibitors of poly(ADP-ribose) polymerase. *Nature* 2005;434:913-7.

17. Hartwell L. Theoretical biology. A robust view of biochemical pathways. *Nature* 1997;387:855, 7.

18. Kaelin WG, Jr. The concept of synthetic lethality in the context of anticancer therapy. *Nat Rev Cancer* 2005;5:689-98.

19. Mateo J, Carreira S, Sandhu S, et al. DNA-Repair Defects and Olaparib in Metastatic Prostate Cancer. *New Engl J Med* 2015;373:1697-708.

20. Mateo J, Porta N, Bianchini D, et al. Olaparib in patients with metastatic castration-resistant prostate cancer with DNA repair gene aberrations (TOPARP-B): a multicentre, open-label, randomised, phase 2 trial. *Lancet Oncol* 2019.

21. Hussain M MJ, Fizazi K, et al. PROfound: Phase 3 study of olaparib versus enzalutamide or abiraterone for metastatic castration-resistant prostate cancer with homologous recombination repair gene alterations. 2019.

22. Coleman RL, Oza AM, Lorusso D, Investigators A. Rucaparib maintenance treatment for recurrent ovarian carcinoma after response to platinum therapy (ARIEL3): a randomised, double-blind, placebo-controlled, phase 3 trial (vol 390, pg 1949, 2017). *Lancet* 2017;390:1948-.

23. Gonzalez-Martin A, Pothuri B, Vergote I, et al. Niraparib in Patients with Newly Diagnosed Advanced Ovarian Cancer. *New Engl J Med* 2019;381:2391-402.

24. Litton JK, Rugo HS, Ettl J, et al. Talazoparib in Patients with Advanced Breast Cancer and a Germline BRCA Mutation. *New Engl J Med* 2018;379:753-63.

25. van der Velden DL, Hoes LR, van der Wijngaart H, et al. The Drug Rediscovery protocol facilitates the expanded use of existing anticancer drugs. *Nature* 2019;574:127-31.

26. Pujade-Lauraine E, Ledermann JA, Selle F, et al. Olaparib tablets as maintenance therapy in patients with platinum-sensitive, relapsed ovarian cancer and a BRCA1/2 mutation (SOLO2/ENGOT-Ov21): a double-blind, randomised, placebo-controlled, phase 3 trial. *Lancet Oncol* 2017;18:1274-84.

27. Bins S, Cirkel GA, Gadellaa-Van Hooijdonk CG, et al. Implementation of a Multicenter Biobanking Collaboration for Next-Generation Sequencing-Based Biomarker Discovery Based on Fresh Frozen Pretreatment Tumor Tissue Biopsies. *Oncologist* 2017;22:33-40.

28. Jung SH, Lee T, Kim K, George SL. Admissible two-stage designs for phase II cancer clinical trials. *Stat Med* 2004;23:561-9.

29. Simon R. Optimal 2-Stage Designs for Phase-II Clinical-Trials. *Control Clin Trials* 1989;10:1-10.

30. van Waalwijk van Doorn-Khosrovani SB, Pisters-van Roy A, van Saase L, et al. Personalised reimbursement: a risk-sharing model for biomarker-driven treatment of rare subgroups of cancer patients. *Ann Oncol* 2019.

31. Priestley P, Baber J, Lolkema MP, et al. Pan-cancer whole-genome analyses of metastatic solid tumours. *Nature* 2019;575:210-+.

32. Forbes SA, Beare D, Boutselakis H, et al. COSMIC: somatic cancer genetics at high-resolution. *Nucleic Acids Res* 2017;45:D777-D83.

33. Nguyen L, Martens JWM, Van Hoeck A, Cuppen E. Pan-cancer landscape of homologous recombination deficiency. *Nature Communications* 2020;11.

34. Davies H, Glodzik D, Morganella S, et al. HRDetect is a predictor of BRCA1 and BRCA2 deficiency based on mutational signatures. *Nature Medicine* 2017;23:517-+.

35. Nguyen L, J WMM, Van Hoeck A, Cuppen E. Pan-cancer landscape of homologous recombination deficiency. *Nat Commun* 2020;11:5584.

36. Van De Haar J, Hoes LR, Roepman P, Cuppen E, Wessels LF, Voest EE. Genomic evolution of metastatic tumours under therapeutic pressure. *Ann Oncol* 2020;31:S274-S.

37. Shimelis H, Mesman RLS, Von Nicolai C, et al. BRCA2 Hypomorphic Missense Variants Confer Moderate Risks of Breast Cancer. *Cancer Research* 2017;77:2789-99.

38. Naipal KAT, Verkaik NS, Ameziane N, et al. Functional Ex Vivo Assay to Select Homologous Recombination-Deficient Breast Tumors for PARP Inhibitor Treatment. *Clinical Cancer Research* 2014;20:4816-26.

39. Fukumoto T, Zhu HR, Karakashev S, et al. The N6-Methylation of Adenosine (M6a) in Fzd10 Mrna Contributes to Resistance to Parp Inhibitor. *Clinical Cancer Research* 2019;25:204-.

40. Angus L, Smid M, Wilting SM, et al. The genomic landscape of metastatic breast cancer highlights changes in mutation and signature frequencies. *Nat Genet* 2019;51:1450-+.

41. Andre F, Bachelot T, Campone M, et al. Targeting FGFR with dovitinib (TKI258): preclinical and clinical data in breast cancer. *Clin Cancer Res* 2013;19:3693-702.

42. Brunello E, Brunelli M, Bogina G, et al. FGFR-1 amplification in metastatic lymph-nodal and haematogenous lobular breast carcinoma. *J Exp Clin Cancer Res* 2012;31:103.

43. Turner N, Pearson A, Sharpe R, et al. FGFR1 amplification drives endocrine therapy resistance and is a therapeutic target in breast cancer. *Cancer Res* 2010;70:2085-94.

44. Wang L, Zhang P, Molkenkine DP, et al. TRIP12 as a mediator of human papillomavirus/p16-related radiation enhancement effects. *Oncogene* 2017;36:820-8.

45. Molkenkine JM, Molkenkine DP, Bridges KA, et al. Targeting DNA damage response in head and neck cancers through abrogation of cell cycle checkpoints. *Int J Radiat Biol* 2020.

46. Liu L, Zhou W, Cheng CT, et al. TGFbeta induces "BRCAness" and sensitivity to PARP inhibition in breast cancer by regulating DNA-repair genes. *Mol Cancer Res* 2014;12:1597-609.

47. Singh A, Misra V, Thimmulappa RK, et al. Dysfunctional KEAP1-NRF2 interaction in non-small-cell lung cancer. *Plos Med* 2006;3:1865-76.

48. Sun CY, Fang Y, Yin J, et al. Rational combination therapy with PARP and MEK inhibitors capitalizes on therapeutic liabilities in RAS mutant cancers. *Science Translational Medicine* 2017;9.

49. de Bono J, Mateo J, Fizazi K, et al. Olaparib for Metastatic Castration-Resistant Prostate Cancer. *N Engl J Med* 2020.

50. Ledermann J, Harter P, Gourley C, et al. Olaparib maintenance therapy in platinum-sensitive relapsed ovarian cancer. *N Engl J Med* 2012;366:1382-92.

51. Moore K, Colombo N, Scambia G, et al. Maintenance Olaparib in Patients with Newly Diagnosed Advanced Ovarian Cancer. *New Engl J Med* 2018;379:2495-505.

52. Robson M, Im SA, Senkus E, et al. Olaparib for Metastatic Breast Cancer in Patients with a Germline BRCA Mutation. *New Engl J Med* 2017;377:523-33.

53. Golan T, Hammel P, Reni M, et al. Maintenance Olaparib for Germline BRCA-Mutated Metastatic Pancreatic Cancer. *N Engl J Med* 2019;381:317-27.

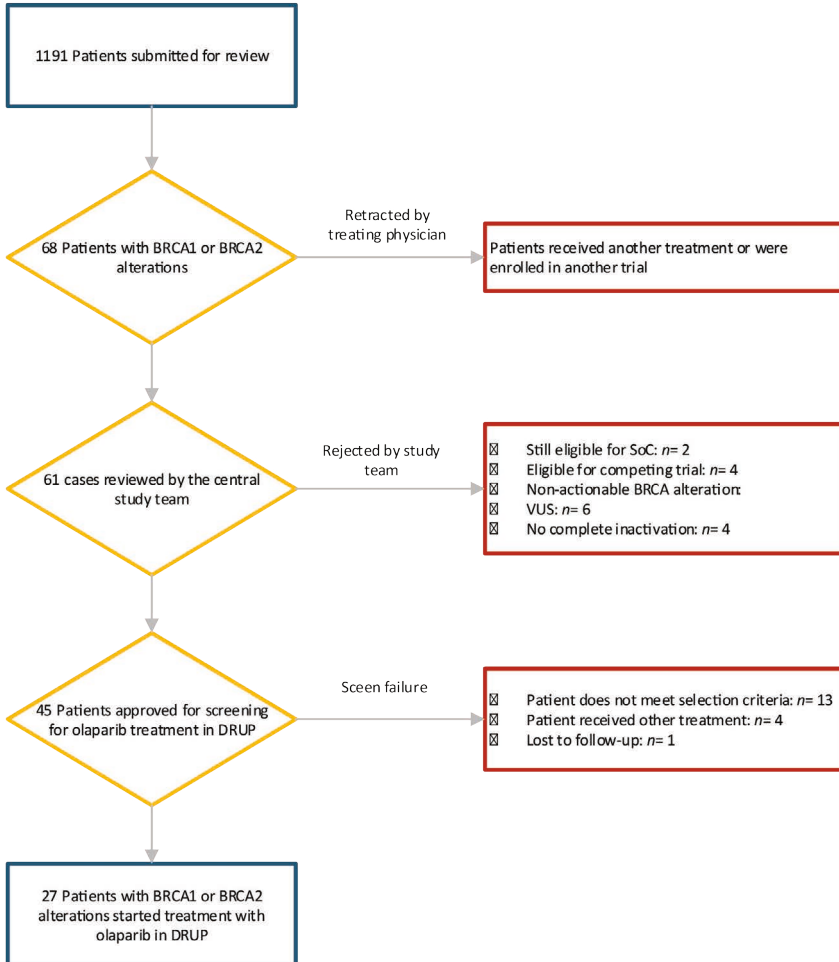
54. Fong PC, Yap TA, Boss DS, et al. Poly(ADP)-ribose polymerase inhibition: frequent durable responses in BRCA carrier ovarian cancer correlating with platinum-free interval. *J Clin Oncol* 2010;28:2512-9.

55. Jiang X, Li X, Li W, Bai H, Zhang Z. PARP inhibitors in ovarian cancer: Sensitivity prediction and resistance mechanisms. *J Cell Mol Med* 2019;23:2303-13.

56. Paul Roepman EdB, Stef van Lieshout, Lieke Schoenmaker, Mirjam C Boelens, Hendrikus J Dubbink, Willemina RR Geurts-Giele, Floris H Groenendijk, Manon MH Huibers, Mariëtte EG Kranendonk, Margaretha GM Roemer, Marloes Steehouwer, Wendy WJ de Leng, Alexander Hoischen, Bauke Ylstra, Kim Monkhorst, Jacobus JM van der Hoeven, Edwin Cuppen. Clinical validation of Whole Genome Sequencing for routine cancer diagnostics. medRxiv 2020.

57. Monkhorst K, Samsom K, Schipper L, et al. Validation of whole genome sequencing in routine clinical practice. *Ann Oncol* 2020;31:S784-S.

SUPPLEMENTARY TABLES AND FIGURES



Supplementary Figure 1. Flow chart of patients with BRCA1/2 alterations submitted to the study team between September 2016 and December 2019, and reasons for drop-out, rejection or screen failure.

Abbreviations: VUS = Variant of Unknown Significance, LOH = Loss of Heterozygosity.

Supplementary Table 1. For each patient, an overview of clinical characteristics (tumor type, response to therapy, previous treatments) and molecular characteristics (pre-enrollment and at baseline) is presented.

[§] = For details regarding the functional tests, please refer to the results section in the main text

	<i>Patient had clinical benefit</i>
	<i>Patient had no clinical benefit</i>
*	<i>Patient was not evaluable for primary end point and was not included in the efficacy analysis</i>

(Table starts on next page)

Patient	Tumortype	Start study treatment	Clinical benefit				
			BOR	PFS (weeks)	Bi-allelic BRCA inactivation	HRD -signature score	Labeled indication as per 01-01-2021?
1	Cholangiocarcinoma	27 Jul 2018	SD	115.6	Yes	0.99	no
2	Castration resistant prostate cancer	16 Aug 2018	PR	72.1	Yes	1.00	yes
3	Hormone Receptor positive Breast cancer	30 Oct 2018	PR	67.3	Yes	1.00	yes
4	Renal cell carcinoma	21 Mar 2018	SD	46.9	yes	0.89	no
5	Ductal triple-negative breast cancer	13 Apr 2017	SD	45.1	Unknown	Unknown	yes
6	Castration resistant prostate cancer	24 Sep 2018	SD	40.7	no	0.00	yes
7	Castration resistant prostate cancer	28 Nov 2018	SD	40.1	Yes	0.88	yes
8	Castration resistant prostate cancer	23 Mar 2018	PR	38.6	Yes	0.94	yes
9	Castration resistant prostate cancer	25 Jan 2019	PR	36.6	Yes	0.98	yes
10	Castration resistant prostate cancer	17 Feb 2018	PR	36.6	Yes	0.99	yes
11	Castration resistant prostate cancer	09 Apr 2019	PR	32.1	Yes	0.98	yes
12	High Grade Serous Ovarian Cancer	15 May 2017	SD	31.6	Unknown	Unknown	yes
13	Cholangiocarcinoma	21 Aug 2018	SD	25.3	Yes	0.98	no

14	Endometrium cancer	21 Nov 2018	PR	25.0	Yes	0.99	no
15	Castration resistant prostate cancer	22 Aug 2019	PD	15.8	Unknown	Unknown	yes
16	Ductal triple-negative breast cancer	23 Dec 2016	PD	9.6	No	0.11	yes
17	Colorectal cancer	07 Jun 2017	PD	8.8	No	0.00	no
18	Castration resistant prostate cancer	01 Mar 2017	PD	8.0	No	0.00	yes
19	Pancreatic cancer	06 Dec 2018	PD	8.0	Yes	1.00	yes
20	Pancreatic cancer	17 Aug 2018	PD	7.8	Yes	0.99	yes
21	Adrenal gland carcinoma	05 Jul 2018	PD	7.6	Yes	0.95	no
22	Ductal Hormone Receptor positive Breast cancer	21 Feb 2017	PD	7.0	Yes	1.00	yes
23	Castration resistant prostate cancer	13 Feb 2018	PD	4.4	No	0.00	yes
24	Colorectal cancer	01 Nov 2017	PD	4.1	No	0.00	no
25	Castration resistant prostate cancer	21 Dec 2017	NE	NE	Yes	0.98	yes
26	High Grade Serous Ovarian Cancer	14 May 2018	NE	NE	Yes	1.00	yes
27	Pancreatic cancer	19 Sep 2018	NE	NE	Yes	0.99	no

Pre-enrollment molecular information									
Patient	Molecular test	Date molecular test result was issued	Germline BRCA variant (VAF)	Somatic BRCA variant 1 (VAF)	Somatic BRCA variant 2 (VAF)	HRD-signature score	Bi-allelic BRCA inactivation	Other oncogenic drivers discovered by WGS	Sample TCP
1	WGS	09 Oct 2017	none	BRCA2 copy loss (0 copies)	n/a	0.97	Yes	FGFR2-TBC1D4 fusion DDR2 amplification	30%
2	WGS	22 May 2018	none	BRCA2 copy loss (0 copies)	BRCA1 c.1961 dupA; p.Ty r655fs (49%)	1.00	Yes	KMT2C c.1837_1843 delACTGAAT; p.Thr613fs (89%); TP53 c.742C>T; p.Arg248Trp (91%)	70%
3	WGS	28 May 2018	BRCA1 c.191G>A; p.Cys641Yr (26%)	BRCA1 c.160C>T; p.Gln54* (73%)	n/a	1.00	Yes	NCOR1 homozygous disruption	70%
4	WGS	03 Apr 2017	BRCA1 p.Asp693fs (50%)	BRCA1 c.2338C>T; p.Gln780* (50%)	n/a	0.89	Yes	KMT2C c.9524C>A; p.Ser3175* (44%); RB1 homozygous disruption	90%
5	Germline test	19 Feb 2013	BRCA1 c.527T>1G>A	n/a	n/a	n/a	Unknown	n/a	n/a
6	smMIP	15 Jun 2018	unknown	BRCA2 c.1147del; p.Ile383fs (24%)	n/a	n/a	Unknown	n/a	60%
7	smMIP	30 Jun 2017	unknown	BRCA2 c.1310_1313del; p.Lys437fs	n/a	n/a	Unknown	n/a	20-30%
8	Germline test + WGS	16 Feb 2018	BRCA2 p.Asp252fs	LOH	BRCA1 c.5618 C>A; p.Thr 1873Asn (83%)	0.94	Yes	TP53 c.524G>A; p.Arg175His (91%)	49%
9	WGS	14 Dec 2018	none	BRCA2 c.9230T>C; p.Phe3077Ser (100%)	BRCA2 c.9254 C>T; p.Thr 3085Ile (100%)	0.98	Yes	JAK1 homozygous disruption TMPRSS2-ERG fusion	21%
10	WGS	31 Oct 2017	none	BRCA2 copy loss (0 copies)	n/a	0.99	Yes	TP53 c.588_605del; p.Val197_Arg202del (82%); PTEN copy loss (0 copies); RNF43 c.582+2_582+15del (splice site) (88%); TMPRSS2-ERG fusion	80%
11	WGS	26 Mar 2018	BRCA2 c.6816_6817delAA; p.Arg2272fs	BRCA2 partial loss (0.7 copies)	n/a	0.98	Yes	PTEN copy loss (0 copies) RB1 homozygous disruption FOXAI c.797_838del; p.Phe266_Ser280delInsCys (39%)	48%
12	Germline test	Unknown	BRCA1 c.2019delA; p.Glu673fs	n/a	n/a	n/a	Unknown	n/a	n/a
13	WGS	14 Sep 2017	BRCA1 c.181T>G; p.Cys61Gly (100%)	LOH	n/a	1.00	Yes	TP53 c.407A>C; p.Gln136Pro (100%); CDKN2A copy loss (0 copies); ARID1A c.3294_3298delGTGT C; p.Gln1098fs (89%)	70%

14	smMIP + MLPA	29 Oct 2018	BRCA1 c.3756_3759del(GTCT); p.Ser1253fs (82%)	LOH	n/a	n/a	Yes	n/a	60%
15	NGS panel (FoundationOne)	29 Jan 2019	unknown	BRCA2 Tyr1762*	n/a	n/a	Unknown	n/a	Unknown
16	Germline test +2 functional HRD-tests ³	Dec 2015	BRCA2 c.9104A>C; p.Y3035S (60%)	Functional 50% decrease in HR; RAD51 staining negative ³	n/a	n/a	No	n/a	Unknown
17	WGS	06 Feb 2017	none	BRCA2 c.2836G>C; p.Asp946His (89%)	BRCA2 c.9519C>A; p.Cys3173* (2.7%)	0.00	No	TP53 c.673>A>C (54%); APC c.895-8A>G (60%); High mutational load 177 mutations across the genome; tumor is MSS	70%
18	WGS	26 Dec 2016	none	BRCA2 c.8524C>T; p.Arg2842Cys (50%)	n/a	0.00	No	RBP1-NTRK3 fusion; AR amplification (46x); PTEN copy-loss (0 copies); RB1 copy-loss (0 copies); TP53 homozygous disruption	50%
19	Germline test	28 Apr 2016	BRCA2 c.9167G>C; p.Asp2723His	unknown	n/a	n/a	Unknown	n/a	n/a
20	Germline test + WGS	18 Jan 2018	BRCA2 c.6357_6370del(TTTT); p.Leu209fs (85%)	none	n/a	0.99	Yes	TP53 1.024C>T; p.Arg3427 (100%); KRAS c.34G>C; p.Gly12Arg (84%); KEAP1 p.Cys434>C; RB1 homozygous disruption	45%
21	WGS	12 May 2018	none	BRCA2 copy loss (0 copies)	n/a	0.95	Yes	TP53 c.759_763delCATCA; p.p.Ile254fs (100%); CTNNB1 c.133T>C; p.Ser45Pro (62%); RB1 copy loss (0 copies)	92%
22	Germline test	Unknown	BRCA2 c.3847_3848del(GT); p.Val1283fs	unknown	n/a	n/a	Unknown	n/a	n/a
23	MLPA	03 May 2017	none	BRCA1 exon 1 deletion	n/a	na	Unknown	n/a	Unknown
24	WGS	10 Jun 2017	none	BRCA2 c.7044delT; p.Phe62349fs (33%)	n/a	0.00	No	TP53 c.626_627del(GA); p.Arg209fs (59%); APC c.3955delC; p.Pro1319fs (68%); KRAS c.35G>A; p.Gly12Asp (49%); SMAD4 c.1282A>G; p.Lys428Glu (62%)	40%
25	WGS	06 Mar 2017	none	BRCA2 copy loss (0 copies)	n/a	0.98	Yes	TP53 c.927delC; p.Pro309fs (81%); PTEN copy loss (0 copies); AR amplification (9x); CTNNB1 c.97T>C; p.Ser33Pro (24%); TMPRSS2-ERG fusion	90%
26	WGS	12 Oct 2017	none	BRCA2 c.1301_1304del(AAAG); p.Lys437fs (100%)	n/a	1.00	Yes	TP53 c.583A>T; p.Ile195Phe (100%)	30%
27	NGS panel (Archer FusionPlex CTL Panel)	03 Sep 2018	none	BRCA2 c.5946delT; p.Ser1982fs (68%)	LOH	n/a	Yes	n/a	50%

Baseline WGS-based molecular information

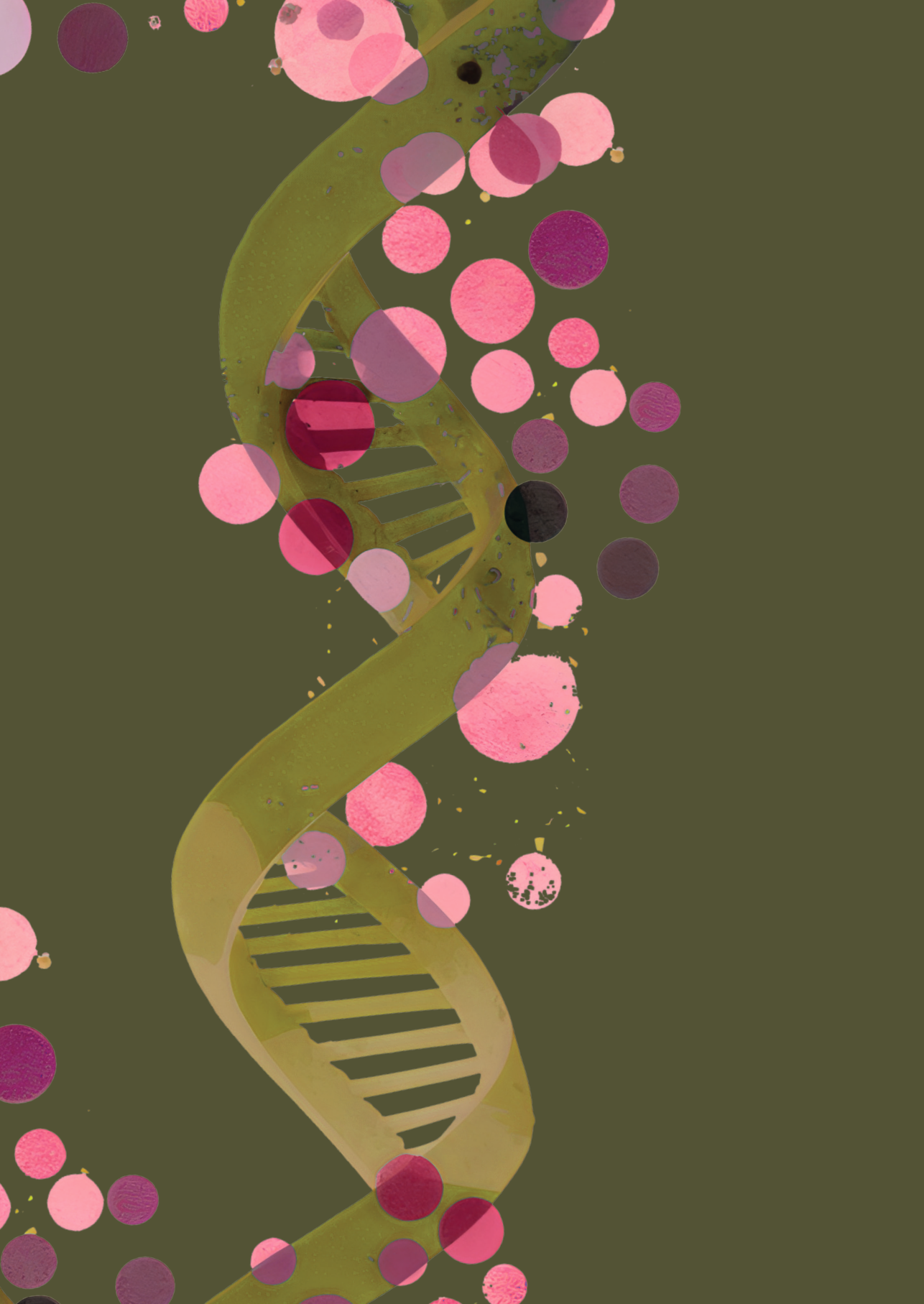
Patient	Germline BRCA variant (tVAF)	Somatic BRCA variant 1 (tVAF)	Somatic BRCA variant 2 (tVAF)	HRD-signature score	Bi-allelic BRCA inactivation	Other oncogenic drivers discovered by WGS	Sample TCP
1	none	BRCA2 copy loss (0 copies)	n/a	0.99	Yes	FGFR2-TBC1D4 fusion DDR2 amplification	26%
2	none	BRCA2 copy loss (0 copies)	BRCA1 c.1961dupA; p.Tyr655fs (49%)	1.00	Yes	KMT2C c.1837_1843delACTGAAAT; p.Thr613fs (100%), TP53 c.742C>T; p.Arg248Trp (91%), CCDC171-NTRK2 fusion	73%
3					TCP < 30%		
4					No baseline biopsy; high risk procedure		
5					No baseline biopsy; leptomeningeal disease localization only		
6	none	none	n/a	0.00	No	PTEN copy loss (0 copies) ACVR2A copy loss (0 copies) KMT2C c.14331dupG; p.Ser4778fs (40%)	22%
7	none	BRCA2 c.1310_1313del; p.Lys437fs	n/a	0.88	Unknown (due to low purity)	KDM6A homozygous disruption KEAP1 c.1075C>T; p.Gln359* (50%)	18%
8					TCP < 30%		
9	none	BRCA2 c.9230T>C; p.Phe3077Ser (100%)	BRCA2 c.9254C>T; p.Thr3085Ile (100%)	0.98	Yes	JAK1 homozygous disruption TMPRSS2-ERG fusion	45%
10					TCP < 30%		
11					TCP < 30%		
12					TCP < 30%		
13					TCP < 30%		

14	BRCA1 c.3756_3759delGTCT; p.Ser1253fs (80%)	none	n/a	0.99	Yes	MECOM amplification (13x), NFI copy loss (0 copies) PIK3CA c.263G>A; p.Arg88Gln (78%), PTEN copy loss (0 copies) TP53 c.818G>A; p.Arg273His (100%)	62%
15	BRCA2 c.5286T>A; p.Tyr1762* (51%)	none	n/a	Unknown (due to low purity)	Unknown (due to low purity)	unknown	Unknown
16	BRCA2 c.9104A>C; p.Tyr3035Ser (50%)	None	n/a	0.11	No	TP53 c.352dupA; p.Thr118fs (70%), CCNE1 amplification (18x) MYC amplification (15x), PTEN copy loss (0 copies), AD21 amplification (16x) SMARCA4 copy loss (0 copies)	90%
17	none	BRCA2 c.2836G>C; p.Asp946His (32%)	BRCA2 c.9519C>A; p.Cys3173* (24%)	0.00	No	TP53 c.673-2A>C (97%) APC c.835-8A>G (100%), KRAS amplification (33 copies), High mutational load 168 mutations across the genome	40%
18	none	BRCA2 c.8524C>T; p.Arg2842Cys (41%)	n/a	0.00	No	BRP1/NTRK3 fusion, AR amplification (46x) PTEN copy loss (0 copies), RB1 copy loss (0 copies) TP53 homozygous disruption	70%
19	BRCA2 c.8167C>C; p.Asp2723His	BRCA2 c.3812C>A; p.Ser1271* (59%)	BRCA1 c.67+1G>T (65%)	1.00	Yes	CDKN2A copy loss (0 copies); TGFBR2 homozygous disruption KRAS c.35G>T; p.Gly12Val	41%
20					TCP < 30%		
21					TCP < 30%		
22	BRCA2 c.3847_3848delGT; p.Val1283fs (59%)	BRCA2 c.9089_9090insA; p.Trp3033fs (25%)	n/a	1.00	Yes	FGFR1 amplification (18 copies); PTEN copy loss (0 copies) CHEK2 c.1223delC; p.Thr410fs (germline), ESR1 c.1610A>C; p.Tyr537Ser (32%)	70%
23	none	none	n/a	0.00	No	TP53 c.1015_1017delGAGinsAA; p.Glu339fs (100%), PTEN copy loss (0 copies) AR amplification (18x)	76%
24	none	BRCA2 c.7044delT; p.Phe2349fs (29%)	n/a	0.00	No	TP53 c.626_627delGA; p.Arg209fs (100%), APC c.3955delC; p.Pro1319fs (100%), KRAS c.35G>A; p.Gly12Asp (85%), SMAD4 c.1282A>G; p.Lys428Glu (100%)	30%
25					TCP < 30%		
26	None	None	n/a	0.00	No	KRAS c.35G>A; p.Gly12Asp (51%) TP53 c.189delT; p.Arg65fs (77%)	21%
27	n/a	BRCA2 p.Ser1982fs; c.5946delT (83%)	n/a	0.99	Yes	APC c.4703A>C; p.Asp1568Ala (21%), KRAS p.Gly12Asp (33%); CDKN2A copy loss (0 copies); MSH2 c.2783C>A; p.Ser928* (42%), germline, tumor is not MSI)	37%

Exhausted standard treatment options?

Patient	
1	Yes
2	yes
3	no palliative chemotherapy
4	yes
5	Yes
6	No cabazitaxel
7	No cabazitaxel
8	yes
9	no palliative chemotherapy
10	yes
11	yes
12	yes
13	yes

14	yes
15	Yes
16	yes
17	yes
18	Yes
19	yes
20	Yes
21	yes
22	yes
23	no enzalutamide/abiraterone
24	yes
25	no enzalutamide/abiraterone
26	yes
27	Yes





CHAPTER 4

Candidate biomarkers for treatment benefit from sunitinib in patients with advanced renal cell carcinoma using mass spectrometry-based (phospho)proteomics

Hanneke van der Wijngaart, Robin Beekhof, Jaco C. Knol, Alex A. Henneman, Richard de Goeij – de Haas, Sander R. Piersma, Thang V. Pham, Connie R. Jimenez, Henk M.W. Verheul, Mariette Labots

ABSTRACT

The tyrosine kinase inhibitor sunitinib is an effective first-line treatment for patients with advanced renal cell carcinoma (RCC). Hypothesizing that a functional read-out by mass spectrometry-based (phospho, *p*-)proteomics will identify predictive biomarkers for treatment outcome of sunitinib, tumor tissues of 26 RCC patients were analyzed. Eight patients had primary resistant (RES) and 18 sensitive (SENS) RCC. A 78 phosphosite signature ($p < 0.05$, fold-change > 2) was identified; 22 *p*-sites were upregulated in RES (unique in RES: BCAR3, NOP58, EIF4A2, GDI1) and 56 in SENS (35 unique). EIF4A1/EIF4A2 were differentially expressed in RES at the (*p*-)proteome and, in an independent cohort, transcriptome level. Inferred kinase activity of MAPK3 ($p = 0.026$) and EGFR ($p = 0.045$) as determined by INKA was higher in SENS. Posttranslational modifications signature enrichment analysis showed that different *p*-site-centric signatures were enriched ($p < 0.05$), of which FGF1 and prolactin pathways in RES and, in SENS, vanadate and thrombin treatment pathways, were most significant.

In conclusion, the RCC (phospho)proteome revealed differential *p*-sites and kinase activities associated with sunitinib resistance and sensitivity. Independent validation is warranted to develop an assay for upfront identification of patients who are intrinsically resistant to sunitinib.

BACKGROUND

The treatment landscape in metastatic renal cell carcinoma (mRCC) has changed dramatically in the past 15 years. Anti-angiogenic tyrosine kinase inhibitors (TKIs), such as sunitinib, sorafenib, axitinib, pazopanib and cabozantinib, are an effective treatment option for patients with mRCC. Since their introduction, the median overall survival (OS) has improved from 15-17 months before 2004¹⁻⁴ to 23-29 months with TKI monotherapy⁵⁻⁷. Combining TKI's with immune checkpoint inhibitors (ICI) has further improved the 12-month overall survival rate from 72%⁸ to 90%^{9,10}. With the vast expansion of therapeutic options, optimization of treatment selection strategies for individual patients becomes more important. Sunitinib is an oral multi-targeted TKI targeting mainly the Vascular Endothelial Growth Factor Receptors (VEGFR 1 and 2), Platelet-Derived Growth Factor Receptors (PDGFR-alpha and PDGFR-beta) and stem cell factor receptor (KIT), though many off-target effects are observed¹¹. Patients receiving first-line treatment with sunitinib have a median progression free survival (PFS) of 8.4 - 11 months, with an objective response rate of 25 - 47%^{7,12}. However, all patients eventually relapse due to acquired resistance, and 13-29% does not benefit from treatment at all¹²⁻¹⁴. Moreover, up to 53% of patients require dose interruptions and in 12% therapy is discontinued because of adverse events¹². Sunitinib remains one of the preferred first-line treatment options for patients with favorable-risk clear cell RCC (ccRCC) and non-ccRCC¹⁵⁻¹⁷. To improve treatment benefit from sunitinib, a predictive biomarker would be of significant clinical value.

Tissue-based baseline predictive biomarkers for sunitinib in RCC are lacking. Although a large number of candidate molecular biomarkers have been under investigation, none have been prospectively validated¹⁸. Thus far, most attempts have applied immunohistochemistry, panel DNA or RNA sequencing and PCR for target detection¹⁹. However, due to multiple resistance mechanisms in RCC, characteristically driven by a multitude of aberrantly activated kinase signaling pathways²⁰ instead of a single oncogenic driver mutation, genomics-based analysis alone is most likely not sufficient to predict response to sunitinib²¹. A functional pathway analysis may be a more promising approach^{22,23}.

Proteins are the driving force of cellular function, including intracellular signaling and immune responses. Post-translational modifications, such as phosphorylation, have a major role in regulation of protein function and activity. (Phospho)proteomics based on liquid chromatography coupled to tandem mass spectrometry (LC-MS/MS) offers insight in aberrantly activated kinase signaling pathways and potential drug targets through the global analysis of phosphorylated proteins. This method has high potential for patient stratification and prediction of therapy response²⁴⁻²⁸. In particular, phosphotyrosine-(pTyr)-phosphoproteomics provides an opportunity for the identification of patient subgroups likely to benefit from TKI's²⁹. As only 1% of all protein phosphorylations occur on tyrosine residues³⁰, enrichment of tyrosine phosphorylated peptides is necessary prior to LC-MS/MS.

We here aimed to identify baseline tissue-based molecular biomarkers for prediction of (lack of) treatment benefit to sunitinib in patients with advanced RCC, using MS-based pTyr-phosphoproteomics and global expression proteomics.

MATERIALS AND METHODS

PATIENT SELECTION

From the hospital pathology database, patients with RCC were selected who had undergone tumor nephrectomy or metastasectomy between 2000 and 2013, and thereafter received palliative treatment with sunitinib in the Amsterdam University Medical Centers (Amsterdam UMC), location VUmc. Clinical data were collected retrospectively from the hospital case records. Patients were classified as “sensitive” if they had PFS \geq 12 weeks and radiological stable disease or objective response, or “primary resistant” if they exhibited radiological progressive disease at first evaluation (PFS < 12 weeks). Since archival tissue was used for the purpose of scientific research, and collected within the context of routine clinical practice procedures, the Dutch Medical Research Involving Human Subjects Act does not apply. Patients treated at Amsterdam UMC had the possibility to opt-out for the use of their data and tissue for research purposes.

TUMOR TISSUE COLLECTION AND SAMPLE PROCESSING FOR LC-MS/MS

Frozen pre-treatment tumor resection specimens, acquired through standard care procedures and stored at -80°C , were collected from the hospital biobank. The tumor samples were cut (Leica CM1850) in $10\text{-}\mu\text{m}$ cryosections at -20°C , transferred to precooled 1.5-ml Eppendorf vials and stored at -80°C . Lysis was performed using approximately 1 ml 9 M urea buffer per sample, followed by 1 min vortexing (maximum speed), sonication ($18\text{-}\mu\text{m}$ amplitude) and centrifugation (15 min, maximum speed). The cleared lysate was aliquotted and stored at -80°C until further use. The BCA protein assay (ThermoPierce, Rockford, IL) was used to determine protein concentration. Cell lysates were reduced in 4 mM DTT for 20 min at 60°C , cooled to room temperature, and subsequently alkylated in 10 mM iodoacetamide for 15 min in the dark. After dilution to 2 M urea using 20 mM HEPES buffer pH 8.0, the lysate was digested with 20 μg Sequencing Grade Modified trypsin/ (Promega, Leiden, The Netherlands) per mg protein by overnight incubation at 22°C . Digestion was then stopped by adding trifluoroacetic acid (TFA) to a final concentration of 1%. Samples were incubated for 15 min on ice, centrifuged for 5 min at $1800 \times g$, and transferred to a new tube. Tryptic digests were desalted using 1-ml Oasis HLB cartridges (Waters, Milford, MA). After pre-wetting with acetonitrile (ACN) and equilibration of the column with 0.1% TFA, peptides were loaded. The column was washed using 0.1% TFA before elution into glass vials with 40% ACN/0.1% TFA. Eluates were lyophilized for 48 h and stored at -80°C until further use.

CONTROL SAMPLES

As quality control samples, the colorectal cancer cell line HCT116 and a reference sample of tissue-mixture (containing pooled lysates of tumor samples of colorectal cancer, melanoma, non-small cell lung cancer and hepatocellular carcinoma) were used. HCT116 cells were obtained from the American Type Culture Collection. Cells were cultured in Dulbecco's Modified Eagle Medium (DMEM), supplemented with 10% fetal bovine serum (FBS), 100 U/ml sodium penicillin and 100 µg/ml streptomycin, and maintained at 37 °C. Plated cells were washed twice with phosphate-buffered saline (PBS) and lysed using 9M urea buffer. Cells were scraped and the lysate was sonicated and centrifuged for 15 minutes at maximum speed. Aliquots of lysate were stored at -80 °C. Further processing was done as described before.

IMMUNOPRECIPITATION AND PROTEIN IDENTIFICATION

Tumor samples were processed in 3 batches, each containing samples from patients with sensitive and resistant tumors. Immunoprecipitation (IP) of tyrosine phospho-peptides was performed using the PTMScan kit (P-Tyr-1000) from Cell Signaling Technology (Leiden, The Netherlands) as described elsewhere^{32,34}. Briefly, lyophilized phosphopeptides were dissolved in IAP buffer (20 mM Tris-HCl pH 7.2, 10 mM sodium phosphate and 50 mM NaCl) and incubated with 2 µl P-Tyr-1000 beads per mg protein at 4 °C for 2 h. After washing in cold IAP buffer and Milli-Q water, peptides were eluted from the beads in two steps in 0.15% TFA, desalted in 20 µl Proxeon Stage Tips (Thermo Scientific) using 0.1% TFA, eluted with 80% ACN/0.1% TFA into LC autosampler vials, and stored at 4 °C until LC-MS/MS measurement on the same day. Peptides were separated on a pepmap Acclaim column (75 µm ID x 500 mm, 1.9 µm C18) connected to a pepmap Acclaim trap column (75 µm ID x 10 mm 3 µm C18) and running at 300 nl/min as described elsewhere^{32,33} on an Ultimate 3000 nanoLC- (Dionex LC-Packings, Amsterdam, The Netherlands) connected to a Q Exactive mass spectrometer (Thermo Fisher, Bremen, Germany) using a 2hr gradient (8-32% acetonitrile in 0.1% formic acid). Intact masses were measured at resolution 70,000 (at m/z 200) in the Orbitrap analyser using an AGC target value of 3E6 charges. The top 10 peptide signals (charge-states 2+ and higher) were submitted to MS/MS in the HCD (higher-energy collision) cell (1.4 u-amu isolation width, 25% normalized collision energy). MS/MS spectra were acquired at resolution 17,500 (at m/z 200) in the Orbitrap using an AGC target value of 1E6 charges, MaxIT of 80 ms and an underfill ratio of 0.1%. Dynamic exclusion was applied with a repeat count of 1 and an exclusion time of 30 s.

LC-MS/MS spectra were searched against the Uniprot human reference proteome FASTA file (release August 2015, 62447 entries, no fragments) using MaxQuant 1.5.2.8³⁵. Enzyme specificity was set to trypsin and up to two missed cleavages were allowed. Cysteine carboxamidomethylation (Cys, +57.021464 Da) was treated as fixed modification and serine, threonine and tyrosine phosphorylation (+79.966330 Da), methionine oxidation (Met, +15.994915 Da) and N-terminal acetylation (N-terminal, +42.010565 Da) as variable modifications. Peptide precursor ions were searched with a maximum mass deviation of 4.5 ppm and fragment ions with a maximum mass deviation of 20 ppm. Peptide, protein and site identifications were filtered at a false discovery rate (FDR) of 1% using the decoy database strategy. The minimal

peptide length was 7 amino acids and the minimum Andromeda score for modified peptides was 40, with the corresponding minimum delta score set at 17³⁶. Proteins that could not be differentiated based on MS/MS spectra alone were grouped into protein groups (default Max-Quant settings). (Phospho)peptide identifications were propagated across samples using the match-between-runs option checked. Searches were performed with the label-free quantification option selected. A normalization factor derived from the total count of matched protein lysates was applied to scale peptide intensities for each pTyr capture.

PROTEIN EXPRESSION PROFILING

Protein lysates (50 µg) were separated on precast 4–12% gradient gels using the NuPAGE SDS-PAGE system (Invitrogen, Carlsbad, CA). Following electrophoresis, gels were fixed in 50% ethanol/3% phosphoric acid solution and stained with Coomassie R-250. Gel lanes were cut into five bands, and each band was cut into ~1 mm³ cubes. Gel cubes were washed with 50 mM ammonium bicarbonate/50% acetonitrile and were transferred to a 1.5 ml microcentrifuge tube, vortexed in 400 µl 50 mM ammonium bicarbonate for 10 min, and pelleted. The supernatant was removed, and the gel cubes were vortexed in 400 µl 50 mM ammonium bicarbonate/50% acetonitrile for 10 min. After pelleting and removal of the supernatant, this wash step was repeated. Subsequently, gel cubes were reduced in 50 mM ammonium bicarbonate supplemented with 10 mM DTT at 56°C for 1 h. The supernatant was removed, and gel cubes were alkylated in 50 mM ammonium bicarbonate supplemented with 50 mM iodoacetamide for 45 min at room temperature in the dark. Next, gel cubes were washed with 50 mM ammonium bicarbonate/50% acetonitrile dried in a vacuum centrifuge at 50°C for 10 min and covered with trypsin solution (6.25 ng/µl in 50 mM ammonium bicarbonate). Following rehydration with trypsin solution and removing excess trypsin, gel cubes were covered with 50 mM ammonium bicarbonate and incubated overnight at 25°C. Peptides were extracted from the gel cubes with 100 µl of 1% formic acid (once) and 100 µl of 5% formic acid/50% acetonitrile (twice). For each sample the three extracts were pooled and stored at –20°C until use. Before LC-MS, the extracts were concentrated in a vacuum centrifuge at 50°C, and volumes were adjusted to 50 µl by adding 0.05% formic acid, filtered through a 0.45 µm spin filter, and transferred to an LC autosampler vial.

STATISTICAL ANALYSIS AND BIOLOGICAL PATHWAY ANALYSIS

Cluster analysis of phosphopeptides and phosphosites was performed using hierarchical clustering. Phosphopeptide intensities were normalized to zero mean and unit variance for each phosphopeptide. Normalization of phosphopeptide intensities and cluster analyses were performed in R version 3.5.1. For comparative analyses, only high confidence class 1 phosphosites were considered. Aiming to distinguish a phosphosite and protein signature predictive of treatment outcome of sunitinib, differential expression patterns were analyzed using the Linear Models for Microarray and RNA-Seq Data (limma) package version 3.36.5 for R^{37,38} (filters: $p < 0.05$, fold change (FC) > 2 , $\geq 30\%$ data presence, i.e. there must be a non-zero value in at least 30% of samples in the group with highest abundance). Differential expression of proteins was analyzed using the filters: $p < 0.05$, FC > 2 and $\geq 50\%$ data presence; here, with

a more complete data matrix, a stricter filter could be applied. No imputation of data was performed. Heatmap visualization and hierarchical clustering was done with the R package ComplexHeatmap version 2.2.0³⁹. Differential proteins were imported into Cytoscape version 3.5⁴⁰, and gene ontology analysis was performed in Cytoscape with the BiNGO app version 3.0.3⁴¹, using ontology and organism annotation definitions downloaded on 8 July 2019 via <http://geneontology.org>.

KINASE ACTIVITY ANALYSIS

Per sample, a ranking of most activated kinases was generated using the Integrative Inferred Kinase Activity (INKA) data analysis pipeline²⁴, taking both information on phosphorylated kinases and their substrates into account. Differentially activated kinases were identified and level of significance was determined by Mann-Whitney U-test.

POST-TRANSLATIONAL MODIFICATIONS SIGNATURE ENRICHMENT ANALYSIS (PTM-SEA)

PTM-SEA⁴² was performed using the Phospho (STY).txt Max Quant search result file after filtering out decoy and contaminant site entries, to identify site-specific signatures of kinase activities and signaling pathways, overrepresented in each of the 2 groups. Phosphosites were ranked using $-10 * \text{sign}(\log\text{FC}) * \log_{10}(\text{P-Value})$ as a measure, where the P-value and logFC were calculated in a differential analysis by limma version 3.38.3. and used as inputs to run the PTM-SEA algorithm in GenePattern⁴³ (<https://cloud.genepattern.org>). The PTM signature sets were those defined in PTMsigDB v1.9.0 (human, flanking sequence format, file `ptm.sig.db.all.flanking.human.v1.9.0.gmt`) downloaded from <https://github.com/broadinstitute/ssGSEA2.0>. Results were visualized in R. Significantly enriched signatures were reported (FDR < 0.25).

EXPLORATION OF (PHOSPHO)PROTEOMICS CANDIDATES IN TRANSCRIPTOME DATA OF AN INDEPENDENT COHORT

Publicly available transcriptomics data from an independent cohort previously described by Beuselinck et al⁴⁴ was used. CEL files containing Affymetrix array signals from 59 patients with ccRCC, treated with sunitinib, were obtained and processed in R (package “oligo”). Group comparison analysis was done in R (package “LIMMA”). All significantly ($p < 0.05$) differentially expressed transcripts were considered. Expression levels of differentially expressed proteins from our proteomics analysis ($p < 0.05$ & $\text{FC} > 2$ & $\geq 50\%$ data points in the highest group) were compared to the expression of matching transcripts in the validation cohort at gene level, the percentage of overlapping proteins/transcripts was reported.

DATA AND MATERIALS AVAILABILITY

The mass spectrometry proteomics data have been deposited to the ProteomeXchange Consortium via the PRIDE⁴⁵ partner repository with the dataset identifier PXD043514.

RESULTS

CLINICOPATHOLOGICAL CHARACTERISTICS

Twenty-six patients with mRCC were identified who underwent resection of a primary tumor ($n=23$) or metastatic lesion ($n=3$) and received sunitinib as first-line palliative therapy upon progression or relapse (**Table 1, Supplementary Table 1**). The median time between surgery and start of sunitinib was six months (range 1-63). Eighteen patients were sensitive to sunitinib, of whom six had an objective response. The median PFS (mPFS) in this group was 8.8 months (range 5 – 62.3). Eight patients had progressive disease as best response (mPFS 2.3 months, range 1.5 – 2.8).

■ **Table 1.** Patient characteristics

¹ Consists of more than one histological type: clear cell + papillary, clear cell + sarcomatoid, clear cell + eosinophilic variant. Time to sunitinib indicates interval between resection and initiation of sunitinib treatment; PFS, progression-free survival.

	All patients (<i>n</i> = 26)	Sensitive (<i>n</i> = 18)	Primary resistant (<i>n</i> = 8)
Age (years), median (range)	60 (20-80)	61 (40-79)	58 (20-80)
Sex, <i>n</i> (%)			
Female	11 (42)	8 (44)	3 (38)
Male	15 (58)	10 (56)	5 (62)
Histology, <i>n</i> (%)			
Clear cell carcinoma	17 (65)	13 (72)	4 (50)
Papillary carcinoma	3 (12)	1 (6)	2 (25)
Mixed type¹	6 (23)	4 (22)	2 (25)
Prior systemic therapy, <i>n</i> (%)			
0	17 (65)	10 (55)	7 (88)
1	8 (31)	7 (39)	1 (12)
2	1 (4)	1 (6)	-
PFS (months), median (range)		8.8 (5-62.3)	2.3 (1.5-2.8)
Time to sunitinib (months), median (range)	6 (1-63)	6 (1-63)	6 (1-24)

TYROSINE-PHOSPHOPROTEOMICS ANALYSIS

Twenty-three out of 26 tumor tissues (16 sensitive and seven primary resistant patients) were evaluable for tyrosine-phosphoproteomics, with a median protein input of 5 mg (range 2-5 mg) per sample. Three samples were considered not evaluable; two had a very low phosphopeptide yield and one had a low protein yield, hindering lysate-based normalization. In total, 2656 unique class 1 phosphosites were identified in tumor and control samples. After eliminating all control sample-specific sites, 1596 unique class 1 phosphosites remained for further comparative analysis between the two groups (86% tyrosine, 9% serine and 5% threonine, showing adequate enrichment for tyrosine phosphorylated peptides), with a median of 415 (range 266

– 713) phosphosites per sample. Identified and quantified phosphosites and phosphopeptides are presented in **Supplementary Tables 2 and 3**. The primary analysis, aiming to identify markers distinguishing sensitive from resistant patients, was performed on phosphosite data. Unsupervised cluster analysis of all identified phosphosites could not separate sensitive from resistant patients (**Supplementary Figure 1a**). After data filtering ($p < 0.05$, $FC > 2$) (**Figure 1a**), a signature of 78 differential phosphosites was identified, comprising 22 upregulated sites in resistant patients; 4 of these were uniquely identified in resistant patients (BCAR3, NOP58, EIF4A2 and GDI1, filtered for $\geq 30\%$ data presence in the group with highest abundance). Fifty-six phosphosites of aforementioned signature were upregulated in sensitive patients; 35 of these were uniquely identified in this subgroup (**Table 2**). This selection of most differential phosphosites split by group is shown in Figure 1b. Top-10 differential phosphosites in each group are shown in Figure 1c. Phosphopeptide clustering data are available in **Supplementary Figure 2a and 2b**.

Figure 1

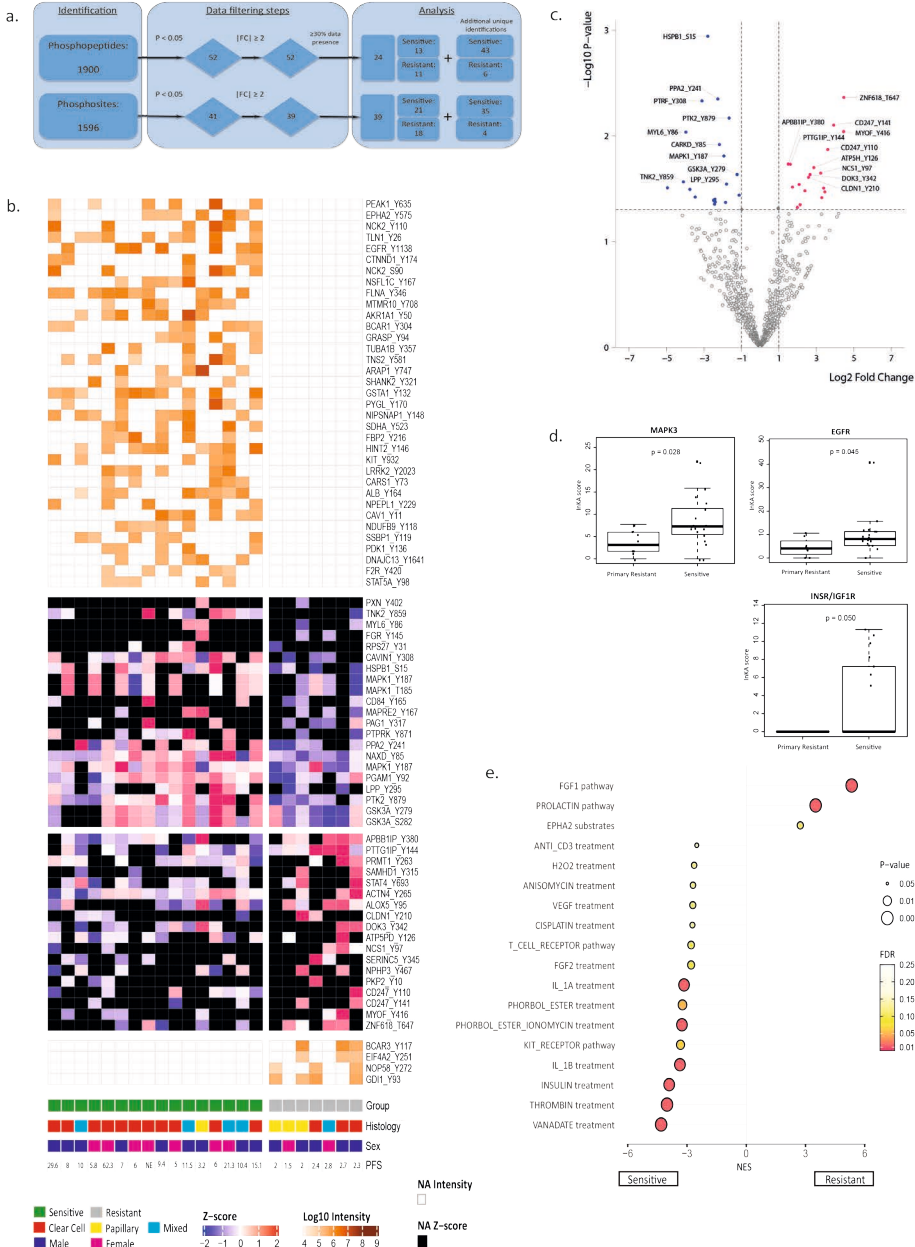


Figure 1. Phosphoproteome analysis of patients with RCC sensitive or resistant to sunitinib

- a. Overview of the data filtering steps applied in phosphosite and phosphopeptide analysis, including the effect of each filter on the total number.
- b. Heatmap of the differentially detected phosphosites ($n = 78$) in sensitive and primary resistant patients, split by group. The heatmap is a concatenation of 3 heatmaps created with R package ComplexHeatmap. The first and third heatmaps were created with log10-transformed intensity values for phosphosites that were uniquely identified (“exclusive”) in the sensitive resp resistant patient group and had a data presence of at least 30%. The second heatmap was created with log10-transformed intensity values for significantly differential phosphosites (“non-exclusive”; $p < 0.05$, $FC \geq 2$). This heatmap was clustered by columns but not by rows. Instead, rows were sorted by fold change and split by the sign of the fold change (down-regulated phosphosites in the upper part, up-regulated phosphosites in the lower part). Column splitting was at the first split of the column clustering dendrogram, and dendrogram plotting was set to FALSE. The column ordering in the resulting concatenated heatmap was determined by the middle heatmap. No imputation of data is performed. Euclidean distance and Ward’s linkage method were used. Black squares indicate non-identified phosphosites in this subgroup. Histology = histological subtype as determined by pathologist review; PFS = progression free survival in months; NE = not evaluable.
- c. Volcano plot of for statistical comparison of differential class 1 phosphosites between the Sensitive and Resistant groups were generated in R with the ggplot2 package. The top 10 significant phosphosites for each group are indicated by labeling. Labels are given for the phosphosite, not the specific type of phosphopeptide in which it was detected.
- d. Boxplots of differentially activated kinases based on INKA analysis. P-values by Mann-Whitney U-test. X-axis: 2 groups (primary resistant versus sensitive patients). Y-axis: INKA score of the kinase, based on kinase- and substrate-centric analyses.
- e. PTM-SEA identified site-specific signatures of kinase activities and signaling pathways, overrepresented in each of the 2 groups. Phosphosites were ranked using the quantity $-10 * \text{sign}(\log FC) * \log_{10}(P\text{-Value})$, where the P-value and logFC were calculated in a differential analysis by limma and used as inputs to the 20161013 version of ssGSEA2.0.R. The PTM-sets were defined in ptm.sig.db.all.flanking.human.v1.9.0.gmt. Significantly enriched signatures are presented in this figure ($p < 0.05$). X-axis represents the enrichment score (negative score = enriched in sensitive patients, positive score = enriched in resistant patients).

■ **Table 2.** Candidate phosphosite signature ($n = 78$) for prediction of sunitinib treatment outcome in RCC
a: phosphosites upregulated in primary resistant patients

	Phosphosite	p-value	FC
Uniquely identified in resistant tumors	BCAR3_Y117	n/a	n/a
	EIF4A2_Y251	n/a	n/a
	NOP58_Y272	n/a	n/a
	GDI1_Y93	n/a	n/a
Differentially upregulated (not unique)	ZNF618_T647	0.004	22.2
	CD247_Y141	0.008	15.2
	MYOF_Y416	0.009	22.0
	CD247_Y110	0.013	12.2
	APBB1IP_Y380	0.018	2.8
	PTTG1IP_Y144	0.018	3.1
	ATP5PD_Y126	0.020	7.3

a: phosphosites upregulated in primary resistant patients (continued)

	Phosphosite	p-value	FC
	NCS1_Y97	0.022	9.4
	DOK3_Y342	0.023	6.3
	CLDN1_Y210	0.025	6.0
	STAT4_Y693	0.029	4.2
	PRMT1_Y263	0.030	3.3
	NPHP3_Y467	0.031	10.5
	ALOX5_Y95	0.033	5.3
	PKP2_Y10	0.034	11.0
	SERINC5_Y345	0.038	9.8
	ACTN4_Y265	0.045	4.4
	SAMHD1_Y315	0.047	3.9

b: phosphosites upregulated in sensitive patients

	Phosphosite	p-value	FC
Uniquely identified in sensitive tumors	PEAK1_Y635	n/a	n/a
	EPHA2_Y575	n/a	n/a
	NCK2_Y110	n/a	n/a
	TLN1_Y26	n/a	n/a
	EGFR_Y1138	n/a	n/a
	CTNND1_Y174	n/a	n/a
	CDK2_S90	n/a	n/a
	NSFL1C_Y167	n/a	n/a
	FLNA_Y346	n/a	n/a
	MTMR10_Y708	n/a	n/a
	AKR1A1_Y50	n/a	n/a
	BCAR1_Y304	n/a	n/a
	GRASP_Y94	n/a	n/a
	TUBA1B_Y357	n/a	n/a
	TNS2_Y581	n/a	n/a
	ARAP1_Y747	n/a	n/a
	SHANK2_Y321	n/a	n/a
	GSTA1_Y132	n/a	n/a
	PYGL_Y170	n/a	n/a
	NIPSNAP1_Y148	n/a	n/a
	SDHA_Y523	n/a	n/a
	FBP2_Y216	n/a	n/a

b: phosphosites upregulated in sensitive patients (continued)

	Phosphosite	p-value	FC
	HINT2_Y146	n/a	n/a
	KIT_Y932	n/a	n/a
	LRRK2_Y2023	n/a	n/a
	CARS1_Y73	n/a	n/a
	ALB_Y164	n/a	n/a
	NPEPL_Y229	n/a	n/a
	CAV1_Y11	n/a	n/a
	NDUFB9_Y118	n/a	n/a
	SSBP1_Y119	n/a	n/a
	PDK1_Y136	n/a	n/a
	DNAJC13_Y1641	n/a	n/a
	F2R_Y420	n/a	n/a
	STAT5A_Y98	n/a	n/a
Differentially upregulated (not unique)	HSPB1_S15	0.001	-6.9
	PPA2_Y241	0.004	-4.8
	CAVIN1_Y308	0.005	-8.6
	PTK2_Y879	0.007	-3.1
	MYL6_Y86	0.009	-15.5
	NAXD_Y85	0.012	-4.5
	MAPK1_Y187	0.015	-3.8
	GSK3A_Y279	0.023	-2.3
	TNK2_Y859	0.027	-16.9
	LPP_Y295	0.028	-3.4
	PXN_Y402	0.031	-30.6
	FGR_Y145	0.032	-13.4
	GSK3A_S282	0.036	-2.2
	RPS27_Y31	0.038	-11.0
	MAPRE2_Y167	0.040	-5.3
	MAPK1_Y187	0.041	-5.6
	MAPK1_T185	0.041	-5.6
	PAG1_Y317	0.042	-5.3
	PTPRK_Y871	0.042	-5.3
	PGAM1_Y92	0.042	-3.6
	CD84_Y165	0.044	-5.4

The 22 phosphosites upregulated in resistant patients, 4 of which were uniquely identified in this group, were linked to various immune processes by gene ontology analysis, such as response to interleukin-18, immune response and immune effector process. The 56 phosphosites upregulated in sensitive patients (of which 35 uniquely identified) were linked to various cellular regulatory and signaling processes, such as enzyme linked receptor protein- and transmembrane receptor protein tyrosine kinase signaling pathways, peptidyl-tyrosine autophosphorylation, positive regulation of cell motility and VEGFR and Epidermal Growth Factor Receptor (EGFR) signaling pathways (**Supplementary Figure 3**). **Supplementary Table 4** lists the role of proteins corresponding to the candidate phosphosite signature according to available literature.

Since tyrosine kinase inhibitors such as sunitinib specifically target aberrant kinase signaling, a functional analysis of activated kinases is essential for a good understanding of sensitivity to sunitinib treatment. To this end, we performed INKA^{24,46-48} analysis to further explore the differences in tumor biology between individual sensitive and resistant patients. Overall, 51 unique tyrosine kinases were identified in 23 patients. For each patient, the top-20 most activated kinases were ranked (**Supplementary Figure 4**). Mitogen-activated Protein Kinase (MAPK3) ($p = 0.028$) and EGFR ($p = 0.045$) showed significantly higher activity in sensitive patients compared to resistant patients. INSR/IGF1R was exclusively activated in a substantial number of sensitive patients (**Figure 1d**). To gain further insight in the biological differences between the groups, a post-translational modifications (PTM) signature enrichment analysis (SEA) was performed. As opposed to gene set enrichment analysis (GSEA), PTM-SEA takes into account the specific combinations of sites of phosphorylation, making it more suitable for analyzing phosphoproteomics data. PTM-SEA showed that three phosphosite-centric signatures were significantly enriched ($p < 0.05$) in resistant patients: “FGF1 and prolactine pathways” and “EPHA substrates”. Fifteen signatures were enriched in sensitive patients, among which “insulin, VEGF and FGF2 treatment” and “KIT receptor pathway” (**Figure 1e**).

PROTEOME ANALYSIS

Expression proteomics was successfully performed on lysate of 25 (17 sensitive and eight resistant) out of 26 samples. In total, 6097 unique proteins were identified (Supplementary Table 3), of which 173 were differentially expressed ($p < 0.05$ & $FC > 2$ & $\geq 50\%$ data presence in group with highest abundance) (**Figure 2**); 109 were upregulated in sensitive and 64 in resistant patients. Of these, FOSL2 was uniquely found in resistant tumors and seven proteins were unique in sensitive tumors (AGMAT, DMGDH, BHMT2, ABCC1, UGT2A3, MEM263 and RBP5). These 173 robust differential proteins are visualized in Figure 2a, split by group. Gene ontology mining revealed that highly abundant proteins in resistant tumors were associated with vesicle mediated transport and excretion from cell processes, while in sensitive tumors, proteins with highest abundance were associated with multiple metabolic processes, such as small molecule-, carboxylic acid-, oxoacid- and glucuronate metabolic processes (**Figure 2c**).

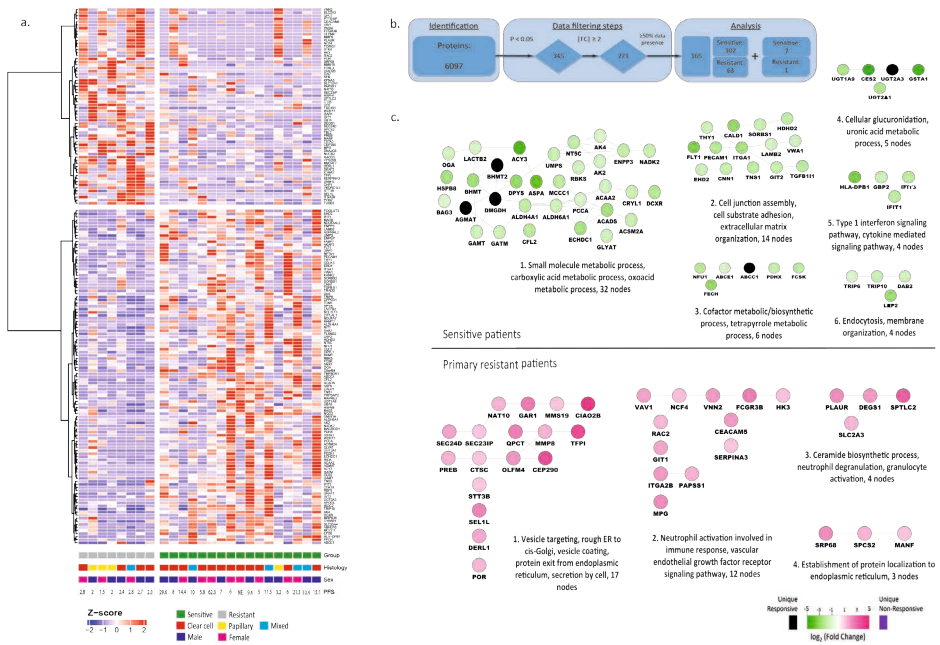


Figure 2. Proteome analysis of patients with RCC sensitive or resistant to sunitinib

- Supervised clustering analysis of the proteome. Supervised cluster analysis of differentially expressed proteins ($n = 173$) in tumor tissue lysates of 25 patients (17 sensitive and 8 resistant to sunitinib) shows one cluster of 13 sensitive patients and a mixed cluster of 8 resistant plus 4 sensitive patients. Filters: $p < 0.05$, $|FC| > 2$, $\geq 50\%$ data presence in the highest group. For clustering, Euclidean distance and Ward's linkage method were used. Histology = histological subtype as determined by pathologist review; PFS = progression free survival in months; NE = not evaluable.
- Overview of the data filtering steps applied in protein analysis, including the effect of each filter on the total number.
- Protein interaction networks. Using STRING and visualization in Cytoscape, major functional protein clusters, corresponding to either sensitive or resistant patients, are shown. Nodes correspond to upregulated proteins and edges symbolize physical or functional associations. Green clusters represent proteins upregulated in lysate of tumors sensitive to sunitinib and purple clusters represent proteins upregulated in lysate of tumors primary resistant to sunitinib. Representative GO terms identified by BiNGO analysis in both sensitive and resistant samples are listed together with the number of proteins (nodes) per cluster. All proteins in this figure are filtered for $p < 0.05$ & $FC > 2$ & $\geq 50\%$ data presence in the group with highest abundance.

EXPLORATION OF PHOSPHO-SITE AND PROTEIN SIGNATURE CANDIDATES IN PUBLICLY AVAILABLE TRANSCRIPTOME DATA

To confirm our findings from this small cohort of patients, we searched the literature for a comparable independent cohort describing ideally phosphoproteome- or proteome-based profiles or an upstream RNA analysis in relation to clinical outcomes of patients treated with sunitinib. We were able to compare our findings to the results of a cohort by Beuselinck et al. describing the transcriptome in relation to sunitinib response⁴⁴. Comparing five primary

resistant patients to 43 sensitive patients in this independent cohort, 815 out of 17,561 transcripts were differentially expressed ($p < 0.05$) between the two groups. Thirty-six of the 173 differentially upregulated proteins in our analysis were also differentially upregulated at the RNA level in the independent cohort (3 in resistant (PLAUR, SLC2A3 and EIF4A1) and 33 in sensitive patients).

DISCUSSION

To our knowledge, this is the first combined mass spectrometry-based tyrosine-phosphoproteomics and expression proteomics analysis on tumor tissue from patients with advanced RCC in order to identify candidate predictive molecular biomarkers for treatment benefit of sunitinib. We report distinctive phosphosite and protein signatures and differential kinase and pathway activities that are associated with sensitive and resistant tumors.

Exploring the differences in biology between sensitive and resistant tumors, we first focused on the characteristics of primary resistant patients. In this group, 22 phosphosites were differentially upregulated, of which 4 phosphosites were uniquely identified in this group (BCAR3_Y117, EIF4A2_Y251, NOP58_Y272, GDI1_Y93) (**Table 2**). BCAR3 and GDI1 have a role in tumor development and progression and are correlated with resistance to systemic therapy in other tumor types, including breast cancer^{28,49-53}. EIF4A2 mutations are found in 0.7% of ccRCC⁵⁴, when found in other types of cancer, these mutations are associated with unfavorable prognosis and resistance to therapy^{55,56}. EIF4A2 is a highly homologous paralog of, and functionally indistinguishable from EIF4A1⁵⁷, which was also differentially expressed in our cohort on the protein level and, in an independent study⁴⁴, on the RNA level. Interestingly, comparing tumor and normal adjacent ccRCC tissue samples, Li et al report EIF4EBP1, another member of the translation initiation complex, as a downstream substrate of mTOR, and EIF4EBP1 phosphorylation was decreased *in vitro* by mTOR inhibition⁵⁸. These four in resistant patients uniquely identified phosphosites have not previously been implied in RCC prognosis or prediction of sunitinib treatment outcome. Other differential phosphosites, yet non-uniquely upregulated in one of the groups, included STAT4_Y693 which is regulated upstream by TYK2, and ALOX5_Y95 which has a role in inflammatory processes^{59,60}.

Looking further into the biology of primary resistant tumors by analyzing enriched phosphosite-centric signatures (PTM-SEA), we found that Fibroblast Growth Factor (FGF) 1 and PROLACTIN pathways and EPHA2 substrates were significantly enriched signatures (**Figure 1e**). FGF is known to play a critical role in driving VEGF-independent tumor angiogenesis and FGFR signaling is an established resistance mechanism of VEGFR inhibition^{61,62}. Prolactin has been reported to be elevated in 45% of ccRCC patients⁶³, acting in a cytokine-like manner and as an important stimulatory regulator of the immune system. EPHA2 is overexpressed in renal cell carcinoma, associated with more advanced disease and angiogenesis⁶⁴ and has been implied as a mediator of sunitinib resistance in RCC⁶⁵.

On protein expression level, gene ontology mining of primary resistant tumors revealed that processes related to vesicle mediated transport and excretion were enriched (**Figure 2c**). One could hypothesize that this possibly reflects enhanced ability of these tumors for drug efflux, contributing to drug resistance^{66,67}. Alternatively, this vesicle mediated transport may reflect activation of immune processes, for example degranulation of mast cells. This would corroborate our phosphoproteomics data, with post-translational modification signatures indicative of enhanced immune processes in resistant patients (**Figure 1e**), which is in line with previously published work linking upregulation of cellular immune pathways and inflammatory markers to an unfavorable response to anti-VEGFR TKI's in ccRCC^{44,68,69}.

Shifting our view towards the group of sensitive patients, we found a different biological profile. At the kinase level, INKA analysis showed significantly increased inferred kinase activity of MAPK3 and EGFR (**Figure 1d**). EGFR is known for its activating effect on the MAPK signaling cascade⁷⁰. Also the downstream substrates MAP2K1 and MAP2K2 were enriched in sensitive patients (**Supplementary Figure 5**), pointing towards MAPK as a contributing signaling pathway in this group. In line with these findings, two MAPK1 sites (T185 and Y187) that are known to induce the activity of the MAPK pathway⁷¹ were differentially phosphorylated in sensitive patients, as well as a uniquely identified EGFR site (Y1138) that is a known regulator of this pathway⁷². Several phosphorylated sites on different peptides identified in sensitive patients are being directly regulated by EGFR (PEAK1, EPHA2, TNK2, RPS27 and CAVIN1)⁷², supporting EGFR activation in sensitive patients. Based on these results, we propose that EGFR-driven MAPK signaling plays an important role in sensitivity to sunitinib in RCC, and may present an alternative target for (combination) treatment⁷³. This corroborates the findings of Li et al who found their P3 phosphoproteomic subtype to be associated with the EGFR pathway and other kinases including MAPK3, that plays a role in VEGF/angiogenesis signaling⁵⁸. PTM signatures associated with sunitinib sensitivity showed enrichment of VEGF, KIT, Thrombin signaling, vanadate and FG2 treatment signatures (**Figure 1e**), pointing towards the anti-angiogenic effects of sunitinib^{74,75}.

Acknowledging the limited sample size of the sensitive (n = 16) and resistant (n = 7) tumors, our analyses may have been influenced by a number of other factors: (i) differences in pre-analytical handling of the frozen, archival specimen may have resulted in different cold ischemia times, potentially altering the phosphorylation profile^{76,77}, (ii) the use of mostly primary tumor tissue, whereas treatment benefit is evaluated based on response of metastases and (iii) the range of intervals (median 6 months) between resection and start of systemic therapy may suggest indolent biology as a cause of longer PFS. However, we found no significant correlation between the time to start sunitinib and the PFS (Spearman's rho -0.018). Also, the influence of longer storage time at -80 °C of samples on the phosphorylation profile is unknown.

Our data are internally consistent based on reproducibly identified phosphosites and -peptides (see Figure 1b and Supplementary Figure 2b) as well as identified kinase-substrate relations (e.g. for INSR/IGF1R and INSULIN treatment; Figure 1c and 1d). Lacking an external data-

set, we have not been able to validate our 78-phosphosite candidate signature that may predict treatment outcome of sunitinib. For most (uniquely identified) differential phosphosites no antibodies were available for (technical) Western blot validation of the phosphoproteomic data. An exploratory comparison of our findings from the (phospho)proteomics analysis to transcriptome data as a proxy for (phospho)protein expression, using a comparable (n = 53) RCC cohort⁴⁴ showed limited overlap (36 of 173) between the differentially regulated proteins and transcripts. In addition to sample size as contributing factor, it is known that transcriptomic and (phospho)proteomic data provide different levels of biological information^{23,78,79}. However, in resistant patients, three proteins/transcripts overlapped: PLAUR, SLC2A3 and EIF4A1. Interestingly, EIF4A1, a regulator of ERK signaling⁸⁰, was differentially upregulated on protein and transcript level, while its nearly identical homolog EIF4A2 was exclusively phosphorylated in resistant patients and represented in the candidate signature, stressing its potential importance in sunitinib resistance. Several identified differential kinases and substrates in our analysis show overlap with previous findings^{23,58}, while some, such as WEE1 and BAP1, did not surface in our study. Although these kinases/substrates are important in RCC pathogenesis, they may not differ between sunitinib sensitive or resistant patients.

CONCLUSIONS

This MS-based analysis of the RCC (tyrosine-phospho)proteome revealed distinctive phosphosite and protein signatures and differential kinase and pathway activities that are associated with sunitinib sensitivity and resistance. One protein (EIF4A1 and its homolog EIF4A2) was confirmed to be differentially expressed on phosphosite, protein and RNA level. These findings warrant validation in an independent cohort and the clinical utility for treatment selection remains to be demonstrated. A targeted assay or immunohistochemistry analysis with a selection of differential phosphosites and/or proteins could facilitate the implementation of these signatures as a decision-making tool for treatment selection in clinical practice. Such an assay would prevent toxicity and enable alternative (combination) treatment in patients upfront predicted to be resistant to sunitinib.

LIST OF ABBREVIATIONS

(cc)RCC	(Clear cell) Renal cell carcinoma
DMEM	Dulbecco's Modified Eagle Medium
EGFR	Epidermal Growth Factor Receptor
FBS	Fetal bovine serum
FC	Fold-change
FDR	False discovery rate
FGF	Fibroblast Growth Factor
GSEA	Gene Set Enrichment Analysis
ICI	Immune checkpoint inhibitors
INKA	Integrative Inferred Kinase Activity
IP	Immunoprecipitation
KIT	Stem cell factor receptor
LC-MS/MS	liquid chromatography coupled to tandem mass spectrometry
MAPK	Mitogen-activated Protein Kinase
mRCC	metastatic renal cell carcinoma
OS	Overall survival
PBS	Phosphate-buffered saline
PDGFR	Platelet-Derived Growth Factor Receptor
PFS	Progression-free survival
P-proteomics	Phosphoproteomics
PTM	Post-translational modification
PTM-SEA	Post-translational modifications signature enrichment analysis
pTyr	Phosphotyrosine
RES	Resistant
SENS	Sensitive
TKI	Tyrosine kinase inhibitor
VEGFR	Vascular Endothelial Growth Factor Receptor

REFERENCES

- 1 Fisher, R. I., Rosenberg, S. A. & Fyfe, G. Long-term survival update for high-dose recombinant interleukin-2 in patients with renal cell carcinoma. *Cancer J Sci Am* **6**, S55-S57 (2000).

- 2 McDermott, D. F. *et al.* Randomized phase III trial of high-dose interleukin-2 versus subcutaneous interleukin-2 and interferon in patients with metastatic renal cell carcinoma. *Journal of Clinical Oncology* **23**, 133-141, doi:10.1200/Jco.2005.03.206 (2005).

- 3 Motzer, R. J. *et al.* Phase III trial of interferon alfa-2a with or without 13-cis-retinoic acid for patients with advanced renal cell carcinoma. *Journal of Clinical Oncology* **18**, 2972-2980, doi:Doi 10.1200/Jco.2000.18.16.2972 (2000).

- 4 Negrier, S. *et al.* Recombinant human interleukin-2, recombinant human interferon alfa-2a, or both in metastatic renal-cell carcinoma. *New Engl J Med* **338**, 1272-1278, doi:Doi 10.1056/Nejm199804303381805 (1998).

- 5 Hutson, T. E. *et al.* Axitinib Versus Sorafenib in First-Line Metastatic Renal Cell Carcinoma: Overall Survival From a Randomized Phase III Trial. *Clin Genitourin Canc* **15**, 72-76, doi:10.1016/j.clgc.2016.05.008 (2017).

- 6 Konishi, S. *et al.* Comparison of axitinib and sunitinib as first-line therapies for metastatic renal cell carcinoma: a real-world multicenter analysis. *Med Oncol* **36**, doi:ARTN 6 10.1007/s12032-018-1231-3 (2019).

- 7 Motzer, R. J. *et al.* Pazopanib versus Sunitinib in Metastatic Renal-Cell Carcinoma. *New Engl J Med* **369**, 722-731, doi:10.1056/NEJMoa1303989 (2013).

- 8 Schmidinger, M. *et al.* Prospective Observational Study of Pazopanib in Patients with Advanced Renal Cell Carcinoma (PRINCIPAL Study). *Oncologist* **24**, 491-497, doi:10.1634/theoncologist.2018-0787 (2019).

- 9 Rini, B. I. *et al.* Pembrolizumab plus Axitinib versus Sunitinib for Advanced Renal-Cell Carcinoma. *New Engl J Med* **380**, 1116-1127, doi:10.1056/NEJMoa1816714 (2019).

- 10 Motzer, R. J. *et al.* Avelumab plus Axitinib versus Sunitinib for Advanced Renal-Cell Carcinoma. *New Engl J Med* **380**, 1103-1115, doi:10.1056/NEJMoa1816047 (2019).

- 11 Kjaeger, S. *et al.* The target landscape of clinical kinase drugs. *Science* **358**, doi:ARTN eaan4368 10.1126/science.aan4368 (2017).

- 12 Motzer, R. *et al.* Nivolumab plus ipilimumab versus sunitinib in first-line treatment for advanced renal cell carcinoma: extended follow-up of efficacy and safety results from a randomised, controlled, phase 3 trial. *Lancet Oncol* **20**, 1370-1385, doi:10.1016/S1470-2045(19)30413-9 (2019).

- 13 Motzer, R. J. *et al.* Overall Survival and Updated Results for Sunitinib Compared With Interferon Alfa in Patients With Metastatic Renal Cell Carcinoma. *Journal of Clinical Oncology* **27**, 3584-3590, doi:10.1200/Jco.2008.20.1293 (2009).

- 14 Gore, M. E. *et al.* Final results from the large sunitinib global expanded-access trial in metastatic renal cell carcinoma. *Brit J Cancer* **113**, 12-19, doi:10.1038/bjc.2015.196 (2015).

- 15 Escudier, B. *et al.* Renal Cell Carcinoma: ESMO clinical practice guidelines for diagnosis, treatment and follow-up. *Ann Oncol* **30(5)**, 706-720, doi:<https://doi.org/10.1093/annonc/mdz056> (2019).
- 16 Network., N. C. C. NCCN clinical practice guidelines in oncology: kidney cancer. Version 3. (2019).
- 17 Urology, E. A. o. Renal Cell Carcinoma Guidelines. (2019).
- 18 Dudani, S., Savard, M. F. & Heng, D. Y. C. An Update on Predictive Biomarkers in Metastatic Renal Cell Carcinoma. *Eur Urol Focus* **6**, 34-36, doi:[10.1016/j.euf.2019.04.004](https://doi.org/10.1016/j.euf.2019.04.004) (2020).
- 19 van der Mijl, J. C., Mier, J. W., Broxterman, H. J. & Verheul, H. M. Predictive biomarkers in renal cell cancer: insights in drug resistance mechanisms. *Drug Resist Updat* **17**, 77-88, doi:[10.1016/j.drup.2014.10.003](https://doi.org/10.1016/j.drup.2014.10.003) (2014).
- 20 Stommel, J. M. *et al.* Coactivation of receptor tyrosine kinases affects the response of tumor cells to targeted therapies. *Science* **318**, 287-290, doi:[10.1126/science.1142946](https://doi.org/10.1126/science.1142946) (2007).
- 21 Fiorentino, M. *et al.* Wide spectrum mutational analysis of metastatic renal cell cancer: a retrospective next generation sequencing approach. *Oncotarget* **8**, 7328-7335, doi:[10.18632/oncotarget.12551](https://doi.org/10.18632/oncotarget.12551) (2017).
- 22 Cutillas, P. R. Role of phosphoproteomics in the development of personalized cancer therapies. *Proteom Clin Appl* **9**, 383-395, doi:[10.1002/prca.201400104](https://doi.org/10.1002/prca.201400104) (2015).
- 23 Clark, D. J. *et al.* Integrated Proteogenomic Characterization of Clear Cell Renal Cell Carcinoma. *Cell* **179**, 964-983 e931, doi:[10.1016/j.cell.2019.10.007](https://doi.org/10.1016/j.cell.2019.10.007) (2019).
- 24 Beekhof, R. *et al.* INKA, an integrative data analysis pipeline for phosphoproteomic inference of active kinases. *Mol Syst Biol* **15(5)**:e8981. doi: [10.15252/msb.20198981](https://doi.org/10.15252/msb.20198981) (2019).
- 25 Labots, M. *et al.* Kinase Inhibitor Treatment of Patients with Advanced Cancer Results in High Tumor Drug Concentrations and in Specific Alterations of the Tumor Phosphoproteome. *Cancers (Basel)* **12**, doi:[10.3390/cancers12020330](https://doi.org/10.3390/cancers12020330) (2020).
- 26 Rikova, K. *et al.* Global survey of phosphotyrosine signaling identifies oncogenic kinases in lung cancer. *Cell* **131**, 1190-1203, doi:[10.1016/j.cell.2007.11.025](https://doi.org/10.1016/j.cell.2007.11.025) (2007).
- 27 Zhang, H. *et al.* Integrated Proteogenomic Characterization of Human High-Grade Serous Ovarian Cancer. *Cell* **166**, 755-765, doi:[10.1016/j.cell.2016.05.069](https://doi.org/10.1016/j.cell.2016.05.069) (2016).
- 28 Mertins, P. *et al.* Proteogenomics connects somatic mutations to signalling in breast cancer. *Nature* **534**, 55-+, doi:[10.1038/nature18003](https://doi.org/10.1038/nature18003) (2016).
- 29 Jimenez, C. R. & Verheul, H. M. Mass spectrometry-based proteomics: from cancer biology to protein biomarkers, drug targets, and clinical applications. *Am Soc Clin Oncol Educ Book*, e504-510, doi:[10.14694/EdBook_AM.2014.34.e504](https://doi.org/10.14694/EdBook_AM.2014.34.e504) (2014).
- 30 Olsen, J. V. *et al.* Global, in vivo, and site-specific phosphorylation dynamics in signaling networks. *Cell* **127**, 635-648, doi:[10.1016/j.cell.2006.09.026](https://doi.org/10.1016/j.cell.2006.09.026) (2006).

- 31 Labots, M. *et al.* Phosphotyrosine-based-phosphoproteomics scaled-down to biopsy level for analysis of individual tumor biology and treatment selection. *J Proteomics* **162**, 99-107, doi:10.1016/j.jprot.2017.04.014 (2017).

- 32 van der Mijn, J. C. *et al.* Evaluation of different phospho-tyrosine antibodies for label-free phosphoproteomics. *Journal of Proteomics* **127**, 259-263, doi:10.1016/j.jprot.2015.04.006 (2015).

- 33 Piersma, S. R. *et al.* Feasibility of label-free phosphoproteomics and application to base-line signaling of colorectal cancer cell lines. *J Proteomics* **127**, 247-258, doi:10.1016/j.jprot.2015.03.019 (2015).

- 34 Rush, J. *et al.* Immunoaffinity profiling of tyrosine phosphorylation in cancer cells. *Nat Biotechnol* **23**, 94-101, doi:10.1038/nbt1046 (2005).

- 35 Cox, J. & Mann, M. MaxQuant enables high peptide identification rates, individualized p.p.b.-range mass accuracies and proteome-wide protein quantification. *Nat Biotechnol* **26**, 1367-1372, doi:10.1038/nbt.1511 (2008).

- 36 Marx, H. *et al.* A large synthetic peptide and phosphopeptide reference library for mass spectrometry-based proteomics. *Nat Biotechnol* **31**, 557-+, doi:10.1038/nbt.2585 (2013).

- 37 Phipson, B., Lee, S., Majewski, I. J., Alexander, W. S. & Smyth, G. K. Robust Hyperparameter Estimation Protects against Hypervariable Genes and Improves Power to Detect Differential Expression. *Ann Appl Stat* **10**, 946-963, doi:10.1214/16-Aoas920 (2016).

- 38 Ritchie, M. E. *et al.* limma powers differential expression analyses for RNA-sequencing and microarray studies. *Nucleic Acids Res* **43**, doi:ARTN e47 10.1093/nar/gkv007 (2015).

- 39 Gu, Z., Eils, R. & Schlesner, M. Complex heatmaps reveal patterns and correlations in multidimensional genomic data. *Bioinformatics* **32**, 2847-2849, doi:10.1093/bioinformatics/btw313 (2016).

- 40 Shannon, P. *et al.* Cytoscape: a software environment for integrated models of biomolecular interaction networks. *Genome Res* **13**, 2498-2504, doi:10.1101/gr.1239303 (2003).

- 41 Maere, S., Heymans, K. & Kuiper, M. BiNGO: a Cytoscape plugin to assess overrepresentation of gene ontology categories in biological networks. *Bioinformatics* **21**, 3448-3449, doi:10.1093/bioinformatics/bti551 (2005).

- 42 Krug, K. *et al.* A Curated Resource for Phosphosite-specific Signature Analysis. *Mol Cell Proteomics* **18**, 576-593, doi:10.1074/mcp.TIR118.000943 (2019).

- 43 Reich, M. *et al.* GenePattern 2.0. *Nat Genet* **38**, 500-501, doi:DOI 10.1038/ng0506-500 (2006).

- 44 Beuselinck, B. *et al.* Molecular Subtypes of Clear Cell Renal Cell Carcinoma Are Associated with Sunitinib Response in the Metastatic Setting. *Clinical Cancer Research* **21**, 1329-1339, doi:10.1158/1078-0432.Ccr-14-1128 (2015).

- 45 Perez-Riverol, Y. *et al.* The PRIDE database and related tools and resources in 2019: improving support for quantification data. *Nucleic Acids Res* **47**, D442-D450, doi:10.1093/nar/gky1106 (2019).

- 46 Cucchi, D. G. J. *et al.* Phosphoproteomic Characterization of Primary AML Samples and Relevance for Response Toward FLT3-inhibitors. *Hemasphere* **5**, doi:ARTN e606 10.1097/HS9.0000000000000606 (2021).

- 47 van Alphen, C. *et al.* Phosphotyrosine-based Phosphoproteomics for Target Identification and Drug Response Prediction in AML Cell Lines. *Mol Cell Proteomics* **19**, 884-899, doi:10.1074/mcp.RA119.001504 (2020).
- 48 van Linde, M. E. *et al.* Tumor Drug Concentration and Phosphoproteomic Profiles After Two Weeks of Treatment With Sunitinib in Patients with Newly Diagnosed Glioblastoma. *Clinical Cancer Research* **28**, 1595-1602, doi:10.1158/1078-0432.Ccr-21-1933 (2022).
- 49 Green, Y. S., Kwon, S. & Christian, J. L. Expression pattern of bcar3, a downstream target of Gata2, and its binding partner, bcar1, during *Xenopus* development. *Gene Expr Patterns* **20**, 55-62, doi:10.1016/j.gep.2015.11.004 (2016).
- 50 Guo, J. M. *et al.* Breast cancer anti-estrogen resistance 3 inhibits transforming growth factor beta/Smad signaling and associates with favorable breast cancer disease outcomes. *Breast Cancer Res* **16**, doi:ARTN 476 10.1186/s13058-014-0476-9 (2014).
- 51 Jenkins, N. C. *et al.* Genetic drivers of metastatic dissemination in sonic hedgehog medulloblastoma. *Acta Neuropathol Commun* **2**, 85, doi:10.1186/s40478-014-0085-y (2014).
- 52 Wallez, Y., Riedl, S. J. & Pasquale, E. B. Association of the Breast Cancer Antiestrogen Resistance Protein 1 (BCAR1) and BCAR3 Scaffolding Proteins in Cell Signaling and Antiestrogen Resistance. *J Biol Chem* **289**, 10431-10444, doi:10.1074/jbc.M113.541839 (2014).
- 53 Zhou, K. *et al.* A tRNA fragment, tRF5-Glu, regulates BCAR3 expression and proliferation in ovarian cancer cells. *Oncotarget* **8**, 95377-95391, doi:10.18632/oncotarget.20709 (2017).
- 54 Creighton, C. J. *et al.* Comprehensive molecular characterization of clear cell renal cell carcinoma. *Nature* **499**, 43-+, doi:10.1038/nature12222 (2013).
- 55 Boussemart, L. *et al.* eIF4F is a nexus of resistance to anti-BRAF and anti-MEK cancer therapies. *Nature* **513**, 105-+, doi:10.1038/nature13572 (2014).
- 56 Chen, Z. H. *et al.* Eukaryotic initiation factor 4A2 promotes experimental metastasis and oxaliplatin resistance in colorectal cancer. *J Exp Clin Cancer Res* **38**, 196, doi:10.1186/s13046-019-1178-z (2019).
- 57 Li, Q. *et al.* Eukaryotic translation initiation factor 4AIII (eIF4AIII) is functionally distinct from eIF4AI and eIF4AII. *Mol Cell Biol* **19**, 7336-7346, doi:10.1128/mcb.19.11.7336 (1999).
- 58 Li, Y. Z. *et al.* Histopathologic and proteogenomic heterogeneity reveals features of clear cell renal cell carcinoma aggressiveness. *Cancer Cell* **41**, 139-+, doi:10.1016/j.ccell.2022.12.001 (2023).
- 59 Tjonahen, E. *et al.* Resolvin E2: Identification and anti-inflammatory actions: Pivotal role of human 5-lipoxygenase in resolvin E series biosynthesis. *Chem Biol* **13**, 1193-1202, doi:10.1016/j.chembiol.2006.09.011 (2006).
- 60 Sun, Q. Y., Zhou, H. H. & Mao, X. Y. Emerging Roles of 5-Lipoxygenase Phosphorylation in Inflammation and Cell Death. *Oxid Med Cell Longev* **2019**, doi:Artn 2749173 10.1155/2019/2749173 (2019).
- 61 Casanovas, O., Hicklin, D. J., Bergers, G. & Hanahan, D. Drug resistance by evasion of antiangiogenic targeting of VEGF signaling in late-stage pancreatic islet tumors. *Cancer Cell* **8**, 299-309, doi:10.1016/j.ccr.2005.09.005 (2005).

- 62 Massari, F. *et al.* Targeting fibroblast growth factor receptor (FGFR) pathway in renal cell carcinoma. *Expert Rev Anticanc* **15**, 1367-1369, doi:10.1586/14737140.2015.1110488 (2015).
-
- 63 Czarnecka, A. M., Niedzwiedzka, M., Porta, C. & Szczylik, C. Hormone signaling pathways as treatment targets in renal cell cancer. *Int J Oncol* **48**, 2221-2235, doi:10.3892/ijo.2016.3460 (2016).
-
- 64 Wang, L. X. *et al.* Expression of EphA2 protein is positively associated with age, tumor size and Fuhrman nuclear grade in clear cell renal cell carcinomas. *Int J Clin Exp Pathol* **8**, 13374-13380 (2015).
-
- 65 Ruan, H. L., Li, S., Bao, L. & Zhang, X. P. Enhanced YB1/EphA2 axis signaling promotes acquired resistance to sunitinib and metastatic potential in renal cell carcinoma. *Oncogene* **39**, 6113-6128, doi:10.1038/s41388-020-01409-6 (2020).
-
- 66 Mc Namee, N. & O'Driscoll, L. Extracellular vesicles and anti-cancer drug resistance. *Bba-Rev Cancer* **1870**, 123-136, doi:10.1016/j.bbcan.2018.07.003 (2018).
-
- 67 Soekmadji, C. & Nelson, C. C. The Emerging Role of Extracellular Vesicle-Mediated Drug Resistance in Cancers: Implications in Advanced Prostate Cancer. *Biomed Research International* **2015**, doi:Artn 454837 10.1155/2015/454837 (2015).
-
- 68 Beuselink, B. *et al.* Prognostic impact of baseline serum C-reactive protein in patients with metastatic renal cell carcinoma (RCC) treated with sunitinib. *BJU Int* **114**, 81-89, doi:10.1111/bju.12494 (2014).
-
- 69 Fujita, T. *et al.* C-reactive protein as a prognostic marker for advanced renal cell carcinoma treated with sunitinib. *Int J Urol* **19**, 908-913, doi:10.1111/j.1442-2042.2012.03071.x (2012).
-
- 70 Wee, P. & Wang, Z. X. Epidermal Growth Factor Receptor Cell Proliferation Signaling Pathways. *Cancers* **9**, doi:ARTN 52 10.3390/cancers9050052 (2017).
-
- 71 Casar, B., Pinto, A. & Crespo, P. Essential role of ERK dimers in the activation of cytoplasmic but not nuclear substrates by ERK-scaffold complexes. *Mol Cell* **31**, 708-721, doi:10.1016/j.molcel.2008.07.024 (2008).
-
- 72 Schulze, W. X., Deng, L. & Mann, M. Phosphotyrosine interactome of the ErbB-receptor kinase family. *Mol Syst Biol* **1**, doi:ARTN 2005.0008 10.1038/msb4100012 (2005).
-
- 73 Diaz-Montero, C. M. *et al.* MEK inhibition abrogates sunitinib resistance in a renal cell carcinoma patient-derived xenograft model. *Br J Cancer* **115**, 920-928, doi:10.1038/bjc.2016.263 (2016).
-
- 74 Welti, J. C. *et al.* Fibroblast growth factor 2 regulates endothelial cell sensitivity to sunitinib. *Oncogene* **30**, 1183-1193, doi:10.1038/onc.2010.503 (2011).
-
- 75 Gao, N. *et al.* Vanadate-induced expression of hypoxia-inducible factor 1 alpha and vascular endothelial growth factor through phosphatidylinositol 3-kinase/Akt pathway and reactive oxygen species. *J Biol Chem* **277**, 31963-31971, doi:10.1074/jbc.M200082200 (2002).
-
- 76 Buffart, T. E. *et al.* Time dependent effect of cold ischemia on the phosphoproteome and protein kinase activity in fresh-frozen colorectal cancer tissue obtained from patients. *Clin Proteom* **18**, doi:ARTN 8 10.1186/s12014-020-09306-6 (2021).
-

- 77 Mertins, P. *et al.* Ischemia in Tumors Induces Early and Sustained Phosphorylation Changes in Stress Kinase Pathways but Does Not Affect Global Protein Levels. *Mol Cell Proteomics* **13**, 1690-1704, doi:10.1074/mcp.M113.036392 (2014).
- 78 Buccitelli, C. & Selbach, M. mRNAs, proteins and the emerging principles of gene expression control. *Nat Rev Genet* **21**, 630-644, doi:10.1038/s41576-020-0258-4 (2020).
- 79 Petralia, F. *et al.* Integrated Proteogenomic Characterization across Major Histological Types of Pediatric Brain Cancer. *Cell* **183**, 1962+, doi:10.1016/j.cell.2020.10.044 (2020).
- 80 Xu, J. N., Wendel, H. G., Pelletier, J., Yao, Z. & Rosen, N. eIF4A regulates ERK activation by controlling the translation of DUSP6. *Mol Cancer Ther* **18**, doi:10.1158/1535-7163.Targ-19-B075 (2019).
- 81 Koster, B. D. *et al.* Autologous tumor cell vaccination combined with systemic CpG-B and IFN-alpha promotes immune activation and induces clinical responses in patients with metastatic renal cell carcinoma: a phase II trial. *Cancer Immunol Immunother* **68**, 1025-1035, doi:10.1007/s00262-019-02320-0 (2019).
- 82 Lopez-Beltran, A. *et al.* The Identification of Immunological Biomarkers in Kidney Cancers. *Front Oncol* **8**, doi:ARTN 456 10.3389/fonc.2018.00456 (2018).
- 83 Chen, F. J. *et al.* Multilevel Genomics-Based Taxonomy of Renal Cell Carcinoma. *Cell Rep* **14**, 2476-2489, doi:10.1016/j.celrep.2016.02.024 (2016).
- 84 An, H. J. *et al.* Myoferlin silencing inhibits VEGFR2-mediated proliferation of metastatic clear cell renal cell carcinoma. *Sci Rep-Uk* **9**, doi:ARTN 12656 10.1038/s41598-019-48968-7 (2019).
- 85 Song, D. H. *et al.* Prognostic role of myoferlin expression in patients with clear cell renal cell carcinoma. *Oncotarget* **8**, 89033-89039, doi:10.18632/oncotarget.21645 (2017).
- 86 Bruggemann, M. *et al.* Systematic Analysis of the Expression of the Mitochondrial ATP Synthase (Complex V) Subunits in Clear Cell Renal Cell Carcinoma. *Transl Oncol* **10**, 661-668, doi:10.1016/j.tranon.2017.06.002 (2017).
- 87 Solarek, W., Koper, M., Lewicki, S., Szczylik, C. & Czarnecka, A. M. Insulin and insulin-like growth factors act as renal cell cancer intratumoral regulators. *J Cell Commun Signal* **13**, 381-394, doi:10.1007/s12079-019-00512-y (2019).
- 88 Bleu, M. *et al.* PAX8 activates metabolic genes via enhancer elements in Renal Cell Carcinoma. *Nature Communications* **10**, doi:ARTN 3739 10.1038/s41467-019-11672-1 (2019).
- 89 Filipovic, J. *et al.* PRMT1 expression in renal cell tumors- application in differential diagnosis and prognostic relevance. *Diagn Pathol* **14**, doi:ARTN 120 10.1186/s13000-019-0901-6 (2019).
- 90 Liu, C. H. *et al.* BTG1 potentiates apoptosis and suppresses proliferation in renal cell carcinoma by interacting with PRMT1. *Oncology Letters* **10**, 619-624, doi:10.3892/ol.2015.3293 (2015).
- 91 Cui, H. *et al.* Identification of the key genes and pathways involved in the tumorigenesis and prognosis of kidney renal clear cell carcinoma. *Sci Rep-Uk* **10**, doi:ARTN 4271 10.1038/s41598-020-61162-4 (2020).

- 92 Faronato, M. *et al.* Increased expression of 5-lipoxygenase is common in clear cell renal cell carcinoma. *Histol Histopathol* **22**, 1109-1118 (2007).
-
- 93 Matsuyama, M. *et al.* 5-Lipoxygenase inhibitors attenuate growth of human renal cell carcinoma and induce apoptosis through arachidonic acid pathway. *Oncol Rep* **14**, 73-79 (2005).
-
- 94 Gudas, L. J., Fu, L. P., Minton, D. R., Mongan, N. P. & Nanus, D. M. The role of HIF1 alpha in renal cell carcinoma tumorigenesis. *J Mol Med* **92**, 825-836, doi:10.1007/s00109-014-1180-z (2014).
-
- 95 Xu, J. S. *et al.* High EphA2 protein expression in renal cell carcinoma is associated with a poor disease outcome. *Oncology Letters* **8**, 687-692, doi:10.3892/ol.2014.2196 (2014).
-
- 96 Feng, Z. H. *et al.* RIN1 promotes renal cell carcinoma malignancy by activating EGFR signaling through Rab25. *Cancer Sci* **108**, 1620-1627, doi:10.1111/cas.13297 (2017).
-
- 97 Lee, S. J. *et al.* Von Hippel-Lindau Tumor Suppressor Gene Loss in Renal Cell Carcinoma Promotes Oncogenic Epidermal Growth Factor Receptor Signaling via Akt-1 and MEK-1. *Eur Urol* **54**, 845-854, doi:10.1016/j.eururo.2008.01.010 (2008).
-
- 98 Minner, S. *et al.* Epidermal growth factor receptor protein expression and genomic alterations in renal cell carcinoma. *Cancer-Am Cancer Soc* **118**, 1268-1275, doi:10.1002/cncr.26436 (2012).
-
- 99 Liu, C. *et al.* VHL-HIF-2 alpha axis-induced SMYD3 upregulation drives renal cell carcinoma progression via direct trans-activation of EGFR. *Oncogene* **39**, 4286-4298, doi:10.1038/s41388-020-1291-7 (2020).
-
- 100 Xu, C. & Zheng, J. H. siRNA against TSG101 reduces proliferation and induces G0/G1 arrest in renal cell carcinoma - involvement of c-myc, cyclin E1, and CDK2. *Cell Mol Biol Lett* **24**, doi:ARTN 7 10.1186/s11658-018-0124-y (2019).
-
- 101 Sun, G. G., Wei, C. D., Jing, S. W. & Hu, W. N. Interactions between Filamin A and MMP-9 Regulate Proliferation and Invasion in Renal Cell Carcinoma. *Asian Pac J Cancer P* **15**, 3789-3795, doi:10.7314/APjcp.2014.15.8.3789 (2014).
-
- 102 De Palma, G. *et al.* The Three-Gene Signature in Urinary Extracellular Vesicles from Patients with Clear Cell Renal Cell Carcinoma. *Journal of Cancer* **7**, 1960-1967, doi:10.7150/jca.16123 (2016).
-
- 103 Tsai, T. H. & Lee, W. Y. Succinate Dehydrogenase-Deficient Renal Cell Carcinoma. *Archives of Pathology & Laboratory Medicine* **143**, 643-647, doi:10.5858/arpa.2018-0024-RS (2019).
-
- 104 Billemont, B. *et al.* Angiogenesis and renal cell carcinoma. *B Cancer* **94**, S232-S240 (2007).
-
- 105 Horstmann, M. *et al.* Evaluation of the KIT/Stem Cell Factor Axis in Renal Tumours. *Anticancer Res* **32**, 4339-4345 (2012).
-
- 106 Shen, C. & Kaelin, W. G. The VHL/HIF axis in clear cell renal carcinoma. *Semin Cancer Biol* **23**, 18-25, doi:10.1016/j.semcancer.2012.06.001 (2013).
-
- 107 Looyenga, B. D. *et al.* Chromosomal amplification of leucine-rich repeat kinase-2 (LRRK2) is required for oncogenic MET signaling in papillary renal and thyroid carcinomas. *P Natl Acad Sci USA* **108**, 1439-1444, doi:10.1073/pnas.1012500108 (2011).
-

- 108 Chen, Z. *et al.* Prognostic role of pretreatment serum albumin in renal cell carcinoma: a systematic review and meta-analysis. *Oncotargets Ther* **9**, 6701-6709, doi:10.2147/Ott.S108469 (2016).
- 109 Campbell, L. *et al.* Caveolin-1 in renal cell carcinoma promotes tumour cell invasion, and in co-operation with pERK predicts metastases in patients with clinically confined disease. *J Transl Med* **11**, doi:Artn 255 10.1186/1479-5876-11-255 (2013).
- 110 Ellinger, J. *et al.* Systematic Expression Analysis of Mitochondrial Complex I Identifies NDUFS1 as a Biomarker in Clear-Cell Renal-Cell Carcinoma. *Clin Genitourin Canc* **15**, E551-E562, doi:10.1016/j.clgc.2016.11.010 (2017).
- 111 Baumunk, D. *et al.* Expression parameters of the metabolic pathway genes pyruvate dehydrogenase kinase-1 (PDK-1) and DJ-1/PARK7 in renal cell carcinoma (RCC). *World J Urol* **31**, 1191-1196, doi:10.1007/s00345-012-0874-5 (2013).
- 112 Zhou, W. M. *et al.* Low expression of PDK1 inhibits renal cell carcinoma cell proliferation, migration, invasion and epithelial mesenchymal transition through inhibition of the PI3K-PDK1-Akt pathway. *Cell Signal* **56**, 1-14, doi:10.1016/j.cellsig.2018.11.016 (2019).
- 113 Pak, S., Kim, W., Kim, Y., Song, C. & Ahn, H. Dihydrotestosterone promotes kidney cancer cell proliferation by activating the STAT5 pathway via androgen and glucocorticoid receptors. *J Cancer Res Clin* **145**, 2293-2301, doi:10.1007/s00432-019-02993-1 (2019).
- 114 Sarto, C. *et al.* Expression of heat shock protein 27 in human renal cell carcinoma. *Proteomics* **4**, 2252-2260, doi:DOI 10.1002/pmic.200300797 (2004).
- 115 Liu, Y. Y. *et al.* Long noncoding RNA BX357664 regulates cell proliferation and epithelial-to-mesenchymal transition via inhibition of TGF-beta 1/p38/HSP27 signaling in renal cell carcinoma. *Oncotarget* **7**, 81410-81422, doi:10.18632/oncotarget.12937 (2016).
- 116 Zhao, Y. B. *et al.* PTRF/CAVIN1, regulated by SHC1 through the EGFR pathway, is found in urine exosomes as a potential biomarker of ccRCC. *Carcinogenesis* **41**, 274-283, doi:10.1093/carcin/bgz147 (2020).
- 117 Beraud, C. *et al.* Targeting FAK scaffold functions inhibits human renal cell carcinoma growth. *International Journal of Cancer* **137**, 1549-1559, doi:10.1002/ijc.29522 (2015).
- 118 Oka, H. *et al.* Constitutive Activation of Mitogen-Activated Protein (Map) Kinases in Human Renal-Cell Carcinoma. *Cancer Research* **55**, 4182-4187 (1995).
- 119 Huang, D. *et al.* Inhibition of MAPK kinase signaling pathways suppressed renal cell carcinoma growth and angiogenesis in vivo. *Cancer Research* **68**, 81-88, doi:10.1158/0008-5472.Can-07-5311 (2008).
- 120 Chua, B. T., Lim, S. J., Tham, S. C., Poh, W. J. & Ullrich, A. Somatic mutation in the ACK1 ubiquitin association domain enhances oncogenic signaling through EGFR regulation in renal cancer derived cells. *Mol Oncol* **4**, 323-334, doi:10.1016/j.molonc.2010.03.001 (2010).
- 121 Jenq, W. M., Cooper, D. R. & Ramirez, G. Integrin expression on cell adhesion function and up-regulation of P125(FAK) and paxillin in metastatic renal carcinoma cells. *Connective Tissue Research* **34**, 161-174, doi:Doi 10.3109/03008209609000696 (1996).

- 122 Qayyum, T. *et al.* Expression and prognostic significance of Src family members in renal clear cell carcinoma. *Brit J Cancer* **107**, 856-863, doi:10.1038/bjc.2012.314 (2012).
-
- 123 Feng, X. *et al.* Overexpression of Csk-binding protein contributes to renal cell carcinogenesis. *Oncogene* **28**, 3320-3331, doi:10.1038/onc.2009.185 (2009).
-
- 124 Li, C. J. *et al.* Expression of PGAM1 in renal clear cell carcinoma and its clinical significance. *Int J Clin Exp Patho* **8**, 9410-9415 (2015).
-

SUPPLEMENTARY TABLES AND FIGURES

■ **Supplementary Table 1.** Clinicopathological data per individual patient

1: RCC = Renal Cell Carcinoma. 2: Gender: M = male, F = female. Age = at start sunitinib. 3: CC = clear cell, AC = adenocarcinoma, P = papillary, S = sarcomatoid, E = eosinophilic variant. 4: ASI trial⁸¹ = vaccination + CpG + GM-CSF, followed by CpG + Interferon. 5: Time in months between nephrectomy or metastasectomy and start sunitinib. 6: Best overall response according to RECIST 1.1. 7: Progression Free Survival in months. 8: Metastatic site: lymph nodes in cavernous sinus. 9: Metastatic site: liver. 10: Metastatic site: local recurrence in renal fossa. *: Measurements of tumor target lesions could not be performed, scan was performed elsewhere, radiology report states “decrease of metastatic lesions”. Patient is considered as sensitive to sunitinib. **: Metastatic lesion was resected after 2 months of therapy. Histological evaluation shows extensive necrosis of the metastatic lesion, therefore patient is considered as sensitive to sunitinib. NA: not applicable. Due to extensive necrotic tumor tissue, the tumor cell percentage could not be determined.

Patient ID ¹	Gender, age ²	Histology ³	Lesion	Prior immuno-therapy ⁴	Time to sunitinib ⁵	Best response ⁶	PFS ⁷	Tumor cell %	Protein input
RCC1	M, 46	CC	Primary	ASI trial	7	PR	29.6	90 %	5 mg
RCC2	M, 59	CC	Primary	ASI trial	4	PR	9.4	90 %	3 mg
RCC3	M, 40	AC/P	Primary	Interferon	5	SD	10	80 %	3 mg
RCC4	M, 60	AC/P	Primary	Interferon	36	SD	11.5	60 %	5 mg
RCC5	M, 60	P	Primary	None	4	SD	3.2	40 %	5 mg
RCC6	M, 79	CC/AC	Primary	None	63	PR	9.5	80 %	5 mg
RCC7	F, 69	CC	Primary	None	2	SD	62.3	80 %	5 mg
RCC8	F, 60	CC	Primary	None	1	SD/PR*	6	80 %	5 mg
RCC9	M, 75	CC	Primary	None	10	SD	8	50 %	5 mg
RCC10	M, 66	CC	Metastatic ⁸	None	4	SD	15.1	90 %	3 mg
RCC11	F, 57	CC	Primary	None	2	PD	2.8	NA	5 mg
RCC12	M, 64	CC	Primary	None	2	PD	2.4	90 %	3 mg
RCC13	F, 64	CC	Primary	Interferon	26	SD	5	90 %	2 mg
RCC14	F, 57	CC/P	Primary	ASI trial	5	PR	21.3	60 %	5 mg
RCC15	F, 42	CC/E	Primary	None	10	PD	2.8	25 %	5 mg
RCC16	F, 62	CC	Primary	ASI trial	13	PR	5.8	50 %	3 mg
RCC17	F, 47	CC	Primary	None	10	SD	14.4	NA	5 mg
RCC18	M, 69	CC	Primary	None	6	SD	7	80 %	5 mg
RCC19	M, 59	CC	Primary	None	4	PD	2.7	25 %	5 mg
RCC20	F, 20	P	Metastatic ⁹	None	1	PD	1.5	60 %	5 mg
RCC21	F, 67	CC	Primary	Interferon	15	SD	6	90 %	5 mg
RCC22	M, 54	CC	Primary	ASI trial	24	PD	2.3	80 %	5 mg
RCC23	M, 75	CC/S	Primary	None	1	PR	10.4	70 %	3 mg
RCC24	M, 80	P	Primary	None	8	PD	2	70 %	5 mg
RCC25	M, 80	P	Primary	None	16	PD	1.8	90 %	5 mg
RCC26	F, 53	CC	Metastatic ¹⁰	None	1	SD	NE**	90 %	5 mg

Supplementary Table 2 and Supplementary Table 3 will be made available online upon publication of the article.

- Supplementary Table 2: All identified and quantified phosphosites
- Supplementary Table 3: All identified and quantified phosphopeptides and proteins

Supplementary Table 4. Role of proteins corresponding to candidate phosphosite signature (n = 78) in RCC

a: phosphosites upregulated in primary resistant patients

	Phosphosite	p-value	FC	Role of corresponding protein in RCC
Uniquely identified in resistant tumors	BCAR3_Y117	n/a	n/a	No literature describing a role in RCC.
	EIF4A2_Y251	n/a	n/a	
	NOP58_Y272	n/a	n/a	
	GDI1_Y93	n/a	n/a	
Differentially upregulated (not unique)	ZNF618_T647	0.004	22.2	No literature describing a role in RCC.
	CD247_Y141	0.008	15.2	A relatively high expression of CD247, which represents a target for immunotherapy, is found in ccRCC compared to normal tissue ^{82,83} .
	MYOF_Y416	0.009	22.0	MYOF influences cellular proliferation of the metastatic CCRCC cell line by regulating VEGFR2 degradation ⁸⁴ and MYOF hyperexpression was significantly associated with disease-free survival ⁸⁵ .
	CD247_Y110	0.013	12.2	A relatively high expression of CD247, which represents a target for immunotherapy, is found in ccRCC compared to normal tissue ^{82,83} .
	APBB1IP_Y380	0.018	2.8	No literature describing a role in RCC.
	PTTG1IP_Y144	0.018	3.1	No literature describing a role in RCC.
	ATP5PD_Y126	0.020	7.3	ATP5PD is differentially expressed between ccRCC tissue en normal renal tissue ⁸⁶ .
	NCS1_Y97	0.022	9.4	No literature describing a role in RCC.
	DOK3_Y342	0.023	6.3	In an <i>in vitro</i> study, DOK3 was downregulated in RCC cell lines after stimulation with insulin and insulin-like growth factors (IGFs), stimulating RCC tumorigenesis and progression ⁸⁷ .
	CLDN1_Y210	0.025	6.0	CLDN1 is expressed in RCC cells in a PAX8-dependent manner ⁸⁸ .
	STAT4_Y693	0.029	4.2	No literature describing a role in RCC.

a: phosphosites upregulated in primary resistant patients (continued)

Phosphosite	p-value	FC	Role of corresponding protein in RCC
PRMT1_Y263	0.030	3.3	Expression may be characteristic for low grade and low stage ccRCC, whole homologous loss of PRMT1 may be significant for high grade and high stage ccRCC ⁸⁹ . BTG1 may inhibit cell growth and promote apoptosis by interacting with PRMT1 in RCC ⁹⁰ .
NPHP3_Y467	0.031	10.5	No literature describing a role in RCC.
ALOX5_Y95	0.033	5.3	Higher expression predicts reduced survival in ccRCC ⁹¹ . Upregulation of ALOX5 is an important step in RCC progression. VEGF expression was strongly inducible by ALOX5 metabolites in vitro ⁹² . ALOX5 inhibition causes marked reduction of RCC cells in vitro through apoptosis ⁹³ .
PKP2_Y10	0.034	11.0	PKP2 is a target gene and component of a protein network regulated by HIF2 α and is associated with a poorer survival of patients with RCC ⁹⁴ .
S E R I N C 5 _ Y345	0.038	9.8	No literature describing a role in RCC.
ACTN4_Y265	0.045	4.4	No literature describing a role in RCC.
SAMHD1_Y315	0.047	3.9	No literature describing a role in RCC.

b: phosphosites upregulated in sensitive patients

	Phosphosite	p-value	FC	Role of corresponding protein in RCC
Uniquely identified in sensitive tumors	PEAK1_Y635	n/a	n/a	No literature describing a role in RCC.
	EPHA2_Y575	n/a	n/a	Expression of EphA2 is positively associated with tumor size and Fuhrman nuclear grade in ccRCC ⁶⁴ and high expression is associated with poor disease outcome ⁹⁵ . Enhanced YB1/EphA2 axis signaling promotes acquired resistance to sunitinib in RCC ⁶⁵ .
	NCK2_Y110	n/a	n/a	No literature describing a role in RCC.
	TLN1_Y26	n/a	n/a	No literature describing a role in RCC.
	EGFR_Y1138	n/a	n/a	The epidermal growth factor receptor (EGFR) is overexpressed in RCC and it plays a critical role in tumorigenesis and progression in RCC ⁹⁶⁻⁹⁸ . EGFR hyperactivity in RCC is mediated by the VHL/HIF-2 α /SMYD3 signaling cascade ⁹⁹ .
	CTNND1_Y174	n/a	n/a	No literature describing a role in RCC.

b: phosphosites upregulated in sensitive patients (continued)

Phosphosite	p-value	FC	Role of corresponding protein in RCC
CDK2_S90	n/a	n/a	CDK2 kinase activity is required for proper cell cycle progression and is involved in oncogenesis of multiple tumor types, among which RCC ¹⁰⁰ .
NSFL1C_Y167	n/a	n/a	No literature describing a role in RCC.
FLNA_Y346	n/a	n/a	FLNA expression is correlated with lymph node metastases, clinical stage, histological grade and poor overall survival in RCC, suggesting that it plays a role as tumor suppressor in RCC ¹⁰¹ .
MTMR10_Y708	n/a	n/a	No literature describing a role in RCC.
AKR1A1_Y50	n/a	n/a	No literature describing a role in RCC.
BCAR1_Y304	n/a	n/a	No literature describing a role in RCC.
GRASP_Y94	n/a	n/a	No literature describing a role in RCC.
TUBA1B_Y357	n/a	n/a	No literature describing a role in RCC.
TNS2_Y581	n/a	n/a	No literature describing a role in RCC.
ARAP1_Y747	n/a	n/a	No literature describing a role in RCC.
SHANK2_Y321	n/a	n/a	No literature describing a role in RCC.
GSTA1_Y132	n/a	n/a	The exosomal shuttle RNA GSTA1 was significantly decreased in the urinary extracellular vesicles of patients with ccRCC compared to healthy subjects ¹⁰² .
PYGL_Y170	n/a	n/a	No literature describing a role in RCC.
NIPSNAP1_Y148	n/a	n/a	No literature describing a role in RCC.
SDHA_Y523	n/a	n/a	SDHA is one of the four subunits of SDH, a well-recognized tumor suppressor gene involved in RCC carcinogenesis by SDH deficiency-driven HIF- α stabilization and activation, leading to increased VEGF-mediated angiogenesis. SDH deficient RCC form a distinct clinicopathological subtype of RCC ¹⁰³ .
FBP2_Y216	n/a	n/a	No literature describing a role in RCC.
HINT2_Y146	n/a	n/a	No literature describing a role in RCC.

b: phosphosites upregulated in sensitive patients (continued)

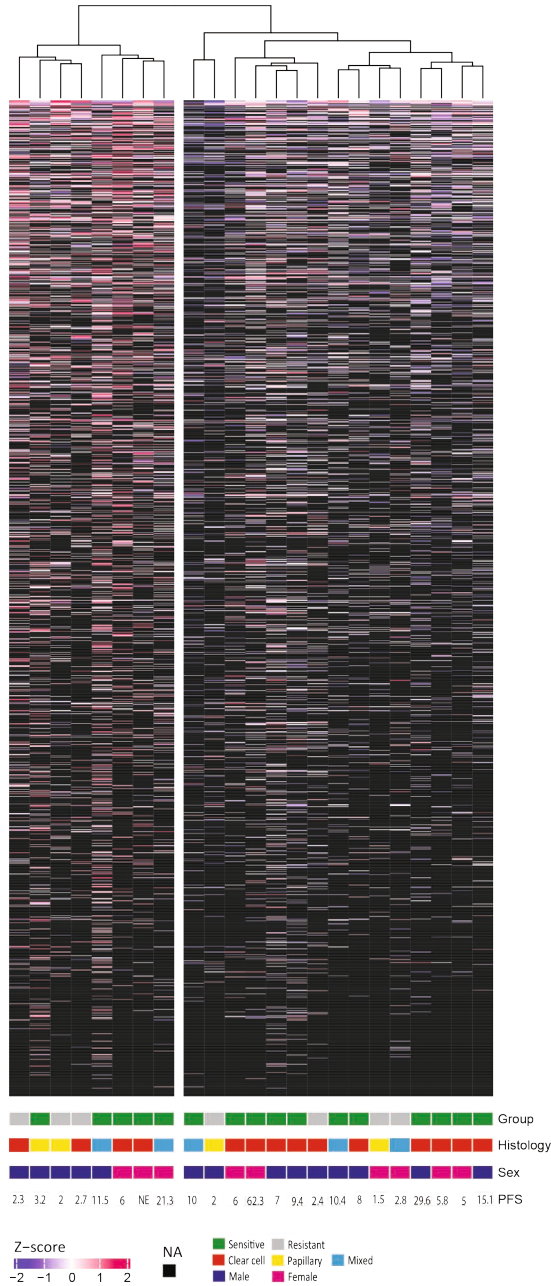
Phosphosite	p-value	FC	Role of corresponding protein in RCC
KIT_Y932	n/a	n/a	The c-KIT receptor is activated by its ligand stem cell factor (SCF) and induces several signal transduction pathways (MAPK, PI3K, AKT) and leads to mast cell activation and secretion of pro-angiogenic cytokines. In RCC, the c-KIT receptor activation induces cross-talk between cancer cells, endothelial cells and mast cells, leading to strengthening of pro-angiogenic signaling ¹⁰⁴⁻¹⁰⁶ . c-KIT receptor is one of the main targets of the multi-kinase inhibitor sunitinib.
LRRK2_Y2023	n/a	n/a	LRRK2 amplification increases MET signaling activation and promotes efficient tumor cell growth and survival in papillary renal cell cancer ¹⁰⁷ .
CARS1_Y73	n/a	n/a	No literature describing a role in RCC.
ALB_Y164	n/a	n/a	A decreased pretreatment serum albumin (ALB) level implies a poor prognosis in RCC patients, with a worse progression free and overall survival ¹⁰⁸ .
NPEPL_Y229	n/a	n/a	No literature describing a role in RCC.
CAV1_Y11	n/a	n/a	CAV1 interacts with the EGFR/RAS/ERK and PI3K/AKT pathways and promotes cell invasion, cell growth and VEGF-A secretion ¹⁰⁹ .
NDUFB9_Y118	n/a	n/a	Seven subunits of the mitochondrial complex I, among which NDUFB9, had downregulated mRNA expression in ccRCC ¹¹⁰ .
SSBP1_Y119	n/a	n/a	No literature describing a role in RCC.
PDK1_Y136	n/a	n/a	PDK1 mRNA expression is upregulated in RCC compared to normal tissue and is negatively correlated with tumor stage ¹¹¹ . In vitro, low expression of PDK1 inhibits proliferation, migration and epithelial mesenchymal transition in RCC ¹¹² .
D N A J C 1 3 _ Y1641	n/a	n/a	No literature describing a role in RCC.
F2R_Y420	n/a	n/a	No literature describing a role in RCC.
STAT5A_Y98	n/a	n/a	Dihydrotestosterone promotes cell proliferation through STAT5 activation in RCC cells ¹¹³ .

b: phosphosites upregulated in sensitive patients (continued)

	Phosphosite	p-value	FC	Role of corresponding protein in RCC
Differentially upregulated (not unique)	HSPB1_S15	0.001	-6.9	HSPB1 (=HSP27) is significantly overexpressed in RCC compared to normal kidney tissue ¹¹⁴ and when activated, attributes to promotion of cancer development and metastatic potential. Inactivation of the pathway may attenuate the invasion and migration capabilities in RCC ¹¹⁵ .
	PPA2_Y241	0.004	-4.8	No literature describing a role in RCC.
	CAVIN1_Y308	0.005	-8.6	CAVIN1/PTRF expression in ccRCC is regulated by SHC1 through the EGFR pathway. Abnormal PTRF, which is detected in exosomes from urine, could be a potential marker for ccRCC diagnosis and treatment ¹¹⁶ .
	PTK2_Y879	0.007	-3.1	Focal Adhesion Kinase (FAK/PTK2) is constitutively expressed in RCC and has a contributing role in proliferation, migration and invasion ¹¹⁷ .
	MYL6_Y86	0.009	-15.5	No literature describing a role in RCC.
	NAXD_Y85	0.012	-4.5	No literature describing a role in RCC.
	MAPK1_Y187	0.015	-3.8	Constitutive activation of the MAPK signaling cascade plays a crucial role in tumorigenesis and metastasis in RCC ¹¹⁸ . MAPK1 (=ERK2) is significantly overexpressed in RCC compared to normal tissue ¹¹⁹ .
	GSK3A_Y279	0.023	-2.3	No literature describing a role in RCC.
	TNK2_Y859	0.027	-16.9	A mutation in the ACK1 (= TNK2) ubiquitin associated domain enhances oncogenic signaling through EGFR regulation in RCC cells ¹²⁰ .
	LPP_Y295	0.028	-3.4	No literature describing a role in RCC.
	PXN_Y402	0.031	-30.6	The mRNA expression of paxillin (PXN) was upregulated in metastatic RCC cells compared to normal renal tissue. Paxillin upregulation may contribute to the pathogenicity and/or metastatic propensity of RCC and may have a role as potential marker of metastasis in RCC cells ¹²¹ .
	FGR_Y145	0.032	-13.4	FGR is one of the five highly expressed Src family kinases in ccRCC. A relation with survival or response to therapy has not been demonstrated ¹²² .
	GSK3A_S282	0.036	-2.2	No literature describing a role in RCC.
	RPS27_Y31	0.038	-11.0	No literature describing a role in RCC.
	MAPRE2_Y167	0.040	-5.3	No literature describing a role in RCC.

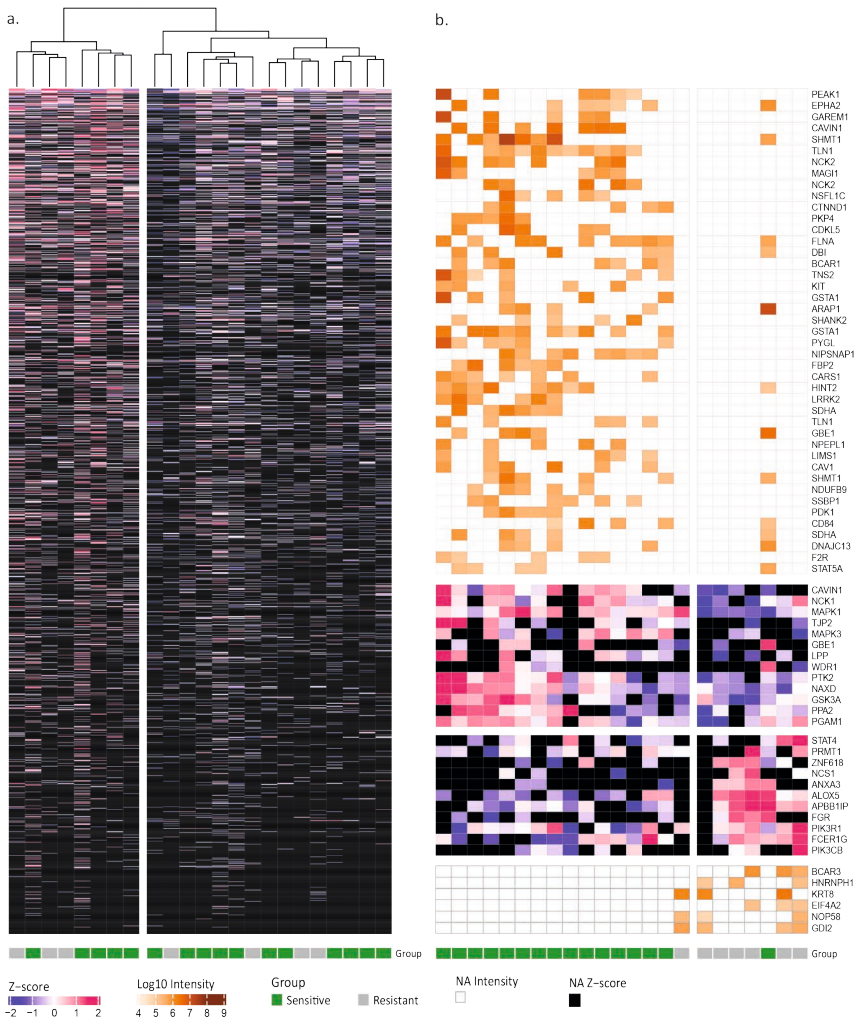
b: phosphosites upregulated in sensitive patients (continued)

Phosphosite	p-value	FC	Role of corresponding protein in RCC
MAPK1_Y187	0.041	-5.6	Constitutive activation of the MAPK signaling cascade plays a crucial role in tumorigenesis and metastasis in RCC ¹¹⁸ . MAPK1 (=ERK2) is significantly overexpressed in RCC compared to normal tissue ¹¹⁹ .
MAPK1_T185	0.041	-5.6	Constitutive activation of the MAPK signaling cascade plays a crucial role in tumorigenesis and metastasis in RCC ¹¹⁸ . MAPK1 (=ERK2) is significantly overexpressed in RCC compared to normal tissue ¹¹⁹ .
PAG1_Y317	0.042	-5.3	Overexpression of Csk-binding protein (= PAG1) is found in over 70% of RCC tissues and contributes to renal cell carcinogenesis ¹²³ .
PTPRK_Y871	0.042	-5.3	No literature describing a role in RCC.
PGAM1_Y92	0.042	-3.6	PGAM1 is highly expressed in ccRCC and correlates with clinicopathological features, such as tumor size ¹²⁴ .
CD84_Y165	0.044	-5.4	No literature describing a role in RCC.



Supplementary Figure 1. Unsupervised cluster analysis of all detected phosphosites

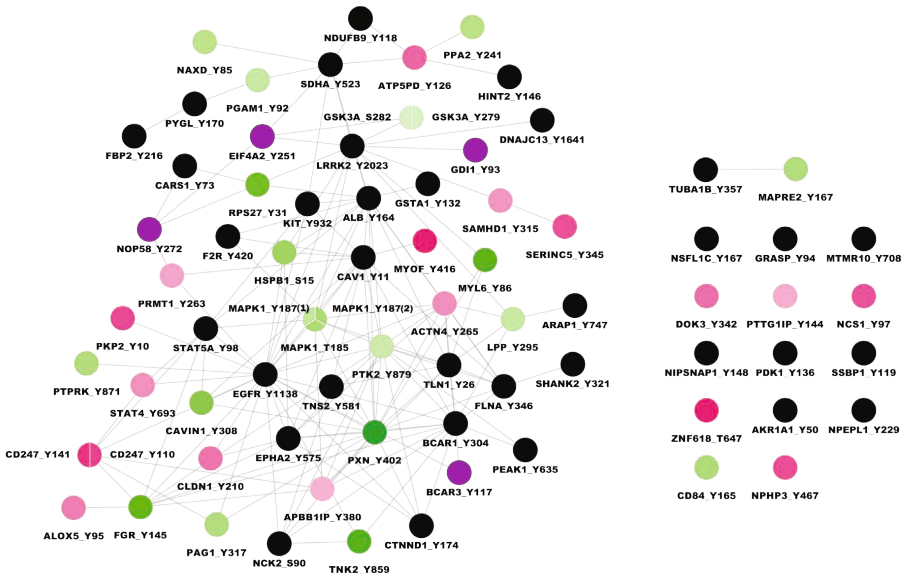
After removal of non-human entries and phosphosites with only zero intensities measured, 1596 phosphosites in 23 samples were analyzed. Group based analysis using LIMMA statistics for differential phosphorylation. No imputation of data is performed. Euclidean distance and Ward’s linkage method were used. Histology = histological subtype as determined by pathologist review; PFS = progression free survival in months; NE = not evaluable.



Supplementary Figure 2. Phosphopeptide cluster analyses in sensitive and primary resistant patients

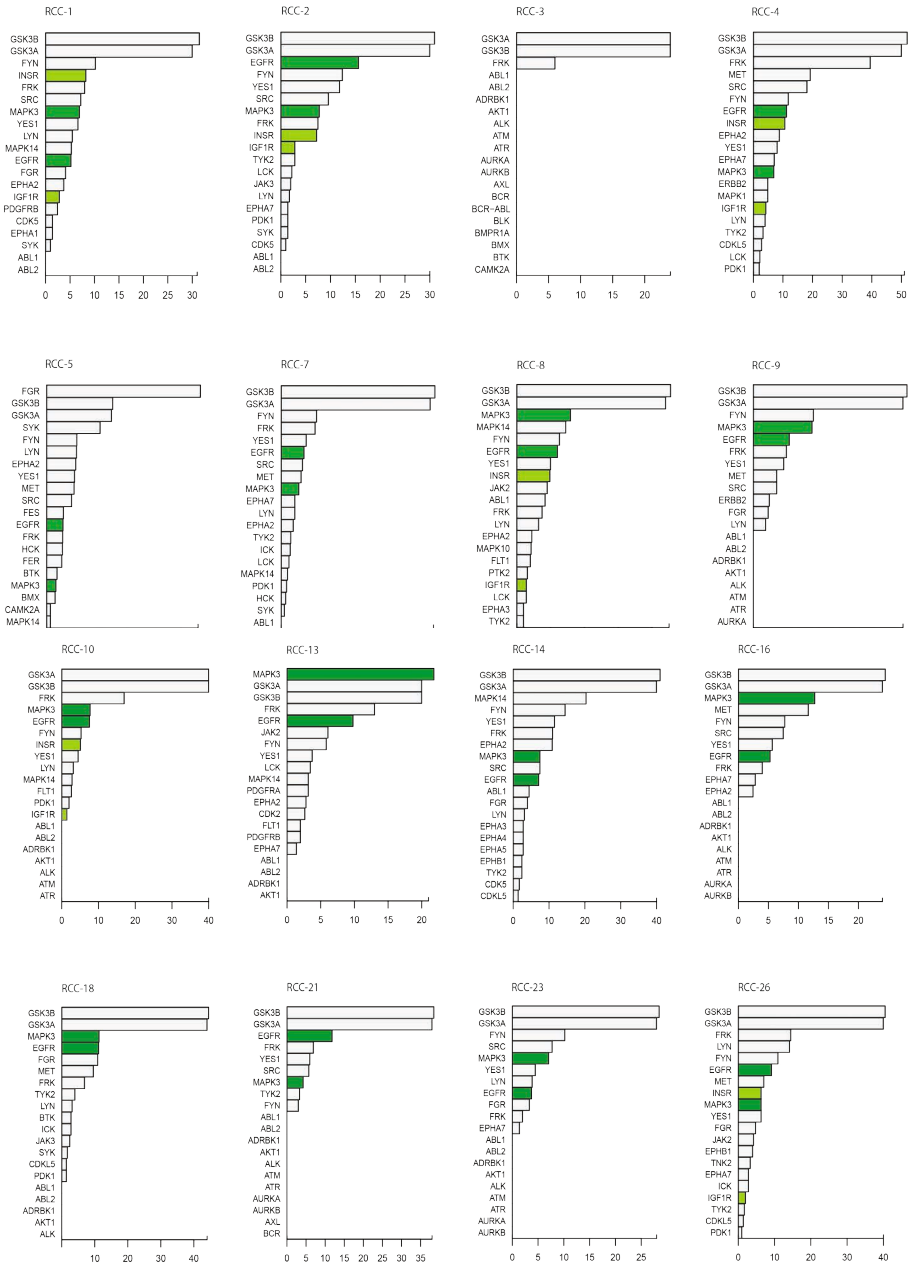
a) Unsupervised cluster analysis of identified phosphopeptides. After removal of non-human entries and phosphopeptides with only zero intensities measured, 1900 phosphopeptides were analyzed.

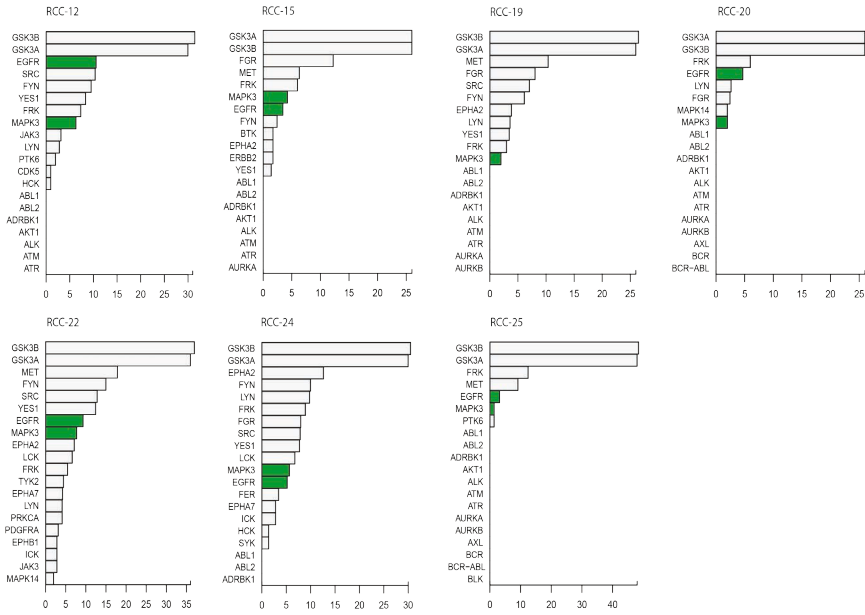
b) Supervised cluster analysis of the differentially detected phosphopeptides (n=73) in sensitive and primary resistant patients. Non-unique phosphopeptides (n=24) are filtered for $p < 0.05$, $|FC| > 2$ and $\geq 30\%$ data presence in the highest group. Unique phosphopeptides (n=49) are filtered for $\geq 30\%$ data presence. Clustering is determined by non-unique phosphopeptides. No imputation of data is performed. Euclidean distance and Ward's linkage method were used.



Supplementary Figure 3. Phosphosite interaction network of sensitive and resistant patients

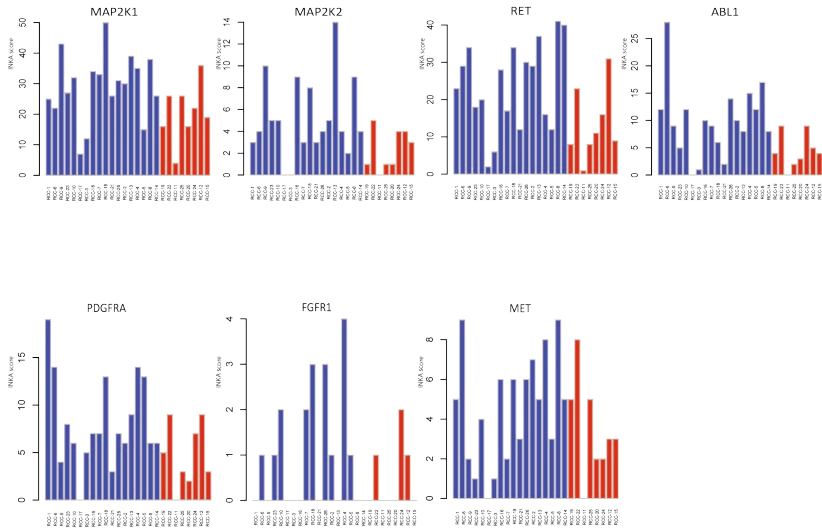
Phosphosite (p-site) interaction network. Using STRING and visualization in Cytoscape, a functional p-site cluster is shown of differentially expressed and unique p-sites in sensitive and resistant patients. Nodes correspond to upregulated p-sites. Green nodes represent p-sites differentially upregulated in tumors sensitive to sunitinib (n=21) and black nodes represent p-sites uniquely identified in tumors sensitive to sunitinib (n=35). Pink nodes represent p-sites differentially upregulated in tumors resistant to sunitinib (n=18) and purple nodes represent p-sites uniquely identified in tumors resistant to sunitinib (n=4). The differential p-sites in this figure are filtered for $p < 0.05$ & $|FC| > 2$. The unique p-sites in this figure are filtered for $\geq 30\%$ data presence in the group with highest abundance. The p-site MAPK1_Y187 is identified twice: once through quantification of a mono-phosphorylated peptide (FC = -3.81) and once through quantification of a diphosphorylated peptide (FC = -5.57).



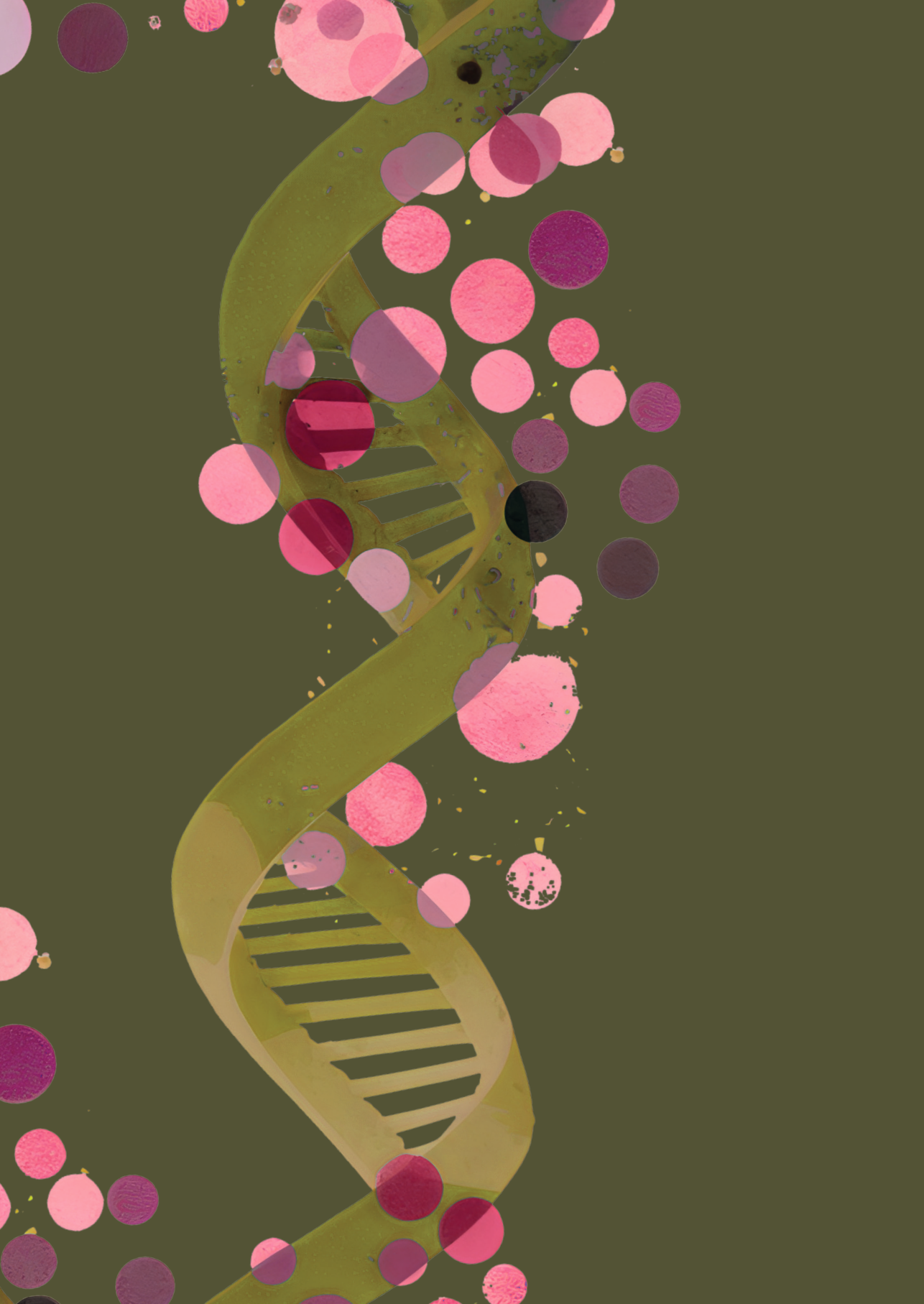


Supplementary Figure 4. Ranking of most activated kinases per sample

Ranking of the top 20 active kinases (Y-axis) in tumors from 16 sensitive and 7 resistant patients. Bar graphs depict kinase ranking based on combined INKA scores of kinase- and substrate-centric analysis of tyrosine phosphoproteomics²⁴. X-axis represents the INKA score for each kinase. Differentially activated kinases between the two groups (Figure 1c) are highlighted with dark (EGFR, MAPK3) and light (INSR/IGF1R) green coloring.



Supplementary Figure 5. Bar plots of activated kinase substrates in sensitive versus resistant patients. Activated kinase substrates that were enriched in sensitive patients (not significant), among which some of the known targets of sunitinib. X-axis: each bar represents a single patient (red = primary resistant, blue = sensitive), y-axis: INKA score of the kinase.





CHAPTER 5

Advancing wide implementation of precision oncology: A liquid nitrogen-free snap freezer preserves molecular profiles of biological samples

*Hanneke van der Wijngaart, Sahil Jagga, Henk Dekker, Richard de Goeij,
Sander R Piersma, Thang V Pham, Jaco C Knol, Babs M Zonderhuis, Harry J Hol-
land, Connie R Jiménez, Henk M W Verheul, Srinivas Vanapalli, Mariette Labots*

ABSTRACT

Purpose: In precision oncology, tumor molecular profiles guide selection of therapy. Standardized snap freezing of tissue biospecimens is necessary to ensure reproducible, high-quality samples that preserve tumor biology for adequate molecular profiling. Quenching in liquid nitrogen (LN_2) is the golden standard method, but LN_2 has several limitations. We developed a LN_2 -independent snap freezer with adjustable cold sink temperature. To benchmark this device against the golden standard, we compared molecular profiles of biospecimens.

Methods: Cancer cell lines and core needle normal tissue biopsies from 5 patients' liver resection specimens were used to compare mass spectrometry (MS)-based global phosphoproteomic and RNA sequencing profiles and RNA integrity obtained by both freezing methods.

Results: Unsupervised cluster analysis of phosphoproteomic and transcriptomic profiles of snap freezer vs LN_2 -frozen K562 samples and liver biopsies showed no separation based on freezing method (with Pearson's r 0.96 (range 0.92-0.98) and >0.99 for K562 profiles, respectively), while samples with +2 hours bench-time formed a separate cluster. RNA integrity was also similar for both snap freezing methods. Molecular profiles of liver biopsies were clearly identified per individual patient regardless of the applied freezing method. Two to 25 seconds freezing time variations did not induce profiling differences in HCT116 samples.

Conclusion: The novel snap freezer preserves high-quality biospecimen and allows identification of individual patients' molecular profiles, while overcoming important limitations of the use of LN_2 . This snap freezer may provide a useful tool in clinical cancer research and practice, enabling a wider implementation of (multi-)omics analyses for precision oncology.

INTRODUCTION

Genomic, transcriptomic and (phospho)proteomic profiling of tumor biopsies plays an increasingly important role in translational cancer research and precision oncology, the selection of therapy for patients with cancer based on their molecular tumor profile¹⁻³. Standardized high-quality (cryo)preservation to most accurately harness tumor biology of assessed tissue is a prerequisite for the generation of complex DNA, RNA and protein data^{4,5}. Cryopreservation of cells and tissues demands swift cooling to sub-freezing temperatures at which biological and enzymatic processes are slowed down or completely stopped^{6,7}. Liquid nitrogen (LN₂, -196 °C or 77K), or pre-cooled isopentane (often -80 °C) are preferred coolants to control cooling rate and prevent cryo-artifacts in tissues, allowing their structural and biochemical preservation⁸⁻¹¹. Tumor biopsies collected for research and precision oncology purposes are generally placed in a cryovial by trained staff and immediately immersed in LN₂. This process is referred to as snap freezing and currently the golden standard¹². Snap freezing is a laborious, potentially hazardous, and not user-friendly procedure. In addition, LN₂ is not widely available and the use of sacrificial LN₂ is non-sustainable due to its energy-intensive synthesis. There is an unmet need for a snap freezing device without these limitations that allows standardized optimal conservation of core needle biopsies or resected tissue for molecular profiling purposes.

We have previously described an electrically powered, novel snap freezer that is not reliant on LN₂ and has adjustable cold sink temperature that will influence the cooling rate^{8,13}. This apparatus consists of a cryocooler, Thermal Energy Storage Unit (TESU) and a gas handling system, which is transportable and easy to handle. Cooling occurs through a narrow gas-gap between the cryovial and the thermal reservoir holding the vial. Recently, we showed that the cooling rate of a vial depends on the thermal properties of the vial material (e.g. aluminum, polypropylene) and on the coolant used. The cooling rate for a LN₂-frozen tissue biopsy in an aluminum vial was about -25 °C/s¹³.

We hypothesize that this novel snap freezer will preserve quality and molecular profiles of tissue biopsies similar to and is more user-friendly than the golden standard of LN₂ quenching. To address this, we benchmarked the performance of the snap freezer prototype to the golden standard with regard to preservation of biology. Molecular profiles of snap frozen cell lines and human tissue biopsies were determined taking phosphoproteomic and transcriptomic profiles as a read out. The secondary aim of this study was to determine whether differences in freezing rate could influence the molecular profile of cancer cells.

METHODS

CELL CULTURE, LYSIS AND PROTEIN DIGESTION

Cells from chronic myeloid leukemia (CML) K562 and the colorectal cancer cell line HCT116 were cultured according to standard methods as described in Supplementary Methods.

TISSUE BIOPSY COLLECTION, LYSIS AND PROTEIN DIGESTION

Normal liver tissue biopsies were collected from five patients with cancer who underwent liver metastasectomy at Amsterdam UMC location VUmc in September 2019. Since the Dutch Medical Research Involving Human Subjects Act does not apply to normal adjacent tissue that is removed, this tissue could be used for research purposes; patients have the possibility to opt-out of the use of their residual tissue for future research. For each patient and immediately after resection, six 14 gauge core needle biopsies of adjacent normal liver tissue were taken from the resection specimen by the surgeon, placed into separate aluminum vials and snap frozen within 5 minutes. After below mentioned freezing procedures, biopsies were longitudinally cut in 10 μm sections (cryomicrotome, Leica CM1850) and processed to tumor lysates for mass spectrometry (MS)-based global phosphoproteomics as described elsewhere^{14,15}. Lysates were stored at -80°C .

BENCHMARKING PERFORMANCE SNAP FREEZER VERSUS LIQUID NITROGEN QUENCHING

Three triplicates of 5-10 ml K562 suspension cell line, each corresponding to 500 μg of protein, and 3-9 normal liver tissue biopsies per patient were snap frozen in aluminum vials by one of the following three methods: (i) cooling to -196°C by immersion in LN_2 (golden standard), (ii) cooling to -73°C in the snap freezer, and (iii) storage at room temperature for 2 hours, followed by immersion in LN_2 to -196°C (+2hr positive control). -73°C (200K) is in general accepted as an adequate temperature to preserve stability of biospecimens for storage^{16,17}. Before start of the experiments, a vessel filled with LN_2 was placed in the laboratory and the electrically powered snap freezer was pre-cooled to -73°C (200K). In each experiment, one vial was placed into the snap freezer and simultaneously another vial was immersed in LN_2 , alternatingly performed for the 2 tissue replicates or 3 cell suspension workflow replicates (Figure 1). After cooling of the vials, all vials in the experiment were transported in LN_2 and stored in a freezer at -80°C until further use.

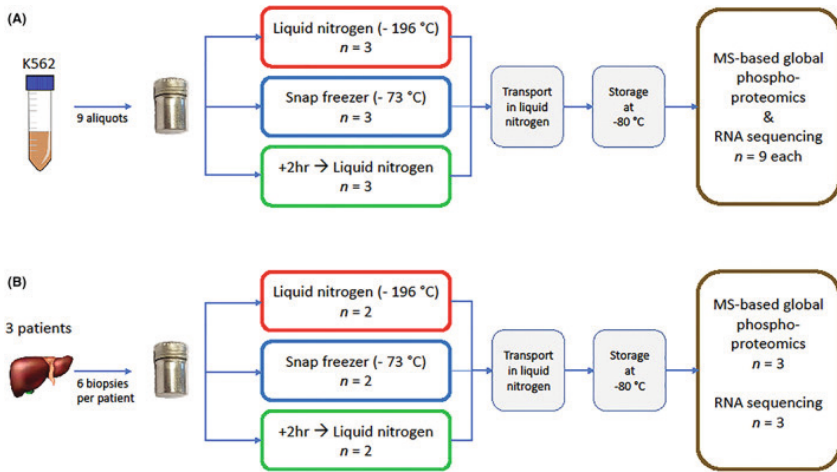


Figure 1. Benchmarking performance of snap freezer versus liquid nitrogen quenching. Study design to compare molecular profiles of biospecimen frozen using the snap freezer vs golden standard of liquid nitrogen quenching.

A. K562 suspension cell line samples frozen using liquid nitrogen ($-196\text{ }^{\circ}\text{C}$) versus snap freezer ($-73\text{ }^{\circ}\text{C}$). Positive control samples were kept at room temperature for two hours before freezing in liquid nitrogen. The surplus lysate of each of the nine samples was used for RNA extraction to perform sequencing and determine RNA integrity scores.

B. Normal human liver tissue frozen using liquid nitrogen versus snap freezer (2 biological replicates per condition). From each biological replicate, one sample was processed for global (TiOx) phosphoproteomics and one sample was processed for RNA extraction to perform sequencing and determine RNA integrity scores.

INFLUENCE OF FREEZING RATE ON PHOSPHOPROTEOMICS PROFILE

Fifteen aliquots of $300\ \mu\text{l}$ HCT116 lysate, each corresponding to $300\text{--}400\ \mu\text{g}$ of protein, were placed in three types of vials with different thermal conduction properties (polypropylene, aluminum and aluminum vials covered in paper tape) to influence their freezing rates. For each condition three vials were individually immersed in either LN_2 or precooled isopentane for 1 minute and cooled to a temperature of $-196\text{ }^{\circ}\text{C}$ or $-80\text{ }^{\circ}\text{C}$, respectively, using a stainless steel vial holder. Pre-cooled isopentane was tested as second coolant, because at room temperature, isopentane (with boiling point of $36.9\text{ }^{\circ}\text{C}$) is in liquid phase. Therefore, no boiling occurs and the cooling rate is not subjected to the Leidenfrost effect, which is the phenomenon that a vapor layer is formed that prevents heat transfer^{18,19}. The aluminum vial covered in paper tape was not immersed in isopentane, because previously published experiments have shown that this vial was not subjected to the Leidenfrost effect in LN_2 ²⁰. After adequate cooling, vials were transported using a LN_2 container and stored at $-80\text{ }^{\circ}\text{C}$ until further use.

PHOSPHOPROTEOMICS: PHOSHOPEPTIDE ENRICHMENT, LC-MS/MS MEASUREMENT, PROTEIN IDENTIFICATION AND LABEL-FREE PHOSHOPEPTIDE QUANTIFICATION

K562 and HCT116 cell lysate aliquots and tissue lysates were reduced, alkylated and digested as described previously¹⁴. Desalted peptides were enriched for phosphopeptides using titanium oxide (TiOx) beads based using aliphatic hydroxy-acid modified metal oxide chromatography^{21,22}. Further sample preparation details are provided in Supplementary Methods. Phosphopeptides were separated by nanoLC and detected as described previously^{21,23,24} on a Q exactive HF mass spectrometer (Thermo Fisher, Bremen, Germany). Protein identification and phosphopeptide quantification were performed as previously described¹⁴. In short, LC-MS/MS spectra were searched against the Uniprot human reference proteome FASTA file (release February 2019, 42417 entries, no fragments) using MaxQuant 1.6.4.0²⁵. (Phospho)peptide identifications were propagated across samples using the match-between-runs option checked. Searches were performed as previously described in detail with the label-free quantification option selected²⁴. Phosphopeptides were quantified by their extracted ion chromatograms ('Intensity' in MaxQuant). For each sample the phosphopeptide intensities were normalized on the median intensity of all identified peptides in the sample ('normalized intensity' from the MaxQuant Evidence table). Further details are provided in the Supplementary Methods.

RNA EXTRACTION AND INTEGRITY, RNA SEQUENCING

Tissue: Dissection of fresh frozen biopsies was performed at -25°C in a cryotome. Twenty micrometer sections were cut and snap frozen in liquid nitrogen and stored at -80°C until RNA extraction. RNA was isolated from the tissue specimens and the surplus of K562 cell suspension samples used for the phosphoproteomics analysis, using the RNeasy Plus Mini K (Qiagen) according to the manufacturers protocol, eluted in 30 μl nuclease free water and quantified using a NanoDrop One UV-Vis Spectrophotometer (Thermo Scientific). To analyze differences in RNA integrity between samples processed in different freezing conditions, the RNA Integrity Number (RIN) was determined using the RNA 6000 Picochip (Bioanalyzer 2100, Agilent). The Bioanalyzer 2100 quality and quantity measures were collected from the automatically generated Bioanalyzer result reports using default settings. Next generation sequencing (NGS) using Illumina's TruSeq Small RNA Sample Preparation protocol and data filtering were performed as previously described²⁶. Illumina's TruSeq Small RNA Sample Preparation protocol was used for the generation of cDNA libraries. These libraries were amplified on the flow cells with Illumina's cluster station (Illumina Inc, San Diego, CA, USA) and sequenced using Illumina's HiSeq 2000 (Illumina Inc, San Diego, CA, USA). Further details are provided in Supplementary Methods.

RESULTS

BENCHMARKING OF SNAP FREEZER VERSUS LIQUID NITROGEN QUENCHING IN MOLECULAR PROFILING

Cancer cell line samples Using a snap freezer at -73°C and the cold sink temperature of LN_2 ¹³, a comparative analysis of the phosphoproteome and transcriptome of suspension cell line K562 was performed (Figure 1A). Mass spectrometry-based global phosphoproteomics was successfully performed on all nine (3 triplicates) K562 cell suspension lysate samples. A total of 16,341 unique peptides were identified of which 14,835 (90.8%) were phosphorylated. The median number of phosphopeptides per sample was 10,357 (range 9,317 – 10,735). The number of identified phosphopeptides did not differ significantly between both freezing methods ($p = 0.44$ by students' t-test). A total of 14,812 unique phosphosites were identified (83.4% serine, 15.2% threonine and 1.4% tyrosine), with a median of 9,502 (range 8,306 – 9,871) per sample. Unsupervised cluster analysis of phosphosites did not show separation of samples processed in LN_2 from samples processed in the snap freezer (Figure 2A). Comparison of the nine study samples with each other showed high Pearson correlations (median r 0.96 (range 0.92-0.98) for either direct freezing method) while the positive control samples with 2 additional hours of bench-time did cluster separately. (Supplementary Figure 1A); 4,789 phosphopeptides (29% of total number of identified phosphopeptides) were shared between all samples (Figure 2B). Next, a read-out at the transcriptomic level was used to compare LN_2 - versus snap freezer-based biospecimen freezing. No significant difference was observed in RNA integrity between cell line samples processed using the two freezing methods, including the +2hr positive controls, indicating that integrity of the RNA molecules is preserved by the snap freezer (Table 1). Also, RNA molecules were shown to be stable after 2 hours at room temperature (Table 1). Unsupervised cluster analysis of the 100 most variably expressed genes showed two main clusters, one smaller consisting of the three positive control samples; the second cluster was a mixed cluster of samples processed using either method (Figure 2C). The two snap freezing methods could not be distinguished based on the RNA expression profiles, even when selecting only the top 100 varying genes between the samples for clustering analysis. Again, comparison of all separate samples with each other showed very high correlation (Pearson's $r > 0.99$, Supplementary Figure 1B).

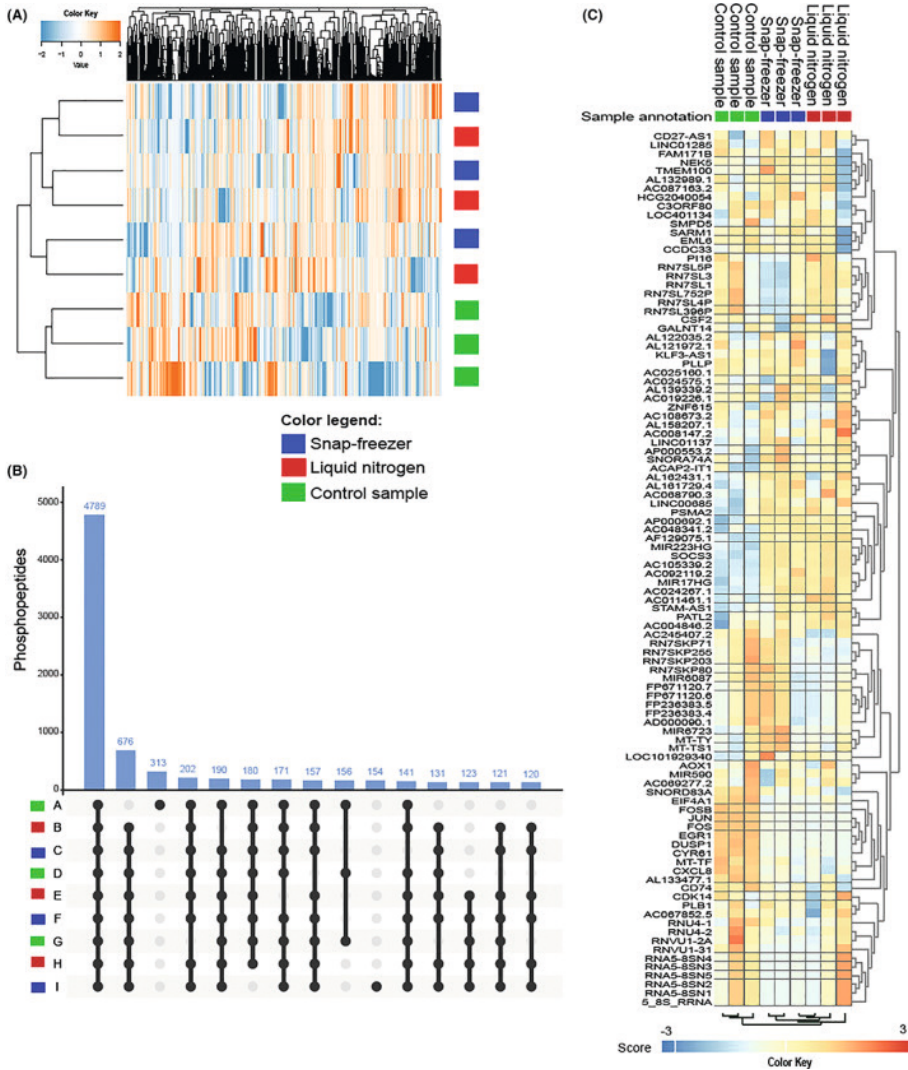


Figure 2. Benchmark of molecular profile preservation using K562 cancer cells. Profile preservation benchmarking using snap freezer vs liquid nitrogen.

A. Unsupervised cluster analysis of all identified phosphosites of K562 suspension aliquots does not cluster samples frozen by liquid nitrogen separately from those frozen by the snap freezer, but clearly separates the +2hr positive control samples. Color key indicates Z-scores.

B. UpSet plot indicating the number of overlapping phosphopeptides shared between (subsets of) the nine K562 samples. Fifteen out of 511 overlaps are shown, covering 51% of the data.

C. Unsupervised cluster analysis of RNA expression of 100 most varying genes does not cluster samples frozen using liquid nitrogen or the snap freezer together, but separates the +2hr positive control samples. Color key indicates Z-scores.

Table 1. RNA integrity of cell line samples processed with different freezing methods. Aluminum vials with lysates of K562 suspension cell line were alternately snap-frozen in the snap freezer or in liquid nitrogen. Three samples were left at room temperature for two hours before freezing in liquid nitrogen as a positive control sample. RIN, RNA integrity numbers.

Freezing method	RIN value		
	Replicate 1	Replicate 2	Replicate 3
Liquid nitrogen	9,40	9,50	9,30
Snap freezer	9,10	9,30	9,20
+2hr Control sample	9,40	9,20	9,30

Normal liver tissue biopsies Characteristics and analysis details of five consecutive patients who underwent liver surgery are presented in Supplementary Table 1. For patient 01 only 3 normal liver tissue biopsies were available (phosphoproteomics) and for patients 02, -03- and -04, 6 biopsies per patient could be evaluated for phosphoproteomics, RNA integrity analysis and RNA sequencing. These biopsies were snap-frozen alternately using the three freezing methods (Figure 1B). In total, twelve 14G core needle biopsies from four patients were processed for global phosphoproteomics, with a median protein input of 500 µg per sample. A total of 15,262 unique peptides were identified, of which 10,395 (68%) were phosphorylated. The median number of phosphopeptides per sample was 6,742 (range 5535 – 7601). A total of 9,966 phosphosites were identified (86% serine, 13% threonine and 1% tyrosine), with a median of 5794 (range 4710 – 6573) per sample. Unsupervised clustering of the phosphoproteome revealed clear separation of replicates from the four patients (Figure 3A). Subclustering of snap freezer- and LN₂-frozen samples, separate from the +2hr controls, was observed in 2 of 4 patients. RNA isolation was successfully performed in tissues from 2 of 3 last mentioned patients. An additional set of nine liver biopsies was obtained from a fifth patient (05, Supplementary Table 1). RNA quality was insufficient in one of the biopsies, leaving 11 samples for downstream analysis. There were no significant differences in RIN values between the samples processed using the 2 freezing methods ($p = 0.89$ by t-test). Samples that were left at room temperature for 2 hours before immersion in LN₂ had RIN values comparable to the other two freezing conditions, indicating that RNA is a stable molecule, even after a prolonged cold ischemia time (Supplementary Table 1). After RNA sequencing, unsupervised cluster analysis of gene expression profiles showed a clear separation of the samples from individual patients (Figure 3B).

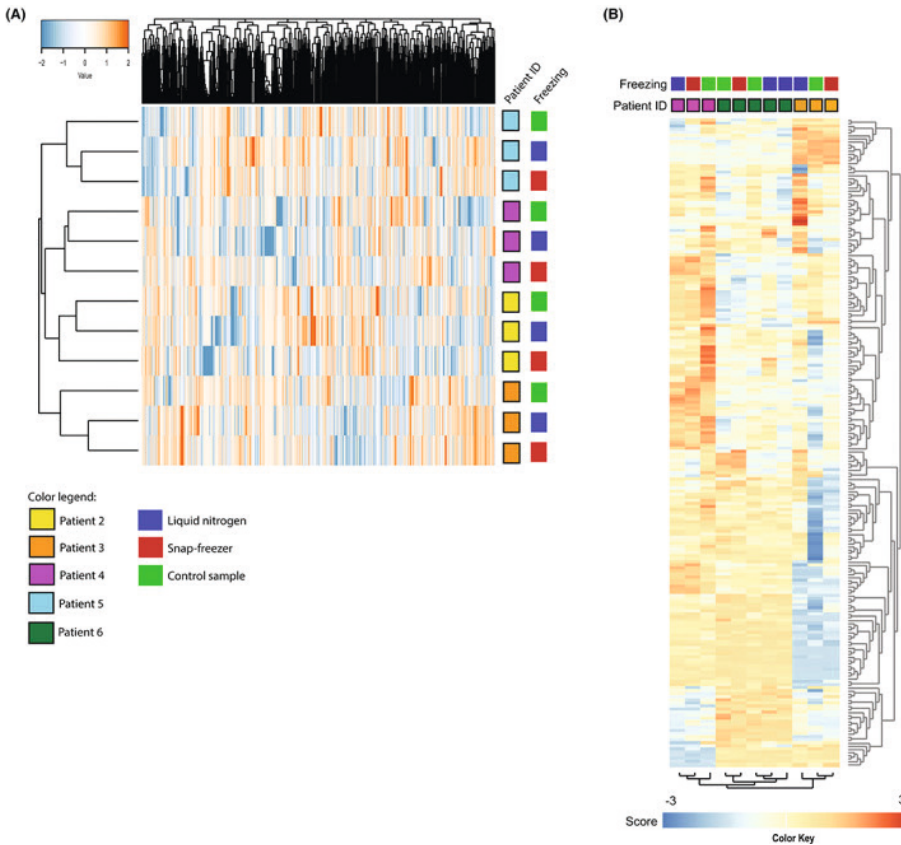


Figure 3. Benchmark of molecular profile preservation of normal liver biopsies from patients with cancer. Molecular profile preservation benchmark of snap freezer vs liquid nitrogen.

A. Unsupervised cluster analysis of the phosphoproteome of liver tissue samples of four individual patients shows that patient-specific profiles can clearly be identified in samples snap frozen in the snap freezer as well as in liquid nitrogen. Color key indicates Z-scores.

B. Unsupervised cluster analysis of RNA expression of 100 most variable genes shows that 3 individual patient profiles can be clearly identified using samples processed in both freezing methods. Color key indicates Z-scores.

EFFECT OF DIFFERENT FREEZING RATES ON PHOSPHOPROTEOMIC PROFILES

Three types of vials with different thermal conduction properties (polypropylene, aluminum and aluminum vials covered in paper tape) and two coolants (LN₂ and pre-cooled isopentane) were used to determine differences in freezing rate of HCT116 cancer cell lines samples to reach -80 °C³ (Supplementary Figure 2). Polypropylene vials immersed in LN₂ versus pre-cooled isopentane had a mean freezing time of 2 versus 25 seconds (s), respectively, while aluminum vials without paper tape covering had freezing times of 4 s in LN₂ and 10 s in isopentane (Table 2). To study whether changes to the phosphoproteome would be detectable in samples from

vials with shortest vs longest (2 vs 25 seconds) freezing time, polypropylene vials frozen in LN₂ vs isopentane were selected for molecular analysis by MS-based global phosphoproteomics. This was successfully performed in five out of six samples. One LN₂-cooled sample was lost due to a technical error in the mass spectrometer. A total of 8597 unique peptides were identified of which 5726 (66.6 %) were phosphorylated, reflecting adequate enrichment for phosphopeptides. The median number of identified phosphopeptides per sample (500 µg protein input/sample) was 4668 (range 4035 - 4780). A total of 5643 unique phosphosites were identified (phosphorylated in 87% at serine residues, 12% threonine and 1% tyrosine), with a median of 4127 (range 3765 - 4251) phosphosites per sample. Unsupervised clustering of the global phosphoproteome did not separate HCT116 samples frozen in polypropylene vials of 2 seconds versus 25 seconds freezing rates (Figure 4A). Fifty-one percent of all identified phosphopeptides were present in all 5 samples and only ≤ 1.6% were uniquely identified in one of the samples; 47-48% of identified phosphopeptides per sample were present in at least one other sample (Figure 4B). The overlap between workflow replicates (47% for LN₂ and 51% for isopentane, data not shown) was comparable to the overlap between the different conditions (51% as per the Venn diagram in Figure 4B). The correlation between all samples was high (Pearson's r 0.93 – 0.99, Figure 4C).

Table 2. Three different types of vials containing HCT116 lysate were immersed in either liquid nitrogen (-196 °C) or pre-cooled isopentane (-80 °C) (Figure 2). The time in seconds (s) elapsed from the point of room temperature until the vials reached a temperature of -80 °C. Three technical replicates per freezing condition were used.

Vial type	Liquid nitrogen	Precooled isopentane
Aluminum	4 s	10 s
Polypropylene	2 s	25 s
Aluminum covered in paper tape	< 2 s	N/A

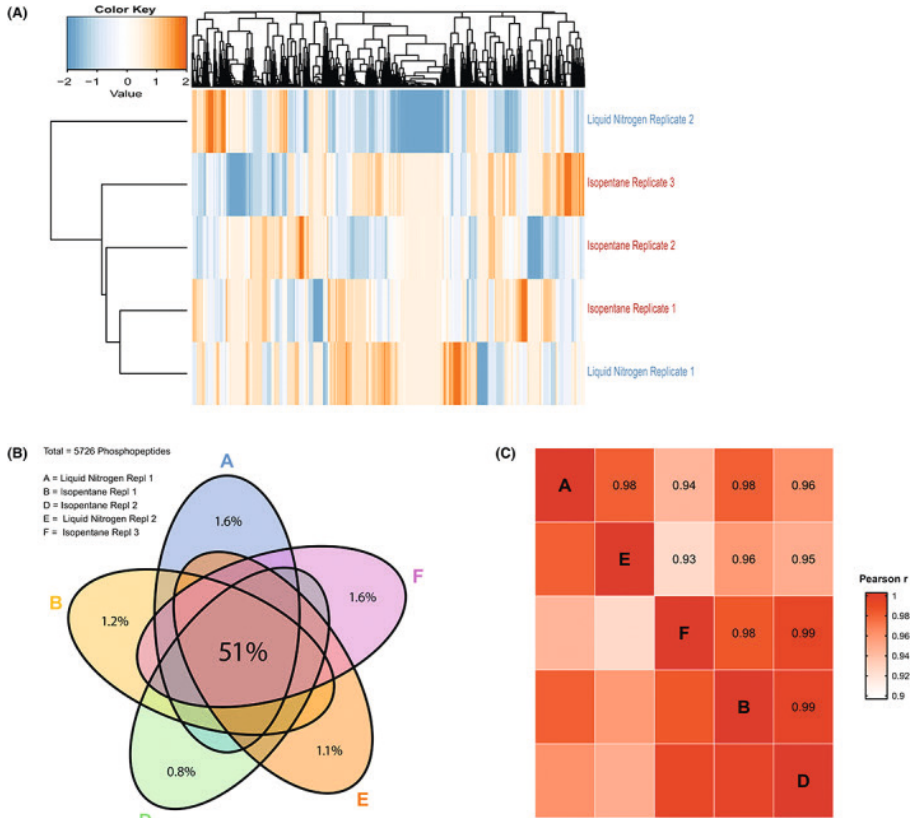


Figure 4. Effect of freezing rate on HCT116 phosphoproteomic profile. Effect of freezing rate on the phosphoproteome of cancer cell line HCT116. HCT116 samples were frozen in polypropylene vials in either liquid nitrogen (-196°C , in 2 seconds, $N = 2$; one sample was lost due to a technical error in the mass spectrometer) or in 25 seconds using pre-cooled isopentane (-80°C , $N = 3$).

A. Unsupervised cluster analysis of all identified phosphopeptides does not separate samples with highest vs lowest freezing rate.

B. Venn diagram of overlapping phosphopeptides between all five samples shows reproducible phosphopeptide identification regardless of freezing rate.

C. Correlation by Pearson's r shows high correlation between phosphoproteomic profiles of samples frozen at high vs lower rate.

DISCUSSION

Snap freezing of core needle biopsies by quenching in liquid nitrogen (LN₂) is the golden standard to preserve tumor biology and allow profiling for precision medicine purposes at the DNA, RNA and (phospho)protein level, but the use of LN₂ has several disadvantages. We have previously developed a LN₂-independent, electrically powered and mobile snap freezer with adjustable cold sink temperature¹³. Comparing the novel snap freezer with the golden standard of LN₂ quenching, we here show that MS-based phosphoproteomic and transcriptomic profiles of cancer cell line K562 and human liver biopsies are preserved (Figure 2 and 3). Phosphoproteome differences between individual patients were larger than potential differences induced by either freezing method (Figure 3A). Gene expression profiling by RNA sequencing corroborated these findings (Figure 3B). These findings are important, because MS-based phosphoproteomics and RNA sequencing profiles are sensitive to variation induced by differences in pre-analytical handling that impact tissue integrity. Ultimately, such variations would hamper extrapolation and implementation of research findings to the general patient population^{27,28}. In particular, cold ischemia time can alter the (phospho)proteome and transcriptome²⁹⁻³¹. While DNA in tumor tissue remains stable after one hour of cold ischemia time^{32,33}, earlier studies describe multiple examples of altered protein and mRNA expression within 15-30 minutes and phosphorylation as early as after 5 minutes of cold ischemia time³⁴⁻³⁷. Remarkably, MS-based phosphotyrosine (pY)-phosphoproteomic profiles from acute myeloid leukemia samples were recently shown to remain relatively stable after a 4-hour delay of sample processing³⁸. These results may indicate that the impact of pre-analytical variation may differ for hematological specimens vs solid tumor biopsies, but need further confirmation. In general, standard methods resulting in reliable results with minimal variation are prerequisites for application in precision oncology. Here, we found that the novel snap freezer is fulfilling this requirement by showing that molecular profiles of cell lines and individual patients' biopsies were maintained.

In addition, the effect of freezing rate differences on the phosphoproteomic profile of a cancer cell line was evaluated. Freezing rates that are too low will damage the cell membrane, likely due to increased solute concentration caused by volume reduction of liquid surrounding the cells³⁹, while ultra-rapid cooling may lead to damage through devitrification and ice crystal formation upon storage including the Leidenfrost phenomenon²⁰. We here found that differences in freezing rate up to 23 seconds to a goal temperature of -73 °C did not induce significant changes in phosphoproteomic profiles (Figure 4) indicating that a freezing rate faster than achieved with the snap freezer and with LN₂ is unnecessary. Increasing the freezing rate by overcoming the Leidenfrost effect will not further improve preservation of the molecular profile of a biological sample. Together, these results imply that this snap freezer is of valid use in clinical setting, eliminating the need for harmful coolants and preventing technical and practical challenges of LN₂ for cryopreservation. Alternative snap freezing solutions have been developed to circumvent the limitations of liquid nitrogen, but each of them has limitations in terms of mobility or cooling performance^{40,41}.

As *in vivo* profiling of (tumor) tissue is impossible, one cannot perform molecular profiling without potentially inducing any procedure-related effect. It is impossible to determine which of both snap freezing methods preserves *in vivo* profiles best. Cancer cell samples left at room temperature for two hours prior to snap freezing were used as a control to show that profiles do change in time. However, when optimal sampling of biospecimens is clinically implemented, no significant differences in molecular profiles are expected based on the freezing rate experiments as described here. This study was designed to compare technical replicates. Although the included clinical sample size was small, results were consistent throughout all comparisons of both phosphoproteomic and RNA sequencing analyses.

In conclusion, the novel snap freezer prototype identifies similar protein- and RNA-based molecular profiles of biological samples including individual patient tissues as obtained with the golden standard of LN₂ quenching. Importantly, this snap freezer overcomes several practical limitations of LN₂ and may provide a useful tool enabling wider implementation of (multi-) omics analyses for precision oncology. Feasibility and usability for snap freezing tumor biopsies in the context of a (precision oncology) clinical trial or the routine clinical setting should be assessed as the next critical step towards its implementation and commercial development.

ACKNOWLEDGEMENT

This publication is part of the project CryoON - Cryogenics meets Oncology: A novel cryogenic device to snap-freeze and transport biopsies (with project number 14014-CryoON) of the research programme which is (partly) financed by the Dutch Research Council (NWO).

REFERENCES

1. Mateo, J., *et al.* Delivering precision oncology to patients with cancer. *Nat Med* **28**, 658-665 (2022).

2. Rodriguez, H., Zenklusen, J.C., Staudt, L.M., Doroshow, J.H. & Lowy, D.R. The next horizon in precision oncology: Proteogenomics to inform cancer diagnosis and treatment. *Cell* **184**, 1661-1670 (2021).

3. Malone, E.R., Oliva, M., Sabatini, P.J.B., Stockley, T.L. & Siu, L.L. Molecular profiling for precision cancer therapies. *Genome Med* **12**, 8 (2020).

4. Barnes, R.O., Parisien, M., Murphy, L.C. & Watson, P.H. Influence of evolution in tumor biobanking on the interpretation of translational research. *Cancer Epidemiol Biomarkers Prev* **17**, 3344-3350 (2008).

5. Tang, W., Hu, Z., Muallem, H. & Gulley, M.L. Quality assurance of RNA expression profiling in clinical laboratories. *J Mol Diagn* **14**, 1-11 (2012).

6. Mazur, P. Stopping biological time. The freezing of living cells. *Ann NY Acad Sci* **541**, 514-531 (1988).

7. Baust, J.G., Gao, D. & Baust, J.M. Cryopreservation: An emerging paradigm change. *Organogenesis* **5**, 90-96 (2009).

8. Srinivas Vanapalli, S.J., Harry Holland, Marcel ter Brake. A tissue snap-freezing apparatus without sacrificial cryogens. *IOP Conf. Ser.: Mater. Sci. Eng.* **278**(2017).

9. Mazur, P. Cryobiology: the freezing of biological systems. *Science* **168**, 939-949 (1970).

10. Hunt, C.J. Cryopreservation: Vitrification and Controlled Rate Cooling. *Methods Mol Biol* **1590**, 41-77 (2017).

11. Steu, S., *et al.* A procedure for tissue freezing and processing applicable to both intra-operative frozen section diagnosis and tissue banking in surgical pathology. *Virchows Arch* **452**, 305-312 (2008).

12. Engel, K.B., Vaught, J. & Moore, H.M. National Cancer Institute Biospecimen Evidence-Based Practices: A Novel Approach to Pre-analytical Standardization. *Biopreservation and Biobanking* **12**, 148-150 (2014).

13. van Limbeek, M.A.J., Jagga, S., Holland, H., Ledebor, K., Ter Brake, M. & Vanapalli, S. Cooling of a vial in a snapfreezing device without using sacrificial cryogens. *Sci Rep* **9**, 3510 (2019).

14. Labots, M., *et al.* Kinase Inhibitor Treatment of Patients with Advanced Cancer Results in High Tumor Drug Concentrations and in Specific Alterations of the Tumor Phosphoproteome. *Cancers (Basel)* **12**(2020).

15. Labots, M., *et al.* Phosphotyrosine-based-phosphoproteomics scaled-down to biopsy level for analysis of individual tumor biology and treatment selection. *J Proteomics* **162**, 99-107 (2017).

16. Jewell, S.D., *et al.* Analysis of the molecular quality of human tissues: an experience from the Co-operative Human Tissue Network. *Am J Clin Pathol* **118**, 733-741 (2002).

17. Hubel, A., Spindler, R. & Skubitz, A.P. Storage of human biospecimens: selection of the optimal storage temperature. *Biopreserv Biobank* **12**, 165-175 (2014).

18. Bourrienne, P., Lv, C. & Quere, D. The cold Leidenfrost regime. *Sci Adv* **5**, eaaw0304 (2019).

19. Song, Y.S., *et al.* Vitrification and levitation of a liquid droplet on liquid nitrogen. *Proc Natl Acad Sci U S A* **107**, 4596-4600 (2010).

20. van Limbeek, M.A.J., Nes T.H., Vanapalli, S. Impact dynamics and heat transfer characteristics of liquid nitrogen drops on a sapphire prism. *International Journal of Heat and Mass Transfer* **148**, 1-8 (2020).

21. Piersma, S.R., *et al.* Feasibility of label-free phosphoproteomics and application to base-line signaling of colorectal cancer cell lines. *J Proteomics* **127**, 247-258 (2015).

22. Sugiyama, N., Masuda, T., Shinoda, K., Nakamura, A., Tomita, M. & Ishihama, Y. Phosphopeptide enrichment by aliphatic hydroxy acid-modified metal oxide chromatography for nano-LC-MS/MS in proteomics applications. *Mol Cell Proteomics* **6**, 1103-1109 (2007).

23. van der Mijn, J.C., *et al.* Evaluation of different phospho-tyrosine antibodies for label-free phosphoproteomics. *Journal of Proteomics* **127**, 259-263 (2015).

24. Beekhof, R., *et al.* INKA, an integrative data analysis pipeline for phosphoproteomic inference of active kinases (vol 15, e8250, 2019). *Mol Syst Biol* **15**(2019).

25. Cox, J. & Mann, M. MaxQuant enables high peptide identification rates, individualized p.p.b.-range mass accuracies and proteome-wide protein quantification. *Nat Biotechnol* **26**, 1367-1372 (2008).

26. Neerinx, M., *et al.* MiR expression profiles of paired primary colorectal cancer and metastases by next-generation sequencing. *Oncogenesis* **4**(2015).

27. Mager, S.R., *et al.* Standard operating procedure for the collection of fresh frozen tissue samples. *Eur J Cancer* **43**, 828-834 (2007).

28. Morente, M.M., *et al.* TuBaFrost 2: Standardising tissue collection and quality control procedures for a European virtual frozen tissue bank network. *Eur J Cancer* **42**, 2684-2691 (2006).

29. Zhou, J.H., Sahin, A.A. & Myers, J.N. Biobanking in genomic medicine. *Arch Pathol Lab Med* **139**, 812-818 (2015).

30. Agrawal, L., Engel, K.B., Greytak, S.R. & Moore, H.M. Understanding preanalytical variables and their effects on clinical biomarkers of oncology and immunotherapy. *Semin Cancer Biol* **52**, 26-38 (2018).

31. Lee, J.E. & Kim, Y.Y. Impact of Preanalytical Variations in Blood-Derived Biospecimens on Omics Studies: Toward Precision Biobanking? *Omics* **21**, 499-508 (2017).

32. Johnsen, I.K., *et al.* Evaluation of a standardized protocol for processing adrenal tumor samples: preparation for a European adrenal tumor bank. *Horm Metab Res* **42**, 93-101 (2010).

33. MG, P. & MS, R. Influence of Cold Ischemia Time and Storage Period on DNA Quality and Biomarker Research in Biobanked Colorectal Cancer Tissues. *Kosin Medical Journal* **35**, 26-37 (2020).

34. Bray, S.E., *et al.* Gene expression in colorectal neoplasia: modifications induced by tissue ischaemic time and tissue handling protocol. *Histopathology* **56**, 240-250 (2010).

35. Buffart, T.E., *et al.* Time dependent effect of cold ischemia on the phosphoproteome and protein kinase activity in fresh-frozen colorectal cancer tissue obtained from patients. *Clinical Proteomics* **18**(2021).

36. Freidin, M.B., Bhudia, N., Lim, E., Nicholson, A.G., Cookson, W.O. & Moffatt, M.F. Impact of collection and storage of lung tumor tissue on whole genome expression profiling. *J Mol Diagn* **14**, 140-148 (2012).

37. Mertins, P., *et al.* Ischemia in Tumors Induces Early and Sustained Phosphorylation Changes in Stress Kinase Pathways but Does Not Affect Global Protein Levels. *Mol Cell Proteomics* **13**, 1690-1704 (2014).

38. van Alphen, C., *et al.* Phosphotyrosine-based Phosphoproteomics for Target Identification and Drug Response Prediction in AML Cell Lines. *Mol Cell Proteomics* **19**, 884-899 (2020).

39. Mazur, P. Freezing of living cells: mechanisms and implications. *Am J Physiol* **247**, C125-142 (1984).

40. Kennedy, J.J., *et al.* Preserving the Phosphoproteome of Clinical Biopsies Using a Quick-Freeze Collection Device. *Biopreservation and Biobanking* **20**, 436-445 (2022).

41. <https://www.cryobiosystem.com/wp-content/uploads/2019/12/Flyer-Digitcool-2019.pdf>.

SUPPLEMENTARY METHODS

PATIENT SAMPLES

This study received approval from the Amsterdam UMC Biobank under study number BUP2019-12. Regular diagnostic procedures were not hindered by the collection of the study biopsies.

CELL LINES

K562 chronic myeloid leukemia (CML) cells were obtained from the ATCC and cultured in DMEM medium supplemented with 10% FBS (Biowest, France). Cells were maintained at 37 °C and expanded in a T175 culture flasks. Nine aliquots of 10 ml cell suspension (exponential growth phase) were transferred into a 50 ml tube and centrifuged for 2 minutes at 300g and the supernatant was removed. Cells were washed twice in phosphate-buffered saline (PBS) and centrifuged for 2 minutes at 300g before being resuspended in 1 ml PBS and transferred in the aluminum vial. The vial was placed into a 50 ml tube and centrifuged for 1 minute at 300g rpm, after which PBS was removed and the pellet of cells remained on the bottom of the vial. The vials subsequently entered their respective freezing procedures, see below, and were stored at -80 °C until further processing.

Cells from the colorectal cancer cell line HCT116 were cultured in biological triplicates in DMEM medium (Lonza Biowhittaker, Verviers, Belgium) containing 10% fetal bovine serum, 2 mM glutamine, 100 IU/ml sodium penicillin and 100 µg/ml streptomycin. Cells were lysed in lysis buffer containing 9 M urea, 20 mM HEPES pH 8.0, 1 mM Na₃VO₄ (orthovanadate), 2.4 mM Na₄P₂O₇ (pyrophosphate), and 1 mM Na₂C₃H₇PO₆ (β-glycerophosphate) by scraping and subsequent sonication. After lysis, protein concentration was determined using the BCA method (ThermoPierce, Rockford, IL). Cell lysate was reduced in 4 mM dithiotreitol (DTT) for 20 minutes at 60 °C, cooled to room temperature and alkylated in 10 mM iodoacetamide for 15 minutes in the dark. Next, the cell lysate was diluted to 2 M urea using 20 mM HEPES buffer pH 8.0 and digested overnight with trypsin (10 µg/mg protein) at 37 °C. Digestion was stopped in 0.1% trifluoroacetic acid (TFA).

PHOSPHOPEPTIDE ENRICHMENT AND LC-MS/MS MEASUREMENT FOR PHOSPHOPROTEOMICS

HCT116 cell lysate aliquots of 300-400 µg protein, K562 cell lysate aliquots of 500 µg protein and tissue lysates were reduced, alkylated and digested as described previously¹. Desalted peptides were enriched for phosphopeptides using titanium oxide (TiOx) beads based using aliphatic hydroxyl-acid modified metal oxide chromatography^{2,3}. In brief, 500 µg desalted peptides (1 µg/µl in 80% ACN, 0.1% TFA) were mixed with 500 µl washing buffer (80% ACN, 0.1% TFA containing 300 mg/ml lactic acid) and applied to 2.5 mg TiOx beads (GL sciences, 10 µm) packed in a 200 µl STAGE tip containing a 16G empore C8 membrane plug (3M, St Paul, MN). The STAGE tip was washed with 200 µl washing buffer followed by 200 µl 80% ACN, 0.1% TFA. Phosphopeptides were eluted in two steps in 50 µl 0.5% and 5% piperidine (Fisher Scientific) and were quenched in 100 µl 20% H₃PO₄. All steps were performed by centrifugation (1500 x

g, 4 min). Phosphopeptides were desalted using a 200 μ l STAGE tip containing a 16G empore SDB-XC membrane plug (3 M, St Paul, MN) using the same solvents as used for the Seppak cartridge (20 μ l, 100 rpm, 1 min). Desalted phosphopeptides were dried in a vacuum centrifuge and redissolved in 20 μ l 4% ACN, 0.5% TFA; 17 μ l was injected on the column. Phosphopeptides were separated by nanoLC and detected as described elsewhere^{2,4,5} on a Q exactive HF mass spectrometer (Thermo Fisher, Bremen, Germany).

PROTEIN IDENTIFICATION

LC-MS/MS spectra were searched against the Uniprot human reference proteome FASTA file (release February 2019, 42417 entries, no fragments) using MaxQuant 1.6.4.0⁶. Enzyme specificity was set to trypsin and up to two missed cleavages were allowed. Cysteine carboxamidomethylation (Cys, +57.021464 Da) was treated as fixed modification and serine, threonine and tyrosine phosphorylation (+79.966330 Da), methionine oxidation (Met, +15.994915 Da) and N-terminal acetylation (N-terminal, +42.010565 Da) as variable modifications. Peptide precursor ions were searched with a maximum mass deviation of 4.5 ppm and fragment ions with a maximum mass deviation of 20 ppm. Peptide, protein and site identifications were filtered at a false discovery rate (FDR) of 1% using the decoy database strategy. The minimal peptide length was 7 amino acids and the minimum Andromeda score for modified peptides was 40, with the corresponding minimum delta score set at 17⁷. Proteins that could not be differentiated based on MS/MS spectra alone were grouped into protein groups (default MaxQuant settings). (Phospho)peptide identifications were propagated across samples using the match-between-runs option checked. Searches were performed with the label-free quantification option selected. (Phospho)peptide identifications were propagated across samples using the match-between-runs option checked. Searches were performed with the label-free quantification option selected.

LABEL-FREE PHOSPHOPEPTIDE QUANTIFICATION

Phosphopeptides were quantified by their extracted ion chromatograms ('Intensity' in MaxQuant). For each sample the phosphopeptide intensities were normalized on the median intensity of all identified peptides in the sample ('normalized intensity' from the MaxQuant Evidence table). Normalization and statistical testing were performed in R. Fold-change and p values were calculated from replicates using a two-tailed Student's t-test; phosphopeptides were considered significantly differential at $p < 0.05$. The match-between-runs option in MaxQuant was used. Missing values were excluded from subsequent statistical analysis. Quantitative values from replicates were averaged prior to biological group comparisons. The t-test requires at least two quantitative values in each group. P-values were not corrected for multiple hypothesis testing. Cluster analysis of differential phosphopeptides was performed using hierarchical clustering in R and repeated for the top10 and 20% most variable peptides. Phosphopeptide intensities were normalized to zero mean and unit variance for each phosphopeptide. Subsequently, the Euclidean distance measure was used for phosphopeptide clustering. For sample clustering metrics, the (1-Pearson correlation) distance and the Ward linkage were used.

RNA SEQUENCING

Next generation sequencing (NGS) using Illumina's TruSeq Small RNA Sample Preparation protocol and data filtering were performed as previously described⁸. Illumina's TruSeq Small RNA Sample Preparation protocol was used for the generation of cDNA libraries. These libraries were amplified on the flow cells with Illumina's cluster station (Illumina Inc, San Diego, CA, USA) and sequenced using Illumina's HiSeq 2000 (Illumina Inc, San Diego, CA, USA). Obtained sequence reads were first quality trimmed, resulting in a >99.9% probability of a correctly identified base of the remaining nucleotides. Secondly, the reads were clipped for adaptor sequences. Thirdly, reads with identical sequences were compiled and counted, resulting in only unique sequences. Finally, each unique sequence was mapped to the reference genome (browser hg19) and only those alignments of at least 18 nucleotides and a maximum of 2 mismatches were retained. Data was visualized on the R2 genomics analysis and visualization platform (<http://r2.amc.nl/>) and the R2 program was used to generate unsupervised clustering heatmaps using the View Geneset option with 100 most varying genes between the groups as found with the TopLister option, with and log₂-score transformation settings, as well as sample correlation analyses using the Sample Correlation Map (SCM) option with data as input and log₂ transformation setting. Genes with Benjamini and Hochberg p-value ≤ 0.01 were considered differentially expressed.

SUPPLEMENTARY TABLES AND FIGURES

■ **Supplementary Table 1.** Patient characteristics and sample processing.

14 Gauge core needle biopsies were obtained from normal liver tissue in resection specimens from five patients undergoing liver surgery in our hospital. Patient details, as well as the individual biopsies acquired from each patient and the type of analysis performed are presented. The freezing condition “control sample” indicates the positive control that was left at room temperature for two hours, before freezing in liquid nitrogen. For patient 01 only 3 normal liver tissue biopsies were available (phosphoproteomics) and for patients 02, -03- and -04, 6 biopsies per patient could be evaluated for phosphoproteomics, RNA integrity analysis and RNA sequencing. RNA isolation from three biopsies from patient 04 and one biopsy from patient 05 failed.
 Abbreviations: LN2 = liquid nitrogen, n/a = not applicable, RIN = RNA integrity number, RNA = ribonucleic acid, TIOX = Titanium Oxide, an enrichment method for label-free quantitative phosphoproteomics.

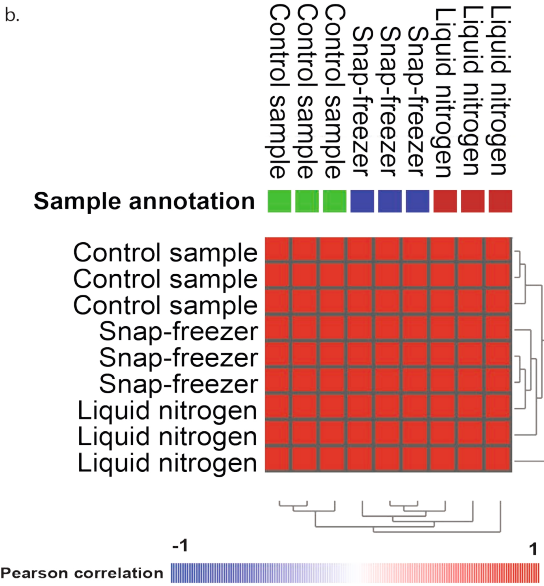
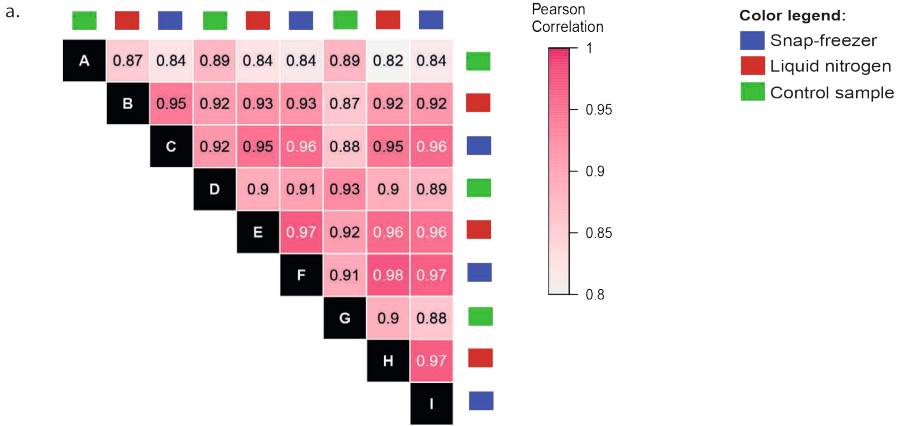
Patient ID	Age (years)	Gender	Primary tumor type	Indication for surgery	Biopsies	Freezing method	Processed for	Number of phospho-peptides	Total number of peptides	RNA Integrity number	Remarks
1	71	M	Cholangio-Carcinoma	Resection of primary tumor	1	Snap-Freezer	TIOX	6054	9225		
					2	LN2	TIOX	6506	9744		
					3	Control sample	TIOX	7067	10346		
2	60	F	Colorectal cancer	Hemi-hepatectomy for liver metastases	1	Snap-freezer	TIOX	7355	11053		
					2	LN2	TIOX	7233	10821		
					3	Control sample	TIOX	7060	10690		
					4	Snap-freezer	RNA			9.50	
					5	LN2	RNA			8.20	
					6	Control sample	RNA			9.30	

■ **Supplementary Table 1.** Patient characteristics and sample processing (continued)

Patient ID	Age (years)	Gender	Primary tumor type	Indication for surgery	Biopsies	Freezing method	Processed for	Number of phospho-peptides	Total number of peptides	RNA Integrity number	Remarks
3	76	M	Colorectal cancer	Hemi-hepatectomy for liver metastases	1	Snap-freezer	TIOX	6456	10036		
					2	LN2	TIOX	5535	8855		
					3	Control sample	TIOX	6003	9513		
					4	Snap-freezer	RNA		6.90		
					5	LN2	RNA		7.80		
					6	Control sample	RNA		6.70		
4	81	M	Hepato-cellular carcinoma	Resection of primary tumor	1	Snap-freezer	TIOX	6978	10121		
					2	LN2	TIOX	7601	11035		
					3	Control sample	TIOX	6293	9338		
					4	Snap-freezer	RNA		n/a	RNA isolation failed	
					5	LN2	RNA		n/a	RNA isolation failed	
					6	Control sample	RNA		n/a	RNA isolation failed	

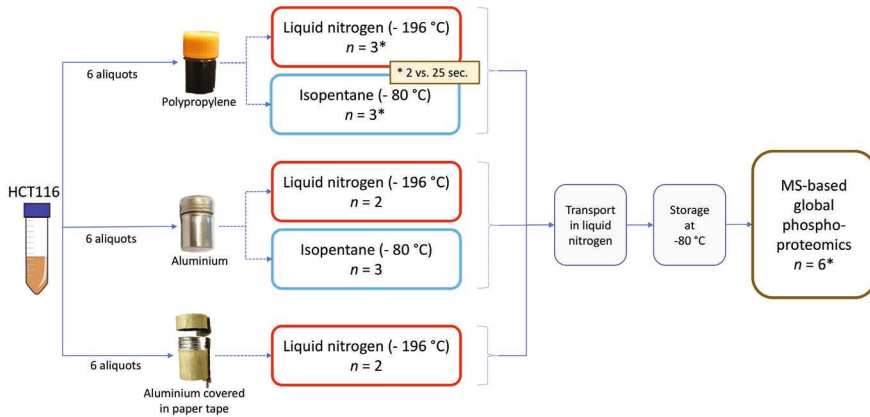
■ **Supplementary Table 1.** Patient characteristics and sample processing (continued)

Patient ID	Age (years)	Gender	Primary tumor type	Indication for surgery	Biopsies	Freezing method	Processed for	Number of phospho-peptides	Total number of peptides	RNA Integrity number	Remarks
5	55	M	Colorectal cancer	Hemi-hepatectomy for liver metastases	1	Snap-freezer	RNA			7.10	
2						LN2	RNA			6.60	
3						Control sample	RNA			8.30	
4						Snap-freezer	RNA			6.90	
5						LN2	RNA			n/a	RNA isolation failed
6						Control sample	RNA			6.20	
7						Snap-freezer	n/a				Sample not processed
8						LN2	n/a				Sample not processed
9						Control sample	n/a				Sample not processed



Supplementary Figure 1. Correlation analyses of K562 cell line samples

- A. Sample correlation map indicating Pearson’s *r* based on phosphoproteomics data of nine K562 samples. The median *r* was 0.96 (range 0.92-0.98) for either direct freezing method.
- B. Sample correlation map indicating Pearson’s *r* based on RNA sequencing data of nine K562 samples. All samples are highly correlated, with Pearson’s *r* > 0.99.



Supplementary Figure 2. Influence of freezing rate on phosphoproteomic profiles

Experimental design of the comparison of the effect of 5 different freezing rates, achieved using 3 different types of vials in 2 different coolants, on the phosphoproteome using cancer cell line HCT116. Aliquots of 300 μ l HCT116 lysate, each corresponding to 300-400 μ g of protein, were placed in three types of vials with different thermal conduction properties (polypropylene, aluminium and aluminium vials covered in paper tape) to influence their freezing rates. For each condition three vials were individually immersed in either LN₂ or precooled isopentane for 1 minute and cooled to a temperature of -196 °C or -80 °C, respectively, using a stainless steel vial holder. The time to reach the goal temperature of -80 °C was registered.

REFERENCES IN SUPPLEMENTARY DATA

1. Labots M, Pham TV, Honeywell RJ, et al: Kinase Inhibitor Treatment of Patients with Advanced Cancer Results in High Tumor Drug Concentrations and in Specific Alterations of the Tumor Phosphoproteome. *Cancers (Basel)* 12, 2020

2. Piersma SR, Knol JC, de Reus I, et al: Feasibility of label-free phosphoproteomics and application to base-line signaling of colorectal cancer cell lines. *J Proteomics* 127:247-58, 2015

3. Sugiyama N, Masuda T, Shinoda K, et al: Phosphopeptide enrichment by aliphatic hydroxy acid-modified metal oxide chromatography for nano-LC-MS/MS in proteomics applications. *Mol Cell Proteomics* 6:1103-9, 2007

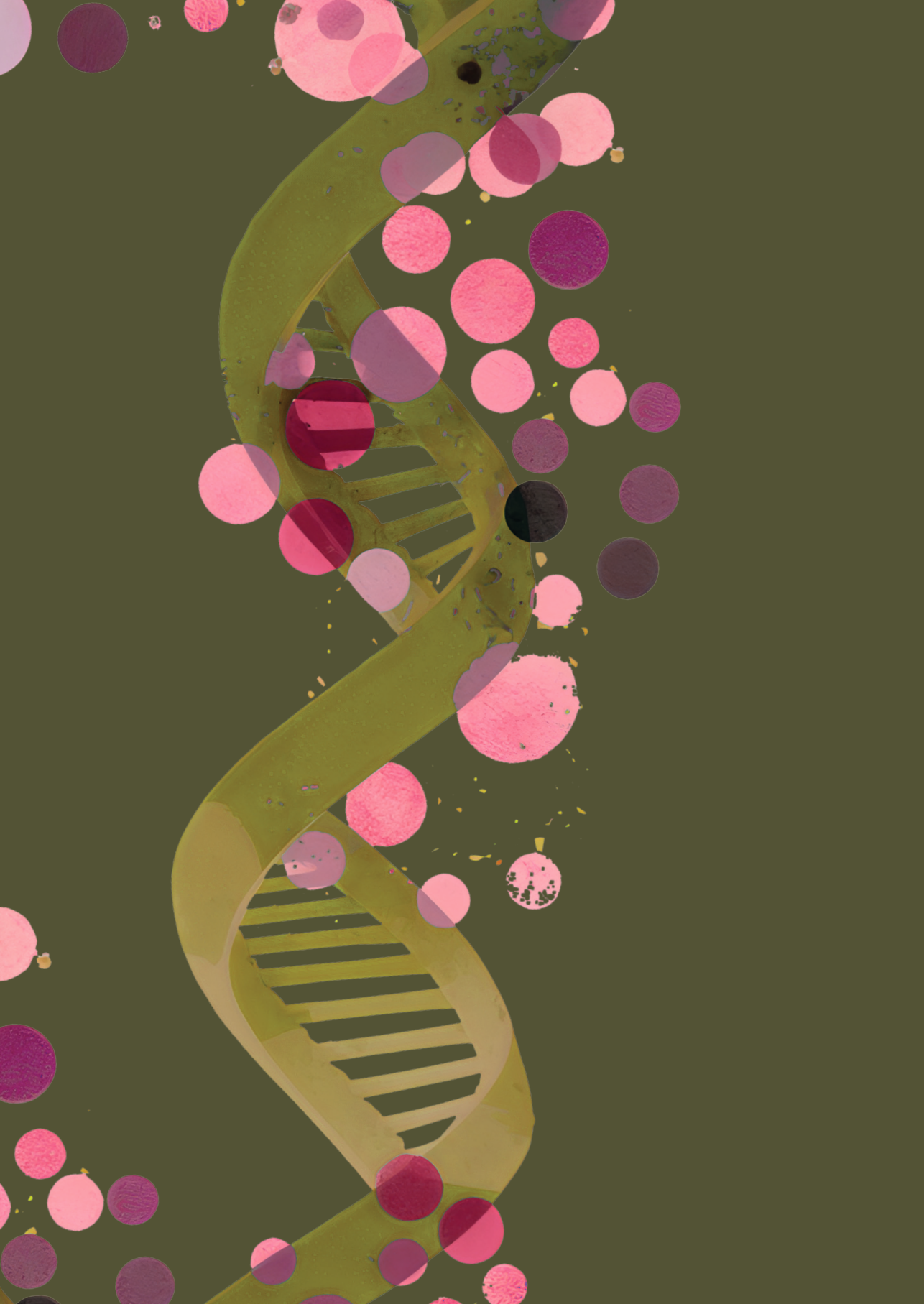
4. van der Mijn JC, Labots M, Piersma SR, et al: Evaluation of different phospho-tyrosine antibodies for label-free phosphoproteomics. *Journal of Proteomics* 127:259-263, 2015

5. Beekhof R, van Alphen C, Henneman AA, et al: INKA, an integrative data analysis pipeline for phosphoproteomic inference of active kinases (vol 15, e8250, 2019). *Molecular Systems Biology* 15, 2019

6. Cox J, Mann M: MaxQuant enables high peptide identification rates, individualized p.p.b.-range mass accuracies and proteome-wide protein quantification. *Nature Biotechnology* 26:1367-1372, 2008

7. Marx H, Lemeer S, Schliep JE, et al: A large synthetic peptide and phosphopeptide reference library for mass spectrometry-based proteomics. *Nature Biotechnology* 31:557-+, 2013

8. Neerincx M, Sie DLS, van de Wiel MA, et al: MiR expression profiles of paired primary colorectal cancer and metastases by next-generation sequencing. *Oncogenesis* 4, 2015





CHAPTER 6

| Summarizing Discussion
| and Future Perspectives

GENERAL DISCUSSION

Advanced cancer continues to be a heavy burden for society. In the Netherlands, 20% of patients who are diagnosed with cancer already have metastatic disease at the time of diagnosis¹. Cancer metastases can also occur later in the course of the disease. Annually, around 38,000 patients in the Netherlands are diagnosed with metastatic cancer¹. Only a minority of patients with metastatic disease can be cured with local therapies such as surgery or radiotherapy or sometimes curative systemic therapy strategies. For most of the patients with metastatic disease, palliative systemic treatment is their last resort, with the aim of disease- and symptom control and thereby prolongation of life while maintaining or improving their quality of life. Since cancer is a genetic disease, characterized by mutations and dysregulated protein kinase signaling², protein kinases (and tyrosine kinases in particular) have become one of the most important drug targets in recent years^{3,4}. Since the introduction of trastuzumab, a monoclonal antibody directed against *ErbB2*⁵ in 1999 as the first targeted treatment, an increasing number of targeted anti-cancer drugs are annually approved by the FDA⁶. Together with the introduction of immune checkpoint inhibitors (ICI), protein kinase inhibitors (PKI's) have made a powerful contribution to the improved survival of patients with advanced cancer⁷. This vast expansion of the targeted therapeutic arsenal broadens opportunities for patients with advanced cancer.

One of the most important questions, which is under extensive evaluation, is how to select the right treatment for the right patient at the right time? What is the biomarker with the best predictive value for response (or resistance) to treatment? And what requirements need to be met before a targeted treatment strategy based on individual tumor characteristics can be offered to each patient with cancer?

The studies in this thesis focus on clinical available pan-cancer genomics-based treatment selection in a drug repurposing clinical trial (chapter 2 and 3), the development of a phosphotyrosine proteomics selection method for a multi-targeted TKI (chapter 4) and the validation of a new liquid nitrogen-free snap freezer for optimal tissue handling to enable (multi)omics analysis on clinical samples (chapter 5).

GENOMICS-BASED TREATMENT SELECTION; DRUG REDISCOVERY PROTOCOL

Each tumor is unique in its genetic and molecular composition. With the improvement and wider implementation of next generation sequencing techniques, extensive molecular information from individual tumors has become available, often revealing unexpected genomic events. In 31% of patients with advanced cancer, an actionable genomic event was identified in the tumor DNA that predicted sensitivity to a targeted drug. In 13% of patients, a genomic target was identified for which targeted drugs are available, but not registered for the specific tumor type⁸.

In **chapter 2**, we described the design and feasibility of the **Drug Rediscovery Protocol (DRUP)** and the results of the first 215 patients enrolled in this multicenter clinical trial, including the results of the first completed cohort. DRUP is an ongoing national prospective multi-drug and pan-cancer phase II clinical trial that started in 2016. Patients with advanced solid tumors, who have exhausted standard-treatment options, are treated with existing targeted anti-cancer drugs (small molecules, monoclonal antibodies and immune checkpoint inhibitors) based on their tumor molecular profile, but outside their labelled indications.

The analysis of the first 215 patients included in the DRUP trial showed that overall, 34% had **clinical benefit**, defined as a confirmed objective response or disease control of at least 16 weeks. The overall clinical benefit rate indicates that the efficacy of the DRUP approach to therapy selection is higher than the disease control rate of 11% in other phase I trials⁹. Chapter 2 also describes the results of the first completed cohort within DRUP. In this cohort, 30 patients with various tumor types with mismatch repair deficiency (dMMR) and microsatellite instability (MSI) were enrolled and treated with nivolumab, an anti-PD-1 monoclonal antibody. The clinical benefit rate in this particular cohort was 63% and the median progression free survival (PFS) was not reached after 16.5 months of follow-up. This impressive result warranted confirmation in an independent cohort, and a “third stage” expansion cohort was created within DRUP and based on the positive outcome of this validation cohort, registration of nivolumab was obtained for patients with dMMR and MSI cancer without standard treatment options.

There is a growing need for a learning health care model which enables early access to potentially effective therapies, where no other established treatment options are available, without overestimating the findings that are based on small cohorts of patients. To this end, we developed a performance-based, **personalized reimbursement model**¹⁰ that enables access to precision medicine in rare biomarker-defined subgroups. Patients are treated with study medication within the DRUP trial stage 3 cohort, and good performance of the regimen (objective response or stable disease for at least 16 weeks) leads to reimbursement by the health insurance. This model allows risk-sharing between the manufacturer of the drugs and payers.

The benefit of genomics-based therapy selection may seem evident today, but that has not always been the case. In the French SHIVA trial, patients with molecular alterations in one of three pathways (hormone receptors, *PI3K/AKT/mTOR* pathway or *RAS/RAF/MEK/ERK* pathway) were randomized between one of ten molecular matched therapy regimens or physicians' choice of treatment. The outcome was not significantly different for both groups ($p=0.41$, HR 0.88) and the authors concluded that off-label use of molecularly targeted agents should be discouraged. However, the study was criticized for lumping genetic profiles without consideration of the tissue context or relative importance of genetic aberrations¹¹. In the WINTHER trial, patients were screened for molecular targets for treatment by DNA and RNA sequencing. An expert panel recommended matched therapies based on the sequencing results, after which the treating physician determined the therapy given. Among other clinical aspects, the eventual choice of therapy depended on drug availability and reimbursement. This trial

reported that 22.4% of patients had a PFS2/PFS1 ratio of ≥ 1.5 , and thereby failed to meet its pre-specified primary end point¹². Despite its negative outcome, the WINTHER trial reports that transcriptome analysis of tumor tissue added substantially to the number of patients treated with a matched targeted drug. By using information from RNA analysis, the matching rate improved from 23% to 35%¹². The **addition of RNA sequencing** and transcriptome-based treatment selection is also considered as a new strategy within DRUP.

One of the factors contributing to the meaningful clinical benefit rate in the DRUP trial may be the **innovative trial design**, which allows evaluation of small groups of patients with rare cancer subtypes to determine the potential benefit of a targeted agent in a group of patients with a specific tumor molecular profile while appreciating the context of histology. DRUP has a wide arsenal of available targeted drugs, with 30 treatments currently available provided through collaboration with 12 pharmaceutical companies, and efforts to further expand are ongoing. A dedicated team of researchers evaluate each case, and alongside the molecular target evaluation, a literature search is performed to appreciate existing (pre-)clinical evidence for the drug-target-histology combination, which substantially impacts the choice of therapy. Another contributing factor may be the increasingly broad molecular testing that is performed in the Netherlands. Since the molecular diagnostic approach is the corner stone of precision oncology, an improvement to the design of DRUP could be to include molecular profiling for target identification on fresh frozen biopsies in the trial. Several other trials have broad-panel sequencing or transcriptome analysis as “prescreening” in their trial design, for example the I-PREDICT¹³ and NCI-MATCH¹⁴ trials. In the latter, patients’ tumor tissue was screened for actionable genomic targets by NGS and matched to a targeted treatment accordingly. Although the NGS results contributed to the knowledge on actionability of genomic events, only a minority of included patients experienced clinical benefit upon targeted treatment¹⁵. As in DRUP, clinical benefit rates differed greatly among various cohorts and targeted pathways.

One of the challenges in many precision-oncology clinical trials is how to generate a sufficient level of evidence for the (lack of) effectivity of a drug in very rare subgroups of cancer patients. Some actionable genomic events occur in such low frequency that timely completion of a DRUP cohort and reporting of the results is considered impossible. One solution to this problem requires **international collaboration of data sharing** with other research groups and participation in collaborative clinical trials. DRUP has formed a global collaboration with two other trial-groups by harmonizing the study protocols: the United States-based Targeted Agent and Profiling Utilization Registry (TAPUR) Study (NCT02693535)¹⁶ and the Canadian Profiling and Targeted Agent Utilization Trial (CAPTUR, NCT03297606). This collaboration comprises a data sharing protocol that allows pooling and combined analysis of comparable cohorts across the three trials¹⁷. As time went on, it became clear that other European countries and research groups also had an interest in starting similar precision oncology trials. Working towards a European precision oncology platform. Therefore, DRUP has also shared its protocol and study documents with these European groups to harmonize protocols and facilitate data sharing closer to home. At the time of writing, several trials have already started enrolling

patients (MEGALiT in Sweden (NCT04185831), IMPRESS in Norway (NCT04817956) and Pro-Target in Denmark (NCT04341181)). Another example of international collaboration is the joint effort of DRUP and the Australian Molecular Screening and Therapeutics clinical trials & immunotherapy (MoST clinical trials). Both DRUP and MoST found in a considerable number of patients with genomic aberrations in the Cyclin D-CDK4/6 pathway treated with off-label CDK4/6 inhibitors no clinical benefit¹⁸. These results were reported as a pooled analysis of all cohorts across the two trials in which patients were treated with CDK4/6 inhibitors palbociclib and ribociclib, achieving a greater level of evidence than reporting of individual small cohorts.

Within the DRUP trial, the vast majority of patients had a **rare subtype of cancer**. Either they had a rare cancer (an incidence less than 6 cases per 100,000 persons per year), or a common tumor type with a rare genomic aberration. Around 33% of enrolled patients in DRUP has a rare cancer, this group has the same overall clinical benefit rate (33%) of genomics-guided off label treatment as the group of patients with non-rare cancers¹⁹. Although it is considered a strength of DRUP that patients with rare cancers are offered an extra, potentially effective, treatment option, it also results in a large number of cohorts with just one or two patients enrolled. One of the challenges following from these small and “incomplete” cohorts is how to gain a sufficient level of evidence for these patients. DRUP has found several solutions for this issue, as described above. But even if cohorts are completed in stage 2 (24 patients), health authorities struggle to appreciate the evidence from small cohorts in a non-randomized non-controlled phase 2 trial. Especially the lack of a proper control group is difficult to overcome. Due to the rarity of these subgroups, conducting a randomized clinical trial is impossible. The use of historical controls is a generally accepted approach, but it has also proven to be nearly impossible to find correctly-matched controls, because patients qualifying for DRUP have exhausted standard-of-care treatments. Historical controls should ideally be matched by molecular subtype, however this information is often not reported in cohorts from the past. Finally, a commonly used endpoint is an intra-patient progression-free survival (PFS) ratio, defined as the PFS interval associated with molecularly guided therapy (PFS2) divided by the PFS interval associated with the last prior systemic therapy (PFS1), above 1.3 or, in some studies, above 1.33 or 1.5²⁰. Using this ratio, the patient serves as his/her own control. Among other issues leading to potential bias²¹, one difficulty in this approach is that the PFS1 data are retrospectively retrieved, while the PFS2 data are prospectively collected.

Another ongoing challenge is to find the most accurate method of prioritizing different molecularly guided treatment options for individual patients. Growing experience with the results of tumor broad panel sequencing or WGS teaches us that tumor DNA often harbors more than one genomic aberration. A large pan-cancer analysis shows that tumors have a mean number of 5.7 candidate genomic driver events per patient⁸, likely occurring at different stages of tumor evolution. Some tumors may have multiple drivers occurring as early events in tumor development. But which genomic feature is the **dominant driver** that should be the target for treatment? It is possible that the answer lies in the administration of combinations of targeted anti-cancer agents. In the I-PREDICT trial, patients were treated with one or more

targeted agents based on their broad panel NGS results. A matching score was computed for each patient, reflecting what percentage of potential targets was covered by the treatment regimen. A higher matching score was associated with a better treatment outcome¹³. In DRUP, the combination treatment approach was also debated, but to date it is considered to be outside the scope of the trial, since some non-established combinations of drugs would require new dose-finding studies before patients could safely be subjected to them. Without a doubt, the implementation of specialized multidisciplinary **Molecular Tumor Boards** (MTBs) plays an essential role in determining the most appropriate molecular-guided treatment strategy²²⁻²⁴. Their experience and expertise may guide physicians' choice for therapy and may suggest extra treatment options within clinical trials, as well as educate physicians in the interpretation of molecular diagnostic test results.

Obviously all the efforts regarding data interpretation, precision oncology clinical trial design and developing algorithms to optimize molecular-guided targeted therapy selection will only succeed if patients have access to the **molecular diagnostics** that are the foundation of precision oncology. If patients cannot access modern diagnostics, all our efforts would reach only few patients, and inequality of healthcare based on geographical location of the patient impends. Surely it will not be possible for each hospital to obtain all technical methods and expertise in house. But strengthening the collaboration and sharing knowledge and resources is necessary to translate advances in precision oncology into benefits for patients with cancer²⁵.

In **chapter 3** we describe the results of a second **positive cohort** in the DRUP trial. Twenty-four patients with nine different histological tumor types harboring deleterious mutation of the *BRCA1* or *BRCA2* gene in their tumor DNA, and with no standard treatment options available, were treated with olaparib, an oral inhibitor of *PARP1*. Pathogenic *BRCA1/2* loss of function (LoF) mutations can result in homologous recombination repair deficiency (HRD) in tumor cells, causing the inability to repair DNA double strand breaks. When *PARP1* is inhibited, DNA single strand break repair is hampered, causing a multitude of double strand breaks, that also cannot be repaired, leading to cancer cell cytotoxicity and apoptosis. Fifty-eight percent had clinical benefit upon treatment with olaparib. Among patients with complete biallelic LoF of *BRCA*, 73% had clinical benefit. Seven out of 24 patients had non-*BRCA*-associated tumor types for which PARPi are not registered to date, and four of them had clinical benefit. This shows that PARPi is a promising treatment strategy for patients with non-*BRCA* associated histologies harboring bi-allelic *BRCA* LoF. The clinical benefit rate in this cohort warrants further investigation and confirmation in patients with non-*BRCA* histologies. This is currently in preparation within DRUP, an independent expansion cohort (stage 3) is planned to open soon, again making use of the personalized reimbursement model¹⁰.

Although our findings strongly suggest that PARP inhibition is an effective treatment option in non-*BRCA* associated tumor types, it is not undisputed whether *BRCA1/2* mutations are valid **tumor-agnostic biomarkers** for PARP inhibitor therapy. A large pan-cancer study by Jonsson et al. showed that (likely) pathogenic germline *BRCA1/2* mutations occur in 2.7% of

patients, and somatic LoF mutations in 1.8% of patients across 38 histological tumor types²⁶. Of these patients, 53% had one of the four *BRCA*-associated tumor types: ovarian, breast, prostate and pancreatic cancer. In these patients, biallelic inactivation of *BRCA* was seen in 61%, while only 28% of patients with non-*BRCA* associated malignancies had bi-allelic inactivation. In fact, somatic loss of the pathogenic germline *BRCA* allele occurred twice as often in the last group. These findings indicate that dependency on *BRCA* pathway dysfunction for tumorigenesis differs between tumor lineages, and in many cases, the *BRCA* mutations are neutral passenger mutations that are rather a consequence of genomic instability than a cause of tumorigenesis²⁶. This is in line with our observation that in patients with bi-allelic *BRCA* LoF who had no benefit upon treatment with olaparib, **another dominant genomic oncogenic driver** was identified. While *BRCA* LoF can cause HRD, *BRCA1/2* mutations are not 100% synonymous with HRD. Approximately 40% of ovarian cancers are HRD without a pathogenic *BRCA1/2* mutation²⁷. And vice versa, in tumors harboring a pathogenic *BRCA1/2* mutation, HRD can be reversed by a secondary mutation that restores *BRCA* function²⁸. Also, an HRD-permissive tumor microenvironment may play an important role in *BRCA*-associated tumors²⁶. Albeit more complex, an accurate estimate of HRD may be a better predictor of response to PARP inhibition and may have more potential as tumor-agnostic biomarker. Various functional HRD assays^{27,29} and classifiers^{30,31} have been developed that can accurately detect HRD in tumor tissue. Histology-agnostic studies in which patients are selected for treatment with PARPi based on a HRD signature have not yet been reported. Within the DRUP trial, the potent PARP inhibitor talazoparib is available for patients with a HRD genomic signature in their tumor DNA, but without a pathogenic mutation or deletion in one of the known HRD genes. This histology-agnostic cohort is currently accruing patients.

DEVELOPMENT OF PHOSPHOPROTEOMICS-BASED BIOMARKERS FOR PRECISION ONCOLOGY

The presence of a clear tissue-based biomarker predictive of treatment outcome is considered a corner stone of precision oncology. A strong example is the *BRAF* V600 mutation as a biomarker for response to treatment with BRAF/MEK-inhibition in advanced melanoma, glioma³² and anaplastic thyroid cancer³³. However, some tyrosine kinase inhibitors (TKI's) are used without the presence of a molecular biomarker, such as sunitinib, which is used as first-line treatment for patients with advanced renal cell cancer (RCC)³⁴. RCC is not a mono-genetic driven disease³⁵ and tissue-based biomarkers for response are lacking. Sunitinib is a multi-targeted TKI targeting mainly the Vascular Endothelial Growth Factor Receptors (*VEGFR* 1 and 2), Platelet-Derived Growth Factor Receptors (*PDGFR-alpha* and *PDGFR-beta*) and stem cell factor receptor (*KIT*), though many off-target effects are observed³⁶. Despite the absence of a **predictive biomarker**, treatment of RCC with sunitinib has proven to be quite effective, resulting in a median progression free survival (PFS) of 8.4 - 11 months^{37,38} and an improved overall survival compared to interferon alfa³⁴, with an objective response rate of 25 - 47%^{37,38}. Upfront identification of patients for whom sunitinib will fail to provide clinical benefit is crucial to prevent unnecessary side effects of the drug.

In **chapter 4**, we performed a **baseline (phospho)proteomics analysis** of 26 patients with RCC, treated with sunitinib. We retrospectively compared samples of patients who were primary resistant to the treatment (PFS < 12 weeks) to patients who had clinical benefit (PFS ≥ 12 weeks), aiming to describe differences in biology between the two groups. We found a discriminatory 78-phosphosite signature and kinase activity associated with sensitive and resistant tumors. p-Tyr phosphoproteomics in resistant tumors showed upregulation of phosphosites that are associated with resistance to treatment in other tumor types, and with inflammatory processes. A comprehensive pathway analysis pointed towards *VEGF*-independent tumor angiogenesis as a possible contributor to sunitinib resistance. We reproducibly identified three differentially upregulated proteins in resistant patients that showed overlap with differential transcripts from an independent cohort³⁹, one of them (EIF4A1/EIF4A2) was also exclusively phosphorylated in resistant patients.

This is the first comprehensive phosphoproteomics analysis on clinical RCC samples in relation to the response to sunitinib. Other phosphoproteomics studies use *in vitro* or *in vivo* models^{40,41}, or use clinical samples to characterize the disease, without correlation to treatment response⁴². **Sunitinib resistance in RCC** remains a hot topic, and many post hoc efforts to find molecular biomarkers for treatment outcome have been reported, assessing other layers of biology in clinical samples. Beuselinck et al. performed a transcriptomics analysis on 53 clinical baseline RCC samples and report four distinct molecular subtypes of ccRCC, associated with different responses to sunitinib³⁹. Motzer et al recently published their integrated multi-omics analysis of 823 baseline tumor samples and found seven molecular subsets of RCC, that correlate with response to angiogenesis blockade and immune checkpoint inhibitors⁴³. To date, only one prospective biomarker-driven trial in metastatic RCC has been published. The randomized phase II BIONIKK trial demonstrates feasibility of treatment allocation based on prospective molecular classification and suggested an improved sunitinib efficacy in one of the four molecular subgroups⁴⁴.

Although a reliable and practical **predictive biomarker** for sunitinib efficacy in RCC is not yet available, many important steps have been taken to improve our understanding of its biology and molecular features. It seems only a matter of time (and effort) before patients can actually profit from the upfront prediction of tumor response to systemic therapy. Our analyses on the role of phosphoproteomics is promising, as it clearly separates primary resistant tumors from sensitive ones based on kinase activity and protein expression. Ultimately, a targeted assay could be developed based on this and future work, computing a simple and practical result that can be interpreted by clinicians in all hospitals.

There are various examples of mass spectrometry-based phosphoproteomics analyses that result in better understanding of cancer biology⁴⁵ and report potential targets for treatment^{46,47} and prognostic biomarkers⁴⁸. These analyses are most often performed on cell lines and patient-derived xenografts (PDX). Phosphoproteomics analyses on tumor tissue samples are scarce and often include low numbers of patients.⁴⁹⁻⁵¹ To our knowledge, no reports are pub-

lished to date on clinical trials using global phosphoproteomics for targeted therapy selection in patients with cancer.

Phosphoproteomics knowledge and facilities are not mainstream and are still confined to centers of expertise, often academic laboratories. At this time, it seems still too early to implement phosphoproteomics analysis for therapy selection in patients with malignancies, due to (i) limited tissue availability, although down-scaling of the pTyr phosphoproteomics protocol now allows for reproducible analysis on only 1 mg of protein input⁵², which is the yield of a 14G core needle biopsy⁵³, (ii) specific logistic requirements and pre-analytical handling of the tissue to allow this complex analysis, (iii) the time-consuming laborious technique and required expertise of the research staff, (iv) required expertise in interpretation of the results, and (v) the lack of clinical validation and reproducibility. A targeted assay or immunohistochemistry analysis with a selection of differential phosphosites and/or proteins could facilitate the implementation of these signatures as a decision-making tool for treatment selection in clinical practice. Such an assay would prevent unnecessary toxicity and enable alternative (combination) treatment in patients upfront predicted to be resistant to sunitinib.

PRE-ANALYTICAL REQUIREMENTS FOR (MULTI)OMICS ANALYSIS ON CLINICAL TISSUE SAMPLES

Increasingly complex molecular analyses of tissue samples require a standardized and controlled method of tissue preservation. To facilitate **multi-omics analysis** on clinical tissue samples, high-quality fresh frozen tissue samples are required. Particularly post-translational modifications in tumor tissue are sensitive to variations in pre-analytical handling⁵⁴⁻⁵⁷. Tumor biopsies collected for research and precision oncology purposes are generally placed in a cryovial by trained staff and immediately immersed in liquid nitrogen (LN₂). This process is referred to as **snap freezing** and currently the golden standard⁵⁸. Snap freezing is a laborious, potentially hazardous, and not user-friendly procedure. In addition, LN₂ is not widely available and the use of sacrificial LN₂ is non-sustainable due to its energy-intensive synthesis. To circumvent the limitations of snap freezing in LN₂, a new liquid nitrogen-free snap freezer was developed for snap freezing biospecimens, to conserve molecular profiles under standardized and optimized pre-analytical conditions⁵⁹.

In **chapter 5**, we benchmarked the performance of the electrically powered **snap freezer** prototype to the golden standard of LN₂-quenching with regard to preservation of biology. We used cancer cell line K562 specimens and core needle biopsies from normal human liver resection specimens, snap frozen using either the golden standard or the new snap freezer, to compare mass spectrometry (MS)-based global phosphoproteomic and transcriptomic profiles and RNA integrity. We found that cell line RNA integrity, phosphoproteomic and transcriptomic profiles of snap freezer versus LN₂ quenching were highly comparable, the samples could not be distinguished based on the freezing method used, while the positive control sample (that was left at room temperature for 2 hours) clearly formed a separate cluster. Molecular profiles of liver tissue biopsy samples clearly clustered per patient, regardless of the applied freezing

method. These findings confirm that the novel snap freezer preserves high-quality biospecimen and allows identification of individual patients' molecular profiles.

The commercial development and wide availability of a mobile, electrically powered snap freezer would greatly benefit precision medicine by placing molecular diagnostics for routine oncology practice within reach in all hospitals. Tissue preservation for complex multi-layer molecular analysis will no longer be confined to the academic hospitals by removing the obstacle of the logistical requirements posed by LN₂. Obviously, the analyses of tissues still need to be performed in expert laboratories that have experience with the techniques and interpretation of the results. But ultimately, by simplifying and **standardizing tissue preservation**, more patients will have access to molecular profiling of their tumors and may benefit from precision oncology.

Optimal preservation of human cancer tissue samples for immediate diagnostic evaluation and also for tissue biobanking has been a hot topic for decades. In the past, local operating procedures for tissue preservation differed per pathology department and were established to ensure optimal morphologic preservation, which does not necessarily correlate with optimal molecular preservation. Around the year 2000, many new biobanks were developed around the world, implementing more stringent standard operating procedures (SOPs) to reduce variability in pre-analytical handling of tissue specimens for research⁶⁰. Early on, the need for rapid cooling of tissues (snap freezing) was recognized. Throughout the years, various methods of fixation and conservation of tissues have been developed⁵⁸. Fixation methods that require a storage medium, such as formalin-fixed paraffin-embedding (FFPE), RNAlater or Optimal Cutting Temperature (OCT) compound, render the tissue useless for some analytical methods such as phosphoproteomics⁶¹, although new techniques are being developed to enable MS-based proteomics⁶²⁻⁶⁴. Medium-free snap freezing methods conserve the tissue for molecular analysis of all layers of biology, but all are laborious and have specific disadvantages, sometimes even damaging the tissue⁵⁸. Examples are snap freezing in pre-cooled (-80 °C) isopentane, carbon dioxide quick-freeze method and the current golden standard of immersion in liquid nitrogen⁶⁵. There is an unmet need for a standardized, widely available, straightforward snap freezing method to circumvent the limitations of the current methods used in pathology labs and biobanks.

Kennedy et al. have developed a portable prototype Quick-Freeze Collection Device, using dimethyl ether/propane as an aerosol cooling system. The device was tested using a melanoma patient derived xenograft (PDX) model and global phosphoproteome profiles were comparable to profiles of samples processed in LN₂. The results however reported an uneven release of coolant, which interfered with the results of the prototype data. The cooling performance of this device is less impressive than that of our snap freezer, as it cools slower, has a higher and non-adjustable maximum cold sink temperature (-30 °C) and the inability to maintain low freezing temperatures for more than 70 minutes⁶⁶.

Other devices for (snap) freezing have already been commercially developed, for example Digitcool freezer (Cryo Bio System, L'Aigle, France), which is a freezing system for biological samples with snap freezing function and adjustable freezing rate and cold sink temperature, but it is not a mobile system. The Portable ULT25NEU freezer (Stirling Ultracold, Athens, Ohio, USA) is a portable device with adjustable temperature, but without the snap freezing function.

In conclusion, our newly developed snap freezer has a promising combination of properties regarding mobility, snap freezing performance and **conservation of molecular profiles** in human tissue samples. It contains favorable properties of the freezing methods that are already in use, while it lacks most of their limitations and obsoletes the use of sacrificial cryogens. The snap freezer will be further developed as a commercial product. Improvements to the design will be implemented to create an intuitive user interface, enhance mobility and allow for multiple cryovials to be snap frozen and stored in parallel. The device will be suitable for use in all types of healthcare facilities, in operating theaters and for imaging-guided biopsies.

OTHER CHALLENGES OF CONDUCTING CLINICAL AND TRANSLATIONAL PRECISION ONCOLOGY TRIALS

In the past decade, tremendous improvements have been made in the personalized care for patients with cancer. These improvements are the direct result of high-quality translational research and many clinical trials, a considerable proportion of which is **investigator-initiated** research. Although researchers are all highly motivated and creative, many challenges hamper the research following from scientific curiosity of clinicians and basic scientists. Aside from the usual suspects that are most often identified as barriers for researchers (time and financial support), we encountered several other challenges as described above.

One example of a hurdle that may jeopardize particularly the investigator initiated translational research in the field of precision oncology is the acquisition of tissue samples for (multi-)omics analysis. Even when patients consent to undergoing extra biopsies for future research purposes, the **regulations** for harvesting and storage of these biopsies have become more strict in recent years, making it difficult to store tissue samples in general biobanks. Tumor-specific biobanking is often possible, but only if a specific research question is already specified in advance, before opening the biobank. The enforcement of the General Data Protection Regulation 2016/679 in 2018 has also made it obligatory for patients to give specific consent for the storage of their genomic data⁶⁷, which puts up an extra barrier for acquiring these data. When samples are requested from other institutes, especially when big data needs to be transferred, contracts may be overly strict, making it almost impossible to come to an agreement between two or more institutes. These regulatory issues, although designed to guard patients' privacy and protect patients' rights, seriously hamper the exchange of useful research data and the development of new ideas and research methods, especially in the field of multi-omics analysis of cancer tissues.

Furthermore, with the rise of multi-omics analyses on clinical cancer tissue samples, there is a high need for computational models to help integrating –omics data from multiple layers of biology⁶⁸. The development of an **integrated bioinformatics pipeline** for data analysis would help advancing precision oncology even more in the future. Knowledge on how genomic features translate to RNA, protein expression and post-translational modifications is still relatively scarce and would benefit our understanding of cancer biology.

PROGRESS MADE IN PRECISION ONCOLOGY AND TARGETED THERAPY SELECTION

Generation of knowledge on cancer biology, the development of molecular diagnostic techniques and the availability of new targeted drugs have fundamentally changed oncology practice worldwide. How did these advances concretely benefit the care for patients with cancer?

For many individual patients with different tumor types, extensive genomic testing revealed unexpected driver mutations, resulting in an **extra treatment option** within a clinical trial such as DRUP. The data resulting from these experimental treatments may ultimately lead to an expansion of the labeled indications of targeted drugs. This has already been the case for nivolumab, which is now approved and reimbursed in the Netherlands for patients with MSI/dMMR tumors, regardless of histology⁶⁹. Another example is the addition of BRCA-mutated prostate cancer to the label for olaparib, a PARP inhibitor, largely based on the PROFOUND data⁷⁰.

Specifically for patients with rare cancers, additional molecular-guided treatment options are highly valued, since they commonly have less treatment opportunities and are understudied at the level of genomic targets¹⁹.

Genomics-guided treatment selection benefits patients in more than one way. Apart from generating extra treatment options, it is also essential to **withhold treatments** if patients have specific molecular or clinical features that render their tumors insensitive to targeted agents. For example, based on molecular profiling, treatment with anti-EGFR monoclonal antibodies for patients with colorectal cancer with a KRAS, NRAS or BRAF mutation has been terminated due to a lack of clinical benefit⁷¹⁻⁷³.

CONCLUDING REMARKS EN FUTURE PERSPECTIVES: EYES ON THE PRIZE

Precision oncology has come a long way since the introduction of the first targeted drug (trastuzumab) in 1999. Broad molecular testing of tumor tissue has vastly expanded our knowledge of the biology of cancer, leading to a steep increase in the number of approved targeted drugs and an expansion of the labeled indications of these drugs. Off-label use of these new classes of targeted drugs is nowadays better documented and often performed in clinical trials to maximize the learning potential of these experimental treatments for the medical community. As long as no “cure for cancer” exists, there will be room for improvement of our knowledge and approach to treating patients with cancer.

General improvements in the logistics, availability of targeted drugs and access to diagnostics and expertise will likely have the greatest impact on direct benefit for patients. In the future, standardized processing and conservation of tumor tissue/biopsies should be possible in all healthcare facilities, and collaborations and sharing of knowledge and resources with the academic institutes will be viable to delivering precision oncology to all patients. If these conditions are met, more patients may potentially benefit from the knowledge and new treatment options resulting from the precision oncology trials. Also, medical oncologists may learn more about molecular testing and interpreting test results from participation in MTBs. To maximize the impact of precision oncology, international collaborations are of utmost importance and research groups throughout the world are encouraged to share best practices and creative solutions to overcome the hurdles that still hamper new initiatives in the field today.

Future clinical research may focus on prospective therapy selection using molecular information from other -omics fields, such as phosphoproteomics, especially in patients where no clear monogenetic driver mutations is identified and a comprehensive pathway analysis may give more direction for potential therapeutic strategies. More knowledge on the best method of prioritizing targets for treatments will be essential, as well as clinical trials investigating new combinations of targeted agents.

With an increasing understanding of cancer biology and improved strategies for treatment selection, precision oncology will be accessible for patients with advanced cancer and more patients will benefit from the knowledge that we gain today and tomorrow. In the future, treatments based on histology alone may be considered old-fashioned, and multi-omics diagnostics may result in a comprehensible report that can be easily interpreted, and will directly guide treatment decisions for individual patients.

REFERENCES

1. Integraal Kankercentrum Nederland. Rapport “Uitgezaaide kanker in beeld”. 2020.

2. Hanahan D, Weinberg RA. Hallmarks of Cancer: The Next Generation. *Cell* 2011;144(5):646-674. (In English). DOI: 10.1016/j.cell.2011.02.013.

3. Cohen P. Protein kinases - the major drug targets of the twenty-first century? *Nat Rev Drug Discov* 2002;1(4):309-315. (In English). DOI: 10.1038/nrd773.

4. Roskoski R. A historical overview of protein kinases and their targeted small molecule inhibitors. *Pharmacol Res* 2015;100:1-23. (In English). DOI: 10.1016/j.phrs.2015.07.010.

5. Goldenberg MM. Trastuzumab, a recombinant DNA-derived humanized monoclonal antibody, a novel agent for the treatment of metastatic breast cancer. *Clin Ther* 1999;21(2):309-318. (In English). DOI: Doi 10.1016/S0149-2918(00)88288-0.

6. Olivier T, Haslam A, Prasad V. Anticancer Drugs Approved by the US Food and Drug Administration From 2009 to 2020 According to Their Mechanism of Action. *Jama Netw Open* 2021;4(12) (In English). DOI: ARTN e2138793 10.1001/jamanetworkopen.2021.38793.

7. Santucci C, Carioli G, Bertuccio P, et al. Progress in cancer mortality, incidence, and survival: a global overview. *Eur J Cancer Prev* 2020;29(5):367-381. (In English). DOI: 10.1097/Cej.0000000000000594.

8. Priestley P, Baber J, Lolkema MP, et al. Pan-cancer whole-genome analyses of metastatic solid tumours. *Nature* 2019;575(7781):210-+. (In English). DOI: 10.1038/s41586-019-1689-y.

9. Garcia VM, Olmos D, Gomez-Roca C, et al. Dose-Response Relationship in Phase I Clinical Trials: A European Drug Development Network (EDDN) Collaboration Study. *Clinical Cancer Research* 2014;20(22):5663-5671. (In English). DOI: 10.1158/1078-0432.Ccr-14-0719.

10. van Waalwijk van Doorn-Khosrovani SB, Pisters-van Roy A, van Saase L, et al. Personalised reimbursement: a risk-sharing model for biomarker-driven treatment of rare subgroups of cancer patients. *Ann Oncol* 2019. DOI: 10.1093/annonc/mdz119.

11. Le Tourneau C, Delord JP, Goncalves A, et al. Molecularly targeted therapy based on tumour molecular profiling versus conventional therapy for advanced cancer (SHIVA): a multicentre, open-label, proof-of-concept, randomised, controlled phase 2 trial. *Lancet Oncol* 2015;16(13):1324-1334. (In English). DOI: 10.1016/S1470-2045(15)00188-6.

12. Rodon J, Soria JC, Berger R, et al. Genomic and transcriptomic profiling expands precision cancer medicine: the WINTHER trial. *Nature Medicine* 2019;25(5):751-+. (In English). DOI: 10.1038/s41591-019-0424-4.

13. Sicklick JK, Kato S, Okamura R, et al. Molecular profiling of cancer patients enables personalized combination therapy: the I-PREDICT study. *Nature Medicine* 2019;25(5):744-+. (In English). DOI: 10.1038/s41591-019-0407-5.

14. Flaherty KT, Gray RJ, Chen AP, et al. Molecular Landscape and Actionable Alterations in a Genomically Guided Cancer Clinical Trial: National Cancer Institute Molecular Analysis for Therapy Choice (NCI-MATCH). *Journal of Clinical Oncology* 2020;38(33) (In English). DOI: 10.1200/Jco.19.03010.

15. NCI-MATCH Sets “Benchmark of Actionability”. *Cancer Discov* 2021;11(1):6-7. DOI: 10.1158/2159-8290.CD-NB2020-100.

16. Mangat PK, Halabi S, Bruinooge SS, et al. Rationale and Design of the Targeted Agent and Profiling Utilization Registry Study. *Jco Precis Oncol* 2018;2:1-14. (In English). DOI: 10.1200/Po.18.00122.

17. Halabi SM, P.; Garrett-Mayer, E.; van der Wijngaart, H.; Verheul, H.M.W.; Voest, E.E.; Siu, L.; Renouf, D.J.; Dancey, J.; Schilsky, R.L. Advancing Precision Oncology: TADRUCA, A Model for Global Collaboration.

18. Zeverijn LJ, Looze EJ, Thavaneswaran S, et al. Limited clinical activity of palbociclib and ribociclib monotherapy in advanced cancers with cyclin D-CDK4/6 pathway alterations in the Dutch DRUP and Australian MoST trials. *International Journal of Cancer* 2023 (In English). DOI: 10.1002/ijc.34649.

19. Hoes LR, Henegouwen JMV, van der Wijngaart H, et al. Patients with Rare Cancers in the Drug Rediscovery Protocol (DRUP) Benefit from Genomics-Guided Treatment. *Clinical Cancer Research* 2022;28(7):1402-1411. (In English). DOI: 10.1158/1078-0432.Ccr-21-3752.

20. Mock A, Heilig CE, Kreutzfeldt S, Gonzalez-Carmona MA. Community-driven development of a modified progression-free survival ratio for precision oncology (vol 4, e000583, 2019). *Esmo Open* 2020;5(1) (In English). DOI: ARTN e000583corr1 10.1136/esmoopen-2019-000583corr1.

21. Wu JR, Chen L, Wei J, Weiss H, Miller RW, Villano JL. Phase II trial design with growth modulation index as the primary endpoint. *Pharm Stat* 2019;18(2):212-222. (In English). DOI: 10.1002/pst.1916.

22. Basse C, Morel C, Alt M, et al. Relevance of a molecular tumour board (MTB) for patients’ enrolment in clinical trials: experience of the Institut Curie. *Esmo Open* 2018;3(3) (In English). DOI: UNSP e000339 10.1136/esmoopen-2018-000339.

23. van de Haar J, Hoes L, Voest E. Advancing molecular tumour boards: highly needed to maximise the impact of precision medicine. *Esmo Open* 2019;4(2) (In English). DOI: UNSP e000516 10.1136/esmoopen-2019-000516.

24. van der Velden DL, van Herpen CML, van Laarhoven HWM, et al. Molecular Tumor Boards: current practice and future needs. *Ann Oncol* 2017;28(12):3070-3075. (In English). DOI: 10.1093/annonc/mdx528.

25. Mateo J, Steuten L, Aftimos P, et al. Delivering precision oncology to patients with cancer. *Nature Medicine* 2022;28(4):658-665. (In English). DOI: 10.1038/s41591-022-01717-2.

26. Jonsson P, Bandlamudi C, Cheng ML, et al. Tumour lineage shapes BRCA-mediated phenotypes. *Nature* 2019;571(7766):576-579. DOI: 10.1038/s41586-019-1382-1.

27. Mukhopadhyay A, Elattar A, Cerbinskaite A, et al. Development of a Functional Assay for Homologous Recombination Status in Primary Cultures of Epithelial Ovarian Tumor and Correlation with Sensitivity to Poly(ADP-Ribose) Polymerase Inhibitors. *Clinical Cancer Research* 2010;16(8):2344-2351. (In English). DOI: 10.1158/1078-0432.Ccr-09-2758.

28. Sakai W, Swisher EM, Karlan BY, et al. Secondary mutations as a mechanism of cisplatin resistance in BRCA2-mutated cancers. *Nature* 2008;451(7182):1116-U9. (In English). DOI: 10.1038/nature06633.

29. Meijer TG, Nguyen L, Van Hoeck A, et al. Functional RECAP (REpair CAPacity) assay identifies homologous recombination deficiency undetected by DNA-based BRCAness tests. *Oncogene* 2022;41(26):3498-3506. (In English). DOI: 10.1038/s41388-022-02363-1.

30. Davies H, Glodzic D, Morganello S, et al. HRDetect is a predictor of BRCA1 and BRCA2 deficiency based on mutational signatures. *Nature Medicine* 2017;23(4):517-+. (In English). DOI: 10.1038/nm.4292.

31. Nguyen L, Martens JWM, Van Hoeck A, Cuppen E. Pan-cancer landscape of homologous recombination deficiency. *Nature Communications* 2020;11(1) (In English). DOI: ARTN 5584 10.1038/s41467-020-19406-4.

32. Wen PY, Stein A, van den Bent M, et al. Dabrafenib plus trametinib in patients with BRAF(V600E)-mutant low-grade and high-grade glioma (ROAR): a multicentre, open-label, single-arm, phase 2, basket trial. *Lancet Oncol* 2022;23(1):53-64. (In English). DOI: 10.1016/S1470-2045(21)00578-7.

33. Subbiah V, Kreitman RJ, Wainberg ZA, et al. Dabrafenib plus trametinib in patients with BRAF V600E-mutant anaplastic thyroid cancer: updated analysis from the phase II ROAR basket study. *Ann Oncol* 2022;33(4):406-415. (In English). DOI: 10.1016/j.annonc.2021.12.014.

34. Motzer RJ, Hutson TE, Tomczak P, et al. Overall Survival and Updated Results for Sunitinib Compared With Interferon Alfa in Patients With Metastatic Renal Cell Carcinoma. *Journal of Clinical Oncology* 2009;27(22):3584-3590. (In English). DOI: 10.1200/Jco.2008.20.1293.

35. Stommel JM, Kimmelman AC, Ying H, et al. Coactivation of receptor tyrosine kinases affects the response of tumor cells to targeted therapies. *Science* 2007;318(5848):287-90. DOI: 10.1126/science.1142946.

36. Klaeger S, Heinzlmeir S, Wilhelm M, et al. The target landscape of clinical kinase drugs. *Science* 2017;358(6367) (In English). DOI: ARTN eaan4368 10.1126/science.aan4368.

37. Motzer R, Rini BI, McDermott DF, et al. Nivolumab plus ipilimumab versus sunitinib in first-line treatment for advanced renal cell carcinoma: extended follow-up of efficacy and safety results from a randomised, controlled, phase 3 trial. *Lancet Oncol* 2019;20(10):1370-1385. (In English). DOI: 10.1016/S1470-2045(19)30413-9.

38. Motzer RJ, Hutson TE, Cella D, et al. Pazopanib versus Sunitinib in Metastatic Renal-Cell Carcinoma. *New Engl J Med* 2013;369(8):722-731. (In English). DOI: 10.1056/NEJMoa1303989.

39. Beuselinck B, Job S, Becht E, et al. Molecular Subtypes of Clear Cell Renal Cell Carcinoma Are Associated with Sunitinib Response in the Metastatic Setting. *Clinical Cancer Research* 2015;21(6):1329-1339. (In English). DOI: 10.1158/1078-0432.Ccr-14-1128.

40. Feng CC, Li YQ, Li KP, et al. PFKFB4 is overexpressed in clear-cell renal cell carcinoma promoting pentose phosphate pathway that mediates Sunitinib resistance (vol 40, 308, 2021). *J Exp Clin Canc Res* 2021;40(1) (In English). DOI: ARTN 379 10.1186/s13046-021-02165-5.

41. van der Mijn JC, Broxterman HJ, Knol JC, et al. Sunitinib activates Axl signaling in renal cell cancer. *Int J Cancer* 2016;138(12):3002-10. DOI: 10.1002/ijc.30022.

42. Clark DJ, Dhanasekaran SM, Petralia F, et al. Integrated Proteogenomic Characterization of Clear Cell Renal Cell Carcinoma. *Cell* 2019;179(4):964-983 e31. DOI: 10.1016/j.cell.2019.10.007.

43. Motzer RJ, Banchereau R, Hamidi H, et al. Molecular Subsets in Renal Cancer Determine Outcome to Checkpoint and Angiogenesis Blockade. *Cancer Cell* 2020;38(6):803-+. (In English). DOI: 10.1016/j.ccell.2020.10.011.

44. Vano YA, Elaidi R, Bennamoun M, et al. Nivolumab, nivolumab-ipilimumab, and VEGFR-tyrosine kinase inhibitors as first-line treatment for metastatic clear-cell renal cell carcinoma (BIONIKK): a biomarker-driven, open-label, non-comparative, randomised, phase 2 trial. *Lancet Oncol* 2022;23(5):612-624. (In English). DOI: 10.1016/S1470-2045(22)00128-0.

45. Hallal M, Braga-Lagache S, Jankovic J, et al. Inference of kinase-signaling networks in human myeloid cell line models by Phosphoproteomics using kinase activity enrichment analysis (KAEA). *Bmc Cancer* 2021;21(1) (In English). DOI: ARTN 789 10.1186/s12885-021-08479-z.

46. Li JJ, Wen SQ, Li B, Li N, Zhan XQ. Phosphorylation-Mediated Molecular Pathway Changes in Human Pituitary Neuroendocrine Tumors Identified by Quantitative Phosphoproteomics. *Cells* 2021;10(9) (In English). DOI: ARTN 2225 10.3390/cells10092225.

47. Khorsandi SE, Dokal AD, Rajeev V, et al. Computational Analysis of Cholangiocarcinoma Phosphoproteomes Identifies Patient-Specific Drug Targets. *Cancer Research* 2021;81(22):5765-5776. (In English). DOI: 10.1158/0008-5472.Can-21-0955.

48. Xu RF, Chen Y, Wang ZJ, et al. Phosphoproteomics Identifies Significant Biomarkers Associated with the Proliferation and Metastasis of Prostate Cancer. *Toxins* 2021;13(8) (In English). DOI: ARTN 554 10.3390/toxins13080554.

49. Hirano H, Abe Y, Nojima Y, et al. Temporal dynamics from phosphoproteomics using endoscopic biopsy specimens provides new therapeutic targets in stage IV gastric cancer. *Sci Rep-Uk* 2022;12(1) (In English). DOI: ARTN 4419 10.1038/s41598-022-08430-7.

50. van Linde ME, Labots M, Brahm CG, et al. Tumor Drug Concentration and Phosphoproteomic Profiles After Two Weeks of Treatment With Sunitinib in Patients with Newly Diagnosed Glioblastoma. *Clinical Cancer Research* 2022;28(8):1595-1602. (In English). DOI: 10.1158/1078-0432.Ccr-21-1933.

51. Labots M, Pham TV, Honeywell RJ, et al. Kinase Inhibitor Treatment of Patients with Advanced Cancer Results in High Tumor Drug Concentrations and in Specific Alterations of the Tumor Phosphoproteome. *Cancers (Basel)* 2020;12(2). DOI: 10.3390/cancers12020330.

52. Labots M, van der Mijn JC, Beekhof R, et al. Phosphotyrosine-based-phosphoproteomics scaled-down to biopsy level for analysis of individual tumor biology and treatment selection. *J Proteomics* 2017;162:99-107. DOI: 10.1016/j.jprot.2017.04.014.

53. Lai HW, Wu HK, Kuo SJ, et al. Differences in accuracy and underestimation rates for 14- versus 16-gauge core needle biopsies in ultrasound-detectable breast lesions. *Asian J Surg* 2013;36(2):83-88. (In English). DOI: 10.1016/j.asjsur.2012.09.003.

54. Bray SE, Paulin FE, Fong SC, et al. Gene expression in colorectal neoplasia: modifications induced by tissue ischaemic time and tissue handling protocol. *Histopathology* 2010;56(2):240-50. DOI: 10.1111/j.1365-2559.2009.03470.x.

55. Buffart TE, van den Oord RAHM, van den Berg A, et al. Time dependent effect of cold ischemia on the phosphoproteome and protein kinase activity in fresh-frozen colorectal cancer tissue obtained from patients. *Clin Proteom* 2021;18(1) (In English). DOI: ARTN 8 10.1186/s12014-020-09306-6.

56. Freidin MB, Bhudia N, Lim E, Nicholson AG, Cookson WO, Moffatt MF. Impact of collection and storage of lung tumor tissue on whole genome expression profiling. *J Mol Diagn* 2012;14(2):140-8. DOI: 10.1016/j.jmoldx.2011.11.002.

57. Mertins P, Yang F, Liu T, et al. Ischemia in tumors induces early and sustained phosphorylation changes in stress kinase pathways but does not affect global protein levels. *Mol Cell Proteomics* 2014;13(7):1690-704. DOI: 10.1074/mcp.M113.036392.

58. Engel KB, Vaught J, Moore HM. National Cancer Institute Biospecimen Evidence-Based Practices: A Novel Approach to Pre-analytical Standardization. *Biopreservation and Biobanking* 2014;12(2):148-150. (In English). DOI: 10.1089/bio.2013.0091.

59. van Limbeek MAJ, Jagga S, Holland H, Ledebøer K, ter Brake M, Vanapalli S. Cooling of a vial in a snapfreezing device without using sacrificial cryogens. *Sci Rep-Uk* 2019;9 (In English). DOI: ARTN 3510 10.1038/s41598-019-40115-6.

60. Barnes RO, Parisien M, Murphy LC, Watson PH. Influence of evolution in tumor biobanking on the interpretation of translational research. *Cancer Epidemiol Biomarkers Prev* 2008;17(12):3344-50. DOI: 10.1158/1055-9965.EPI-08-0622.

61. Schwartz SA, Reyzer ML, Caprioli RM. Direct tissue analysis using matrix-assisted laser desorption/ionization mass spectrometry: practical aspects of sample preparation. *J Mass Spectrom* 2003;38(7):699-708. (In English). DOI: 10.1002/jms.505.

62. Wisniewski JR. Filter-Aided Sample Preparation: The Versatile and Efficient Method for Proteomic Analysis. *Method Enzymol* 2017;585:15-27. (In English). DOI: 10.1016/bs.mie.2016.09.013.

63. Holfeld A, Valdes A, Malmstrom PU, Segersten U, Lind SB. Parallel Proteomic Workflow for Mass Spectrometric Analysis of Tissue Samples Preserved by Different Methods. *Anal Chem* 2018;90(9):5841-5849. (In English). DOI: 10.1021/acs.analchem.8b00379.

64. Coscia F, Doll S, Bech JM, et al. A streamlined mass spectrometry-based proteomics workflow for large-scale FFPE tissue analysis. *Journal of Pathology* 2020;251(1):100-112. (In English). DOI: 10.1002/path.5420.

65. Steu S, Baucamp M, von Dach G, et al. A procedure for tissue freezing and processing applicable to both intra-operative frozen section diagnosis and tissue banking in surgical pathology. *Virchows Arch* 2008;452(3):305-12. DOI: 10.1007/s00428-008-0584-y.

66. Kennedy JJ, Woodcock A, Ivey RG, et al. Preserving the Phosphoproteome of Clinical Biopsies Using a Quick-Freeze Collection Device. *Biopreservation and Biobanking* 2022;20(5):436-445.

67. Council EPa. Regulation (EU) 2016/679 of the European Parliament and of the Council of 27 April 2016, On the protection of natural persons with regard to the processing of personal data and on the free movement of such data, and repealing Directive 95/46/EC (General Data Protection Regulation). 2016.

68. Olivier M, Asmis R, Hawkins GA, Howard TD, Cox LA. The Need for Multi-Omics Biomarker Signatures in Precision Medicine. *Int J Mol Sci* 2019;20(19) (In English). DOI: ARTN 4781 10.3390/ijms20194781.

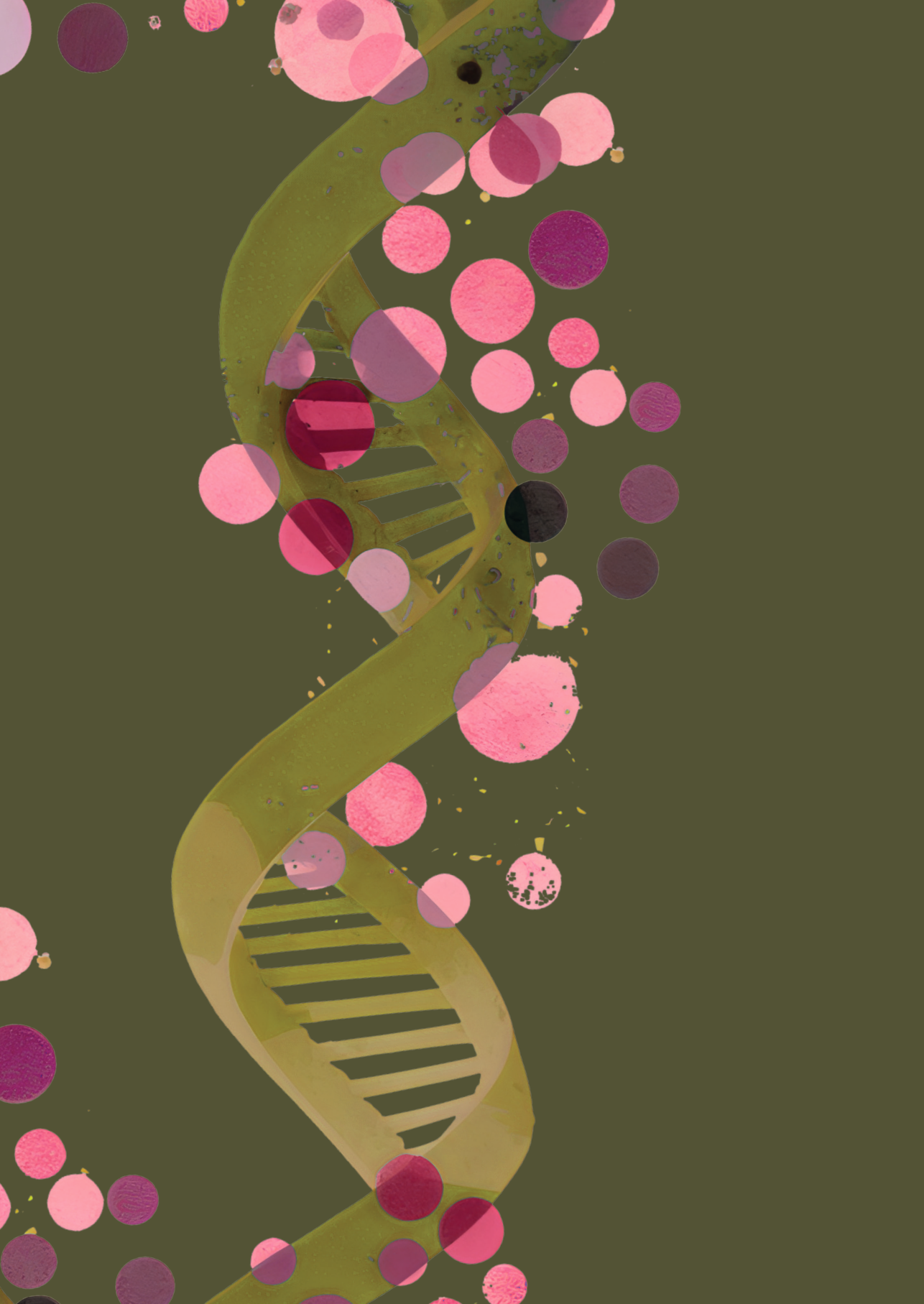
69. Nederland Z. Standpunt nivolumab (Opdivo®) voor de behandeling van bepaalde patiënten met dMMR- of MSI-tumoren - Zorginstituut Nederland. 2022.

70. de Bono J, Mateo J, Fizazi K, et al. Olaparib for Metastatic Castration-Resistant Prostate Cancer. *N Engl J Med* 2020. DOI: 10.1056/NEJMoa1911440.

71. Pietrantonio F, Petrelli F, Coinu A, et al. Predictive role of BRAF mutations in patients with advanced colorectal cancer receiving cetuximab and panitumumab: A meta-analysis. *Eur J Cancer* 2015;51(5):587-594. (In English). DOI: 10.1016/j.ejca.2015.01.054.

72. Rowland A, Dias MM, Wiese MD, et al. Meta-analysis of BRAF mutation as a predictive biomarker of benefit from anti-EGFR monoclonal antibody therapy for RAS wild-type metastatic colorectal cancer. *Brit J Cancer* 2015;112(12):1888-1894. (In English). DOI: 10.1038/bjc.2015.173.

73. Sorich MJ, Wiese MD, Rowland A, Kichenadasse G, McKinnon RA, Karapetis CS. Extended RAS mutations and anti-EGFR monoclonal antibody survival benefit in metastatic colorectal cancer: a meta-analysis of randomized, controlled trials. *Ann Oncol* 2015;26(1):13-21. (In English). DOI: 10.1093/annonc/mdu378.





CHAPTER 7

| Nederlandse samenvatting

NEDERLANDSE SAMENVATTING

Jaarlijks worden in Nederland zo'n 38.000 mensen getroffen door uitgezaaide kanker. Bij een op de vijf mensen met kanker zijn op het moment van diagnose al uitzaaiingen aanwezig. Voor slechts een kleine minderheid van hen is een genezende behandeling voorhanden, maar voor de meeste mensen met gevorderde kanker is de behandeling palliatief. Dat wil zeggen, gericht op het verminderen van ziekte-gerelateerde klachten en verlengen van het leven terwijl de kwaliteit van leven behouden blijft. Tot voorkort bestond een palliatieve behandeling veelal uit chemotherapie, voor alle mensen met hetzelfde type kanker dezelfde behandeling. Sommigen hebben daar baat bij, anderen niet. Dat is op voorhand vaak niet goed te voorspellen. De meeste mensen hebben echter wel bijwerkingen van chemotherapie die hun kwaliteit van leven kan bedreigen.

Kanker is een ziekte van het genoom, die gekarakteriseerd wordt door veranderingen in het DNA (mutaties) en mede daardoor stoornissen in de overdracht van groeisignalen in de cel, met ongeremde en ongecontroleerde groei en celdeling tot gevolg. De eiwitten die betrokken zijn bij deze verstoorde signaaloverdracht zijn mogelijk belangrijke doelwitten (targets) voor doelgerichte behandeling tegen kanker. In de afgelopen 25 jaar zijn veel nieuwe doelgerichte medicijnen ontwikkeld en op de markt gekomen die specifiek ingrijpen op deze afwijkende signaaloverdracht in kankercellen. Deze zogenaemde proteïnekinaseremmers hebben, samen met de opkomst van de immunotherapie, de behandelmogelijkheden en vooruitzichten van patiënten met gevorderde kanker in belangrijke mate verbeterd.

Een belangrijke vraag blijft echter: hoe selecteren we de juiste behandeling voor de juiste patiënt op het juiste moment? Hoe kunnen we op voorhand het meest nauwkeurig bepalen of een individuele patiënt wel of geen baat zal hebben bij een behandeling? En hoe zorgen we ervoor dat in de toekomst een gepersonaliseerde behandeling gericht op de kenmerken van een individuele tumor voor iedere patiënt met kanker tot de mogelijkheden behoort?

Het onderzoek beschreven in dit proefschrift richt zich op de klinische toepassing van een aantal methoden voor de selectie van doelgerichte behandelingen op basis van specifieke moleculaire tumorprofielen, gebruik makend van genetische profielen (hoofdstuk 2 en 3) en gefosforyleerde eiwitprofielen (hoofdstuk 4), en de ontwikkeling en validatie van een nieuwe snap freezer (hoofdstuk 5) om de moleculaire profielen van vriesbiopten zo goed mogelijk te behouden en daarmee de analyses benodigd voor therapieselectie te faciliteren.

THERAPIESELECTIE OP BASIS VAN GENETISCHE PROFIELEN: DRUG REDISCOVERY PROTOCOL

Iedere tumor heeft een unieke genetische en moleculaire samenstelling. De technieken om grootschalige DNA-analyses te doen worden steeds beter en zijn op steeds meer plaatsen beschikbaar. Hiermee wordt in toenemende mate kennis opgedaan over de genetische eigenschappen van verschillende tumoren. Specifieke mutaties die kenmerkend waren voor een bepaald tumortype, bleken ook bij andere tumortypes met regelmaat voor te komen. Helaas

zijn de beschikbare geneesmiddelen gericht tegen deze mutaties vaak slechts voor een of enkele tumortypes geregistreerd, waardoor een mens met andere tumortypes met deze mutatie geen aanspraak kunnen maken op deze mogelijk effectieve behandeling.

In **hoofdstuk 2** beschreven wij de opzet en de uitvoerbaarheid van het Drug Rediscovery Protocol (DRUP studie) en de resultaten van de eerste 215 patiënten die in deze studie behandeld werden, inclusief de resultaten van het eerste complete cohort. DRUP is een landelijke prospectieve fase 2 klinische studie met meerdere medicijnen, voor patiënten met alle vormen van kanker. Sinds de start van de studie in 2016 worden patiënten met gevorderde solide tumoren, voor wie geen standaard behandelopties (meer) voorhanden zijn, behandeld met bestaande doelgerichte anti-kanker medicijnen op basis van hun moleculaire tumorprofielen, buiten de bestaande indicaties om. Patiënten worden behandeld in meerdere parallelle cohorten die allen gekenmerkt worden door hetzelfde tumortype, met mutaties in hetzelfde gen, en dezelfde doelgerichte behandeling. In enkele cohorten speelt het tumortype geen rol en kunnen patiënten met iedere vorm van kanker geïncludeerd worden, zolang ze de benodigde genmutatie hebben.

Analyse van de resultaten van de eerste 215 patiënten in de studie toonde aan dat 34% van hen baat had bij de doelgerichte behandeling. “Baat” wordt binnen DRUP gedefinieerd als een objectieve respons (afname van meetbare ziekte) of stabiele ziekte (het uitblijven van progressie) gedurende ten minste 16 weken vanaf de start van de behandeling. In andere ongeselecteerde fase 1 studies, in een vergelijkbare patiëntenpopulatie, heeft doorgaans slechts ongeveer 11% van de patiënten baat bij de studiebehandeling, dit geeft aan dat de DRUP-aanpak van therapieselectie op basis van genetische informatie in de tumor een potentieel veelbelovende strategie is. Uiteindelijk zijn de behandelresultaten per individueel cohort het meest interessant. Dit hoofdstuk beschrijft tevens de resultaten van het eerste complete cohort in de DRUP studie. In dit cohort werden 30 patiënten met 8 verschillende tumortypes bij wie microsatelliet instabiliteit (MSI) was vastgesteld in de tumor, behandeld met nivolumab, een vorm van immunotherapie. In dit cohort had 63% van de patiënten baat bij de behandeling, en de mediane progressievrije overleving was nog niet bereikt na 16.5 maanden follow-up. Dit mooie resultaat werd bevestigd in een nieuw expansiecohort binnen DRUP, waarin nog eens 130 patiënten met MSI tumoren werden geïncludeerd. De resultaten van deze cohorten leidden in Nederland in 2022 tot vergoeding van nivolumab als off-label behandeling voor patiënten met MSI tumoren in de laatste lijn, nadat geen andere standaard behandelopties meer voorhanden zijn.

In dit expansiecohort binnen DRUP werd ook voor het eerst gewerkt met een nieuw ontwikkeld persoonlijk vergoedingsmodel. Voordat potentieel effectieve behandelingen vergoed kunnen worden voor patiënten in Nederland moet eerst aangetoond worden dat de betreffende behandeling de stand der wetenschap en praktijk is. Voor zeldzame subgroepen van kanker met een specifieke biomarker kan het vergaren van voldoende wetenschappelijke bewijslast binnen afzienbare tijd tot problemen leiden, waardoor mogelijk effectieve behandelingen pas

laat beschikbaar komen. Met het nieuwe persoonlijke vergoedingsmodel worden patiënten gedurende de eerste 16 weken met studiemedicatie behandeld, beschikbaar gesteld door de fabrikant. Indien de patiënt baat heeft bij de behandeling na 16 weken wordt dit gezien als “stand der wetenschap en praktijk” voor deze individuele patiënt, en wordt daarmee vanaf dat moment vergoede zorg. Hiermee komt ook voor meer patiënten met zeldzame vormen van kanker met een specifieke biomarker een mogelijk effectieve behandeling met doelgerichte medicijnen weer een stap dichterbij.

In **hoofdstuk 3** beschreven wij de resultaten van een tweede cohort binnen de DRUP studie. In dit cohort werden 24 patiënten met 9 verschillende tumortypes, bij wie in het tumor-DNA een inactivatie van het BRCA1- of BRCA2-gen werd vastgesteld, behandeld met de PARP-remmer olaparib. Genmutaties in BRCA1/2, met name in de kiembaan, kennen we vooral bij eierstokkanker en borstkanker. Echter deze mutaties komen ook voor bij 1.8% (verworven) - 2.7% (kiembaan) van alle andere vormen van kanker. Inactivatie van BRCA1/2 veroorzaakt een defect in het DNA reparatiesysteem, waardoor een specifieke vorm van DNA-schade niet meer gerepareerd kan worden (homologe recombinatie deficiëntie). Deze eigenschap maakt de kankercellen gevoelig voor behandeling met een PARP-remmer. Olaparib zorgt voor ophoping van DNA-schade in de kankercel door blokkade van een ander essentieel reparatie-eiwit, waardoor de kankercel sterft. In ons cohort had 58% van de 24 patiënten baat bij een behandeling met olaparib. Wanneer we inzoomen op de patiënten die een *volledig verlies* van BRCA1/2 functie had, had 73% van hen baat bij de behandeling. Onder hen waren ook meerdere patiënten met tumortypes die voor zover bekend niet “BRCA-geassocieerd” zijn. Van de zogenaamde “BRCA-geassocieerde tumortypes (borstkanker, eierstokkanker, prostaatcancer en alveolierkanker) weten we inmiddels dat BRCA-mutaties vaker voorkomen en dat zij doorgaans gevoelig lijken te zijn voor behandeling met PARP-remmers. Onze resultaten tonen aan dat ook bij andere tumortypes in aanwezigheid van volledig functieverlies van BRCA1/2 een behandeling met een PARP-remmer overwogen kan worden. Bevestiging van de resultaten van dit cohort in een onafhankelijk expansiecohort binnen de DRUP studie is momenteel in voorbereiding.

Interessant genoeg waren er in ons cohort ook patiënten met volledig verlies van BRCA functie, maar die geen baat hadden bij een behandeling met olaparib. Bij vrijwel al deze patiënten werd naast de BRCA mutatie ook een andere oncogene drivermutatie gevonden. Ondanks de aanwezigheid van de BRCA-mutatie lijkt in die gevallen de tumorgroei niet afhankelijk te zijn van de BRCA-signaleringsroute, en is behandeling met een PARP-remmer waarschijnlijk niet opportuun. Toekomstig onderzoek zal moeten uitwijzen of respons op een PARP-remmer mogelijk beter op een andere manier voorspeld zou kunnen worden, bijvoorbeeld door gebruik te maken van de Homologe Recombinatie Deficiëntie-score (HRD-score) als biomarker, een maat voor hoe goed (of slecht) de kankercellen in staat zijn om DNA-schade te herstellen.

THERAPIESELECTIE OP BASIS VAN FOSFO-EIWIT PROFIELEN

De aanwezigheid van een duidelijke genetische biomarker in kankercellen die voorspellend is voor de respons op een behandeling is een van de hoekstenen van de precisie-oncologie.

Een mooi voorbeeld hiervan is een mutatie in het BRAF-gen, welke voorspellend is voor een respons op BRAF- en MEK remmers in bijvoorbeeld het gevorderd melanoom, hooggradige hersentumoren en het anaplastisch schildkliercarcinoom. Deze proteïnekinaseremmers zijn uitsluitend geïndiceerd bij patiënten met een BRAF-mutatie in hun kankercellen. Echter, sommige andere tyrosinekinaseremmers worden gebruikt zonder de aanwezigheid van een genetische biomarker, bijvoorbeeld sunitinib als eerstelijns behandeling van het gemetastaseerd niercelcarcinoom. Het niercelcarcinoom is een ziekte die niet gedreven wordt door één specifieke driver-mutatie, maar waarschijnlijk door meerdere afwijkend gereguleerde signaleringsroutes in de kankercellen. Ondanks dat er nog geen moleculaire biomarker voor respons op sunitinib is gevonden, heeft meer dan de helft van de patiënten met niercelcarcinoom baat bij deze behandeling. De mogelijkheid om per patiënt voorafgaand aan de behandeling met sunitinib te kunnen voorspellen of hij/zij daar baat bij zal hebben, zou mogelijk onnodige bijwerkingen kunnen voorkomen.

Phosphoproteomics richt zich specifiek op het identificeren en karakteriseren van eiwitten die gefosforyleerd zijn. Fosforylatie is een belangrijk biochemisch proces waarbij fosfaatgroepen worden toegevoegd aan eiwitten door kinases. Dit proces reguleert veel cellulaire functies en is van cruciaal belang voor de signaaloverdracht binnen cellen. Phosphoproteomics kan helpen begrijpen hoe eiwitten functioneren, hoe cellulaire processen worden gereguleerd en hoe ze betrokken zijn bij ziekten. Hiermee kunnen nieuwe inzichten vergaard worden in potentiële nieuwe targets voor doelgerichte behandeling van kanker, specifiek met proteïnekinaseremmers.

In **hoofdstuk 4** beschreven wij een phosphoproteomics analyse van tumorweefsel van 26 patiënten met niercelcarcinoom, die vervolgens werden behandeld met sunitinib. We vergeleken de fosfo-eiwit profielen van patiënten die wel of geen baat hadden bij de behandeling. Baat werd gedefinieerd als “geen progressie in de eerste 12 weken na start van de behandeling”. Het doel van deze analyse was het beschrijven van biologische verschillen tussen deze twee groepen die mogelijk samenhangen met respons op de behandeling. Hierbij vonden wij een set van 78 onderscheidende gefosforyleerde eiwitten en tevens verschillen in kinase activiteit, die wijst op activatie van verschillende signaleringsroutes in de tumoren van patiënten met en zonder baat bij behandeling met sunitinib. Drie eiwitten die verhoogd tot expressie kwamen in de groep *zonder* baat bij sunitinib toonden overlap met een vergelijkende transcriptoom (RNA) analyse in een onafhankelijk cohort van patiënten met niercelcarcinoom, één van deze eiwitten was ook uitsluitend gefosforyleerd in patiënten zonder baat. Deze onderscheiden (fosfo-)eiwitten spelen mogelijk een rol bij resistentiemechanismen in de tumorcellen en zouden mogelijk in de toekomst behulpzaam kunnen zijn bij het voorspellen van respons op een behandeling met sunitinib. Na validatie van deze bevindingen zou uiteindelijk een nieuwe test ontwikkeld kunnen worden die resistentie kan voorspellen. Een dergelijke test moet voor clinic gemakkelijk te interpreteren zijn, om zo klinische beslissingen ten aanzien van therapiekeuze bij individuele patiënten met niercelcarcinoom te kunnen ondersteunen.

OPTIMAAL BEHOUD VAN MOLECULAIRE PROFIELEN IN TUMORWEEFSEL SAMPLES

Met de opkomst van nieuwe technieken om grootschalige moleculaire analyses op tumorweefsel mogelijk te maken, komen ook nieuwe uitdagingen op ons af. Wanneer op grote schaal verschillende lagen van de celbiologie parallel onderzocht worden, bijvoorbeeld genomics (DNA), transcriptomics (RNA), proteomics (eiwitten), noemen we dit “multi-omics”. Er moeten voor een dergelijke gecombineerde analyse meerdere technieken worden toegepast op hetzelfde stukje weefsel. Veelal wordt gebruik gemaakt van naaldbiopten van tumorweefsel, die verkregen worden via echo- of CT-geleide punctie. Een aantal van de moleculaire kenmerken van kankercellen kunnen veranderen of verloren gaan na afname van het biopt door de plotselinge hypoxie in het gebiopteerde weefsel. Vooral fosforylatie is hier gevoelig voor. Om deze veranderingen in de moleculaire samenstelling van de cellen te minimaliseren, wordt een biopt na afname zo snel mogelijk ingevroren en opgeslagen bij een temperatuur van -80°C . Dit supersnel invriezen noemen we snap-freezing, en in de praktijk gebeurt dit vrijwel altijd door onderdompeling in vloeibaar stikstof, dat een temperatuur heeft van -196°C . Het gebruik van vloeibaar stikstof heeft echter een aantal belangrijke nadelen met betrekking tot gebruiksgemak en milieuvriendelijkheid. Om deze reden is een nieuwe snap freezer ontwikkeld die geen gebruik maakt van vloeibaar stikstof, om biopten zo gestandaardiseerd en eenvoudig mogelijk in te kunnen vriezen en daarmee de moleculaire profielen in tumorweefsel zo goed mogelijk te behouden voor het verrichten van (multi)omics analyse.

In **hoofdstuk 5** vergeleken wij de prestaties van deze nieuwe snap freezer met betrekking tot het behoud van moleculaire profielen (phosphoproteomics en transcriptomics) met samples die in vloeibaar stikstof verwerkt zijn. Hiervoor gebruikten wij de kanker cellijn K562 en tevens naaldbiopten van normaal leverweefsel van verschillende patiënten die als onderdeel van een reguliere behandeling een resectie van een deel van de lever ondergingen. We hebben cellijn samples en leverweefsel ingevroren met gebruik van vloeibaar stikstof en met de snap freezer. Vervolgens vergeleken we de moleculaire profielen van deze samples en beschreven we de mate van overlap, waarbij de hypothese was dat de samples verwerkt met de snap freezer even goed geconserveerd bleven als de samples in vloeibaar stikstof. We verwachtten dus een grote mate van overlap in profielen te vinden bij vergelijkende analyse. Uit de vergelijking met cellijn samples bleek dat de RNA integriteit, RNA profielen en gefosforyleerde eiwitprofielen zeer sterk overeen kwamen, en dat de samples die met de verschillende vriesmethoden verwerkt waren niet van elkaar te onderscheiden waren. Het controle-sample, dat 2 uur op kamertemperatuur bewaard werd alvorens het ingevroren werd, toonde wel duidelijke verschillen ten opzichte van de andere samples. De vergelijkende analyse van de leverweefsel samples toonde aan dat middels beide snap freezing methoden de moleculaire profielen van individuele patiënten van elkaar onderscheiden konden worden. Deze resultaten bevestigen dat de nieuwe snap freezer net zo goed als vloeibaar stikstof in staat is om hoge kwaliteit biologische samples te conserveren en geeft de mogelijkheid om verschillende patiënt-specifieke moleculaire profielen van elkaar te onderscheiden. Dit laatste is in de klinische praktijk van de precisie-oncologie zeer relevant, omdat beslissingen omtrent welke behandeling geschikt is

voor welke patiënt gemaakt worden met behulp van hun individuele moleculaire tumorprofielen. De snap freezer heeft een combinatie van gunstige eigenschappen wat betreft mobiliteit, gebruiksgemak en technische prestaties, terwijl het apparaat niet de beperkingen van het gebruik van vloeibaar stikstof heeft.

De commerciële ontwikkeling van een snap freezer die geen vloeibaar stikstof bevat, mobiel is en die op gestandaardiseerde wijze biopten zeer snel en eenvoudig kan invriezen zou een mooie aanwinst zijn voor de precisie-oncologie. Op deze manier is het conserveren van biopten voor multi-omics diagnostiek in ieder ziekenhuis mogelijk en hebben alle patiënten toegang tot dezelfde diagnostiek en de kans om baat te hebben bij een gepersonaliseerde behandeling, onafhankelijk van de plaats waar zij hun behandeling krijgen.

CONCLUSIE EN BLIK OP DE TOEKOMST

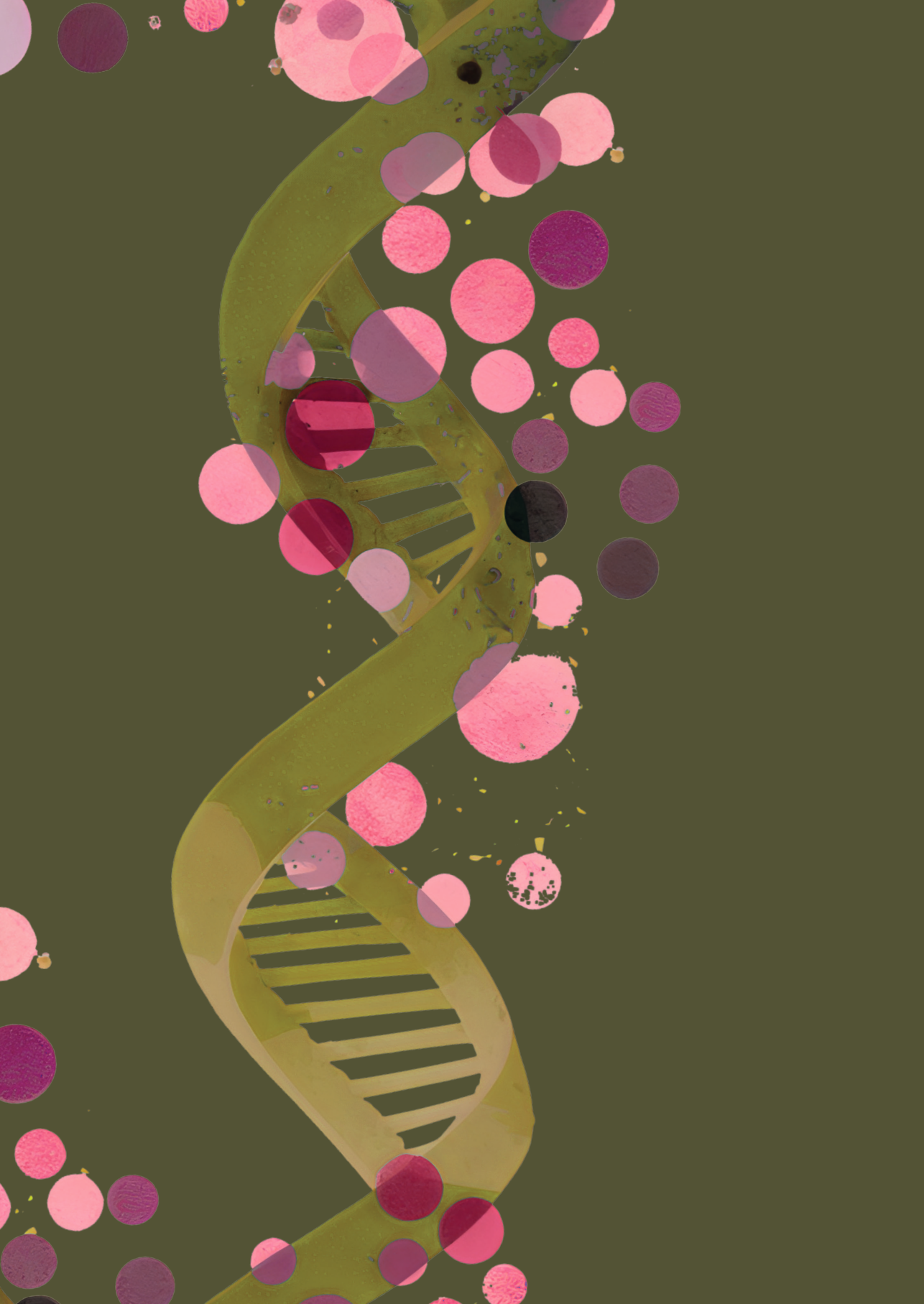
Precisie-oncologie heeft sinds de introductie van het eerste doelgerichte medicijn (trastuzumab) in 1999 een lange weg afgelegd. Breed moleculair onderzoek van tumorweefsel heeft onze kennis van de biologie van kanker aanzienlijk vergroot, wat heeft geleid tot een steile toename van het aantal goedgekeurde doelgerichte medicijnen en een uitbreiding van de geregistreerde indicaties van deze medicijnen. Het off-label gebruik van deze nieuwe doelgerichte medicijnen is tegenwoordig beter gedocumenteerd en wordt vaak uitgevoerd in de context van klinische onderzoeken om het leerpotentieel van deze experimentele behandelingen voor de medische gemeenschap te maximaliseren. Zolang er geen algemene “genezing voor kanker” bestaat, zal er ruimte zijn voor verbetering van onze kennis en aanpak van de behandeling van patiënten met kanker.

Algemene verbeteringen in de logistiek, beschikbaarheid van doelgerichte medicijnen en toegang tot diagnostiek en expertise zullen waarschijnlijk de grootste invloed hebben op direct voordeel voor patiënten. In de toekomst zou gestandaardiseerde verwerking en conservering van tumorweefsel/biopten mogelijk moeten zijn in alle ziekenhuizen, en samenwerking en het delen van kennis en middelen tussen perifere en academische instellingen zijn noodzakelijk om precisie-oncologie aan alle patiënten te kunnen leveren. Als aan deze voorwaarden wordt voldaan, kunnen meer patiënten mogelijk profiteren van de kennis en nieuwe behandelopties die voortkomen uit de precisie-oncologieonderzoeken. Ook kunnen medisch oncologen meer leren over moleculaire tests en het interpreteren van testresultaten door deelname aan Moleculaire TumorBoards. Om het effect van precisie-oncologie te maximaliseren, zijn internationale samenwerkingen van groot belang en worden onderzoeksgroepen over de hele wereld aangemoedigd om beste ervaringen en creatieve oplossingen te delen om de obstakels te overwinnen die nieuwe initiatieven op dit gebied vandaag de dag nog belemmeren.

Toekomstig klinisch onderzoek kan zich richten op prospectieve selectie van doelgerichte therapie op basis van moleculaire informatie uit andere -omics-velden, zoals phosphoproteomics, vooral bij patiënten waarbij niet één duidelijke genetische drivermutatie geïdentificeerd is en een uitgebreide pathway-analyse meer richting kan geven voor mogelijke therapeutische

strategieën. Meer kennis over de beste methode om targets voor behandelingen te prioriteren, evenals klinische onderzoeken naar nieuwe combinaties van doelgerichte middelen, zullen essentieel zijn.

Met een toenemend begrip van de kankerbiologie en verbeterde strategieën voor behandelkeuze zal precisie-oncologie toegankelijk worden voor patiënten met gevorderde kanker, en meer patiënten zullen profiteren van de kennis die we vandaag en morgen opdoen. In de toekomst zullen behandelingen op basis van histologie mogelijk als ouderwets worden beschouwd, en resultaten van multi-omics diagnostiek zullen worden weergegeven in een overzichtelijk en begrijpelijk rapport dat gemakkelijk kan worden geïnterpreteerd door een behandelend arts, zodat het directe behandelbeslissingen kan sturen voor individuele patiënten.





APPENDICES

Dankwoord

Curriculum vitae

List of publications

DANKWOORD

Het zit erop! Met het voltooien van dit proefschrift komt een einde aan mijn onderzoekstijd bij de afdeling medische oncologie van het Amsterdam UMC en het Cancer Center Amsterdam. De beslissing om in 2017 mijn opleiding tot internist-oncoloog te onderbreken voor een promotie-onderzoek was, ondanks de verrassende timing, een van de beste beslissingen van mijn professionele leven. Ik had het voorrecht om tijdens mijn onderzoekstijd heel veel enthousiaste, inspirerende en gezellige mensen te ontmoeten. Zij hebben in belangrijke mate bijgedragen aan de totstandkoming van dit proefschrift en aan de geweldige tijd die ik heb gehad. Een aantal van hen wil ik hier in het bijzonder bedanken.

Allereerst veel dank aan alle *patiënten* die deelnamen aan de DRUP en CPCT-02 studies en hun naasten. Ik heb veel bewondering voor hun motivatie om in de meest kwetsbare periode van hun leven een bijdrage te willen leveren aan de wetenschap.

Ik prijs me gelukkig met een zeer bevlogen, enthousiast, (terecht) kritisch en bovenal optimistisch promotieteam. Jullie hebben mij gestimuleerd om steeds het beste uit mijzelf te halen, niet te snel tevreden te zijn en niet in begrenzingsen maar juist in mogelijkheden te denken.

Prof. dr. Henk M.W. Verheul, promotor. Beste *Henk*, heel veel dank voor de kans die je me hebt gegeven om aan dit promotie-onderzoek te beginnen. Ik had het avontuur met niemand anders aangedurfd en heb er veel van geleerd. Bijzonder hoe je altijd precies de juiste vragen weet te stellen, je scherpe blik, maar altijd met het perspectief van de patiënt (of de promovendus) in beeld. Onze fietstochtjes naar het AVL, de werkbesprekingen, de retreats in Nes a/d Amstel, met als (culinair) hoogtepunt een kookworkshop, ik denk er graag aan terug. Jouw optimisme en aansporing waren vaak precies wat ik nodig had. De ritjes naar Nijmegen en Rotterdam waren altijd de moeite meer dan waard. Maar het meest waardeer ik ons persoonlijke contact en je vertrouwen in mij als oncoloog en onderzoeker. Onze gesprekken aan de keukentafel hebben mij richting gegeven en ik ben dankbaar voor je adviezen en hulp. Ik hoop van harte dat we in de toekomst kunnen blijven samenwerken, maar vooral dat we elkaar nog regelmatig kunnen opzoeken voor een kop koffie en een goed gesprek!

Prof. dr. Emile E. Voest, promotor. Beste *Emile*, wat was het bijzonder om met jou samen te werken. Je bezit een zeldzame combinatie van kwaliteiten. Naast een grote inhoudelijke kennis van zaken en visie voor de toekomst van de oncologische zorg heb je het talent om partijen bij elkaar te brengen en gemeenschappelijkheden te vinden waardoor alle neuzen dezelfde kant op komen te staan. Als onderdeel van het DRUP studieteam kreeg ik de kans om van dichtbij te observeren hoe je dat allemaal aanpakt, ontzettend leerzaam! Ik heb fijne herinneringen aan de vroege werkbesprekingen om 7.30 uur, de wetenschapsbesprekingen (“het moet een beetje schuren”), ESMO x2, BBQ in Soest, de ontelbare keren dat ik binnen 1 minuut na verzending “akkoord, gr Emile” zag binnenkomen in mijn mailbox, en de talloze discussies, successen en vraagstukken van de DRUP. Veel dank voor alles!

Dr. Mariette Labots, co-promotor. Beste *Mariette*, ik weet nog goed dat jij mij bij aanvang van het promotietraject tijdens een eerste werkbespreking probeerde uit te leggen wat phosphoproteomics is, en waarom we ons onderzoek daarop zouden moeten focussen. Na een uur aandachtig geknikt te hebben, begreep ik er helaas nog maar weinig van (dat lag niet aan jou!), maar omdat we het *samen* zouden doen had ik vertrouwen dat het goed zou komen. Dat vertrouwen is er, dankzij jouw aanhoudende steun en hulp, altijd gebleven. Ik vond het een voorrecht om zo intensief met je te kunnen samenwerken al die tijd. In veel opzichten ben je een voorbeeld voor mij. Jouw aanmoediging, expertise en kritische blik, maar ook je menselijke maat en ons persoonlijke contact gaven me de rugwind die ik nodig had om dit proefschrift af te maken. Uit het oog is niet uit het hart: ik hoop van harte dat we ook op afstand de samenwerking kunnen blijven opzoeken!

I am grateful to all members of the reading committee for the time and attention spent on reviewing this thesis manuscript and for their participation in the opposition: prof. dr. J. Berkhof, prof. dr. M.J.L. Ligtenberg, prof. dr. K. Taskén, prof. dr. C.M.L. van Herpen, dr. M.A.J. van Limbeek, dr. M.G.J. van Dongen and dr. M.E. van Linde.

Prof. dr. Hans Gelderblom, beste *Hans*, als een van de 3 PI's van de DRUP studie was het altijd fijn om met je samen te werken. Dank voor je laagdrempeligheid, de goede discussies en je gezelligheid tijdens etentjes met het studieteam. Ik ben blij dat we onze vertrouwde samenwerking nu weer kunnen voortzetten.

De DRUP studie is als investigator initiated studie een mega-project, waarbij zeer veel mensen vanuit het hele land betrokken zijn. Dankzij hen loopt de soms ingewikkelde logistiek toch opvallend soepel.

Allereerst wil ik noemen alle enthousiaste mensen die in het AVL, de sponsorsite, de schouders onder deze studie zetten. De apotheek, onder leiding van prof. dr. *Alwin Huitema*, dank voor de fijne samenwerking en altijd jullie bereidheid om mee te denken. Het centraal datamanagement, onder leiding van *Henk Botma*, dank voor de overzichten en jullie nauwkeurigheid. De monitors, in het bijzonder *Karin Kaptijn*, dank voor je opmerkzaamheid en de fijne manier waarop je zaken kon oppakken met de lokale teams. De afdeling contracten, in het bijzonder *Steven Vanhoutvin*, dank voor al je inspanningen om de vele contracten binnen deze studie rond te krijgen en ons op gedoseerde wijze mee te nemen in de procedures. En natuurlijk de statistici, *Erik van Werkhoven* en *Vincent van der Noort*, dank voor jullie talloze analyses en de sessies met uitleg, en voor het meedenken als we weer eens out-of-the-box wilden gaan.

Dankzij de lokale onderzoeksteams is de DRUP uitgegroeid tot een van de studies met het grootste aantal deelnemende patiënten in ons land. Dank aan alle lokale datamanagers, research verpleegkundigen, coördinatoren en lokale apotheken voor de fijne communicatie en samenwerking! Speciale dank aan alle lokale PI's en behandelend oncologen/longartsen voor het actief includeren en begeleiden van de studiepatiënten.

Alle vertegenwoordigers van de farma-bedrijven die betrokken zijn bij de DRUP studie: het was mooi om steeds jullie enthousiasme, maar ook jullie kritische vragen te kunnen horen tijdens de halfjaarlijkse farma-meetings. Veel dank voor de soepele communicatie en jullie inspanningen om de studie mogelijk te maken.

De bevrogen mensen bij Hartig Medical Foundation, waaronder *Hans, Edwin, Lieke* en *Immy*: dank voor de altijd vlotte terugkoppelingen en de laagdrempeligheid. *Korneel*, geen verzoek leek jou te gek, altijd bereid om even verder te kijken of om iets uit te leggen aan een simpele clinicus.

Paul, Anne en *Wendy*, wat zijn jullie als Molecular Expert Board een belangrijke hoeksteen van de DRUP studie, en wat heb ik onbeschrijflijk veel van jullie geleerd over de technische details, maar vooral over de interpretatie van NGS/WGS rapporten. Het heeft me een veel dieper begrip van de biologie van kanker gegeven, waar ik in mijn klinisch werk nu nog dagelijks van profiteer.

It has been a pleasure working with so many other international study groups. The study teams of TAPUR and CAPTUR: data sharing was much more complex than I had imagined, but it has been an interesting journey, thank you for the collaboration. The study teams of the European collaborating precision oncology trials: wonderful to see that so many of your trials are now recruiting patients and that the European cancer medicine trial network is now established, I will continue to follow your activities with great interest.

Mijn geweldige collega studietoelators van de DRUP studie. *Daphne*, ik heb bewondering voor hoe gestructureerd jij de studie hebt opgezet en al het werk dat je verzet hebt. Dank voor je geduld en uitleg in het begin, het zorgde voor een vliegende start. Lieve *Louisa, Maxime* en *Laurien*, wat waren we een goede 4-eenheid. We konden lezen en schrijven met elkaar en konden op elkaar terugvallen. Ik had me geen betere DRUP-collega's kunnen wensen! Heel veel succes in jullie verder carrières. *Birgit, Ilse, Karlijn* en *Soemeya*, heel veel plezier nog met dit mooie en bijzondere project! *Lena*, je hebt je een zeer moeilijke taak goed eigen kunnen maken, veel dank voor de fijne samenwerking.

Met het research team van de afdeling oncologie in het Amsterdam UMC was de samenwerking altijd bijzonder fijn. Heel veel dank *Mieke, Mikkjal, Rita, Ellen, Lonneke, Jannemieke, Anne Marije* en *Annet*, voor jullie betrokkenheid bij alle DRUP patiënten van het Amsterdam UMC, en voor het laagdrempelige overleg. Altijd fijn om even met jullie te sparren. Dank ook aan het datamanagement team betrokken bij de DRUP, in het bijzonder *Selma* en *Laurien*. *Tamara* en *Babette*, dank voor de data-invoer, fijn dat we elkaar altijd snel wisten te vinden voor overleg. Dank ook aan alle interventieradiologen en laboranten voor jullie hulp bij de afname van heel veel studiebipten voor de CPCT-02 en DRUP studie.

Naast de klinische studie lag er voor mij een mooie uitdaging in de ontdekking van de wondere wereld van (phospho)proteomics, waarvan ik voorafgaand aan de start van mijn promotieon-

derzoek nog nooit gehoord had. Het was niet eenvoudig om alle details en nuanceringen goed onder de knie te krijgen, en er is binnenskamers weleens een onvertogen woord gevallen als ik weer eens door de kleurtjes de heatmaps niet meer zag. Dankzij de gedreven en geduldige mensen van het oncoproteomics lab van het Cancer Center Amsterdam ben ik toch een eind gekomen.

Connie, jouw bevoegenheid en optimisme ten aanzien van de potentie van phosphoproteomics is aanstekelijk. Je zeer snelle en scherpe feedback op stukken, schat aan ervaring en altijd de bereidheid om mee te denken, ik heb er enorm veel van geleerd! Dank voor de waardevolle discussies en al je hulp bij het RCC en het CryoOn project!

Sander, altijd een vriendelijk gezicht in de buurt van de massaspectrometer. Indrukwekkend hoe jij zeer ingewikkelde materie op een begrijpelijke manier kunt uitleggen, zodat zelfs een eenvoudige dokter het snapt, dank daarvoor. *Richard*, dank je voor je hulp bij het plannen en uitvoeren van de experimenten en het meedenken over de praktische zaken. *Thang*, veel dank voor je hulp bij het verwerken en weergeven van de enorme hoeveelheid phospho-data. *Alex*, dank je voor je hulp met de INKA-data en voor de gezamenlijke R-sessies, ik heb er veel van geleerd. *Jaco*, bedankt voor je eindeloze geduld en voor de enorme hoeveelheid analyses die je hebt gedaan voor mijn projecten. Je mails zijn een taalkundig feestje, wel jammer dat die 9-way venn er nog niet van gekomen is!

Henk Dekker, uiteindelijk betrokken bij ieder van mijn projecten. Biopten snijden, RNA-extractie, meedenken over materialen en methodes, maar ook samen met Mariette in jouw auto naar de CryoOn meetings en natuurlijk de ontelbare biopten die jij hebt opgevangen voor de DRUP en CPCT studies. Dank voor alles.

Allen die betrokken waren bij het CryoOn project wil ik heel hartelijk bedanken voor de fijne samenwerking. In het bijzonder *Srinivas Vanapalli* en *Sahil Jagga* van de Universiteit Twente, wat heb ik veel van jullie geleerd. De fysica en thermodynamica vraagstukken waren voor mij een aangename en uitdagende afwisseling.

Alle arts-onderzoekers van de afdeling medische oncologie, dankzij jullie was het promotie-traject een feestje! *Joeri* en *Esther*, wat hebben we het gezellig gehad als burens op 3A. Het vrijdagmiddag-colaatje, muzikale traktaties en congressen, ik denk er graag aan terug. Inmiddels word ik wel minder vaak "gepest op mijn werk"... jammer! *Sophie*, we liepen grotendeels samen op, zowel in het onderzoek als daarbuiten. Samen een tutorgroepje, tegelijk zwanger en samen op phospho-cursus, en altijd zo fijn sparren met jou! Dank je voor je vriendschap, ik hoop dat we die nog lang kunnen voortzetten. *Cyrillo*, dank je voor het kritisch meedenken en voor de gezellige lunches en congressen, ik heb veel van je geleerd en erg met je gelachen! *Iris*, *Ramsha*, *Ruben*, *Elisa*, *Robin*, *Dennis*, *Marieke* en *Caroline*, bedankt voor al jullie gezelligheid en input tijdens de lab meetings. *Tessa* en *Lune*, fijn dat jullie het aandurfdn met mij als stagebegeleider. Dank voor jullie hulp bij de CPCT en DRUP en voor de gezelligheid.

Iris en *Mariska*, bedankt voor de gezellige gesprekjes en jullie hulp met allerlei vragen in de afgelopen jaren. Altijd een vriendelijk gezicht en een glimlach op het secretariaat, jullie zijn van grote waarde voor de afdeling!

Alle *oncologen* van het Amsterdam UMC, bedankt voor jullie aanhoudende belangstelling voor (de voortgang van) mijn onderzoek, en voor jullie inspanningen voor de DRUP patiënten. Zowel in het onderzoek als in de patiëntenzorg heb ik de samenwerking met ieder van jullie enorm gewaardeerd. Op wereldschaal is Maastricht helemaal niet zo ver, ik hoop van harte dat we het fijne contact kunnen onderhouden.

Tineke, *Kathelijn*, *Elske* en *Sarah*, bedankt voor jullie adviezen (niet geheel zonder bias) toen ik twijfelde of ik aan dit promotie-onderzoek zou beginnen. Zoals jullie zien heeft het me veel gebracht. Dank ook voor de gezellige avondjes, bijvoorbeeld op de NVMO-dagen, aan de keukentafel, verschillende ESMO edities, etc, ik heb er erg van genoten.

Alle *oncologie-fellows*, van toen en nu, heel veel dank voor jullie oprechte interesse in mijn onderzoek en voor jullie hulp en gezelligheid. Ik prijs me gelukkig dat ik aan zowel het begin als aan het eind van mijn fellowship een warme groep collega's trof, die elkaar opvangt als het moeilijk is en toejuicht bij de successen. Ik weet zeker dat we elkaar nog tegen zullen komen.

Na de mooie tijd in het Amsterdam UMC sta ik nu aan de vooravond van een nieuw avontuur in het mooie Zuiden van ons land. Ik dank de afdeling medische oncologie van het Maastricht UMC+ voor het in mij gestelde vertrouwen en kijk erg uit naar onze samenwerking.

Lotte en Jessica, roomies! Wie had gedacht dat we naast kamergenoten ook zulke goede vriendinnen zouden worden. Lieve *Lot*, vanaf het moment dat we elkaar ontmoetten was er een klik. Ik hou van je oprechtheid, je humor en je positiviteit. Dank je voor je hulp en adviezen door de jaren heen. Lieve *Jessica*, jouw Twentse nuchterheid en relativiseringsvermogen zijn een verademing. Ik heb veel bewondering voor je doorzettingsvermogen, je discipline en je dansmoves. Meiden, wat hebben we samen veel meegemaakt in korte tijd! Van de uitdagingen van het overstappen naar een ander instituut (met meenemen van de studie) of naar een volledig ander onderzoeksonderwerp, tot bruiloften, banen en baby's. Ik ben dankbaar dat jullie mij op 15 december zullen bijstaan als *paranimfen*, en kan me niet voorstellen dat ik hier met iemand anders dan met jullie aan mijn zijde zou staan. Bedankt voor jullie warme vriendschap, en proost op al het moois dat ons nog te wachten staat.

En dan is er gelukkig ook nog een mooi en rijk gevuld leven naast het werk. Ik heb het geluk om omringd te zijn door de liefste vrienden en fijnste familie!

Alieke, Michelle, Sanne, Esther en Marloes, wat ben ik blij dat we al 19 jaar lief en leed met elkaar kunnen delen. Ik denk graag terug aan alle fijne etentjes, weekendjes Antwerpen, feestjes en kopjes thee (met bokkenpootjes) samen. Lieve *Sanne*, wat maak je mij vaak aan het

lachen met jouw kurkdroge humor en nuchtere blik op de wereld. Jouw relativiseringsvermogen heeft mij meer dan eens de nodige lucht in het hoofd gegeven. Lieve *Alieke*, wie had kunnen bedenken dat de persoon naast wie ik ging zitten op die allereerste dag bij het introductiecollege geneeskunde, in die grote collegezaal, nu nog steeds een van mijn beste vriendinnen zou zijn! Ik hou van je eigenheid en je heldere kijk op de dingen, en hoop dat we nog steeds af en toe een wandeldate kunnen organiseren. Lieve *Michelle*, Giaaaa! Vanaf de eerste logeerpartij in het eerste studiejaar (ik opgekruld op de grond onder jouw bureau in die veel te kleine studentenkamer in Utrecht) zijn we nooit van elkaars spreekwoordelijke zijde geweken. Van samen studeren en cabaret kijken op de avond voor het tentamen tot een luisterend oor en praktische adviezen bij de grote levensvraagstukken (“waarom slaapt mijn baby niet?”). Dank je voor je zorgzaamheid, eerlijkheid, aanmoediging, en ook de afleiding als het nodig was. Meiden, ik hoop dat het langste deel van onze vriendschap nog voor ons ligt!

Lieve *Daisy*, bijzonder hoe we in korte tijd zo'n hechte vriendschap hebben gekregen! Ik geniet van de frequente speeltuin/bibliotheek-dates met Kai, Ava, Kiera en Tom, die ons allebei wat lucht geven op uitdagende dagen. Maar ook de kopjes koffie zonder de kinderen en natuurlijk onze gezamenlijke hobby. En mocht je het toch weer eens vergeten: you got this!

Lieve familie, “*De Groep*”, dank voor jullie betrokkenheid en jullie niet-aflatende interesse in mijn onderzoek en carrière. En natuurlijk voor de heerlijke weekendjes weg samen, de familiedagen en de Sinterklaasvieringen. Ik weet zeker dat oma vanaf haar wolkje mee geniet en onze samenkomsten voorziet van gevat commentaar.

Lieve ome *Frans*, *Esther*, *Noortje* en *Joost*, wat ben ik blij dat we elkaar vanaf nu veel vaker gaan zien! Veel dank voor jullie enthousiasme en hulp bij “de transfer” naar Maastricht, ik kijk uit naar laagdrempelige bezoeken over en weer.

Ondanks de grote afstand heb ik geluk met een fijne schoonfamilie. Lieve *Pae* en *Mae*, *Nette* en *Ponto*, ik hoop dat we snel weer met ons gezin naar Suriname kunnen komen om te genieten van elkaars aanwezigheid en het lekkere eten. *Tampy* and *Andrew*, thank you for your visits and for your interest in our children. We hope to come visit you in Canada in the near future.

Dankzij mijn liefdevolle opvoeding had ik een goede basis die mij de mogelijkheid gaf mijn dromen en ambities achterna te gaan.

Mama en Jack, dank jullie wel voor jullie onvoorwaardelijke steun en liefde, en al jullie hulp door de jaren heen. Lieve *Jack*, jouw daadkracht, gestructureerde overzichtjes en handigheid hebben ons meer dan eens enorm geholpen. Ik waardeer je oprechte interesse in mijn onderzoek en carrière en je enthousiasme en aanmoediging. Je geeft me het gevoel dat ik altijd bij je terecht kan, dank je voor je niet aflatende steun. Lieve *mamp*, mijn grote voorbeeld. Jij bent altijd mijn stabiele basis geweest. Van thee met een koekje na schooltijd en samen in een volleybalteam, tot een luisterend oor voor al mijn belevenissen en praktische adviezen in de

uitdagende tijden. Dank je dat je er altijd voor mij bent geweest, dat je me hebt geleerd door te zetten en mijn eigen gevoel te volgen. Je vermogen tot bedenken van creatieve oplossingen heb je met mij gedeeld, daarvan heb ik nog dagelijks profijt in mijn werk en in de opvoeding. Dankzij jouw steun en liefde ben ik geworden wie ik nu ben, een gelukkig en tevreden mens. Ik ben dankbaar voor de goede band die jullie als opa en oma hebben met Ava en Tom. In al jullie bescheidenheid willen jullie voor alle hulp nooit een bedankje, maar bij deze komen jullie toch aan de beurt. Dank jullie wel voor *alles*, ik hou van jullie!

Lieve *Tjipto*, op een dansvloer in Paramaribo sloeg de vonk over, en kijk ons nu eens, 8 jaar later! Jij geeft me rust en welkome afleiding van het werk. Dank je voor de vrijheid die je mij geeft om mijn carrière vorm te geven en voor alles wat je voor ons gezin doet. Ik kijk uit naar onze mooie toekomst, met hopelijk weer iets vaker tijd voor een dansje samen. Aku seneng karo kowe!

Ava en Tom, de lichtjes in mijn leven. Wat ben ik ontzettend trots op jullie. Er bestaat geen woord om te beschrijven hoeveel ik van jullie hou. Lieve *Ava*, mijn knappe, slimme, creatieve, lieve dochter. Ik geniet enorm van jouw liedjes, dansjes, verhaaltjes, acrobaten-kunsten en knuffels. Lieve *Tom*, mijn vrolijke, ondeugende, slimme, ondernemende mannetje. Wat word ik vrolijk van jouw schaterlach, je onbevreesdheid, het klimmen en klauteren en je kletspraatjes. Vol verwondering zie ik hoe jullie steeds weer nieuwe dingen leren. Ik kijk uit naar alle avonturen die we nog met z'n allen zullen beleven. Samen zijn jullie mijn hele wereld, ik hou van jullie!

CURRICULUM VITAE



Hanneke van der Wijngaart was born on December 8th 1985 in Ridderkerk, the Netherlands. She finished secondary school at the Libanon Lyceum in Rotterdam in 2004. Subsequently she started her medical training at the VU University Medical Center in Amsterdam. During her medical training, Hanneke has been an active member of the European Medical Students Association (EMSA), where she served the European Executive Board as Vice-President (2006-2007) and as President (2008-2009). She paused her studies for 8 months for an internship at the Standing Committee of European Doctors (CPME) in Brussels, Belgium (2008). Hanneke obtained her medical degree in 2011.

After having worked as a resident not in training at the department of internal medicine at the Zaans Medisch Centrum in Zaandam for one year, she started her training to become an internist at Medisch Centrum Alkmaar (MCA, nowadays NoordWest Ziekenhuisgroep). After four years of training in Alkmaar, including a four-month internship in the Diaconessenhuis in Paramaribo, Surinam, she transferred to the Amsterdam University Medical Centers in 2016 to continue her training as a fellow in medical oncology. During her fellowship, Hanneke developed an interest for academic research and was given the opportunity to start a PhD project.

In 2017 she paused her medical oncology training for four years to embark on a PhD project, under supervision of prof. dr. H.M.W. Verheul, prof. dr. E.E. Voest and dr. M. Labots. During these four years, Hanneke worked as one of the national coordinators of the Drug Rediscovery Protocol (DRUP, trial), an ongoing investigator initiated, multi-center, multi-drug, pan-cancer phase 2 basket/umbrella trial in which patients with advanced cancer are treated with targeted anti-cancer drugs based on their tumor molecular profiles. She also engaged in a translational project on renal cell cancer, aiming to use global phosphoproteomics to find tissue-based biomarkers for response to sunitinib. In a collaborative project with the Thermal Physics department of the University of Twente, Hanneke worked on benchmarking a newly developed snap freezer for optimal preservation of tissues to facilitate molecular profiling on clinical samples.

In September 2023, Hanneke finished her training and became a medical oncologist. Since November 2023 she works as a medical oncologist in the Maastricht University Medical Center (MUMC+) in Maastricht, where she focuses on the care for patient with skin cancer, renal-, prostate- bladder- and testicular cancer and tumors with unknown primary origin. She plans to continue her clinical research in the field of precision oncology and tissue molecular profiling.

Hanneke currently lives in Maastricht with her partner Tjipto and their two children Ava (2018) and Tom (2021).

LIST OF PUBLICATIONS

Laurien Zeverijn, Birgit Geurts, Thomas Battaglia, Jade van Berge Henegouwen, Gijsbrecht de Wit, Louisa Hoes, [Hanneke van der Wijngaart](#), Vincent van der Noort, Paul Roepman, Wendy de Leng, Anne Jansen, Myriam Chalabi, Carla van Herpen, Lot Devriese, Frans Erdkamp, Mariette Labots, Maja Dejonge, Emile Kerver, Adriaan Bins, Lindsay Leek, Jessica Notohardjo, Alfonsus J.M. van den Eertwegh, Lodewyk Wessels, Henk Verheul, Hans Gelderblom, Joris van de Haar, Emile Voest. **The innate immune landscape of dMMR/MSI cancers predicts outcome of nivolumab treatment**

Submitted

Jade M. van Berge Henegouwen; Laurien J. Zeverijn; Birgit S. Geurts; Gijs F. de Wit; Louisa R. Hoes; [Hanneke van der Wijngaart](#); Vincent van der Noort; Alwin D.R. Huitema; Filip Y.F. de Vos; Katrien Grunberg; Haiko J. Bloemendal; Henk M.W. Verheul; Emile E. Voest; Hans Gelderblom. **Maximizing “real life” treatment opportunities in the Drug Rediscovery Protocol (DRUP): consequence evaluation of protocol waivers on safety and outcome**

Submitted

[H. van der Wijngaart](#), R. Beekhof, J.C. Knol, A.A. Henneman, R. de Goeij – de Haas, S.R. Piersma, T.V. Pham, C.R. Jimenez, H.M.W. Verheul, M. Labots. **Candidate biomarkers for treatment benefit from sunitinib in patients with advanced Renal Cell Carcinoma using mass spectrometry-based (phospho)proteomics**

Clin Proteomics 2023. Accepted

L. Zeverijn, E. Looze, S. Thavaneswaran, J.M. van Berge Henegouwen, J. Simes, L.R. Hoes, K. Sjoquist, [H. van der Wijngaart](#), L. Sebastian, B. Geurts, C. Lee, G. de Wit, D. Espinoza, P. Roepman, F. Lin, A.M.L. Jansen, W.W.J. de Leng, V. van der Noort, L. Leek, F. de Vos, C.M.L. van Herpen, H. Gelderblom, H.M.W. Verheul, D. Thomas, E.E. Voest. **Limited clinical activity of palbociclib and ribociclib monotherapy in advanced cancers with Cyclin D-CDK4/6 pathway alterations in the Dutch DRUP and Australian MoST trials**

Int J Cancer. 2023 Oct 1;153(7):1413-1422. doi: 10.1002/ijc.34649

[H. van der Wijngaart](#), S. Jagga, H. Dekker, R. de Goeij, S.R. Piersma, T.V. Pham, J.C. Knol, B. Zonderhuis, H.J. Holland, C.R. Jiménez, H.M.W. Verheul, S. Vanapalli, M. Labots. **Advancing wide implementation of precision oncology: a liquid nitrogen-free snap freezer preserves molecular profiles of biological samples**

Cancer Med. 2023 Mar 14. doi: 10.1002

BS Geurts, TW Battaglia, JM van Berge Henegouwen, LJ Zeverijn, GF de Wit, LR Hoes, [H van der Wijngaart](#), V van der Noort, P Roepman, WWJ de Leng, AML Jansen, FL Opdam, MJA de Jonge, GA Cirkel, M Labots, A Hoeben, ED Kerver, AD Bins, FGL Erdkamp, JM van Rooijen, D Houtsma, MP Hendriks, JB de Groot, HMW Verheul, H Gelderblom, EE Voest. **Efficacy, safety and biomarker analysis of durvalumab in patients with mismatch-repair deficient or microsatellite instability-high solid tumours**

BMC Cancer 2023 Mar 4;23(1):205. doi: 10.1186

van Berge Henegouwen JM, Jebbink M, Hoes LR, [van der Wijngaart H](#), Zeverijn LJ, van der Velden DL, Roepman P, de Leng WWJ, Jansen AML, van Werkhoven E, van der Noort V, van der Wekken AJ, de Langen AJ, Voest EE, Verheul HMW, Smit EF, Gelderblom H. **Trastuzumab and pertuzumab combination therapy for advanced pre-treated HER2 exon 20-mutated non-small cell lung cancer**

Eur J Cancer. 2022 Aug;171:114-123. doi: 10.1016

van Berge Henegouwen JM, [van der Wijngaart H](#), Zeverijn LJ, Hoes LR, Meertens M, Huitema ADR, Devriese LA, Labots M, Verheul HMW, Voest EE, Gelderblom H. **Efficacy and toxicity of vemurafenib and cobimetinib in relation to plasma concentrations, after administration via feeding tube in patients with BRAF-mutated thyroid cancer: a case series and review of literature**

Cancer Chemother Pharmacol. 2022 Jul;90(1):97-104. doi: 10.1007

Hoes LR, van Berge Henegouwen JM, [van der Wijngaart H](#), Zeverijn LJ, van der Velden DL, van de Haar J, Roepman P, de Leng WJ, Jansen AML, van Werkhoven E, van der Noort V, Huitema ADR, Gort EH, de Groot JWB, Kerver ED, de Groot DJ, Erdkamp F, Beerepoot LV, Hendriks MP, Smit EF, van der Graaf WTA, van Herpen CML, Labots M, Hoeben A, Morreau H, Lolkema MP, Cuppen E, Gelderblom H, Verheul HMW, Voest EE. **Patients with Rare Cancers in the Drug Rediscovery Protocol (DRUP) Benefit from Genomics-Guided Treatment**

Clin Cancer Res. 2022 Apr 1;28(7):1402-1411. doi: 10.1158

[van der Wijngaart H](#), Hoes LR, van Berge Henegouwen JM, van der Velden DL, Zeverijn LJ, Roepman P, van Werkhoven E, de Leng WWJ, Jansen AML, Mehra N, Robbrecht DGJ, Labots M, de Groot DJA, Hoeben A, Hamberg P, Gelderblom H, Voest EE, Verheul HMW. **Patients with Biallelic BRCA1/2 Inactivation Respond to Olaparib Treatment Across Histologic Tumor Types**

Clin Cancer Res. 2021 Nov 15;27(22):6106-6114. doi: 10.1158

van der Wijngaart H*, van der Velden DL*, Hoes LR*, van Berge Henegouwen JM*, van Werkhoven E, Roepman P, Schilsky RL, de Leng WWJ, Huitema ADR, Nuijen B, Nederlof PM, van Herpen CML, de Groot DJA, Devriese LA, Hoeben A, de Jonge MJA, Chalabi M, Smit EF, de Langen AJ, Mehra N, Labots M, Kapiteijn E, Sleijfer S, Cuppen E, Verheul HMW, Gelderblom H, Voest EE. **The Drug Rediscovery protocol facilitates the expanded use of existing anticancer drugs**

Nature. 2019 Oct;574(7776):127-131. doi: 10.1038

van Waalwijk van Doorn-Khosrovani SB, Pisters-van Roy A, van Saase L, van der Graaff M, Gijzen J, Sleijfer S, Hoes LR, van Berge Henegouwen JM, van der Wijngaart H, van der Velden DL, van Werkhoven E, Retel VP, van Harten WH, Huitema ADR, Timmers L, Gelderblom H, Verheul HMW, Voest EE. **Personalised reimbursement: a risk-sharing model for biomarker-driven treatment of rare subgroups of cancer patients**

Ann Oncol. 2019 May 1;30(5):663-665. doi: 10.1093

Neefjes ECW, van der Wijngaart H, van der Vorst MJDL, Ten Oever D, van der Vliet HJ, Beeker A, Rhodius CA, van den Berg HP, Berkhof J, Verheul HMW. **Optimal treatment of opioid induced constipation in daily clinical practice - an observational study**

BMC Palliat Care. 2019 Mar 29;18(1):31. doi: 10.1186

van der Wijngaart H, van Dam B, van den Berg JG, Krul-Poel YH, Klemt-Kropp M, Bax WA. **A 73-year-old male with jaundice and acute kidney injury. Bile cast nephropathy**

Neth J Med. 2014 Feb;72(2):95, 99

* *These authors contributed equally to the work*

